AD-A126 809 EFFECT OF HF HEATING ARRAY DIRECTIVITY PATTERN ON THE FREQUENCY RESPONSE O..(U) PENNSYLVANIA STATE UNIV UNIVERSITY PARK IONOSPHERE RESEARCH L.. 1/3

UNCLASSIFIED K J CARROLL ET AL. JAN 83 PSU-IRL-SCI-475 F/G 20/14 NL

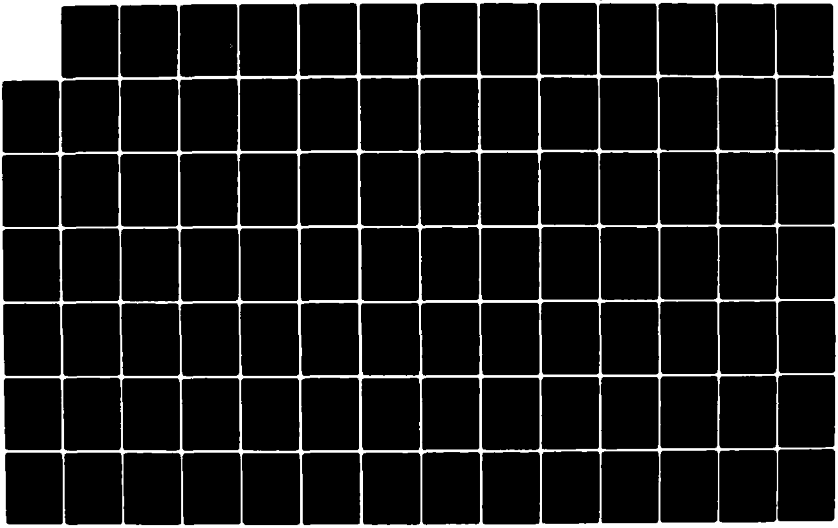

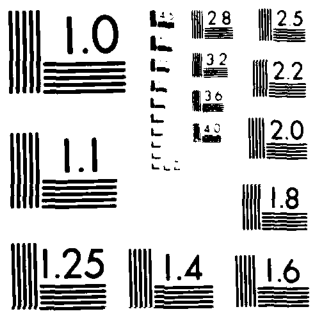

MICROCOPY RESOLUTION TEST CHART
NATIONAL BUREAU OF STANDARDS 1963-A

(2)

AD A126809

PSU-IRL-SCI-475
Classification Numbers: 1.5.1, 3.1.4, 3.2.1, 3.3

THE PENNSYLVANIA
STATE UNIVERSITY

IONOSPHERIC RESEARCH

Scientific Report 475

EFFECT OF HF HEATING ARRAY DIRECTIVITY PATTERN ON THE FREQUENCY RESPONSE OF GENERATED ELF/VLF

by

Kenneth J. Carroll, A. J. Ferraro
H. S. Lee, Roger Allshouse
Bruce Long, Ray J. Lunnen

January 1983

The research reported in this document has been supported by the Office of Naval Research under Contract No. N00014-81-K-0276.

IONOSPHERE RESEARCH LABORATORY

University Park, Pennsylvania

UNCLASSIFIED

SECURITY CLASSIFICATION OF THIS PAGE (When Data Entered)

REPORT DOCUMENTATION PAGE		READ INSTRUCTIONS BEFORE COMPLETING FORM
1. REPORT NUMBER Scientific Report 475	2. GOVT ACCESSION NO. AD-A126809	3. RECIPIENT'S CATALOG NUMBER
4. TITLE (and Subtitle) Effect of HF Heating Array Directivity Pattern on the Frequency Response of Generated ELF/VLF		5. TYPE OF REPORT & PERIOD COVERED Annual Technical CY1982
		6. PERFORMING ORG. REPORT NUMBER 475
7. AUTHOR(s) Kenneth J. Carroll, A. J. Ferraro, H. S. Lee, Roger Allshouse, Bruce Long, Ray J. Lunnen		8. CONTRACT OR GRANT NUMBER(s) N00014-81-K-0276
9. PERFORMING ORGANIZATION NAME AND ADDRESS The Pennsylvania State University 318 Electrical Engineering East University Park, PA 16802		10. PROGRAM ELEMENT, PROJECT, TASK AREA & WORK UNIT NUMBERS RR032-08-01;1-AE SR0-108 3208-010
11. CONTROLLING OFFICE NAME AND ADDRESS Office of Naval Research Code 414 Arlington, Virginia 22217		12. REPORT DATE January 1983
		13. NUMBER OF PAGES 203
14. MONITORING AGENCY NAME & ADDRESS(if different from Controlling Office)		15. SECURITY CLASS. (of this report) Unclassified
		15a. DECLASSIFICATION/DOWNGRADING SCHEDULE

16. DISTRIBUTION STATEMENT (of this Report)

Approved for public release and sale, distribution unlimited.

17. DISTRIBUTION STATEMENT (of the abstract entered in Block 20, if different from Report)

18. SUPPLEMENTARY NOTES

19. KEY WORDS (Continue on reverse side if necessary and identify by block number)

D-Region
Numerical Techniques and Computations
Ground-Based Techniques and Measurements
Instrumentation and Facilities for Ionospheric Measurements

20. ABSTRACT (Continue on reverse side if necessary and identify by block number)

Directivity patterns at 3.17 MHz and 5.1 MHz are calculated for the HF antenna array at the high power HF heating facility at the Arecibo Observatory in Puerto Rico. The pattern was calculated using pattern multiplication and method of moment techniques. The calculated pattern is shown to be a good approximation to an experimentally measured pattern in one plane of the array. A simple model was used to approximate the effect of the pattern on the frequency response of ELF/VLF signals generated by the HF

DD FORM 1 JAN 73 1473 EDITION OF 1 NOV 65 IS OBSOLETE
S N 0102-LF-014-6601

UNCLASSIFIED

SECURITY CLASSIFICATION OF THIS PAGE (When Data Entered)

heating. The frequency response was determined at two ELF/VLF receiver sites. Results show that ELF/VLF generated by side lobes of the HF pattern have sufficient strength to create a ELF/VLF interference pattern at receiving locations.

PSU-IRL-SCI-475
Classification Numbers: 1.5.1, 3.1.4, 3.2.1, 3.3

Scientific Report 475

EFFECT OF HF HEATING ARRAY DIRECTIVITY PATTERN ON THE FREQUENCY RESPONSE OF GENERATED ELF/VLF

by

Kenneth J. Carroll, A. J. Ferraro
H. S. Lee, Roger Allshouse
Bruce Long, Ray J. Lunnen

January, 1983

The research reported in this document has been supported by the Office of Naval Research under Contract No. N00014-81-K-0276.

Submitted by: ______________________
A. J. Ferraro
Professor of Electrical Engineering

Approved by: ______________________
John S. Nisbet
~~Director~~, Ionosphere Research Laboratory

Ionosphere Research Laboratory
Department of Electrical Engineering
The Pennsylvania State University
University Park, Pennsylvania 16802

TABLE OF CONTENTS

ACKNOWLEDGEMENTS

I wish to thank Dr. A. Veldhuis for the sharing of his work and knowledge of the Arecibo HF heating antenna. He provided information through informal discussions and correspondence. Dr. Veldhuis' suggestions on the approach to analyze the antenna as well as his providing physical data about the antenna were invaluable.

This study was supported by the Office of Naval Research under Contract No. N00014-81-K-0276.

Arecibo Observatory is operated by Cornell University under a contract with the National Science Foundation.

LIST OF TABLES

LIST OF FIGURES

ABSTRACT

Directivity patterns at 3.17 MHz and 5.1 MHz are calculated for the HF antenna array at the high power HF heating facility at the Arecibo Observatory in Puerto Rico. The pattern was calculated using pattern multiplication and method of moment techniques. The calculated pattern is shown to be a good approximation to an experimentally measured pattern in one plane of the array. A simple model was used to approximate the effect of the pattern on the frequency response of ELF/VLF signals generated by the HF heating. The frequency response was determined at two ELF/VLF receiver sites. Results show that ELF/VLF generated by side lobes of the HF pattern have sufficient strength to create a ELF/VLF interference pattern at receiving locations.

EFFECT OF HF HEATING ARRAY DIRECTIVITY PATTERN ON THE FREQUENCY RESPONSE OF GENERATED ELF/VLF

INTRODUCTION

ELF/VLF generation experiments were conducted at the Arecibo Observatory (A.O.) in Puerto Rico. The HF heating faciltiy for A.O. is located at 18° 29' N and 66° 40' W geographic latitude and longitude respectively. The ELF/VLF receiving site was located 7.7 km from the heating facility and 238° to the east.

The motion of the ionospheric plasma, in the presence of the earth's magnetic field, causes natural ionospheric currents to flow. By changing the conductivity of a small portion of the ionosphere, the natural currents within that portion can be modulated. Modulating the currents in the ELF/VLF range causes a ELF/VLF signal to be radiated by the ionosphere.

The conductivity in the ionosphere is dependent upon the electron collision frequency, which is in turn dependent upon the electron temperature. An HF electromagnetic wave is absorbed by the ionosphere. The EM wave adds kinetic energy to the electrons, which in effect increases the electron temperature. Thus, by modulating the HF transmission at a ELF/VLF rate, the ionospheric conductivities will be modulated at the same rate, and a ELF/VLF signal will be radiated from the ionosphere.

The antenna, radiating the HF signal heating the ionosphere, has a pattern consisting of a main beam, side lobes, and possibly grating lobes. Heating occurs where each of these penetrates the ionosphere. By determining the pattern of the HF antenna, the spatial distribution

of the heating in the ionosphere can be determined. Thus, the location in the ionosphere and the intensity of each of the ELF/VLF radiating sources can be determined. From this the characteristics of the ELF/VLF radiation from the ionosphere can be calculated.

This section will describe the calculation of an approximation to the Arecibo HF heating array directive gain pattern and apply the results to find a zero order approximation to an ELF/VLF radiating array. The technique employed to calculate the HF array pattern is one which uses the combination of pattern multiplication techniques and computer numerical analysis. The numerical program used was the Antenna Modeling Program (AMP)[(1)]. The AMP output was then used with analytical equations in a program written at the Ionosphere Research Laboratory at Penn State University to carry out the pattern multiplication.

PATTERN MULTIPLICATION THEORY

The pattern multiplication technique is based upon the calculation of the total pattern of an array by taking the product of an array factor (AF) with the elemental pattern. The array is made up of identical elements. The elemental pattern is the pattern of an individual element of the array. The AF is obtained by replacing each of the elements of the array with an isotropic radiator and calculating the pattern for the array of isotropic radiators. A detailed discussion of pattern multiplication can be found in reference (2). A description of the theory used in this analysis follows.

For example, assume there are an even number "N" of colinear isotropic radiators separated by a distance "d" as shown in figure (1-1). The far field, at a point "P", due to the n^{th} radiator, is proportional to a complex current amplitude, I_n, a phase factor, $e^{-j\beta R_n}$, and is inversely proportional to the distance from the radiator to "P", equation (1-1).

$$E_n \alpha I_n[e^{-j\beta R_n}/(4\pi R_n)] \qquad (1-1)$$

The far field approximation states that "P" is far enough away that "R_n" can be assumed to be parallel to "R", and the length of "R_n" is approximately equal to "R". Under these conditions the approximations in equation (1-2) can be made.

$$1/R \approx 1/R_n \qquad (1-2a)$$

$$R_n \approx (2|n|-1)(d/2)\cos\alpha + R \quad ; n < 0 \qquad (1-2b)$$

$$R_n \approx R - (2|n|-1)(d/2)\cos\alpha \quad ; n > 0 \qquad (1-2c)$$

While the small difference in length of "R_n" can be neglected in the "$1/R_n$" term, these differences can have a significant effect on the phase term, $e^{-j\beta R_n}$. Incorporating the far field approximation equation (1-2) with equation (1-1), the total field at "P" can be expressed (1-3).

$$E = \sum_{n=(-N/2)}^{-1} E_n + \sum_{n=1}^{N/2} E_n = [\sum_{n=(-N/2)}^{-1} I_n e^{-j\beta[(2|n|-1)(d/2)\cos\alpha + R]}$$

$$+ \sum_{n=1}^{N/2} I_n e^{-j\beta[R-(2|n|-1)(d/2)\cos\alpha]}][1/(4\pi R)] \qquad (1-3)$$

Assume that "I_n" is equal to a constant "I_o" and collect all the like terms. Equation (1-3) reduces to equation (1-4).

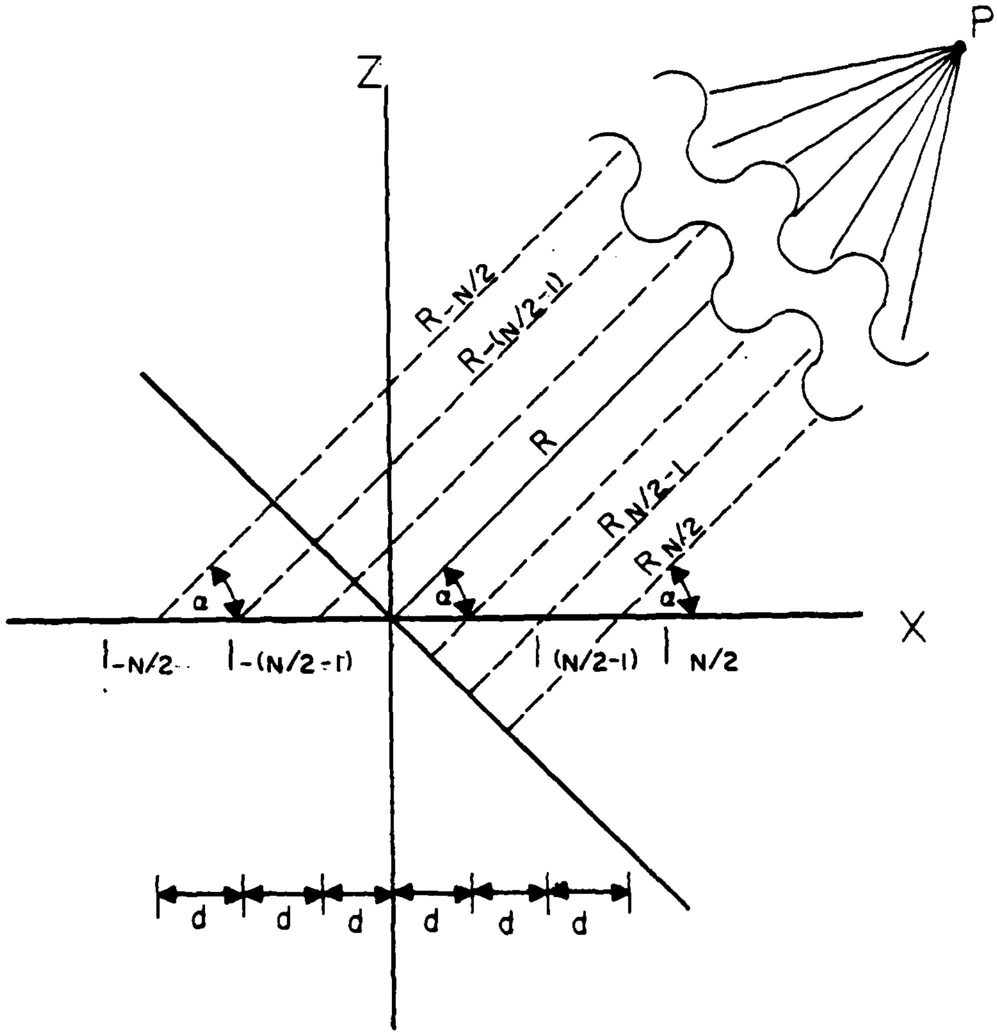

Figure 1-1 N colinear isotropic radiators

$$E = (I_o/4\pi R)\, e^{-j\beta R}\left[\sum_{n=(-N/2)}^{-1} e^{-j\gamma_n} + \sum_{n=1}^{N/2} e^{j\gamma_n}\right] \qquad (1\text{-}4)$$

$$\gamma_n = \beta(2\,|n| - 1)(d/2)\cos\alpha$$

The first term is a constant for a fixed value of "R". The second term is dependent on alpha. It defines the antenna pattern and is the AF. The AF is given in equation (1-5).

$$AF = \sum_{n=(-N/2)}^{N-1} e^{-j\gamma_n} + \sum_{n=1}^{N/2} e^{-j\gamma_n} \qquad (1\text{-}5)$$

Noting that γ_{-n} is equal to γ_n, equation (1-5) can be simplified to equation (1-6).

$$AF = \sum_{n=1}^{N/2} (e^{j\gamma_n} + e^{-j\gamma_n}) = 2\sum_{n=1}^{N/2} \cos\gamma_n = 2\sum_{n=1}^{N/2} \cos[\beta(2n-1)(d/2)\cos\alpha] \qquad (1\text{-}6)$$

Since the 2 in equation (1-6) is a constant, it may be dropped from the array factor. In addition, in equation (1-6) 2n-1 can be replaced with n, and the result simplified to equation (1-7).

$$AF = \sum_{n=1,3,5...}^{n-1} \cos[n\beta(d/2)\cos\alpha] \qquad (1\text{-}7)$$

Equation (1-7) is the array factor for a colinear array of an even number of N isotropic radiators with equal current amplitudes. The angle α is measured from the line of the array to the observation point.

ANTENNA MODELING PROGRAM (AMP) THEORY

The Antenna Modeling Program (AMP) was used to analyze the array element. This program was developed by MBA/Information Systems.[1] The computer program applies the method of moments to the thin wire approximation of the integral equation for the electric field due to a volume current distribution, equation (1-8).[1]

$$E(\bar{r}_o) = \iiint_V i\mu_o \, \omega \bar{J}(\bar{r}) \cdot (\bar{\bar{G}}(\bar{r},\bar{r}_o) d\bar{v} \tag{1-8}$$

$\bar{\bar{G}}(\bar{r},\bar{r}_o) = -(1/4\pi)[\bar{\bar{I}}+(1/k^2)\nabla\nabla]g$

$g = (e^{-ik|\bar{r}-\bar{r}_o|} / |\bar{r}-\bar{r}_o|)$

$k = \omega\sqrt{\mu_o\varepsilon_o}$, $\bar{\bar{I}}$ = unit 2nd rank tensor

$|\bar{r}-\bar{r}_o|$ = distance measured from wire axis (source point) to observation point on the surface.

The thin wire approximation requires that the diameter of the wire be small compared with the wavelength. Thus azimuthel current flow around the wire can be neglected and the volume integral in equation (1-8) can be changed to a line integral, equation (1-9).[1]

$$-\hat{s}_o \cdot \bar{E}^I(\bar{r}_o) = (-i\omega\mu_o/4\pi) \int_L I(s)[\hat{s}\cdot\hat{s}_o-(1/k^2)\ (\partial^2/\partial s\partial s_o]g(\bar{r},\bar{r}_o)ds \tag{1-9}$$

$\hat{s}$ = unit tangent at source point

$\hat{s}_o$ = unit tangent at observation point

$I = (\pi a^2 J)2\pi a$

a = wire radius

Included in equation (1-9) is also the boundary condition for a metal surface, equation (1-10).

$$E^{I}_{tan} + E^{s}_{tan} = 0 \qquad (1\text{-}10)$$

E^{I}_{tan} = Tangential component of incident electric field

E^{s}_{tan} = Tangential component of scattered electric field

AMP solves equation (1-9) numerically by converting it into matrix form. This is accomplished by expanding the unknown currents, I, in terms of a set of basis functions, I_n, and taking the inner product of both sides of equation (1-9) with a set of weighting functions w_m. A general discussion on this method of solution can be found in reference (3).

Equation (1-11) is obtained by expressing equation (1-9) in operational format, where the operator L_{op} denotes the integral and "<A,B>" denotes the inner product of quantities A and B.

$$\sum_{n}^{N} A_n \langle w_m, L_{op}\ I_n\rangle = \langle w_m, E^{I}\rangle \qquad (1\text{-}11)$$

$$\text{where } I = \sum_{n}^{N} A_n\ I_n$$

Equation (1-11) must be true for each w_m, and thus may be written in matrix form as expressed in equation (1-12).

$$\begin{bmatrix} \langle w_1, L_{op}\ I_1\rangle & \langle w_1, L_{op}\ I_2\rangle & \ldots\langle w_1, L_{op}\ I_n\rangle \\ \langle w_2, L_{op}\ I_1\rangle & \langle w_2, L_{op}\ I_2\rangle & \ldots\langle w_2, L_{op}\ I_n\rangle \\ '' & '' & '' \\ '' & '' & '' \\ '' & '' & '' \\ '' & '' & '' \\ \langle w_N, L_{op}\ I_1\rangle & \langle w_N, L_{op}\ I_2\rangle & \ldots\langle w_N, L_{op}\ I_N\rangle \end{bmatrix} \begin{bmatrix} A_1 \\ A_2 \\ '' \\ '' \\ '' \\ '' \\ A_N \end{bmatrix} = \begin{bmatrix} \langle w_1, E^{I}\rangle \\ \langle w_2, E^{I}\rangle \\ '' \\ '' \\ '' \\ '' \\ \langle w_N, E^{I}\rangle \end{bmatrix}$$

(1-12)

Since E^I, I_n and w_m are known, by matrix inversion the values of A_n can be calculated.

Specifically, AMP uses sine and cosine functions as basis functions and employs a method of collocation, or point matching, by choosing the weighting functions as δ functions.

THEORY APPLIED TO A.O. ARRAY

To apply the techniques of AMP and pattern multiplication to the A.O. heating array, the array's physical characteristics must be known.* The HF antenna consists of a 4x8 array of radiating elements. This array is oriented as shown in figure (1-2). Each of the elements in the array is constructed in the shape of an inverted pyramid with four sides. The faces of the pyramid are at an angle of 45° with the ground and contain two nonplanar log-periodic antennas (NLPA). One NLPA is contained in the north and south faces, and the other is contained in the east and west faces. A sketch of an array element is shown in figure (1-3). Note that the elements in the south and west faces have been rotated 180° about the corresponding face's NLPA elements feed lines. A diagram looking down at the top elements of the pyramid is shown in figure (1-4).

Both NLPAS are designed with a τ of .88. The dimensions of the array elements in the north and south faces are shown in figure (1-5). The dimensions of the east and west faces are scaled to $\tau^{1/4}$ of the north and south faces. This will result in right hand circular polarization radiation when the north and south faces are fed 180° out

*Note: See appendix III for additional information on HF antenna geometry.

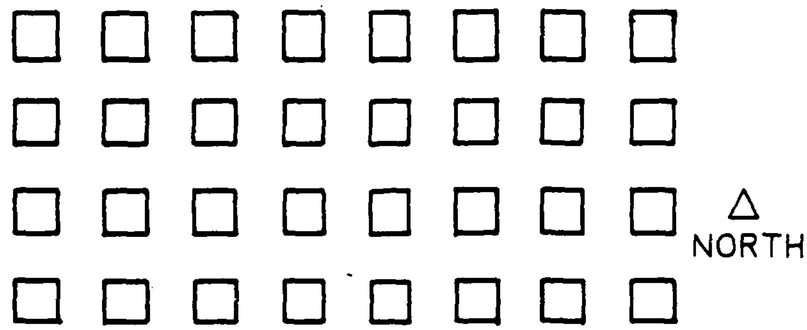

Figure 1-2 HF heating array

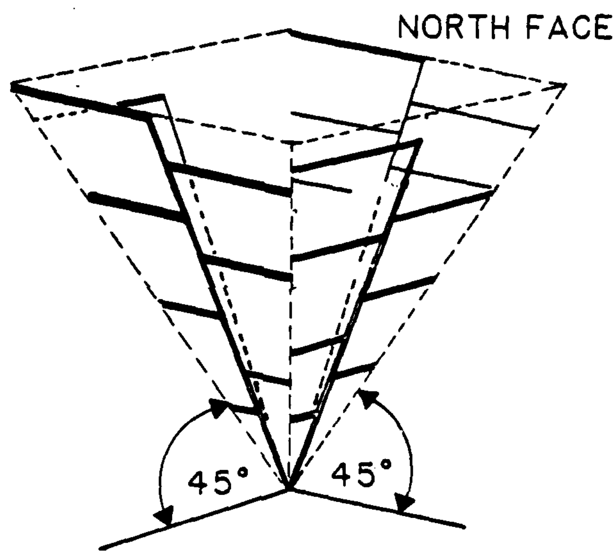

Figure 1-3 HF heating array element

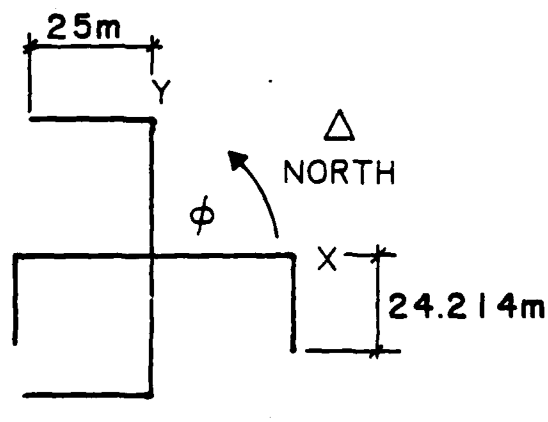

Figure 1-4 View of top elements looking down at pyramid

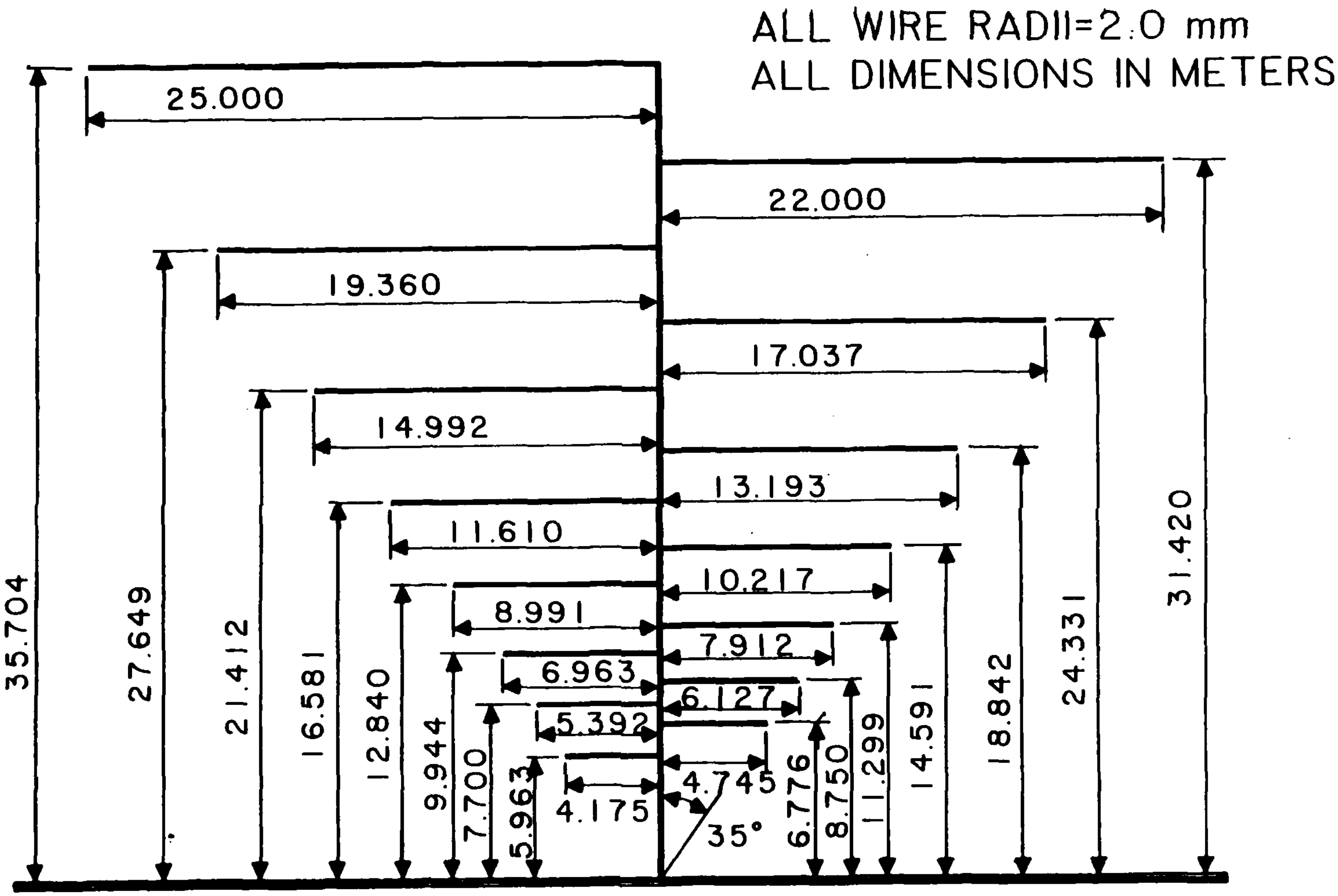

Figure 1-5 Non-planar log-periodic antenna semi-structure dimensions

of phase with the east and west faces. When fed in phase, left hand circular polarization radiation will be transmitted.[4] The north and south and the east and west faces are fed against ground by separate transmitters. This gives the capability to adjust the phase between different faces and thus change the radiation polarization.

The array element was analyzed using the AMP computer program. Then the pattern multiplication technique was used to calculate the total array pattern.

The array element was analyzed using AMP for frequencies of 3.17 MHz and 5.1 MHz. The data file used is listed in Appendix I program 1. The GW and GM cards generate the antenna structure depicted in figure (1-3) and orient it with respect to the coordinate axis shown in figure (1-4). The GN card specified the conductivity (.03 ℧/m) and relative permativity (20) of the ground below the HF array. The actual conductivity and permativity for the heater site was not known, but based on the fact that maps indicate the heater array is located on marshy ground, a conductivity and a relative permativity for "good" earth[5] were used. As shown in the RP card, the power gain was computed for 2.5 degree steps in "theta" and 5 degree steps in "phi."

In order to use the output of AMP in the pattern multiplication, it was necessary to develop an elemental pattern function. Given a "theta" and "phi", the function returns a value of the power gain in that direction. To accomplish this, the power gains form the AMP output for selected constant "phi" surfaces were combined with a linear interpolation scheme. The selected values of "phi" are listed in table I.

Figures (1-6) and (1-7) show the comparison of the interpolated values (shown by X) with the AMP results (shown by ·). The maximum error is approximately one db. Figure (1-6) is a plot of power gain as a function of "phi" for a constant "theta." The power gain decreases as the radius of the polar plot increases. The unsymmetrical nature of the plot is due to the unsymmetrical nature of the array element. Figure (1-7) is a plot of power gain as a function of "theta" for a constant "phi."

3.17 MHz Phi (deg)	5.1 MHz Phi (deg)
0	10
90	60
130	90
180	110
210	150
270	180
320	215
360	270
	320

Table I. Selected Values of Phi for Interpolation Routines

The total array pattern for the A.O. array shown in figure (1-1) was calculated by taking the product of two separate array factors. In essence this is a pattern multiplication. The array pattern of one array becomes the elemental pattern of the other array. One array is the 4-element array on the north and south line. The other array is an 8-element array on an east and west line.

The expansion of equation (1-7) for the 4-element and 8-element arrays can be simplified by using trigonometric identities. These trigonometric identities were obtained from Chebysheff polynomials, as shown in Appendix II. The simplified equation for the antenna factors are given in equations (1-13) and (1-14). The 4-element array factor

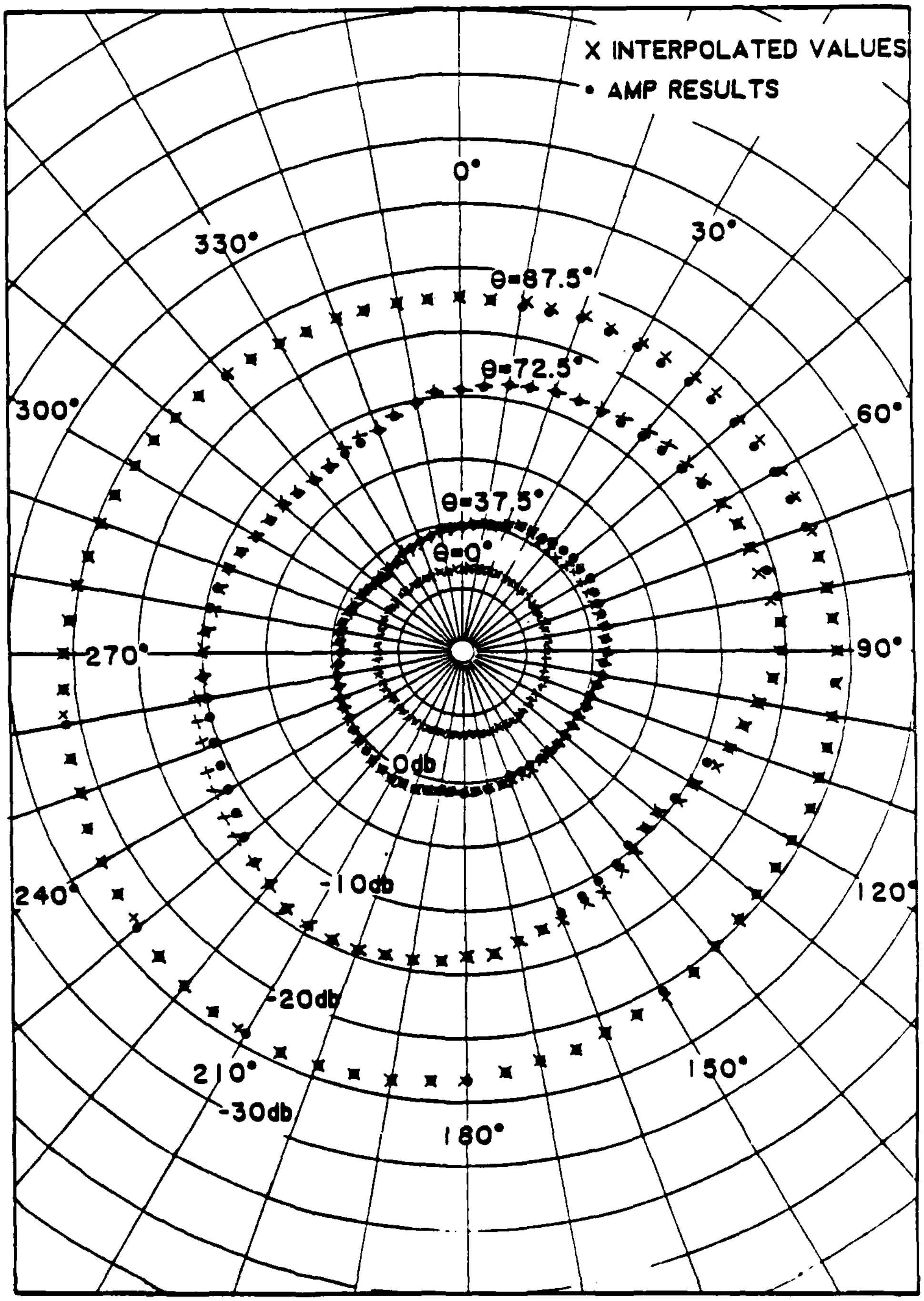

Figure 1-6a Power gain vs. phi for a constant theta, 3.17 MHz

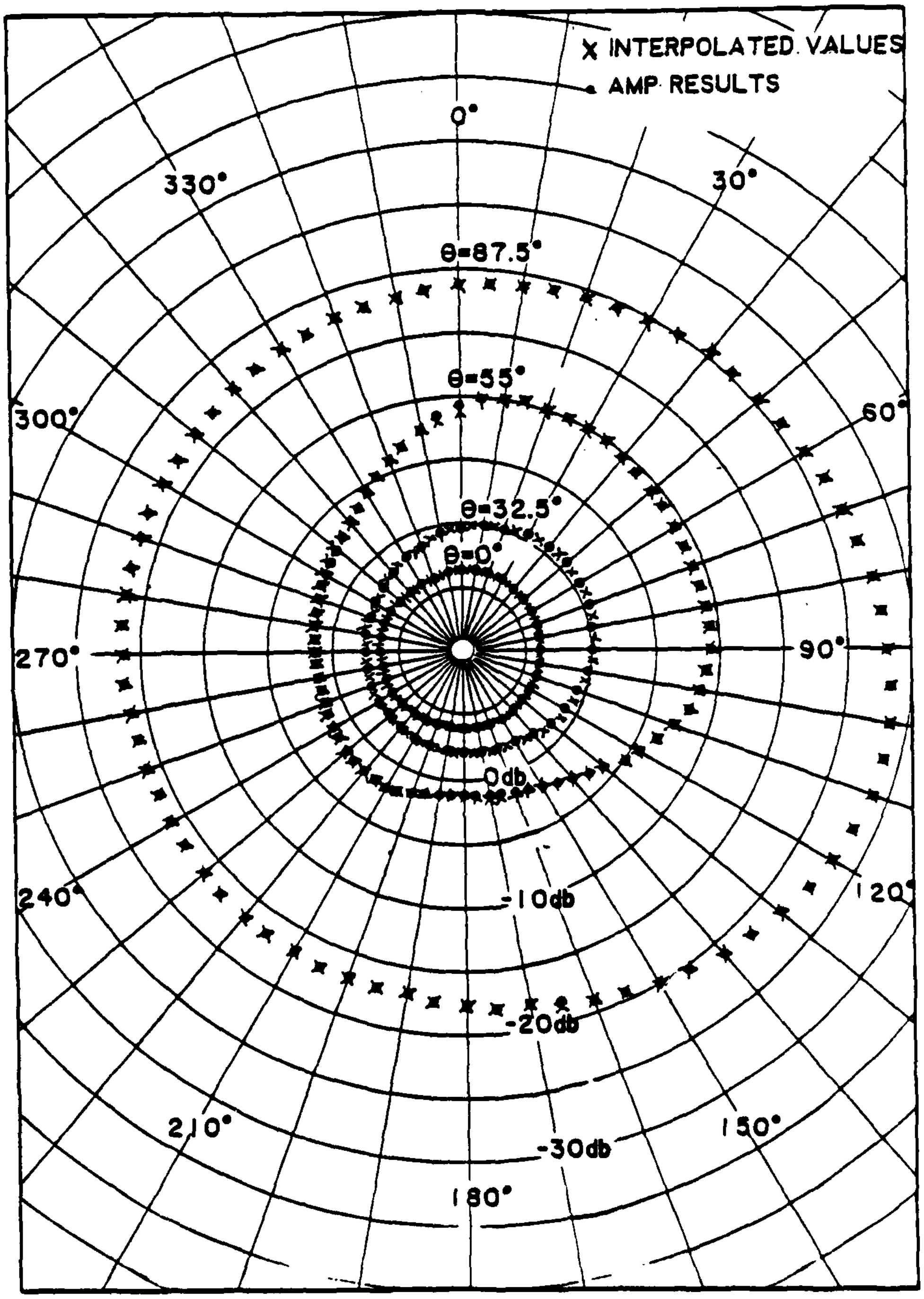

Figure 1-6b Power gain vs. phi for a constant theta, 5.1 MHz

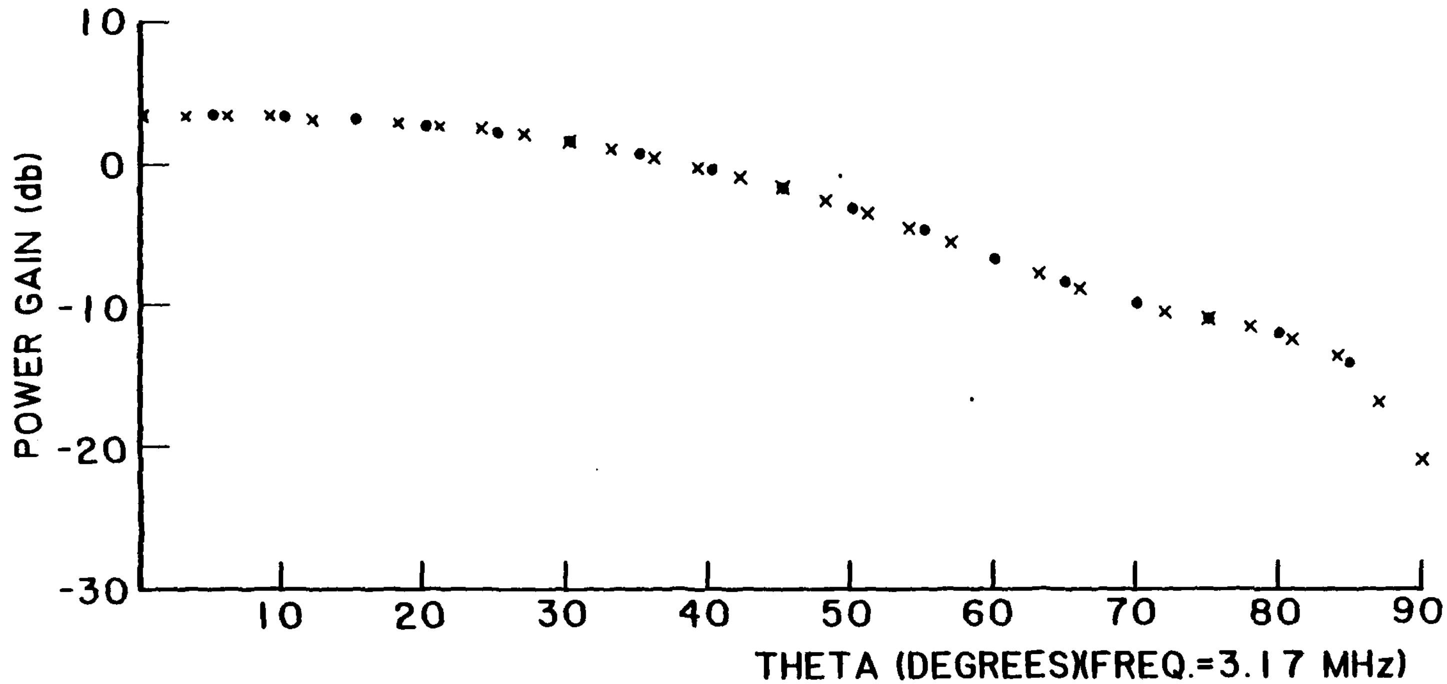

Figure 1-7a.1 Power gain vs. theta for phi $=0^{\circ}$, 3.17 MHz

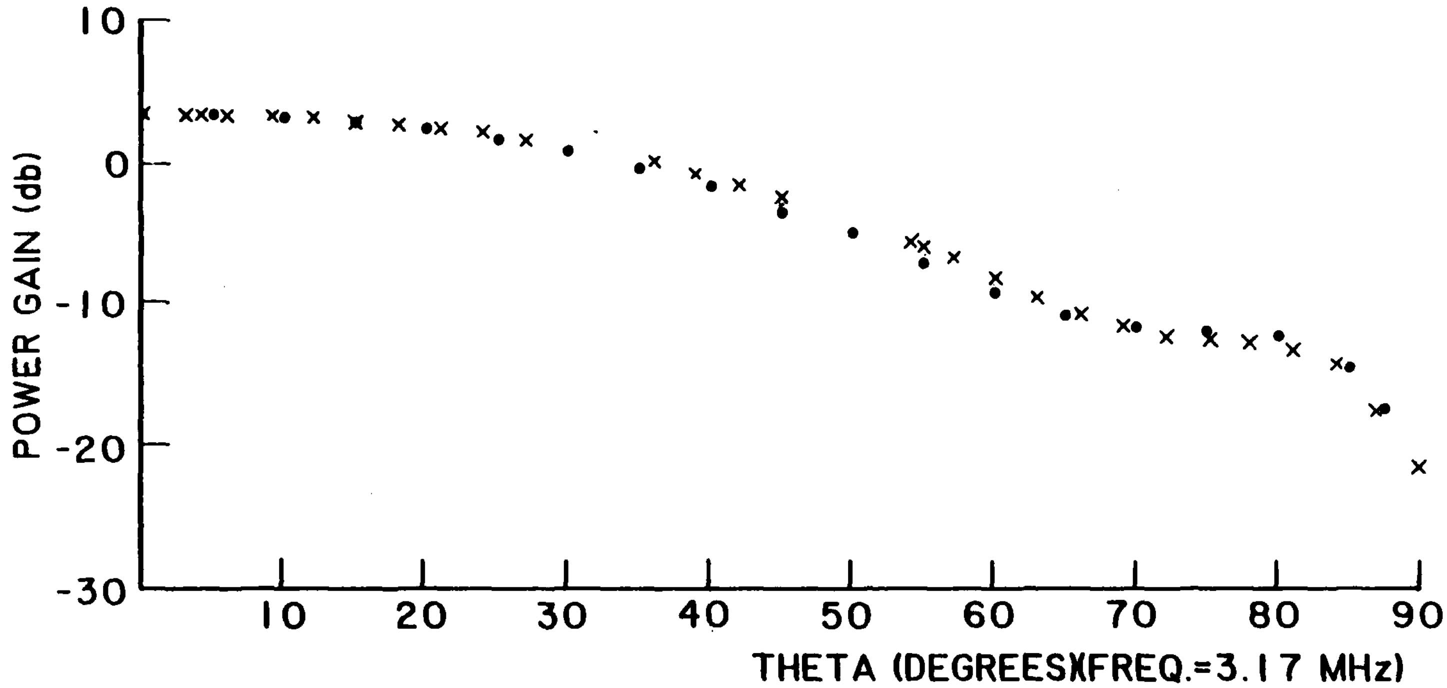

Figure 1-7a.2 Power gain vs. theta for phi=40°, 3.17 MHz

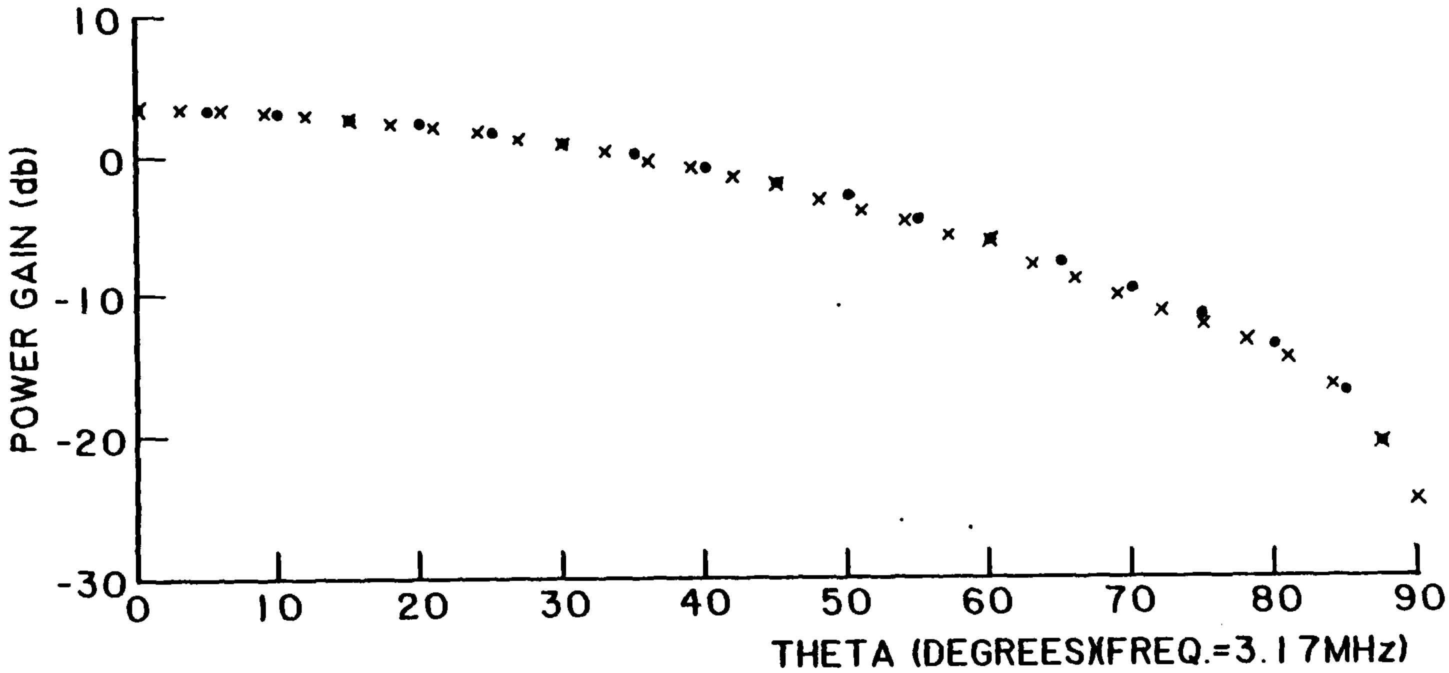

Figure 1-7a.3 Power gain vs. theta for phi=150°, 3.17 MHz

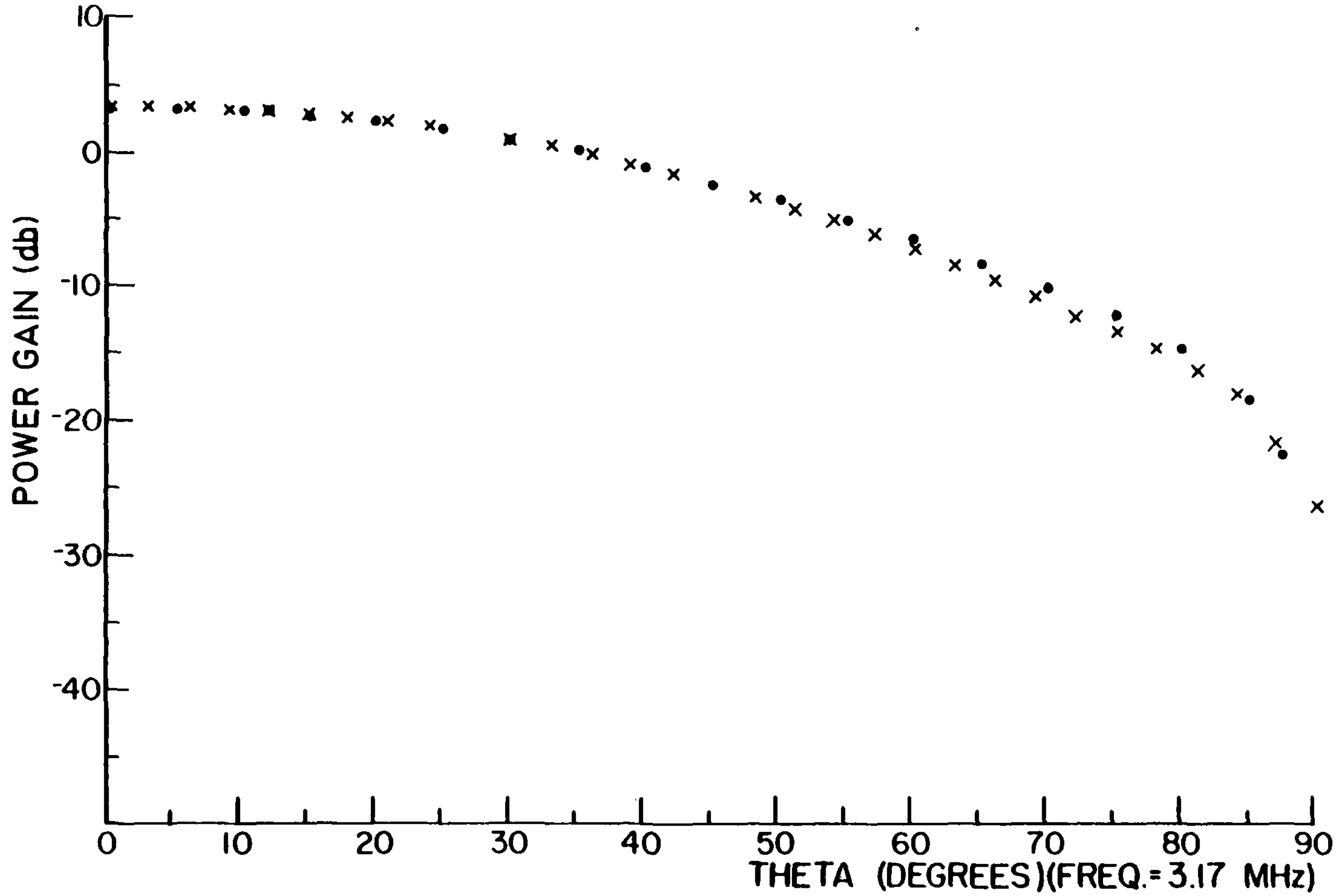

Figure 1-7a.4 Power gain vs. theta for phi=240°, 3.17 MHz

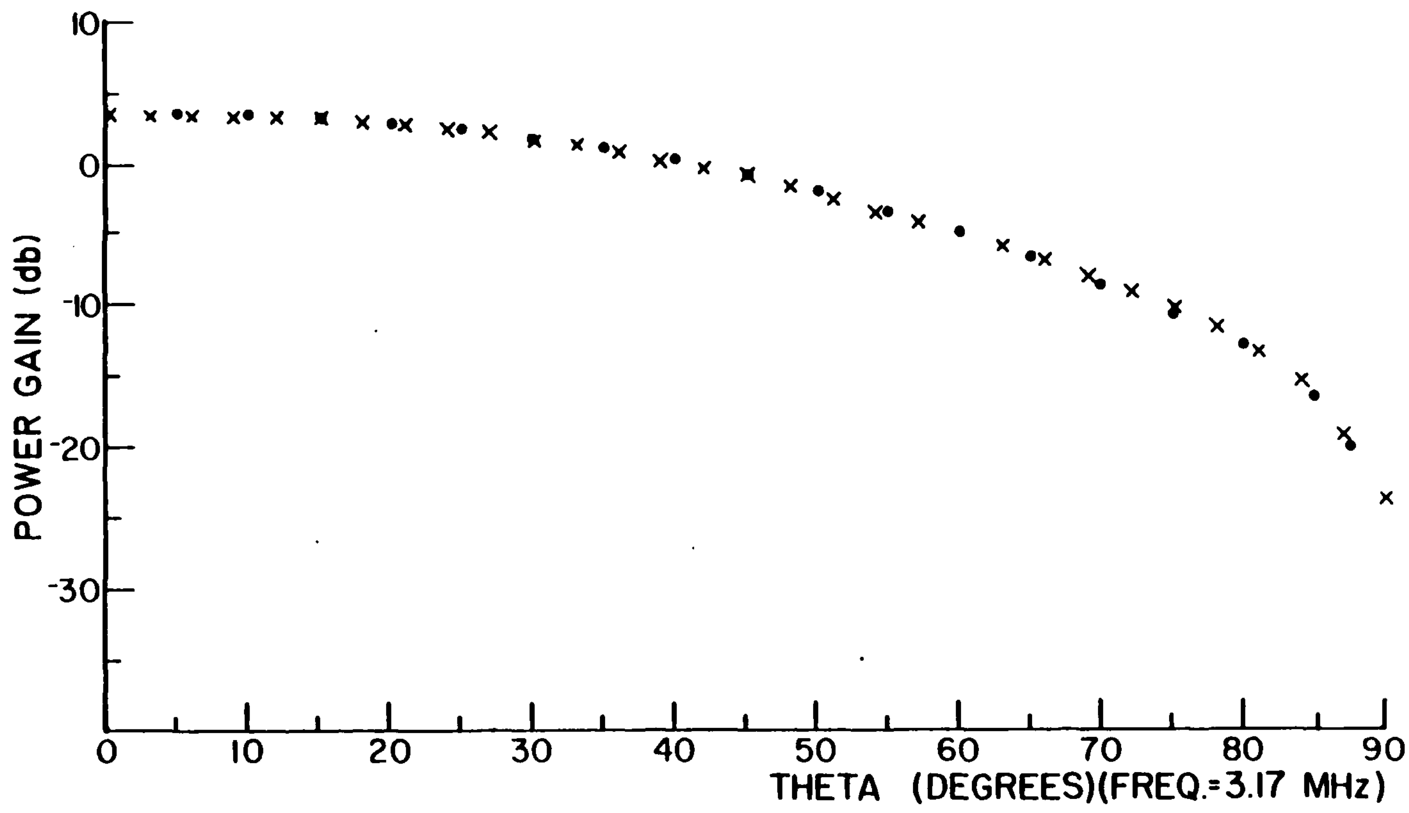

Figure 1-7a.5 Power gain vs. theta for phi=280^{o}, 3.17 MHz

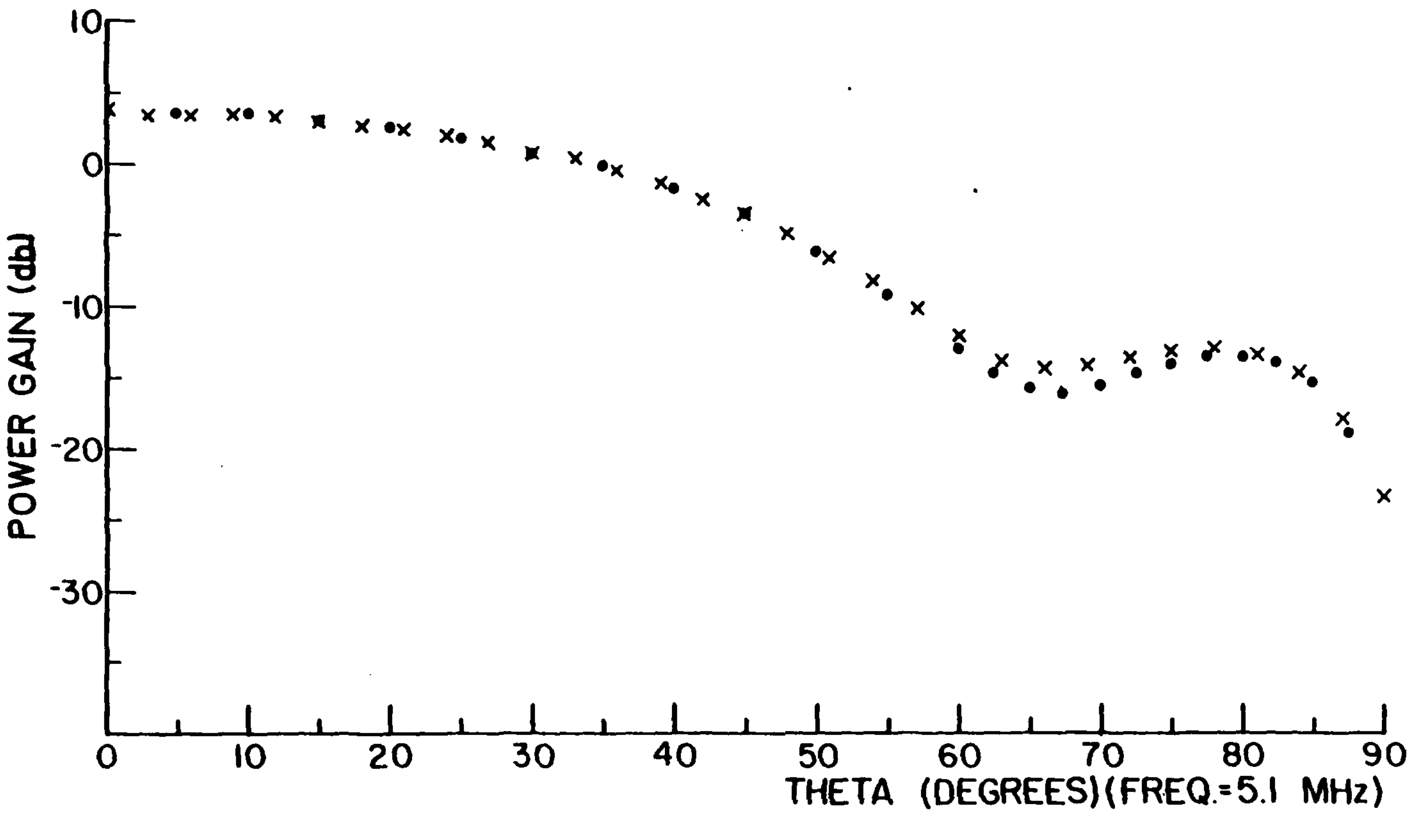

Figure 1-7b.1 Power gain vs. theta for phi=0^{o}, 5.1 MHz

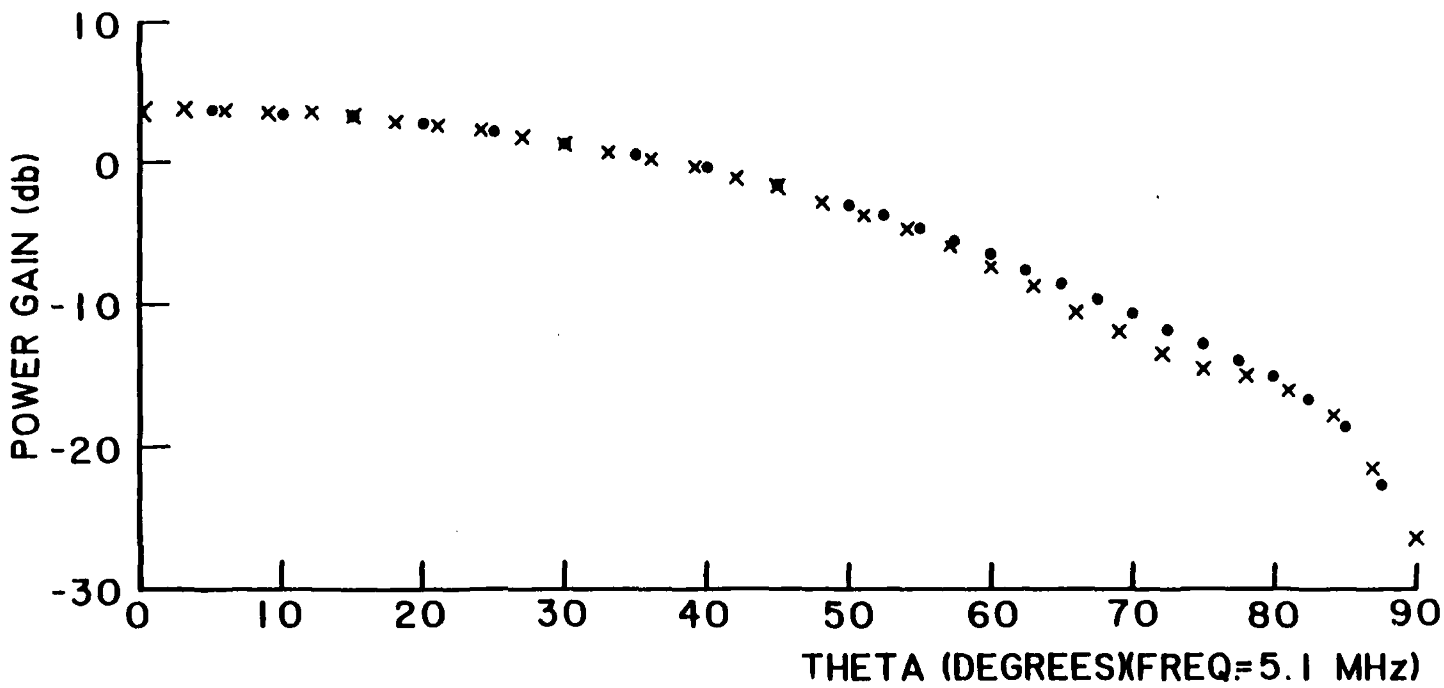

Figure 1-7b.2 Power gain vs. theta for phi=130°, 5.1 Mhz

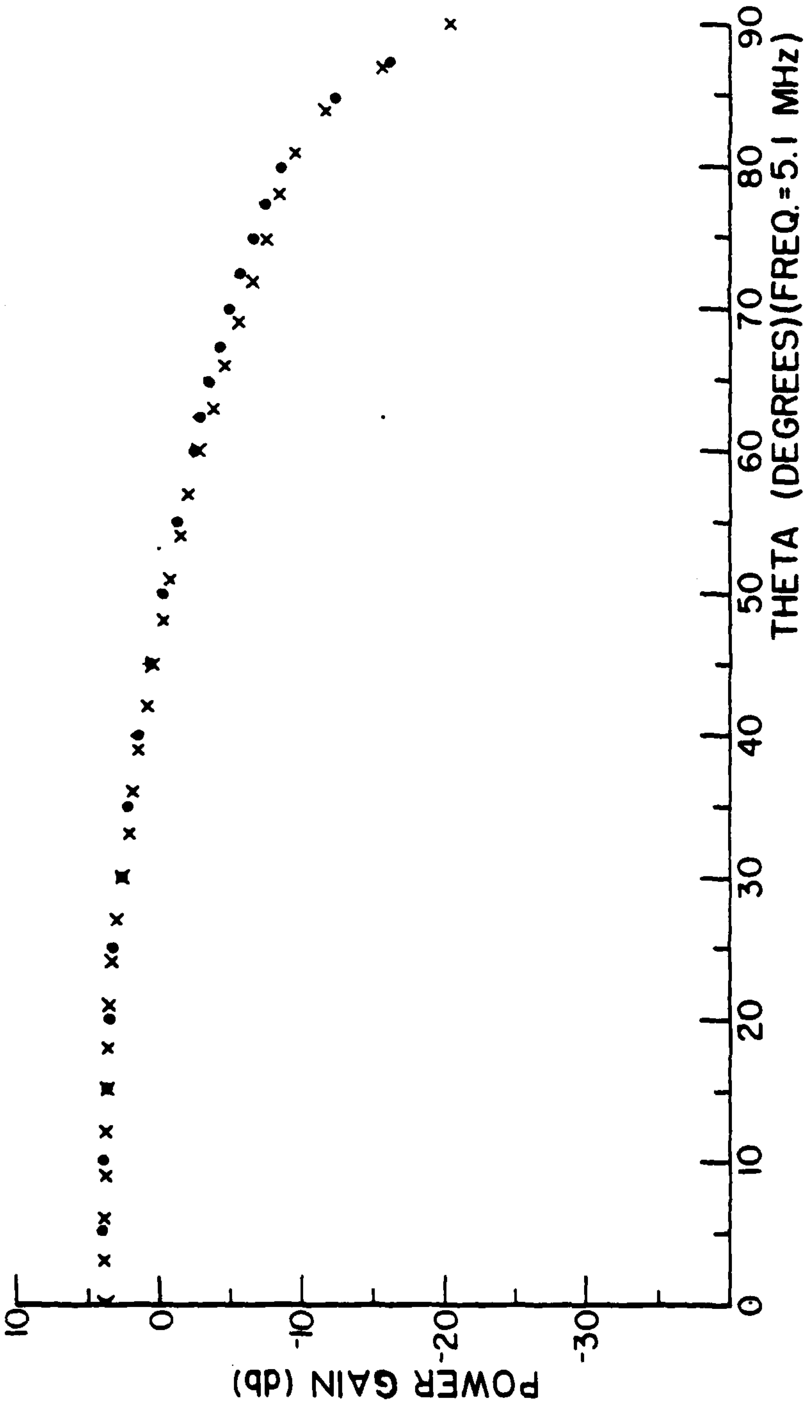

Figure 1-7b.3 Power gain vs. theta for phi=250^{o}, 5.1 Mhz

is equation (1-13), and the 8-element array factor is equation (1-14). Figure (1-8) shows the orientation of the 4- and 8-element arrays on an X,Y,Z coordiate system. The Y-axis was taken to be north and the X-axis as east.

$$AF_1 = [\sin(4\beta(d/2)\cos\xi_1]/\sin(\beta(d/2)\cos\xi_1) \qquad (1\text{-}13)$$

$$AF_2 = [\sin(8\beta(d/2)\cos\xi_2)]/\sin(\beta(d/2)\cos\xi_2) \qquad (1\text{-}14)$$

The array pattern of the 8-element array is solid of revolution about the X-axis, and the 4-element array pattern is a solid of revolution about the Y-axis.

Using the transformation in equation (1-15), AF_1 and AF_2 can be transformed to spherical coordinates. The total array factor AF, equation (1-16), is the product of AF_1 and AF_2.

$$\begin{aligned}\cos\xi_1 &= \sin\Theta\sin\phi \\ \cos\xi_2 &= \sin\Theta\cos\phi\end{aligned} \qquad (1\text{-}15)$$

$$AF = AF_1 \times AF_2 = \frac{\sin[4\beta(d/2)\sin\Theta\sin\phi]}{\sin[\beta(d/2)\sin\Theta\sin\phi]}\ \frac{\sin[8\beta(d/2)\sin\Theta\cos\phi]}{\sin[\beta(d/2)\sin\Theta\cos\phi]} \qquad (1\text{-}16)$$

The total array power pattern can be calculated by taking the square of the total array factor, AF, and multiplying it by the elemental pattern function, which is an interpolation of the AMP results. To achieve the goal of the calculation of a directive gain pattern, a correction factor must be determined. This factor is a result of neglecting the constants in calculating the array factor.

The directive gain "in a given direction is defined as the ratio of the radiation intensity in that direction to the average radiated power."[5] Since the constants which were neglected in calculating AF are also contained in the calculation of the average radiated power

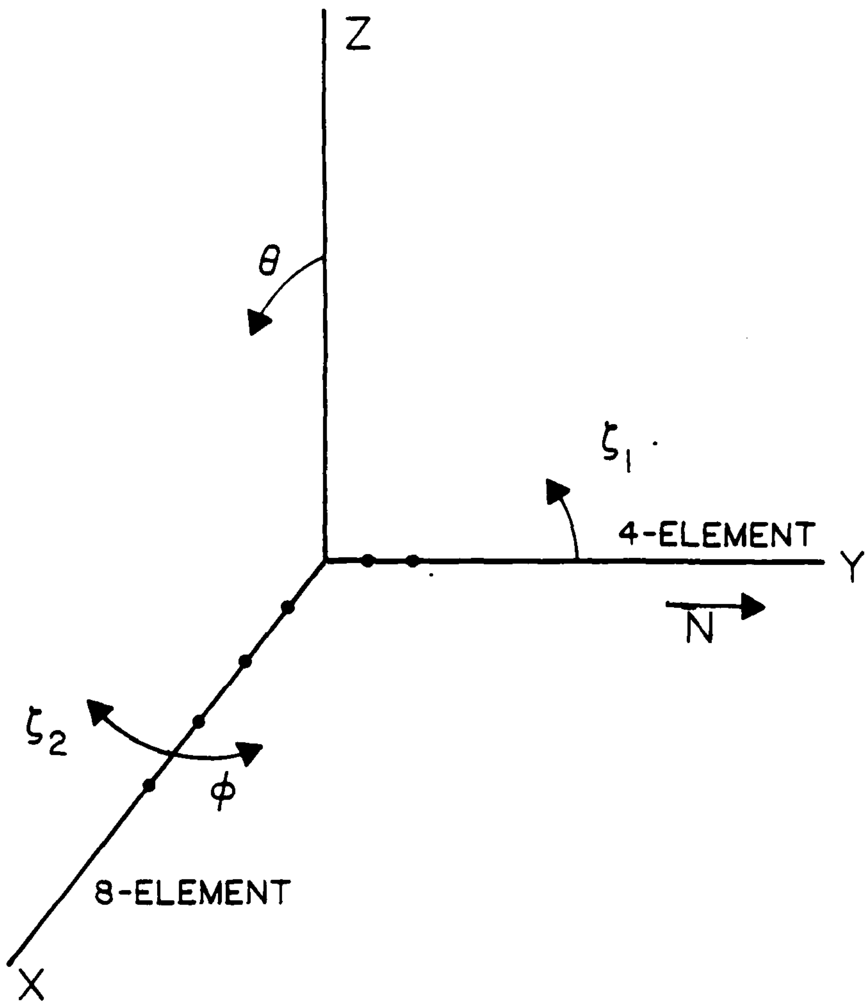

Figure 1-8 Orientation of 4- and 8-element arrays

and the directive gain is a ratio, these same constants must also be neglected in calculation of the average radiated power. Thus the calculation of the average radiated power becomes the correction factor necessary to convert the array power pattern to an array directivity pattern.

Equation (1-17) was used to calculate the average radiated power, W_r.

$$W_r = \int_0^{2\pi}\int_0^{\pi/2} \frac{[AF(\Theta,\phi)]^2 \text{ X } 10^{(ELF(\Theta,\phi)/10)} \sin\Theta \, d\Theta \, d\phi}{4\pi} \qquad (1\text{-}17)$$

$ELF(\Theta, \phi)$ = Elemental Power gain from interpolated AMP output
$AF(\Theta, \phi)$ = Total Array Factor

The integration was performed numerically using Simpson integration, equation[6] (1-18). The programs are given in Appendix I, programs 2 and 3.

$$\int_a^b f(x)dx = (\Delta x/3)\ [f(x_o)+4f(x_1)+2f(x_2)+4f(x_3)+2f(x_4)+\ldots \qquad (1\text{-}18)$$
$$+2f(x_{2n-2})+4f(x_{2n-1})+f(x_{2n})]$$

$\Delta x = (b-a)/(2n)$

The first quardrant integration was carried out for two cases. One case was with a "phi" step size of 2.5 degrees; the other case was with a "phi" step size of 1 degree. A "theta" step size of 1 degree was used in both cases. No significant difference was found in the result of the integrations. Based on this result, the step sizes chosen for the total integral were 1 degree and 2.5 degrees for "theta" and "phi" respectively. The correction factors determined were 9.82 db and 8.62 db for 5.1 MHz and 3.17 MHz respectively.

Equation (1-19) combines the total array factor AF, the elemental pattern ELF, and the correction factor to calculate the directive gain pattern for the A.O. heating array.

$$D(\Theta,\phi) = 20 \log[AF(\Theta,\phi)] + ELF(\Theta,\phi) - \text{Correction factor} \qquad (1\text{-}19)$$

Figure (1-9) is a plot of the pattern in the "phi" equal zero plane (north-south plane). The "x's" are experimentally measured values.[7] The values were measured from a Boeing 707 aircraft at 2900 ft (8.84 km). The plane was flown over the A.O. array on a north-south line, while the heater was operating at 5.1 MHz. The plot shows that the array pattern obtained by the combination of pattern multiplication and numerical techniques is a good approximation of the A.O. array pattern.

Figures (1-10) and (1-11) are plots of the directivity pattern of the A.O. heater array for 3.17 MHz and 5.1 MHz respectively. Each plot is the variation of the directive gain with "theta" in a constant "phi" plane. "Phi" is varied in 5 degree steps from 0 degrees to 180 degrees. Two additional "phi" plane patterns have been plotted in figures (1-12) and (1-13). These two figures are the directivity patterns in the "phi" equal 121.5^{o} and 146^{o} planes respectively. These patterns are in planes corresponding to the direction of Los Canos and the A.O., respectively. The programs used to make the directivity patterns are given in Appendix I, programs 4 and 5 for 3.17 MHz and 5.1 MHz respectively.

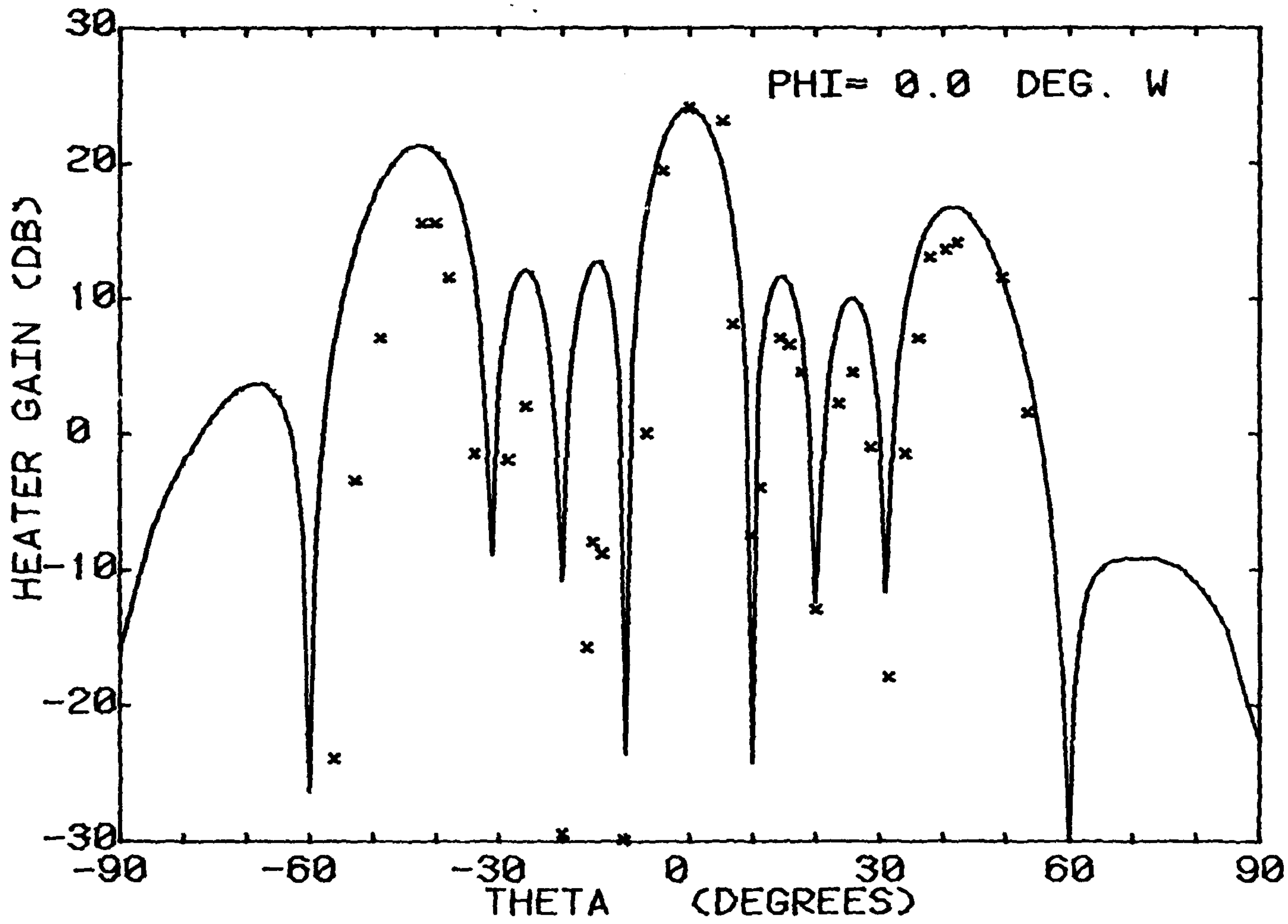

Figure 1-9 Comparison of experimental and theoretical patterns

Figure 1-10 Directive gain pattern for Arecibo Observatory HF heating array. Frequency = 3.17 MHz.

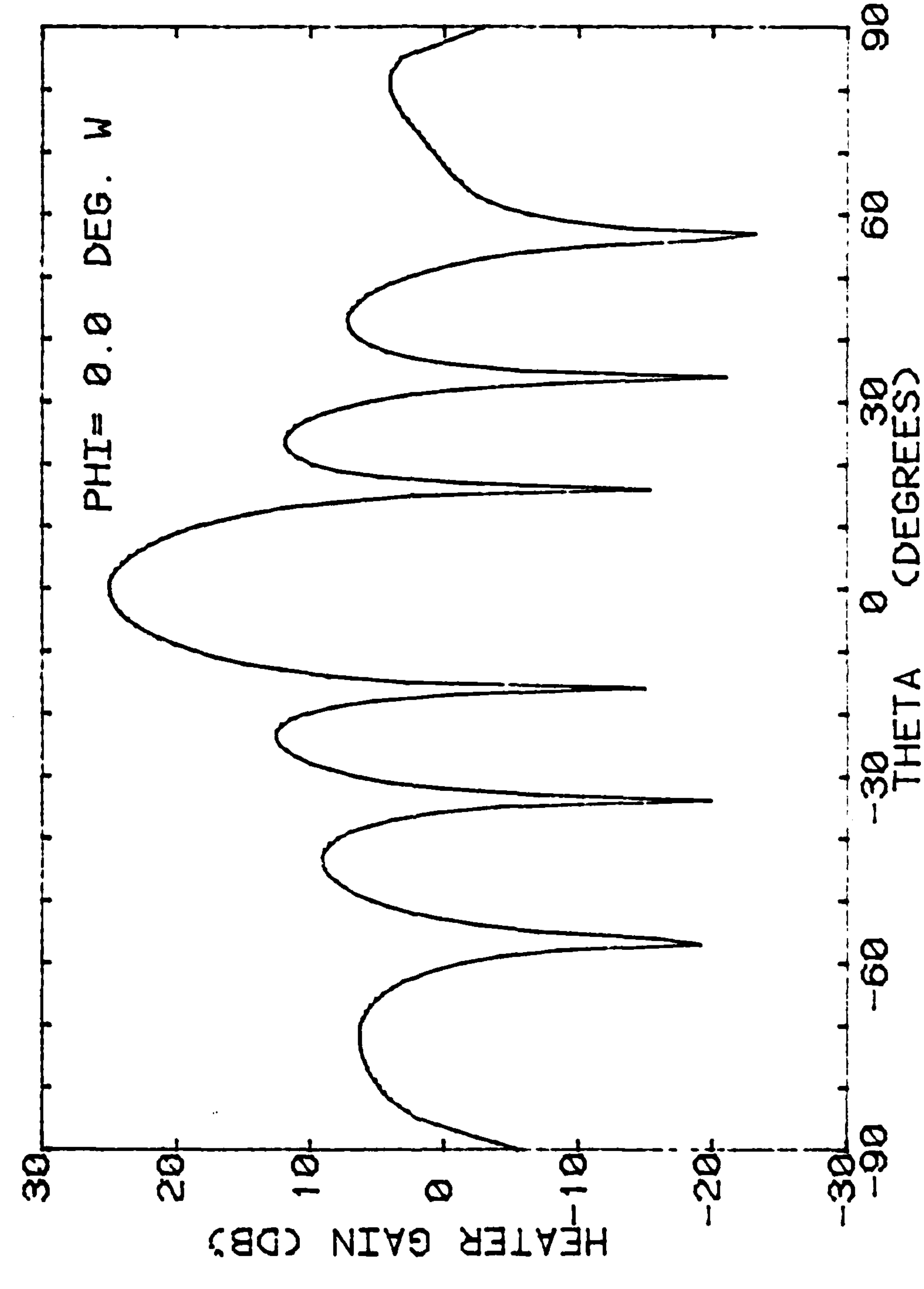
PHI= 0.0 DEG. W
HEATER GAIN (DB)
30
20
10
0
-10
-20
-30
THETA (DEGREES)
-90
-60
-30
0
30
60
90

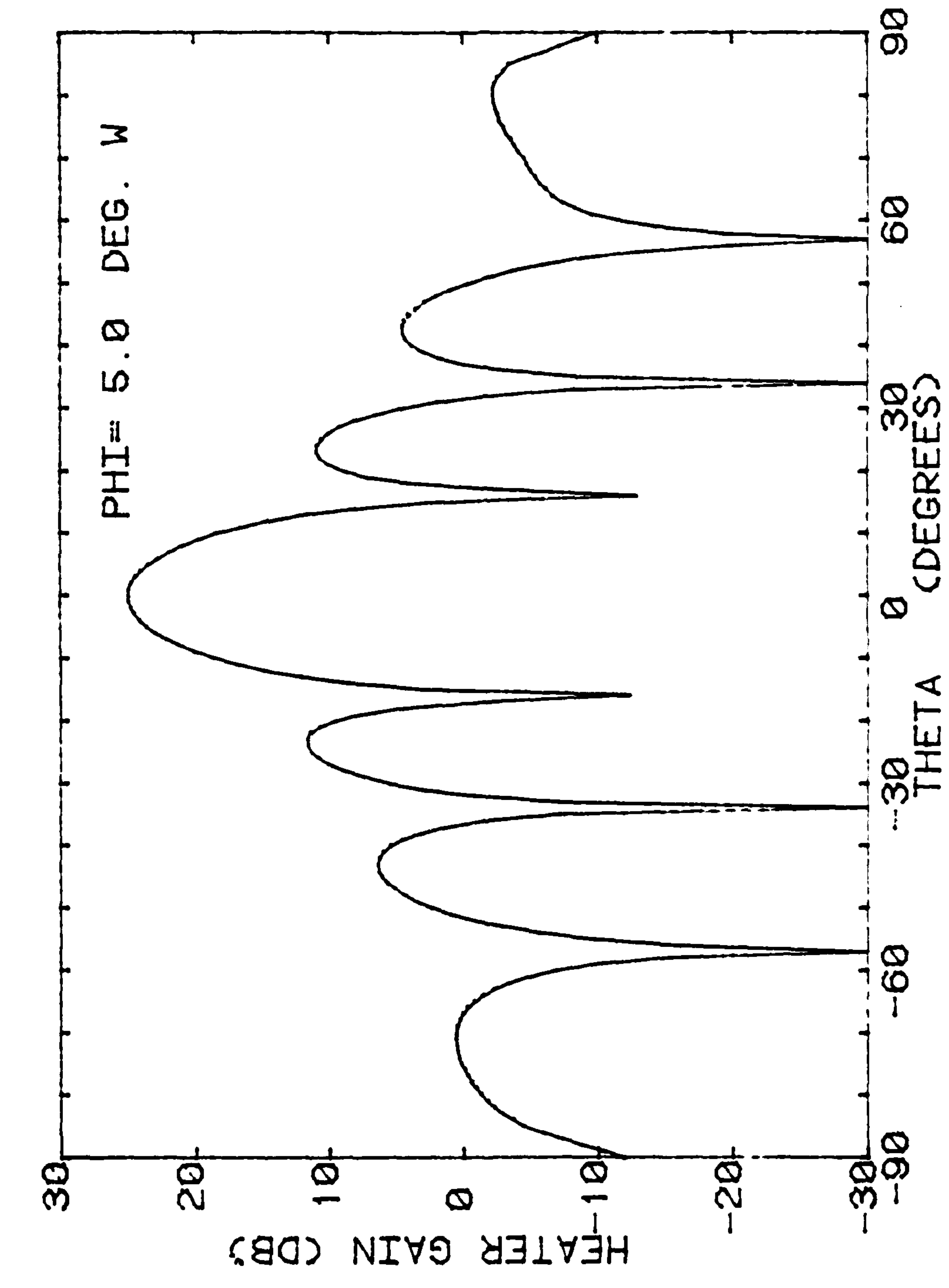
PHI= 5.0 DEG. W
HEATER GAIN (DB)
30
20
10
0
-10
-20
-30
-90
-60
-30
0
30
60
90
THETA (DEGREES)

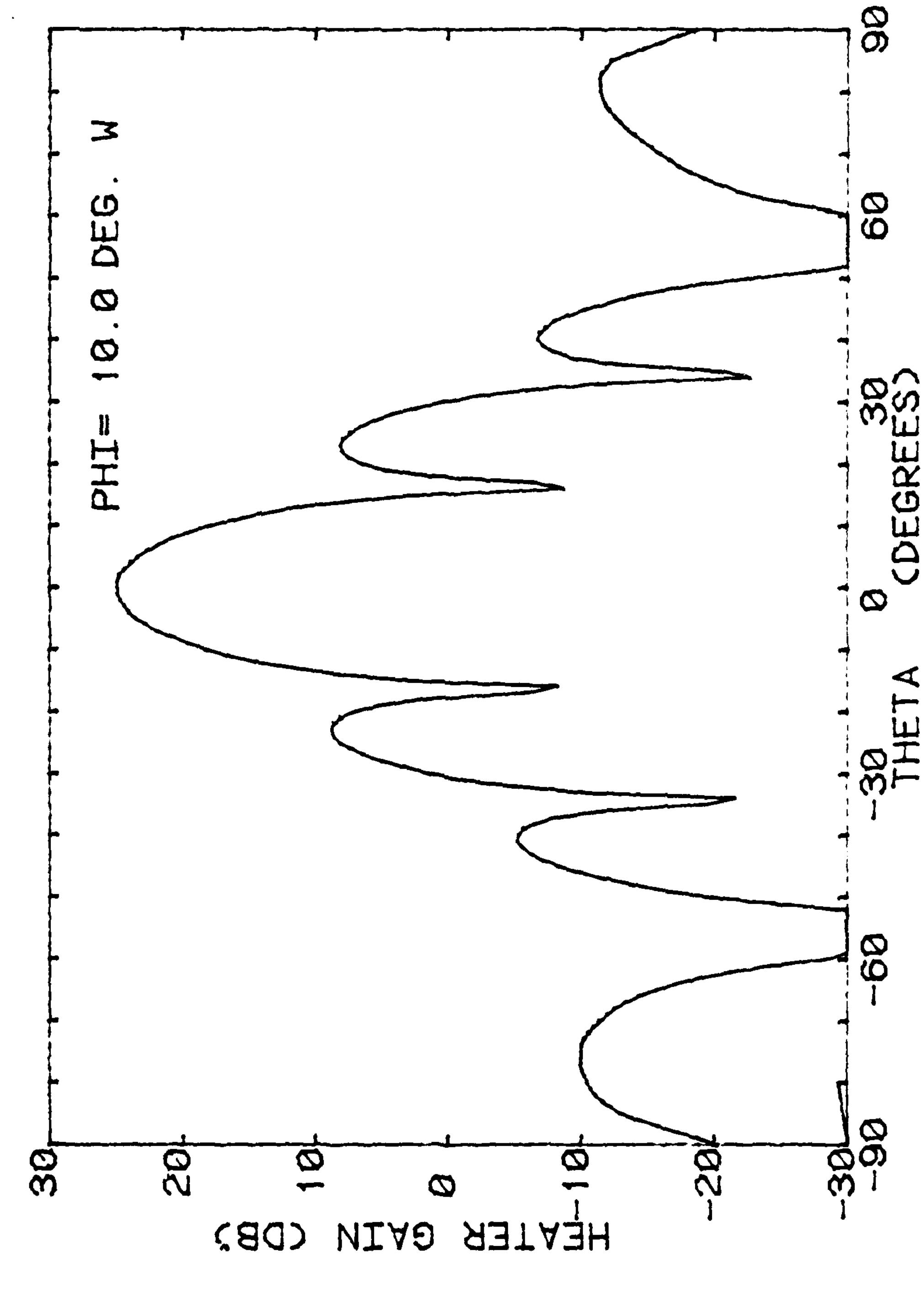
PHI= 10.0 DEG. W
HEATER GAIN (DB)
30
20
10
0
-10
-20
-30
-90
-60
-30
0
30
60
90
THETA (DEGREES)

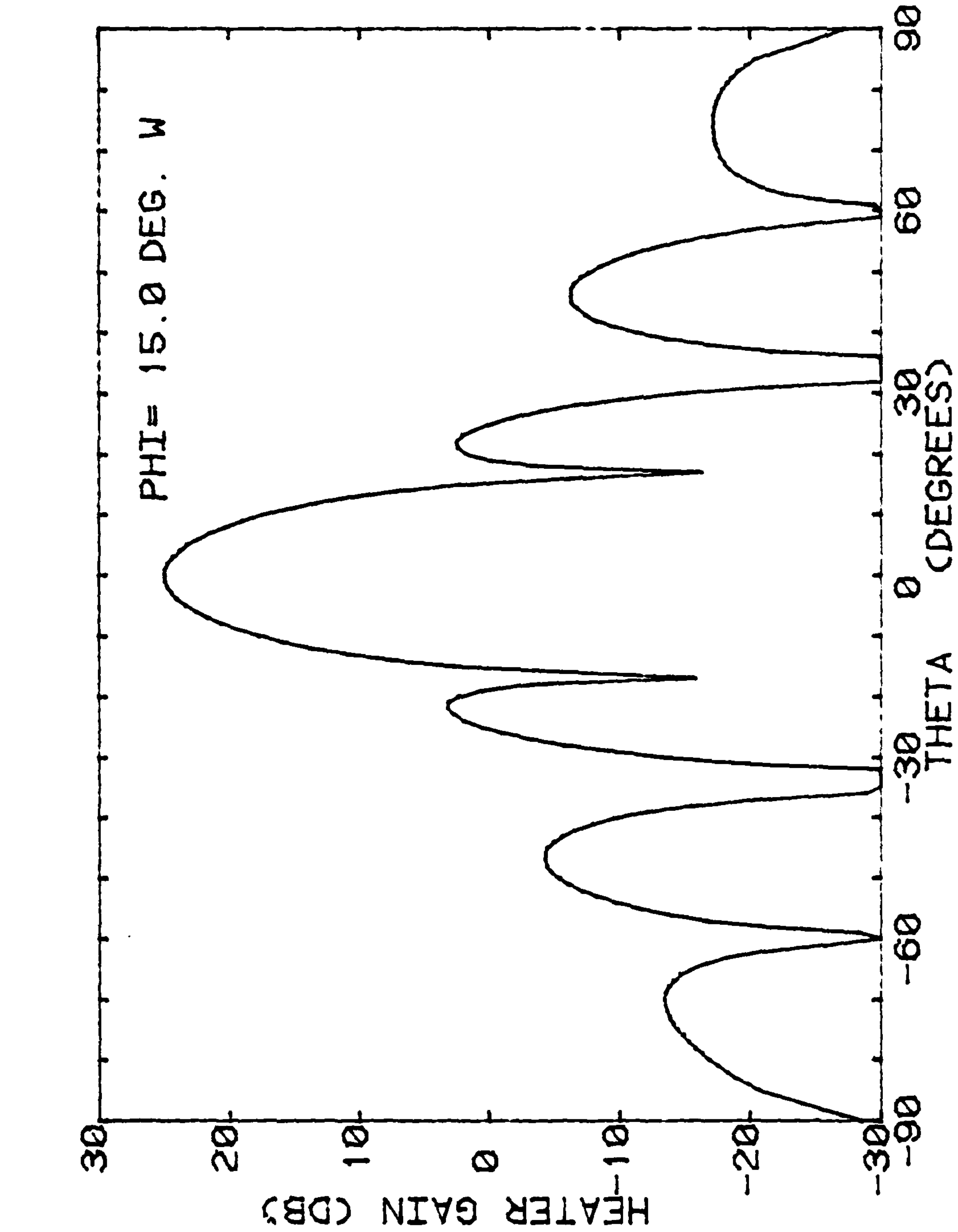
PHI= 15.0 DEG. W
HEATER GAIN (DB)
THETA (DEGREES)
30
20
10
0
-10
-20
-30
-90
-60
-30
0
30
60
90

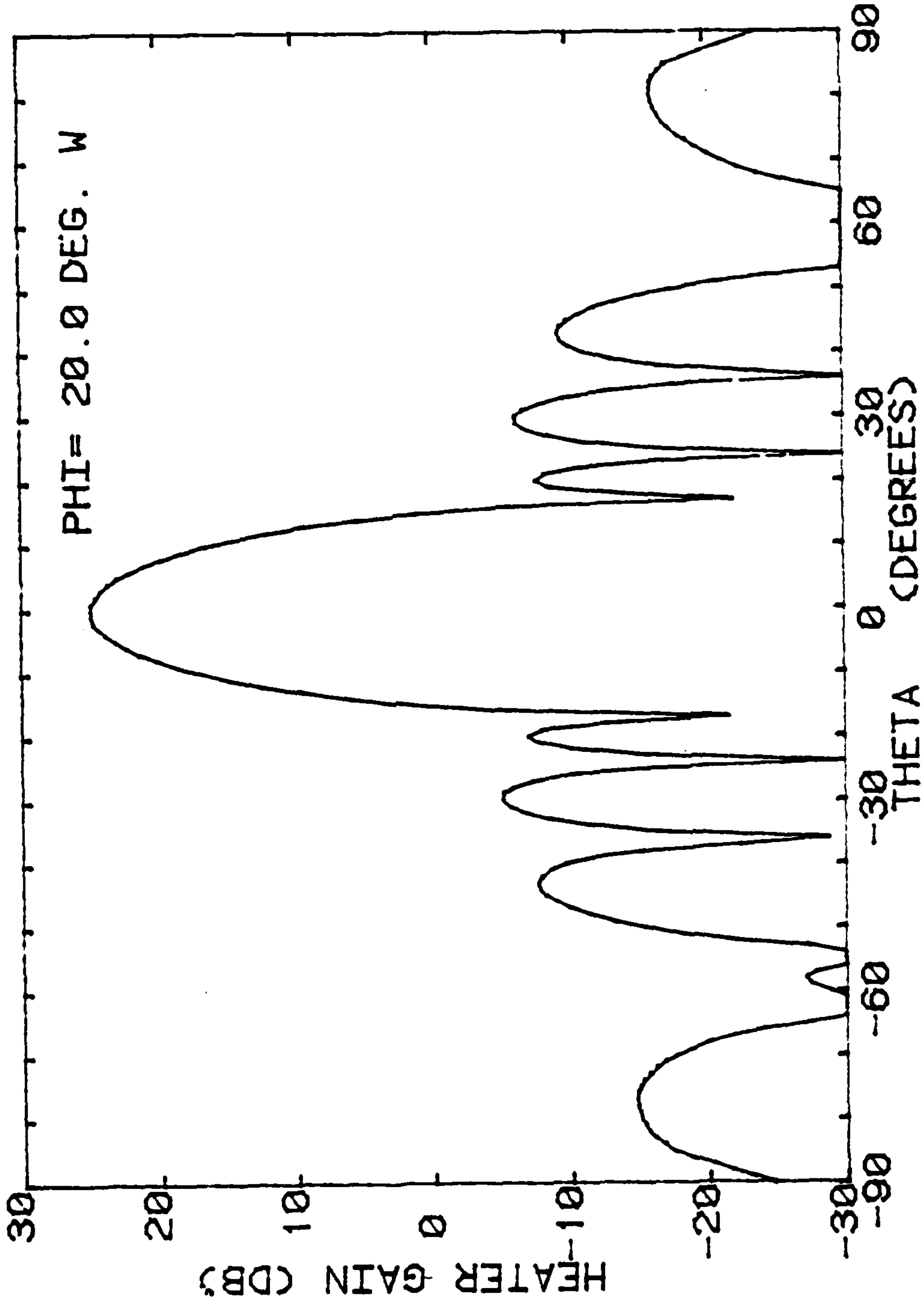
PHI= 20.0 DEG. W
30
20
10
0
-10
-20
-30
HEATER GAIN (DB)
-90
-60
-30
0
30
60
90
THETA (DEGREES)

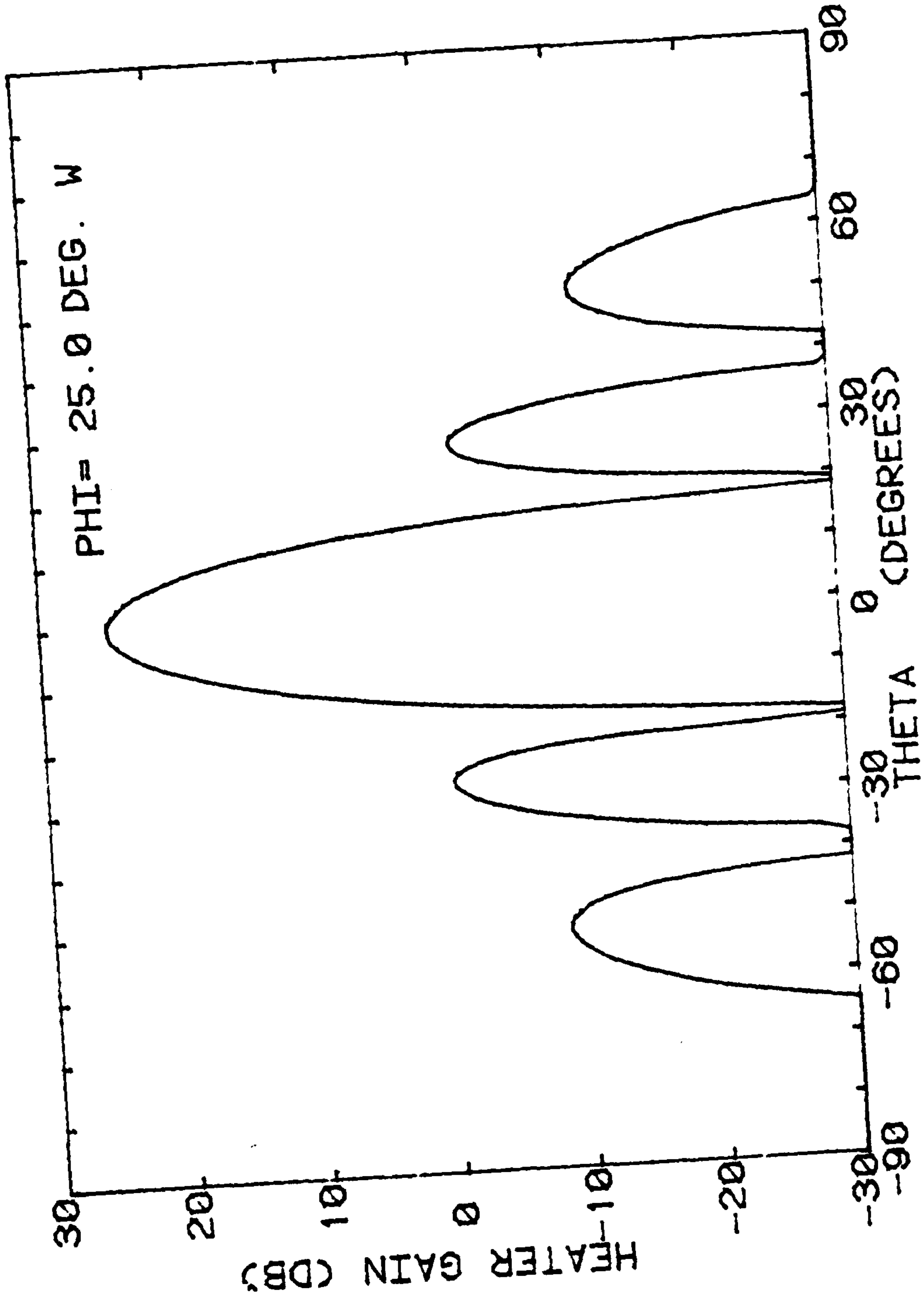
PHI= 25.0 DEG. W
HEATER GAIN (DB)
30
20
10
0
-10
-20
-30
-90
-60
-30
0
30
60
90
THETA (DEGREES)

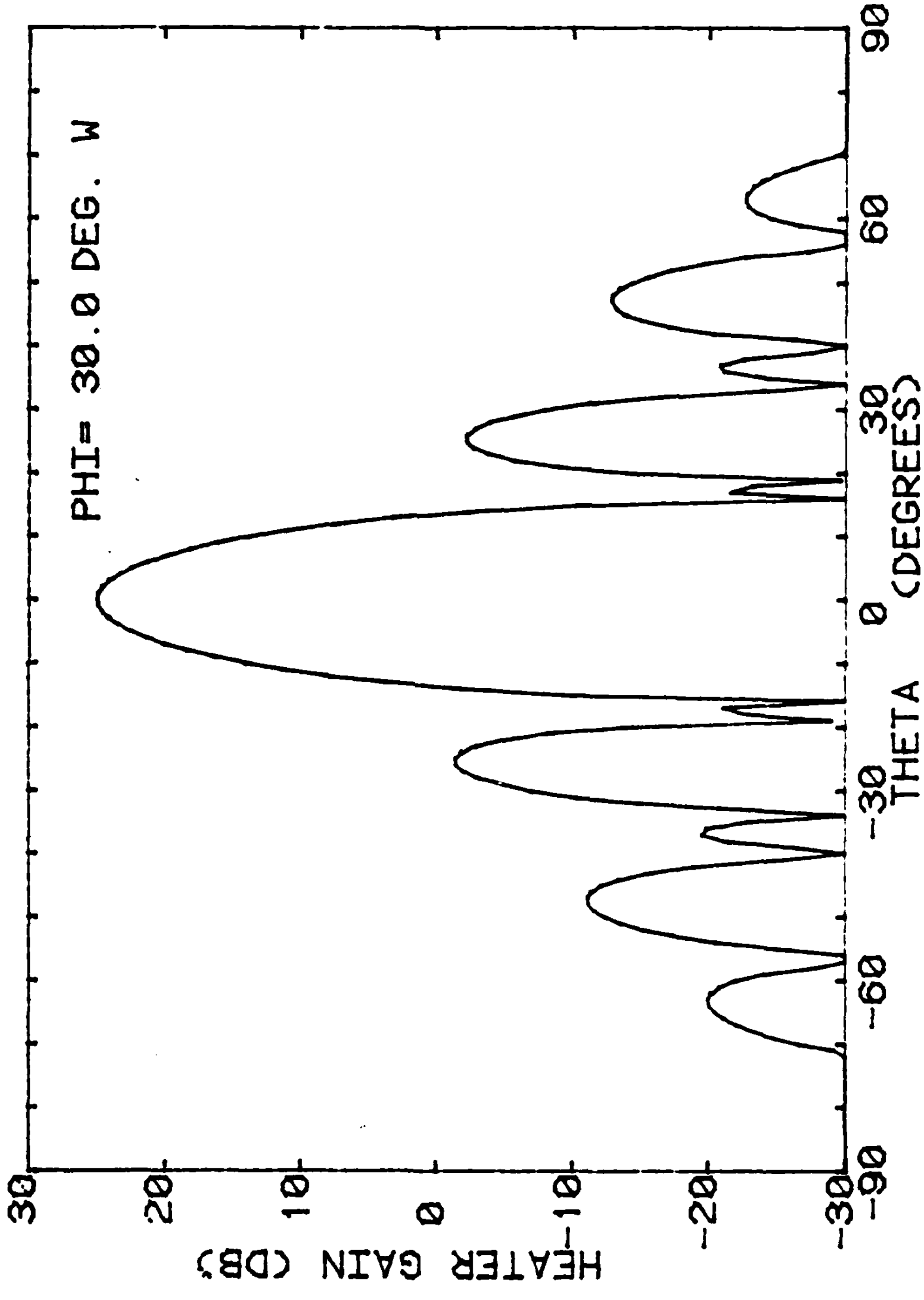
PHI= 30.0 DEG. W
HEATER GAIN (DB)
30
20
10
0
-10
-20
-30
THETA (DEGREES)
-90
-60
-30
0
30
60
90

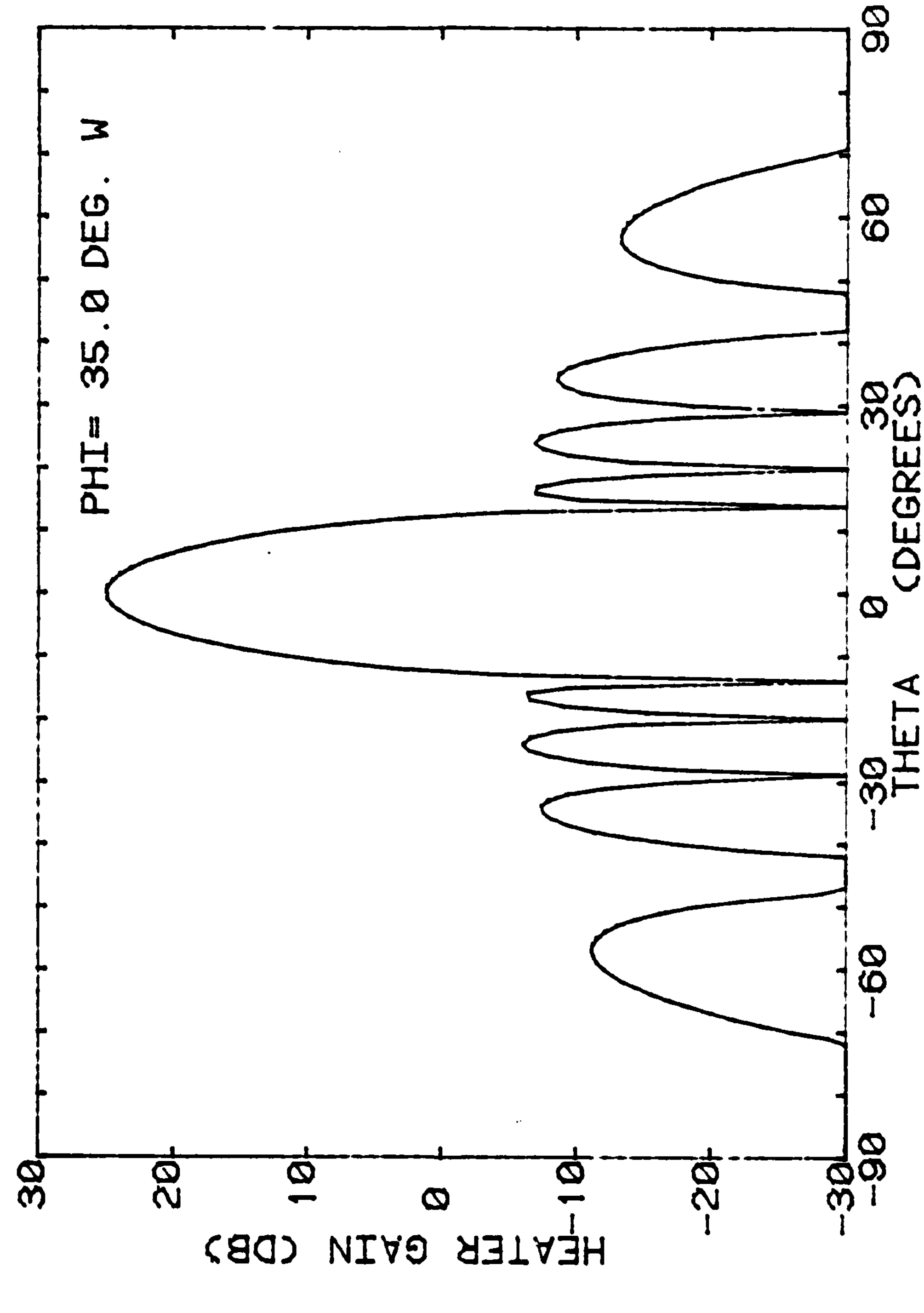
PHI= 35.0 DEG. W
HEATER GAIN (DB)
THETA (DEGREES)
30
20
10
0
-10
-20
-30
-90
-60
-30
0
30
60
90

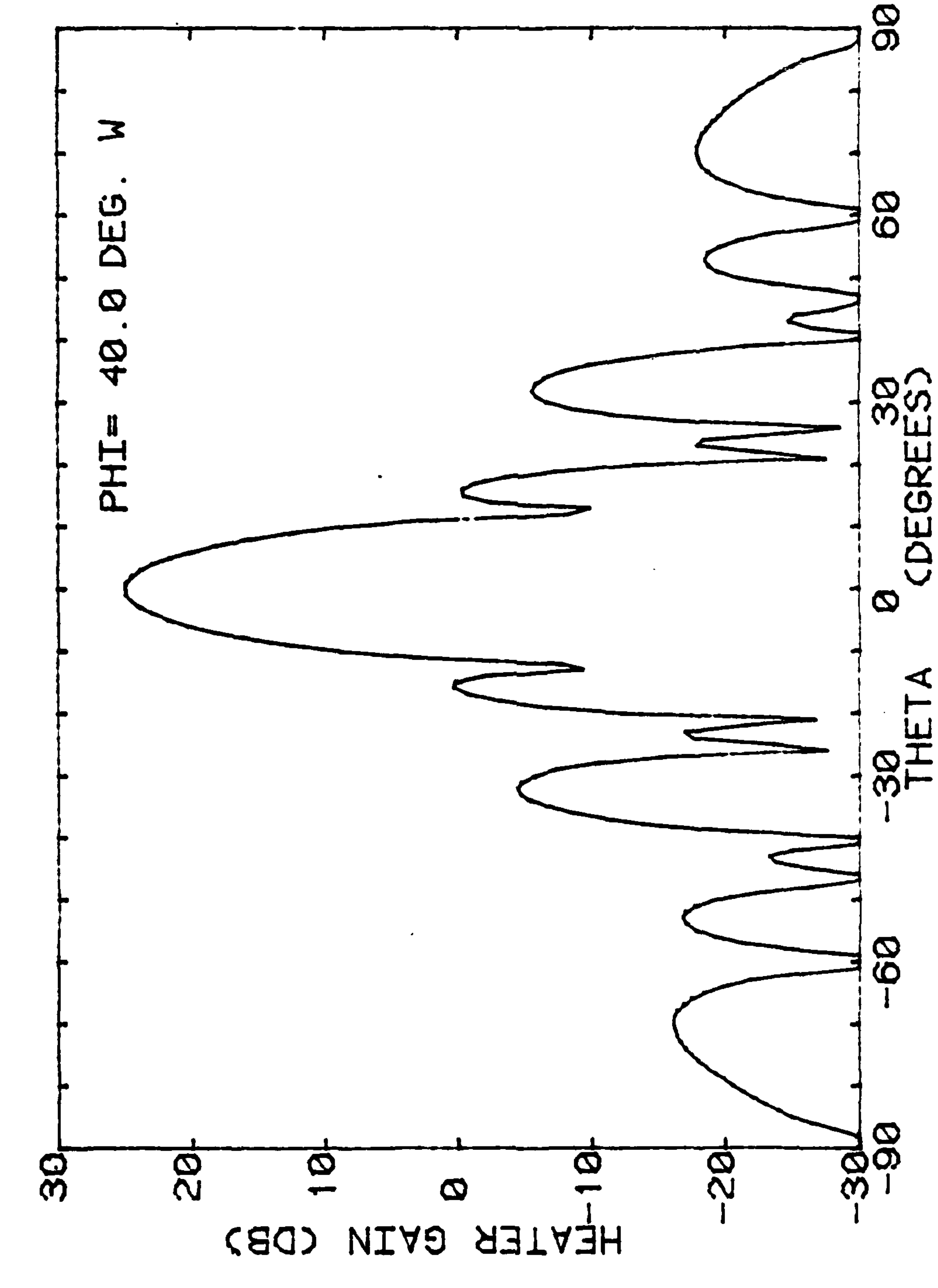

PHI= 40.0 DEG. W
HEATER GAIN (DB)
30
20
10
0
-10
-20
-30
-90
-60
-30
0
30
60
90
THETA (DEGREES)

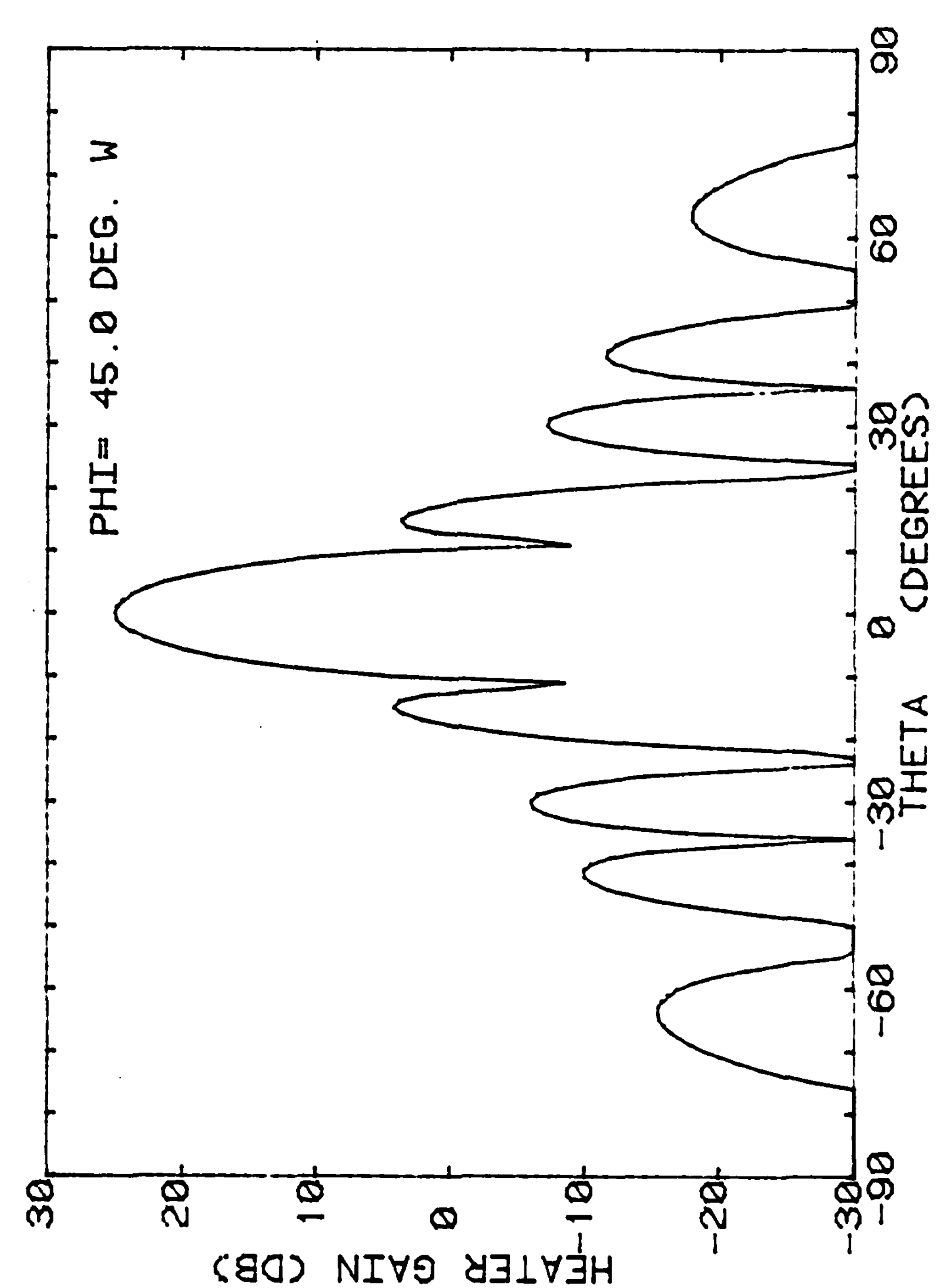
PHI= 45.0 DEG. W
HEATER GAIN (DB)
30
20
10
0
-10
-20
-30
-90
-60
-30
0
30
60
90
THETA (DEGREES)

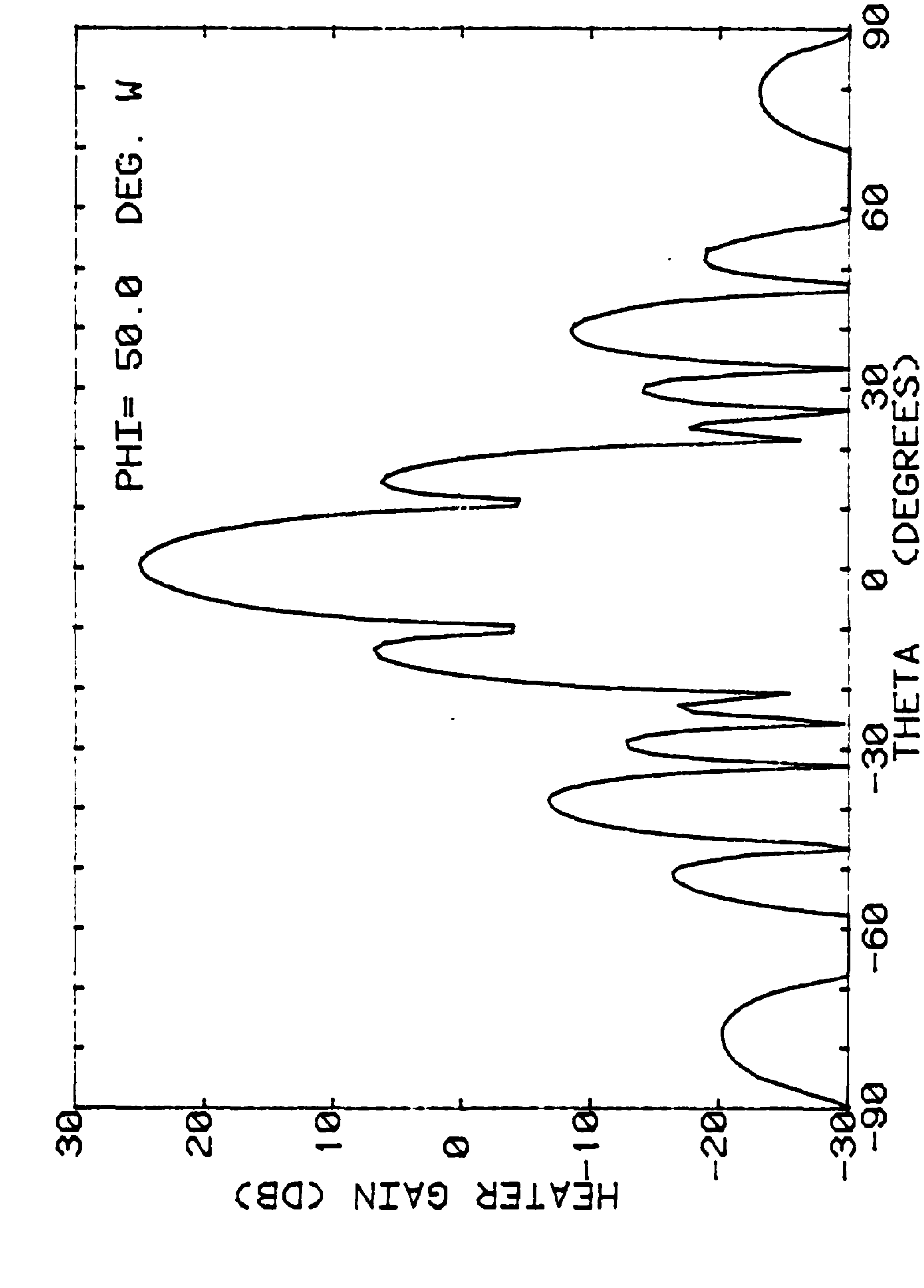
PHI= 50.0 DEG. W
HEATER GAIN (DB)
30
20
10
0
-10
-20
-30
-90
-60
-30
0
30
60
90
THETA (DEGREES)

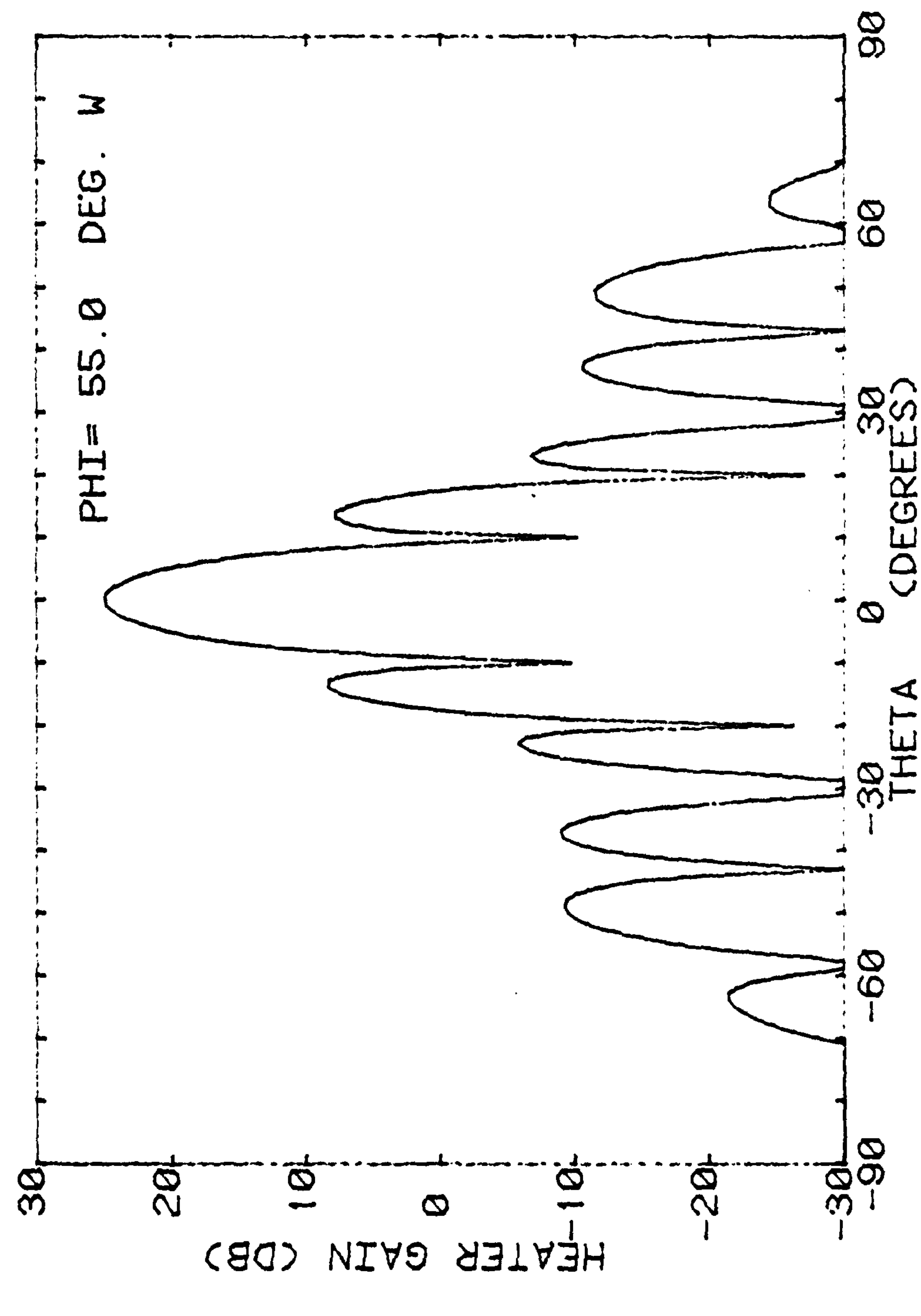
PHI= 55.0 DEG. W
HEATER GAIN (DB)
30
20
10
0
-10
-20
-30
-90
-60
-30
0
30
60
90
THETA (DEGREES)

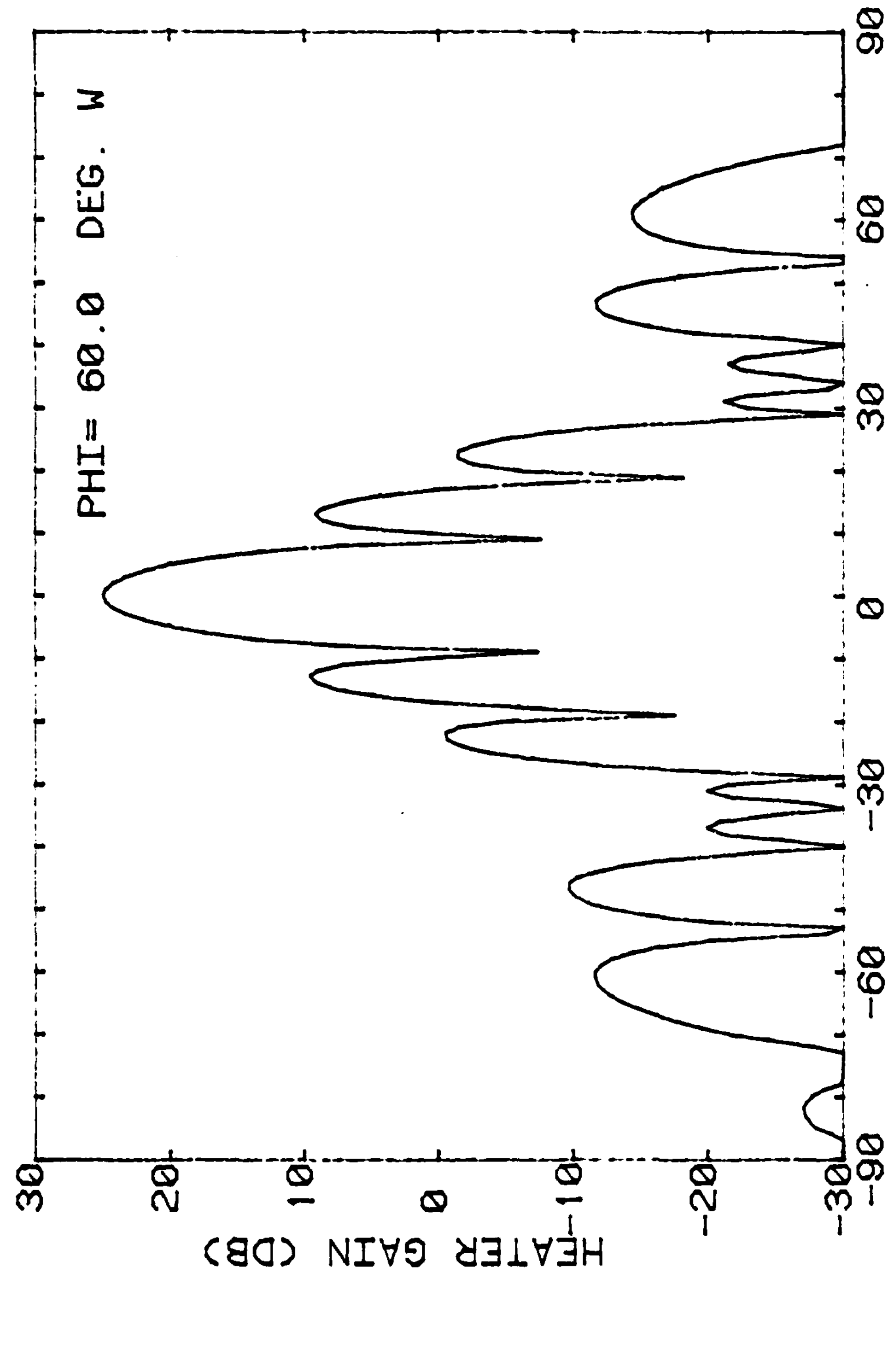
PHI= 60.0 DEG. W
HEATER GAIN (DB)
30
20
10
0
-10
-20
-30
-90
-60
-30
0
30
60
90
THETA (DEGREES)

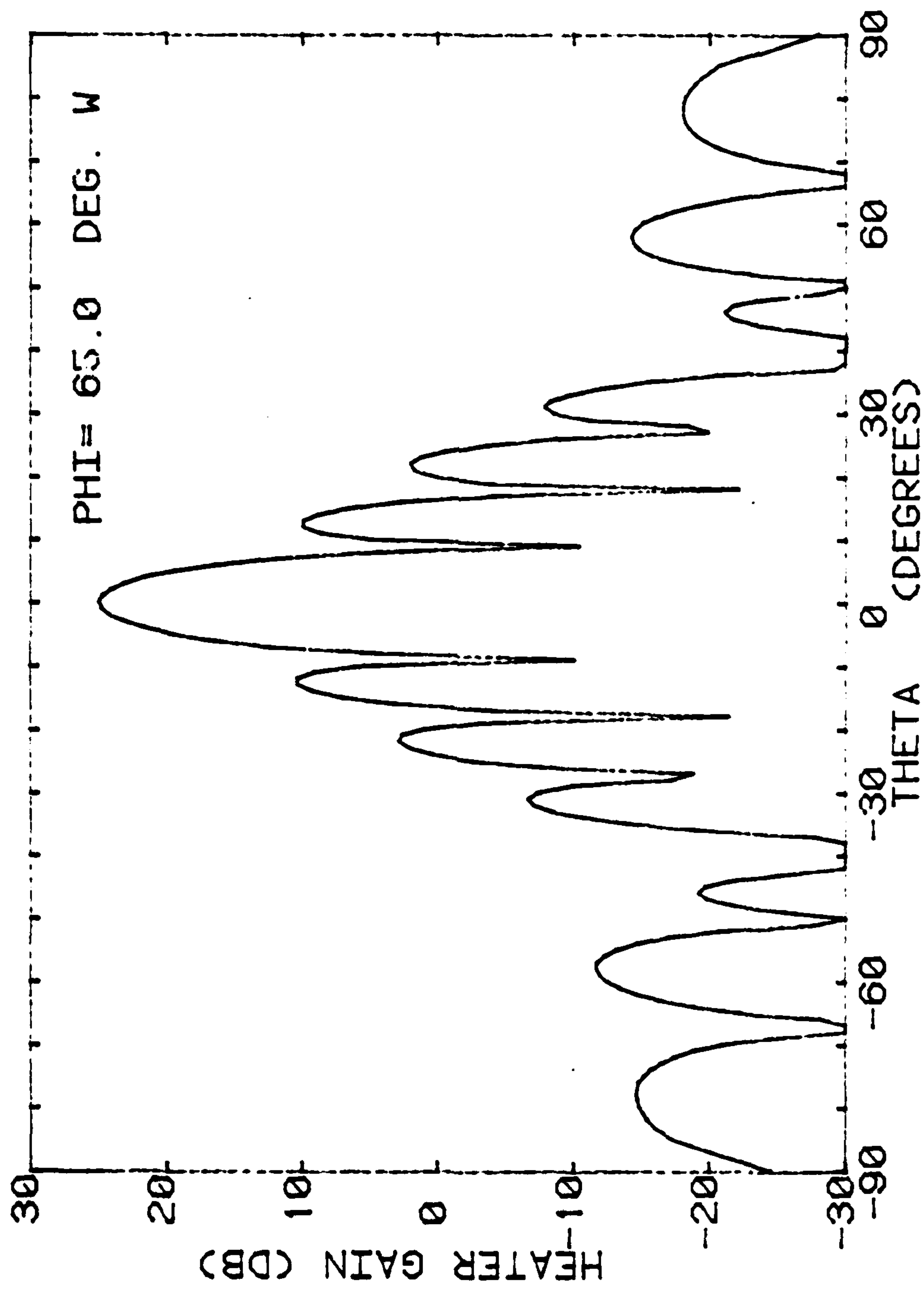

PHI= 65.0 DEG. W
HEATER GAIN (DB)
30
20
10
0
-10
-20
-30
THETA (DEGREES)
-90
-60
-30
0
30
60
90

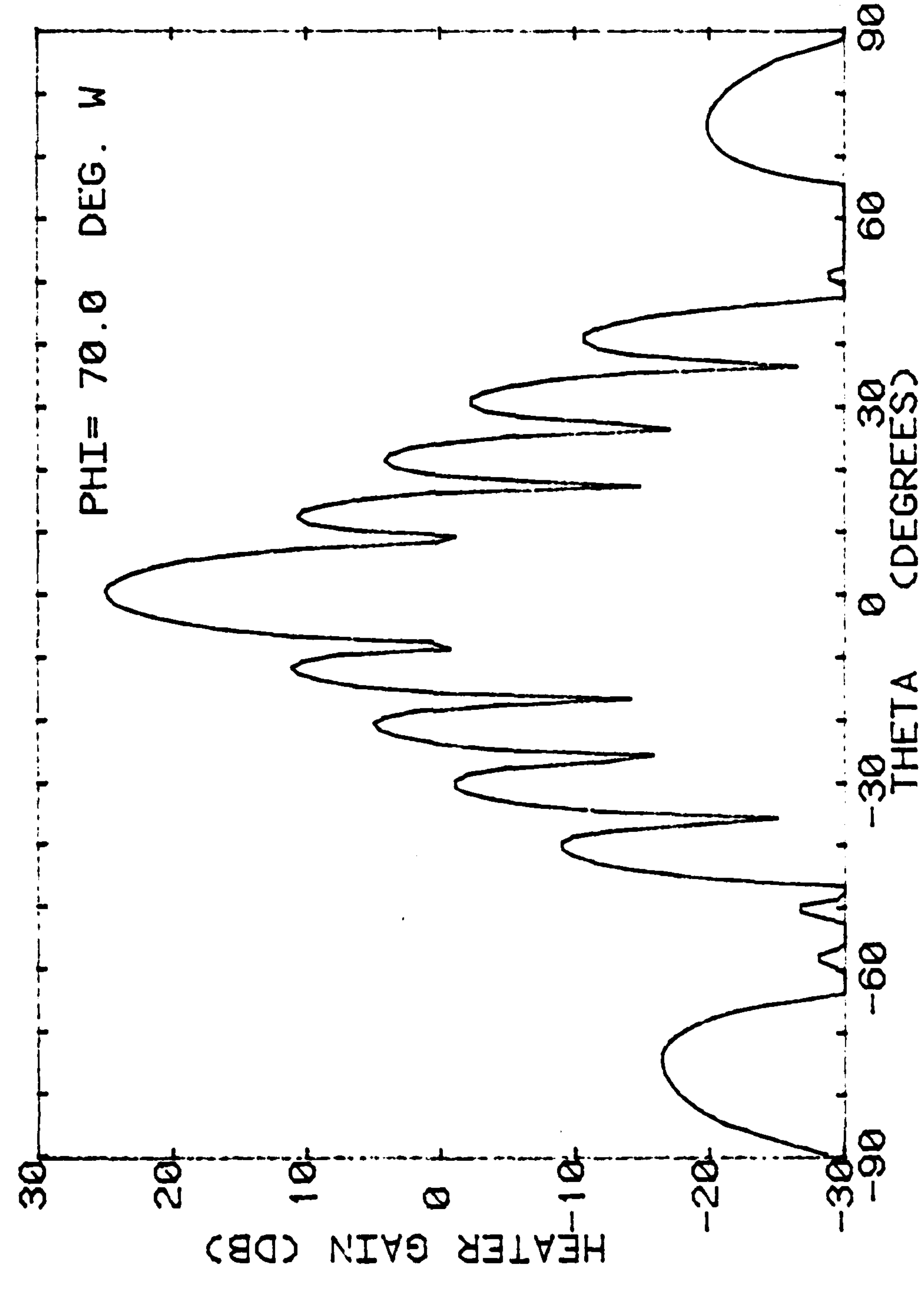
PHI= 70.0 DEG. W
HEATER GAIN (DB)
THETA (DEGREES)
30
20
10
0
-10
-20
-30
-90
-60
-30
0
30
60
90

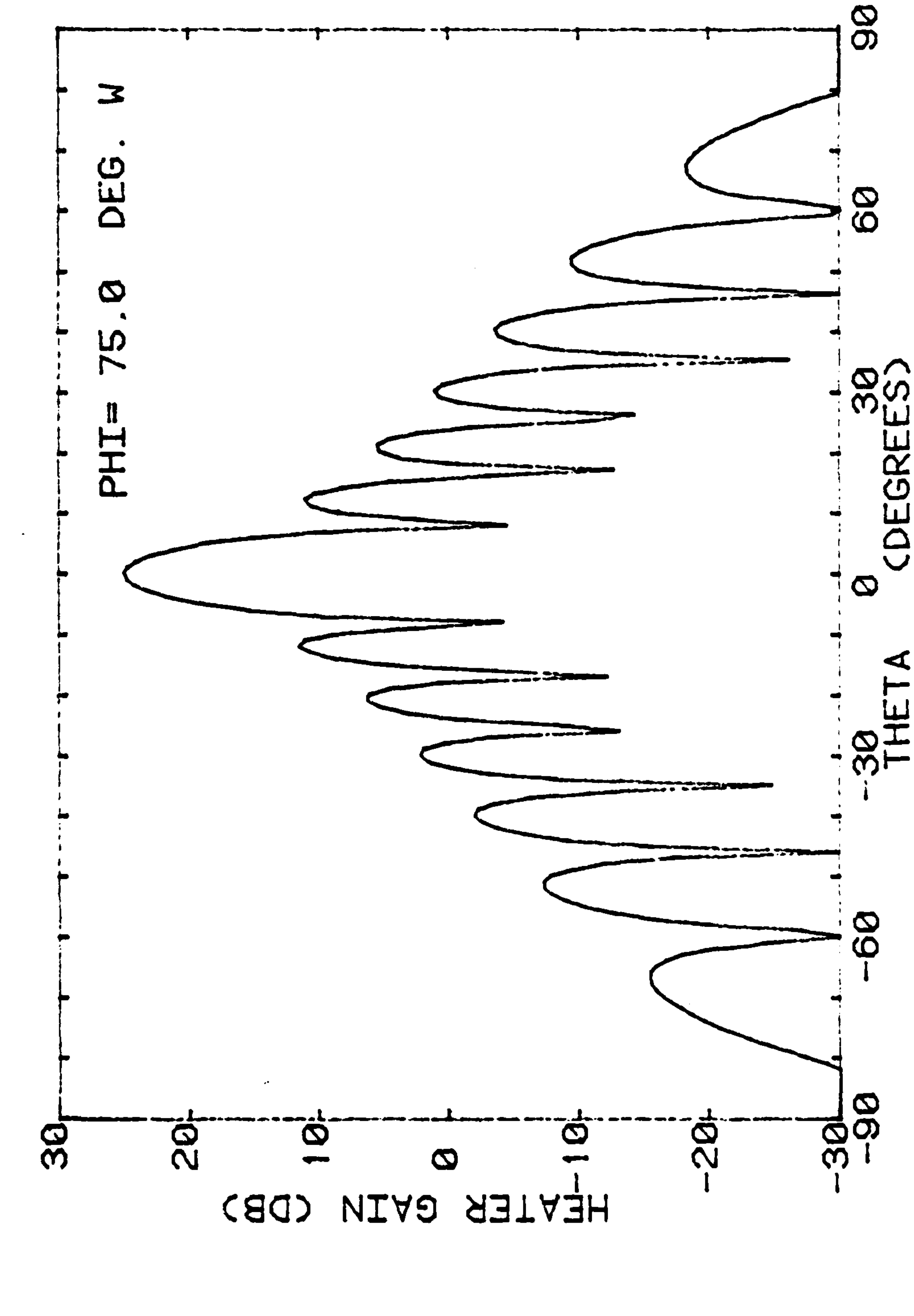
PHI= 75.0 DEG. W
HEATER GAIN (DB)
30
20
10
0
-10
-20
-30
-90
-60
-30
0
30
60
90
THETA (DEGREES)

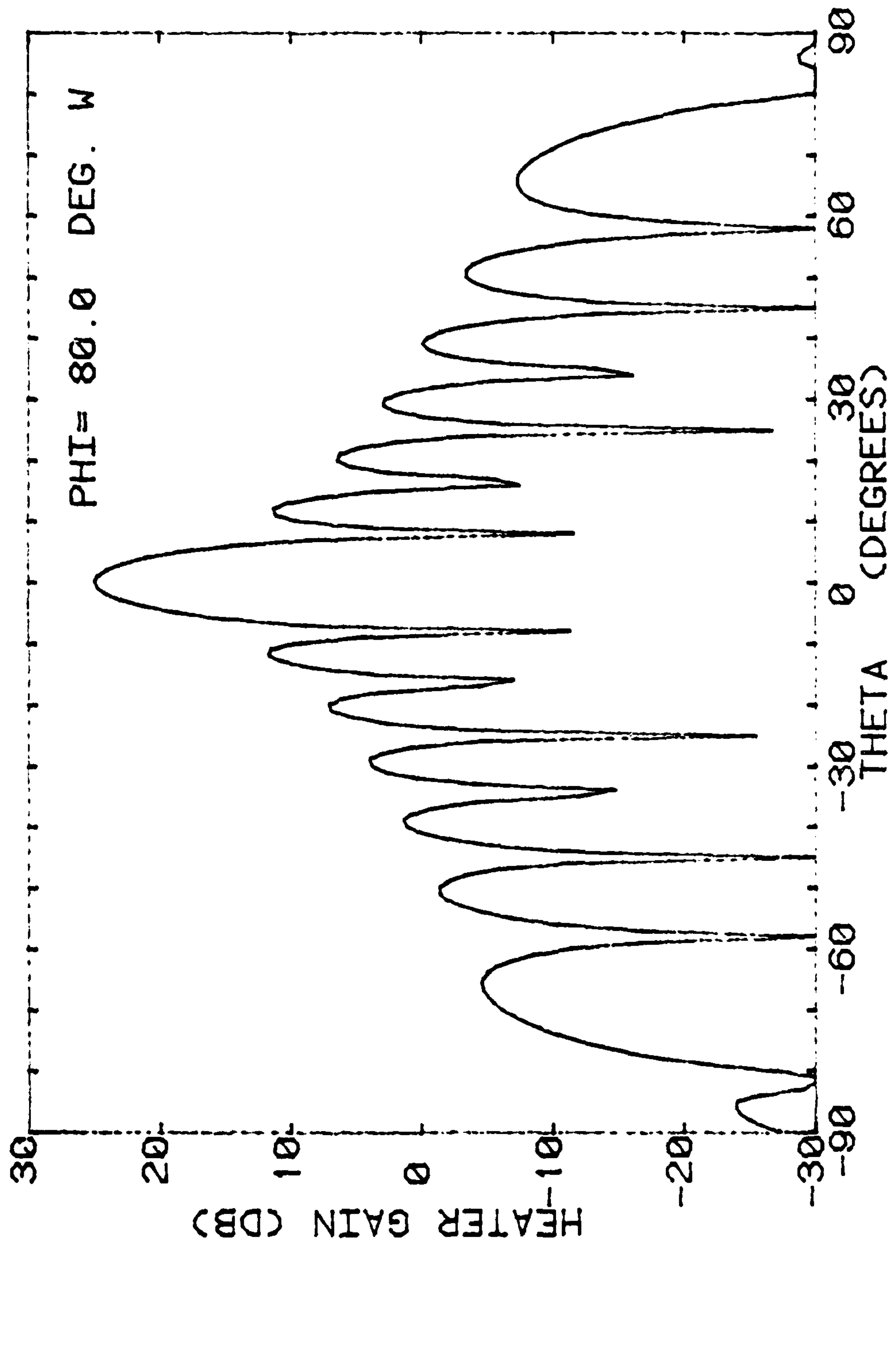
PHI= 80.0 DEG. W
HEATER GAIN (DB)
30
20
10
0
-10
-20
-30
THETA (DEGREES)
-90
-60
-30
0
30
60
90

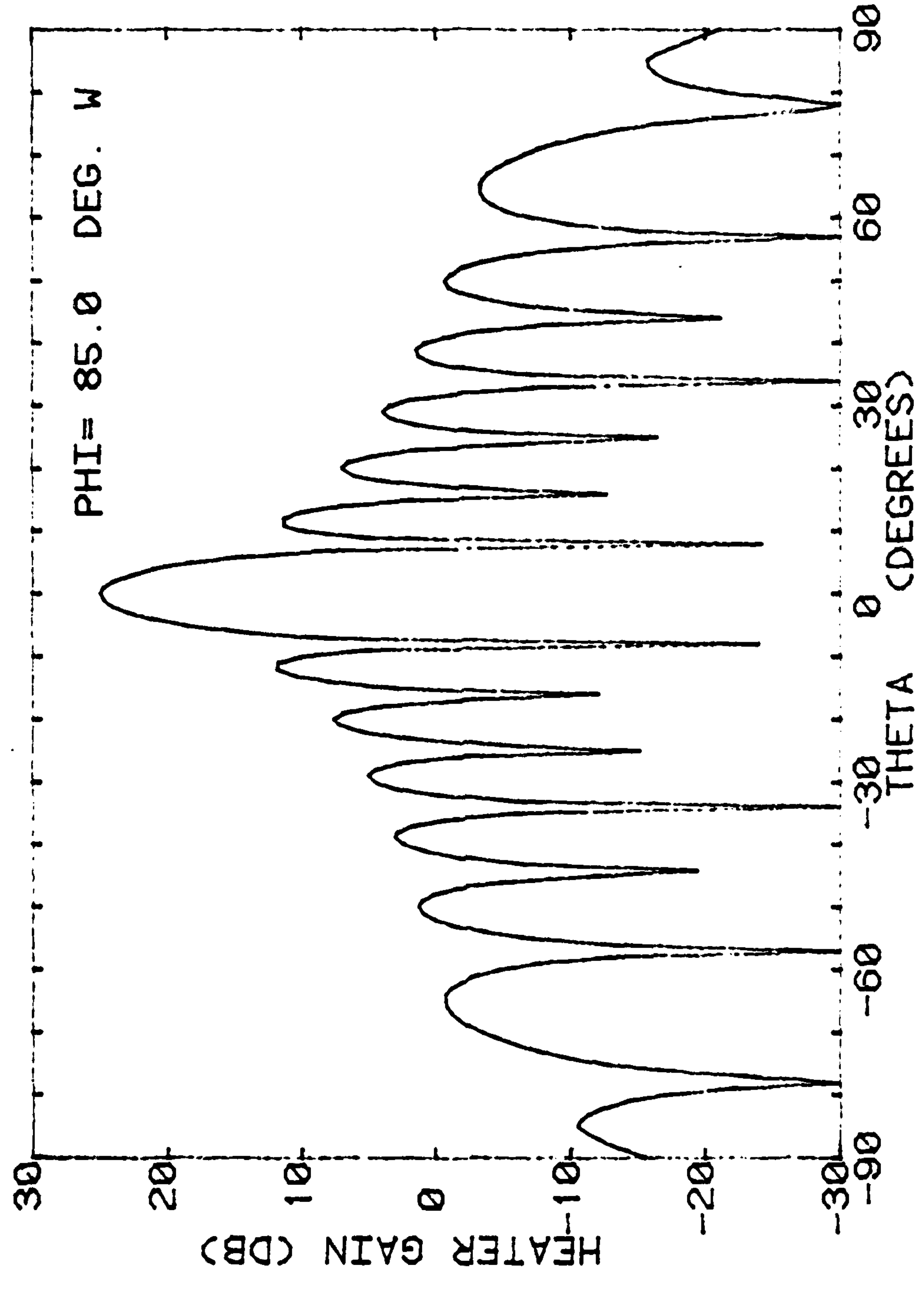
PHI= 85.0 DEG. W
HEATER GAIN (DB)
30
20
10
0
-10
-20
-30
THETA (DEGREES)
-90
-60
-30
0
30
60
90

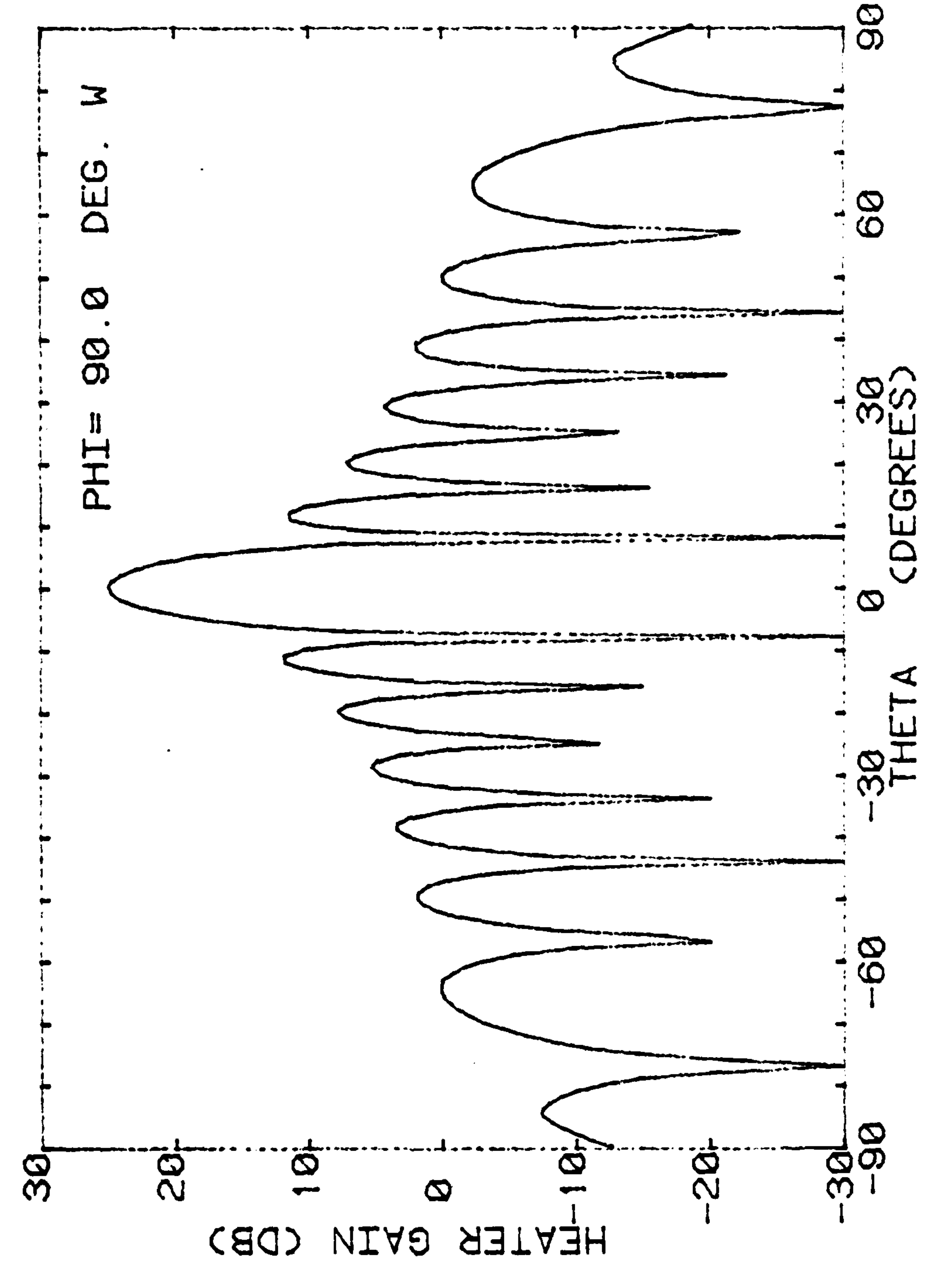
PHI= 90.0 DEG. W
HEATER GAIN (DB)
30
20
10
0
-10
-20
-30
-90
-60
-30
0
30
60
90
THETA (DEGREES)

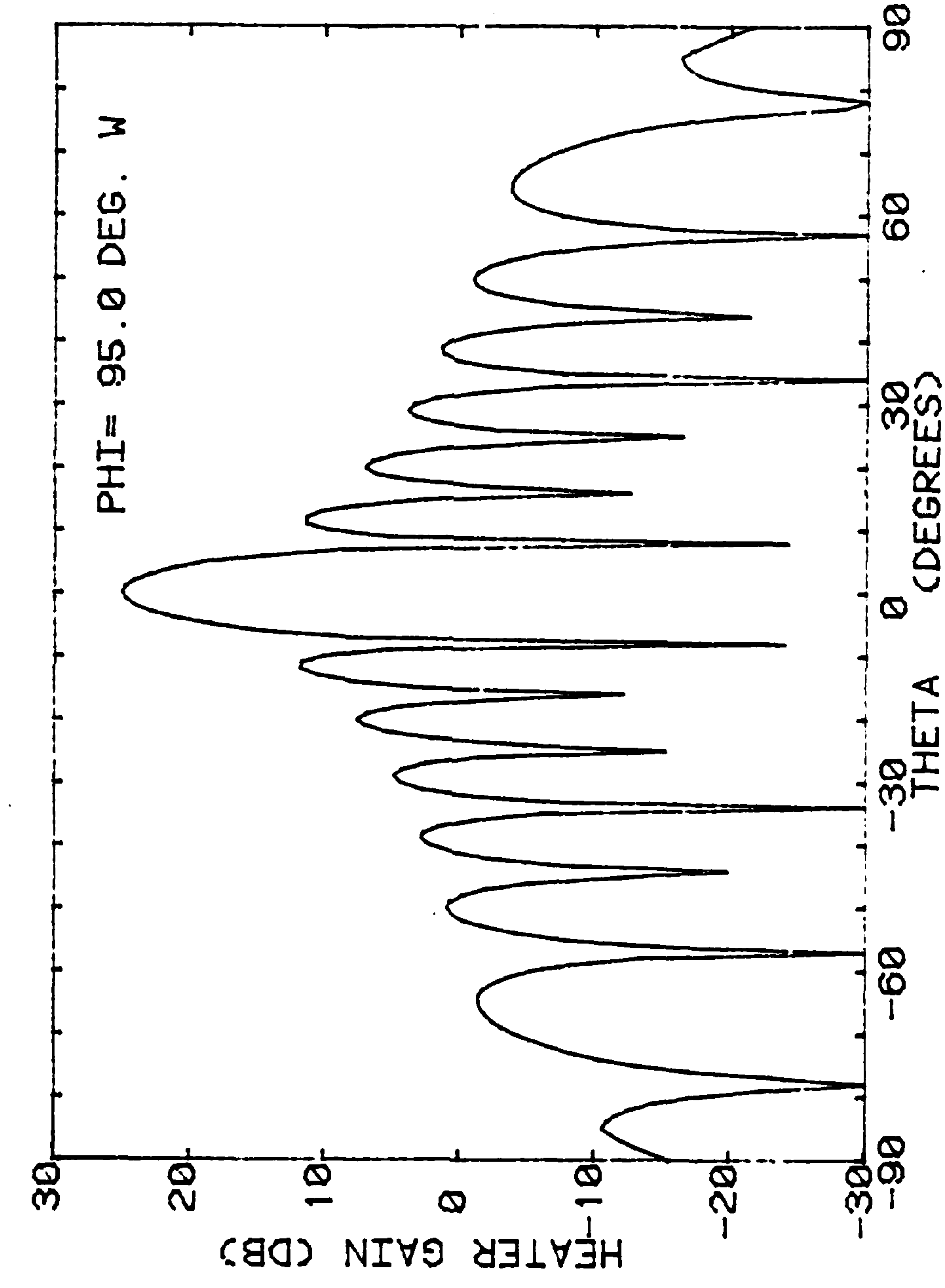
PHI= 95.0 DEG. W
HEATER GAIN (DB)
30
20
10
0
-10
-20
-30
-90
-60
-30
0
30
60
90
THETA (DEGREES)

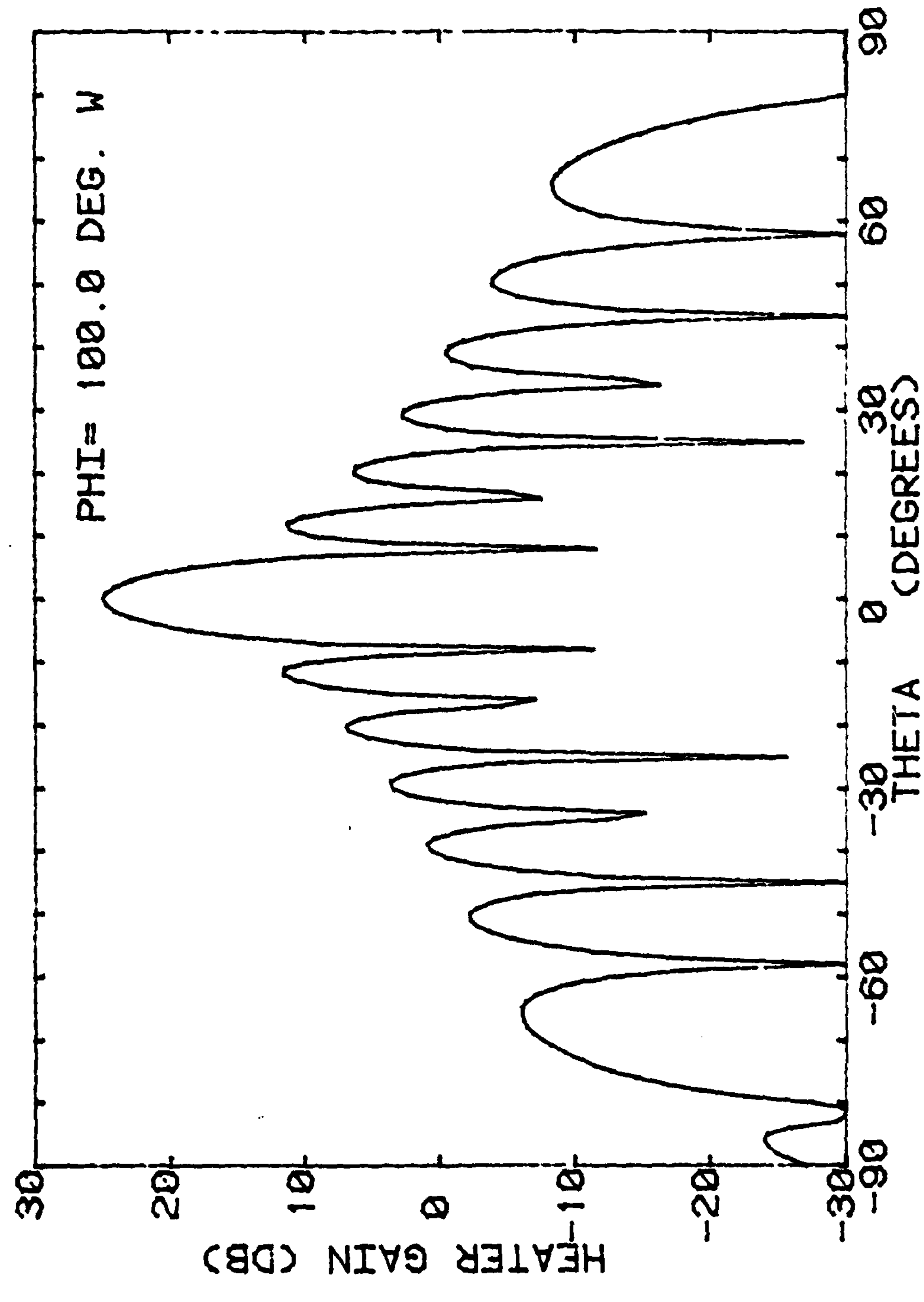
PHI= 100.0 DEG. W
HEATER GAIN (DB)
30
20
10
0
-10
-20
-30
THETA (DEGREES)
-90
-60
-30
0
30
60
90

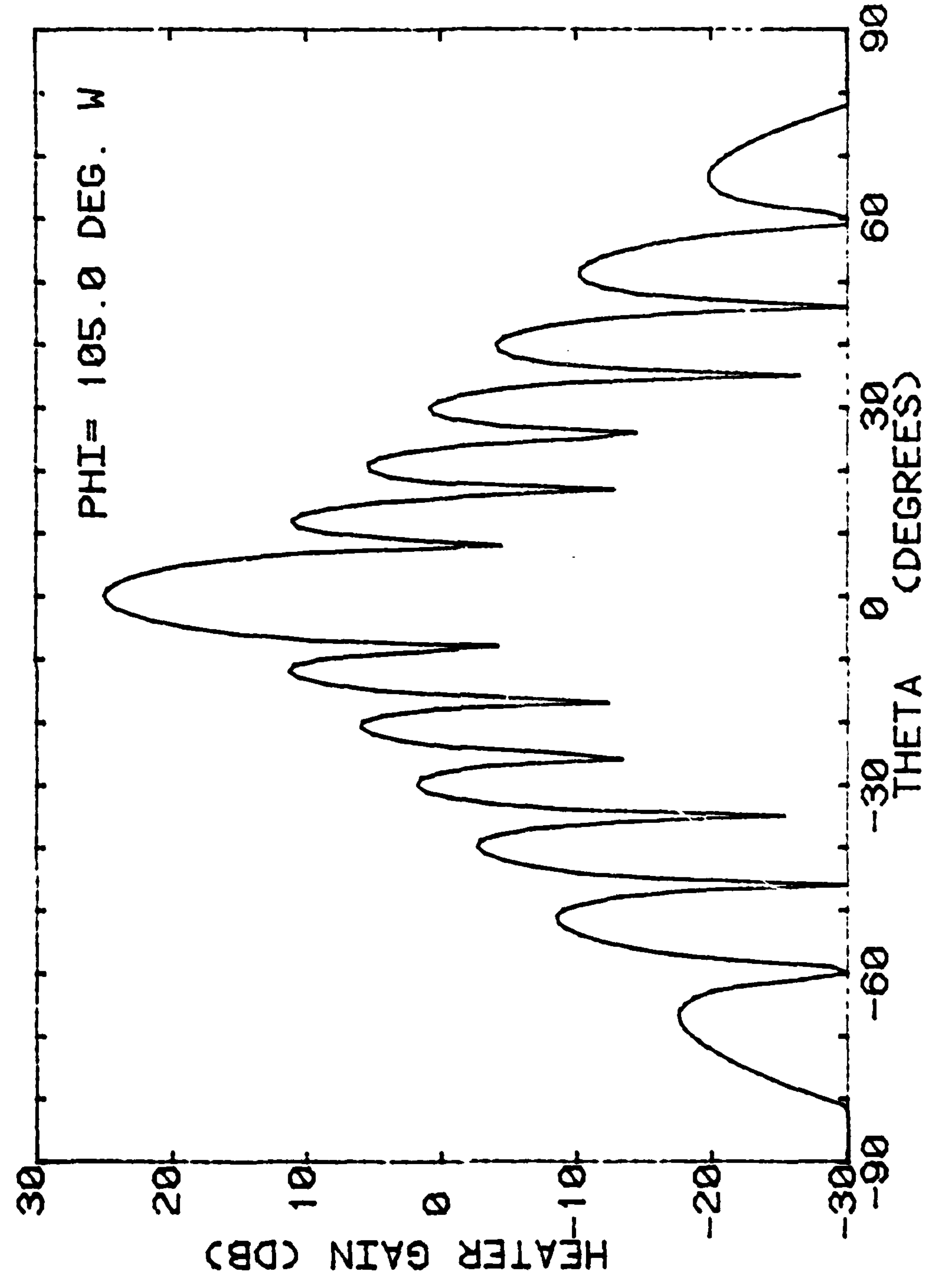
PHI= 105.0 DEG. W
HEATER GAIN (DB)
THETA (DEGREES)
30
20
10
0
-10
-20
-30
-90
-60
-30
0
30
60
90

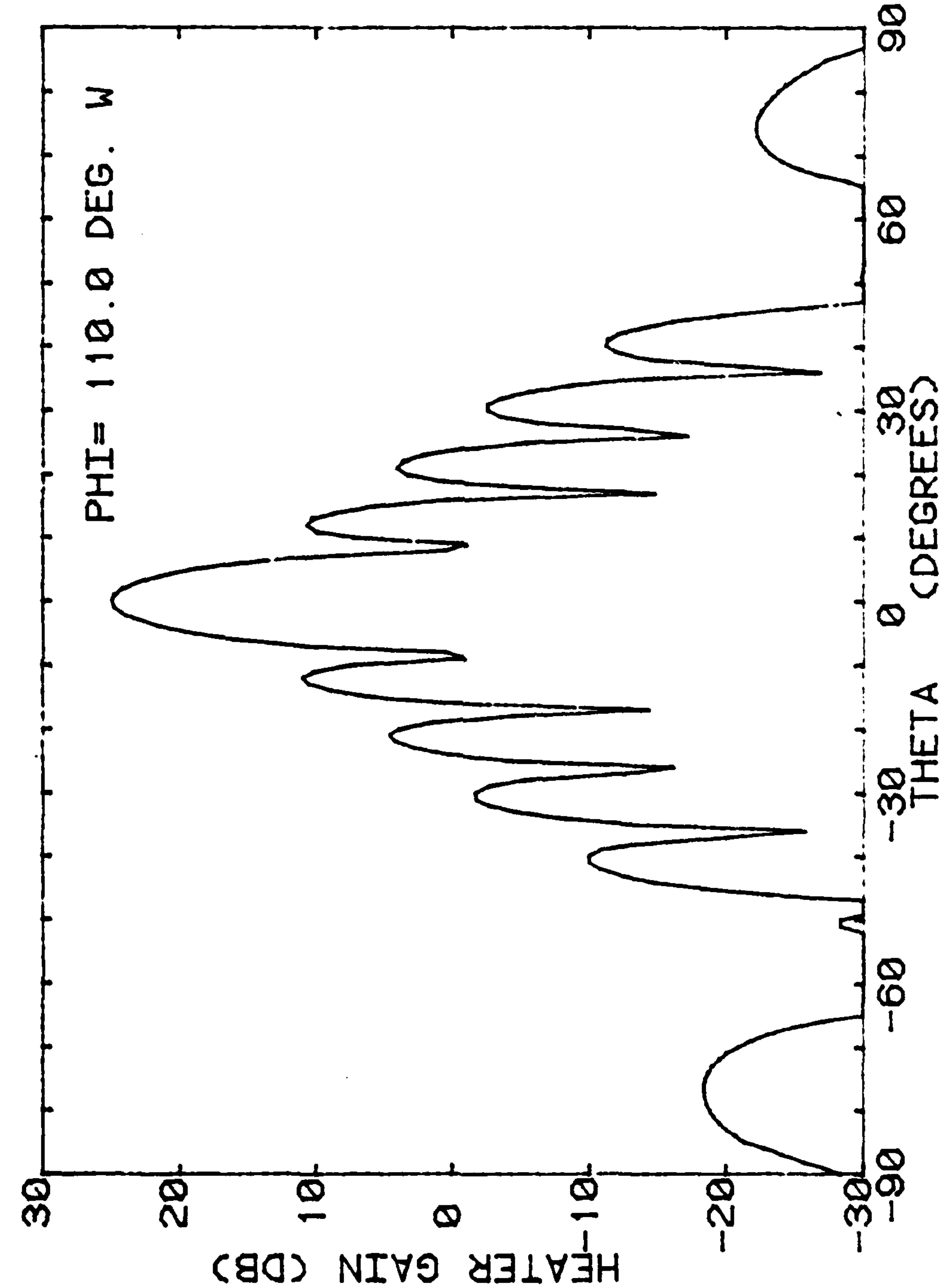
PHI= 110.0 DEG. W
HEATER GAIN (DB)
30
20
10
0
-10
-20
-30
-90
-60
-30
0
30
60
90
THETA (DEGREES)

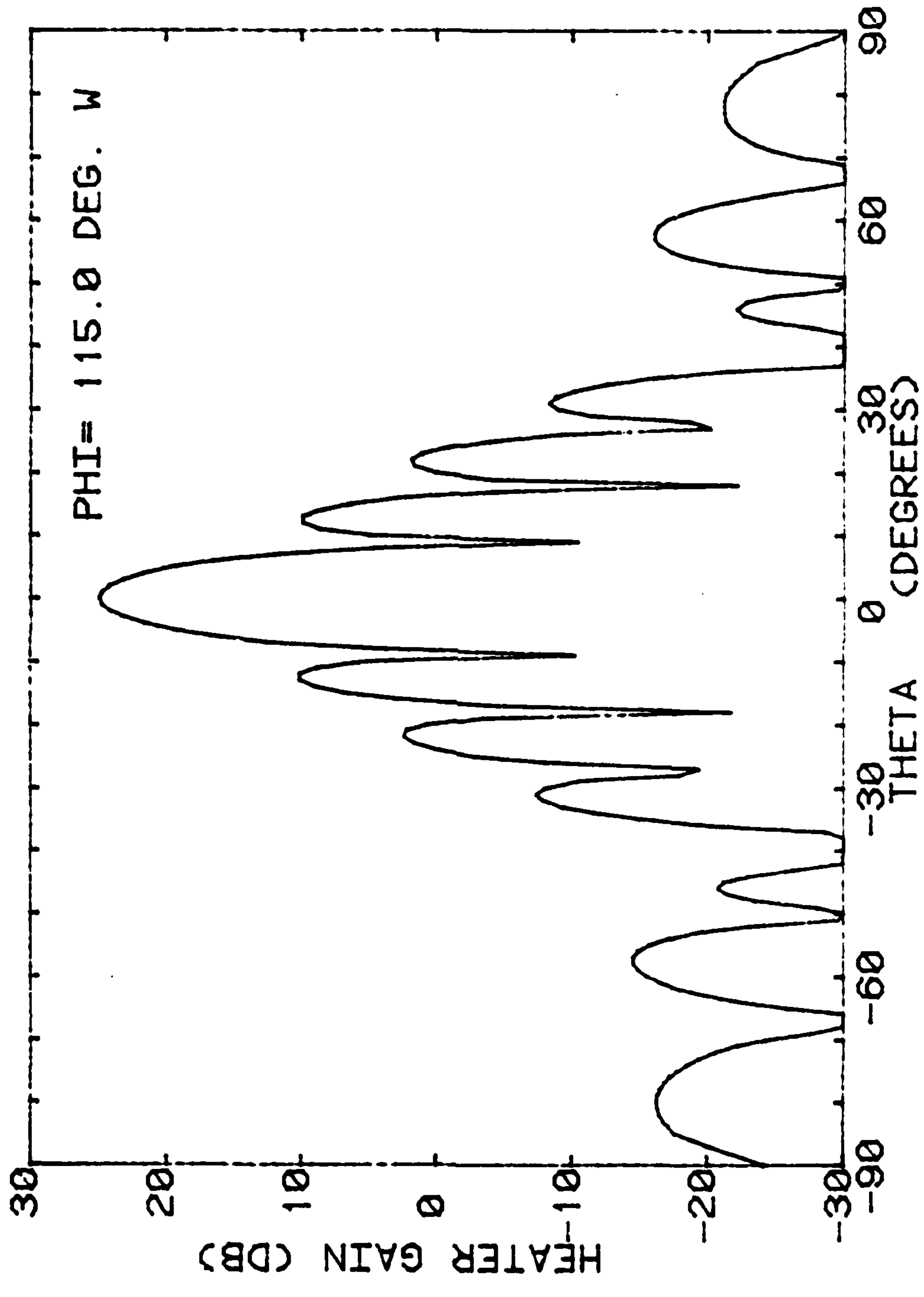
PHI= 115.0 DEG. W
HEATER GAIN (DB)
30
20
10
0
-10
-20
-30
-90
-60
-30
0
30
60
90
THETA (DEGREES)

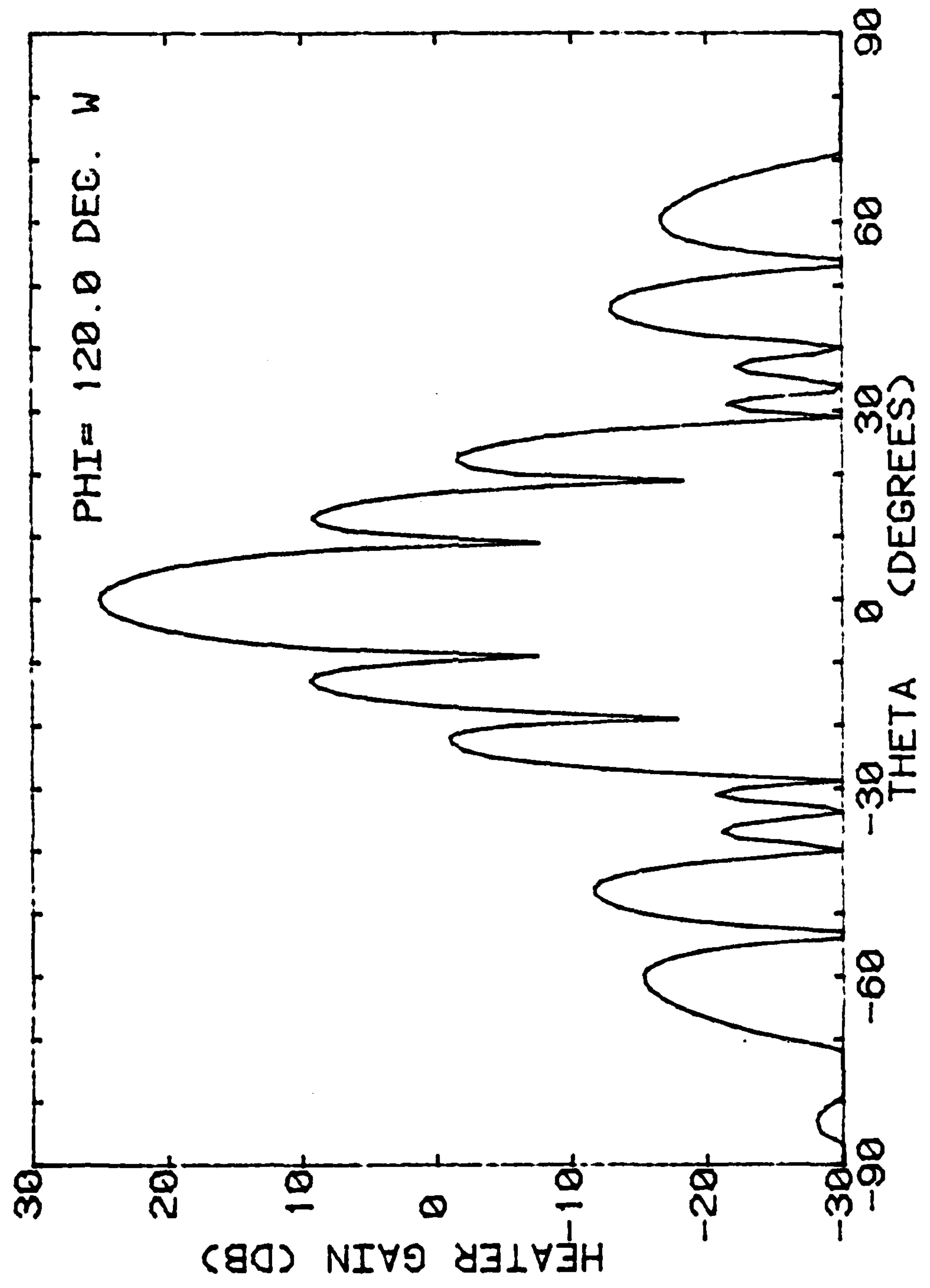
PHI= 120.0 DEG. W
HEATER GAIN (DB)
30
20
10
0
-10
-20
-30
-90
-60
-30
0
30
60
90
THETA (DEGREES)

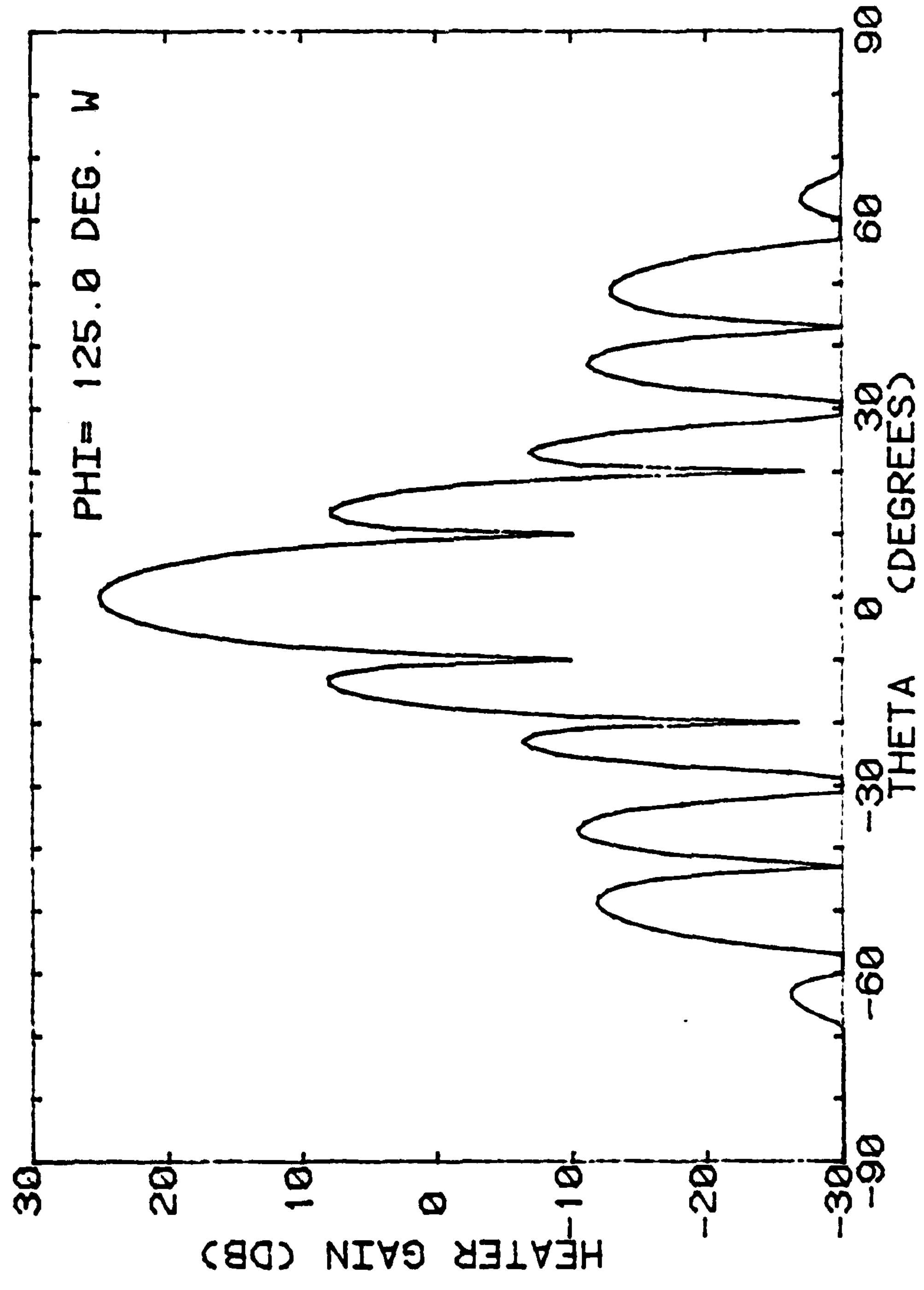
PHI= 125.0 DEG. W
HEATER GAIN (DB)
30
20
10
0
-10
-20
-30
-90
-60
-30
0
30
60
90
THETA (DEGREES)

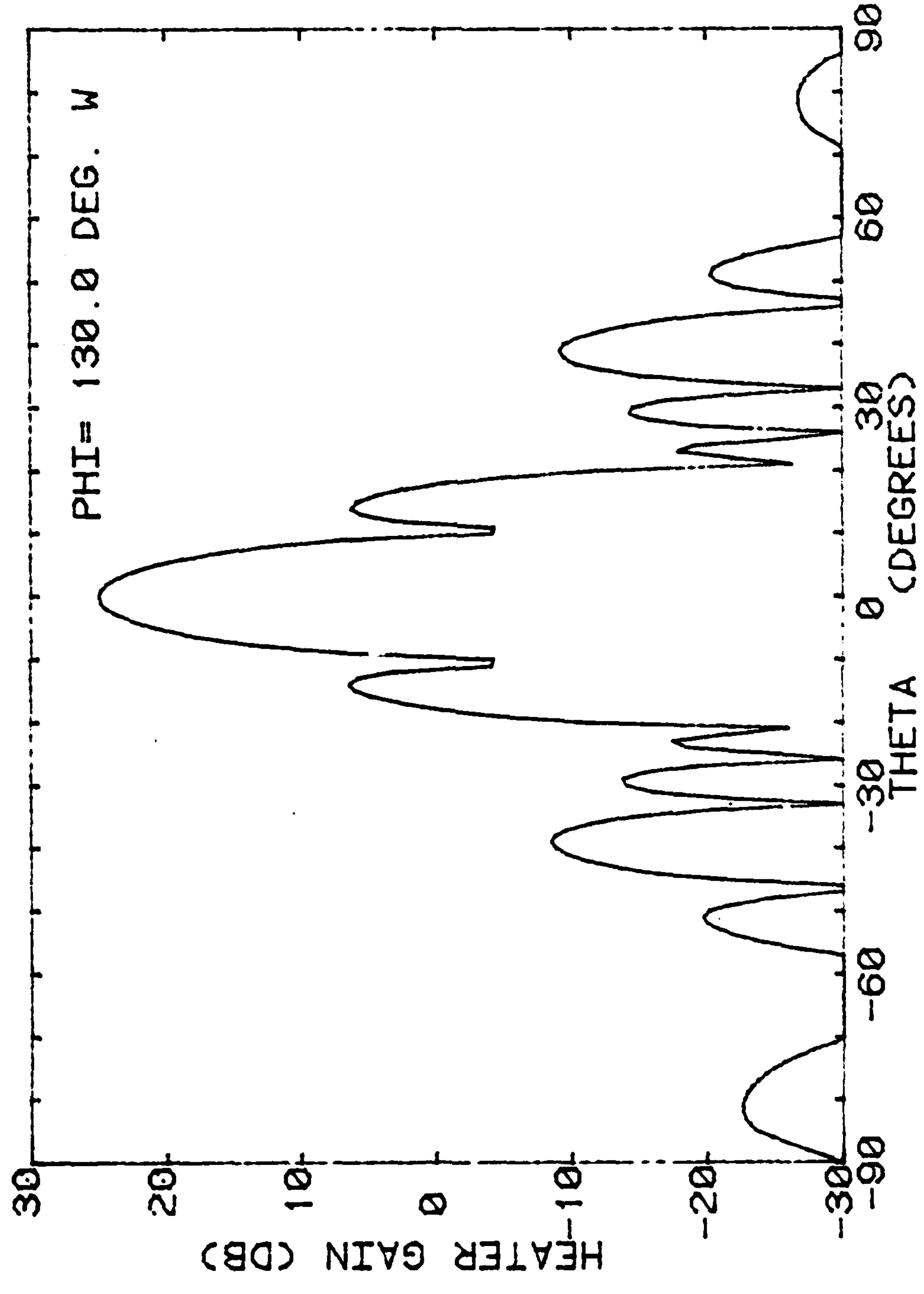
PHI= 130.0 DEG. W
HEATER GAIN (DB)
30
20
10
0
-10
-20
-30
-90
-60
-30
0
30
60
90
THETA (DEGREES)

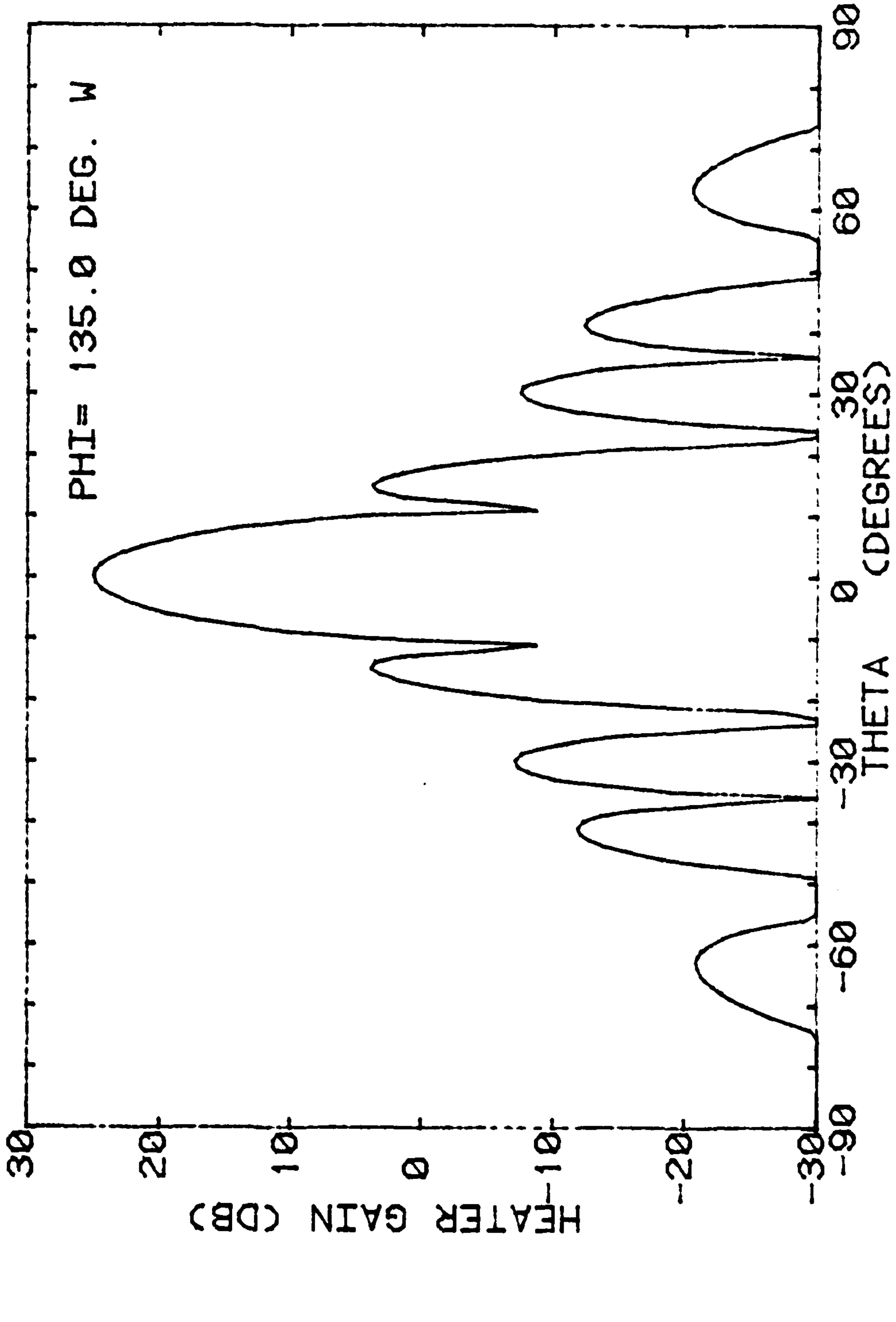
PHI= 135.0 DEG. W
HEATER GAIN (DB)
THETA (DEGREES)
30
20
10
0
-10
-20
-30
-90
-60
-30
0
30
60
90

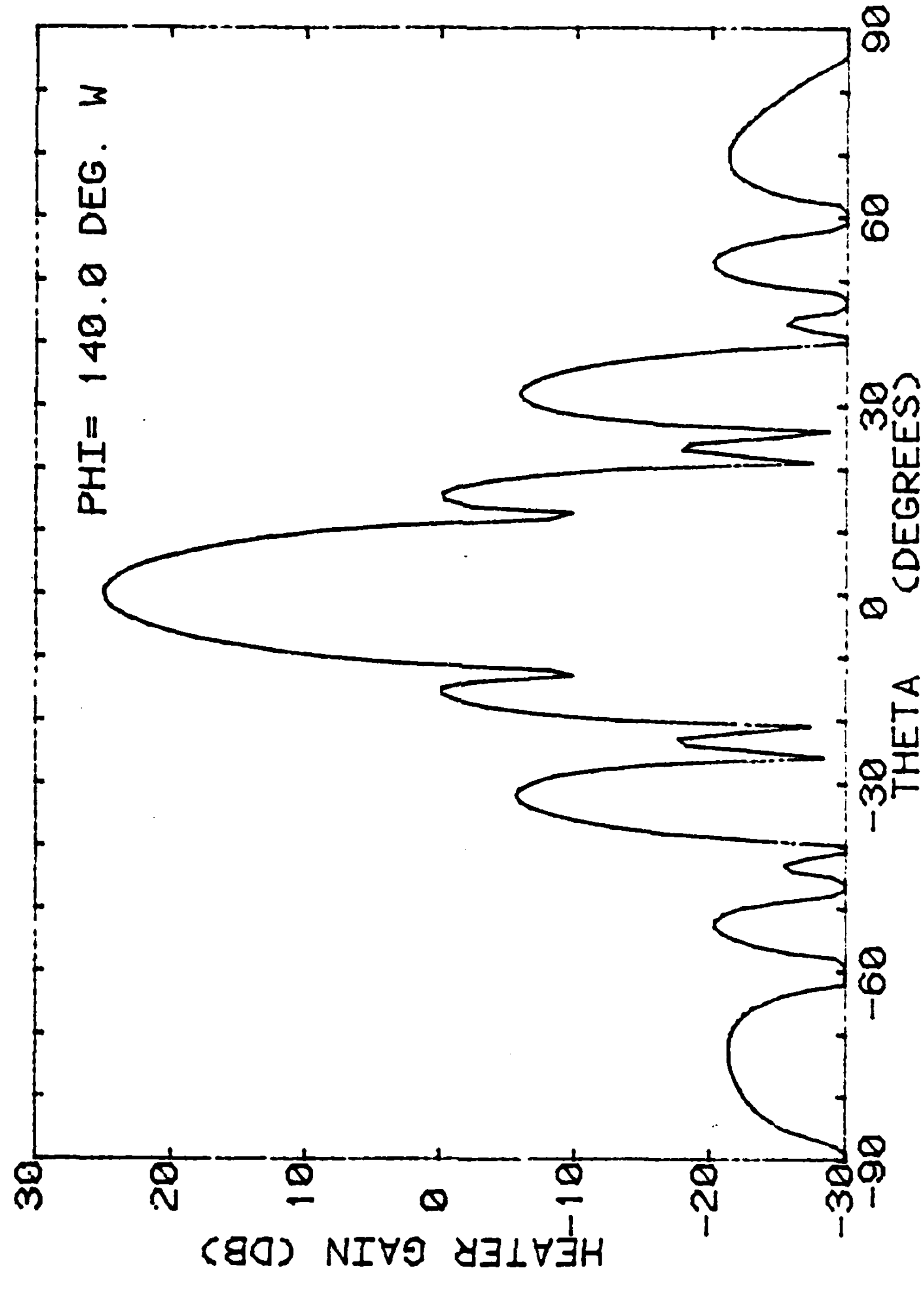
PHI= 140.0 DEG. W
HEATER GAIN (DB)
30
20
10
0
-10
-20
-30
-90
-60
-30
0
30
60
90
THETA (DEGREES)

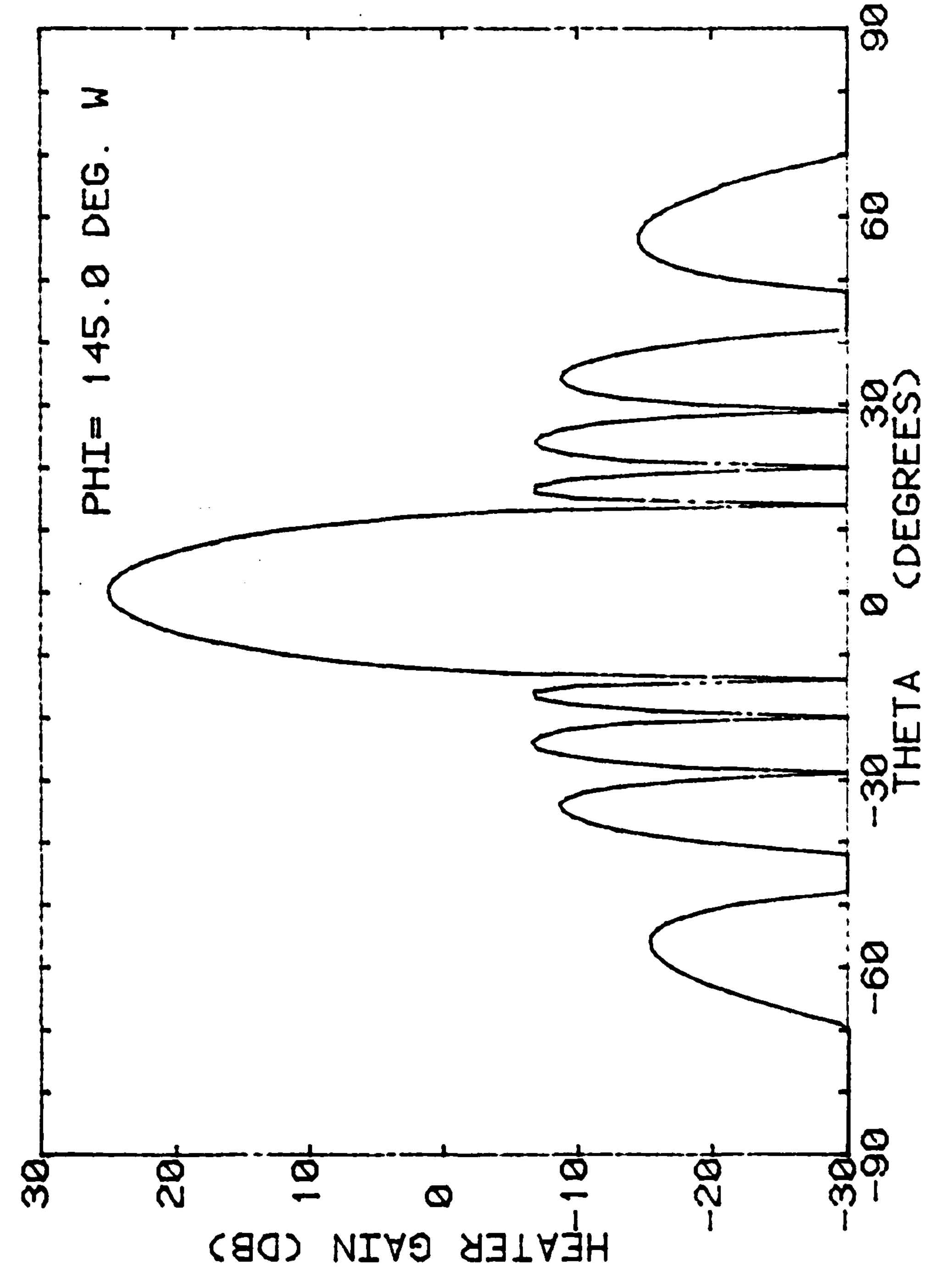
PHI= 145.0 DEG. W
HEATER GAIN (DB)
30
20
10
0
-10
-20
-30
-90
-60
-30
0
30
60
90
THETA (DEGREES)

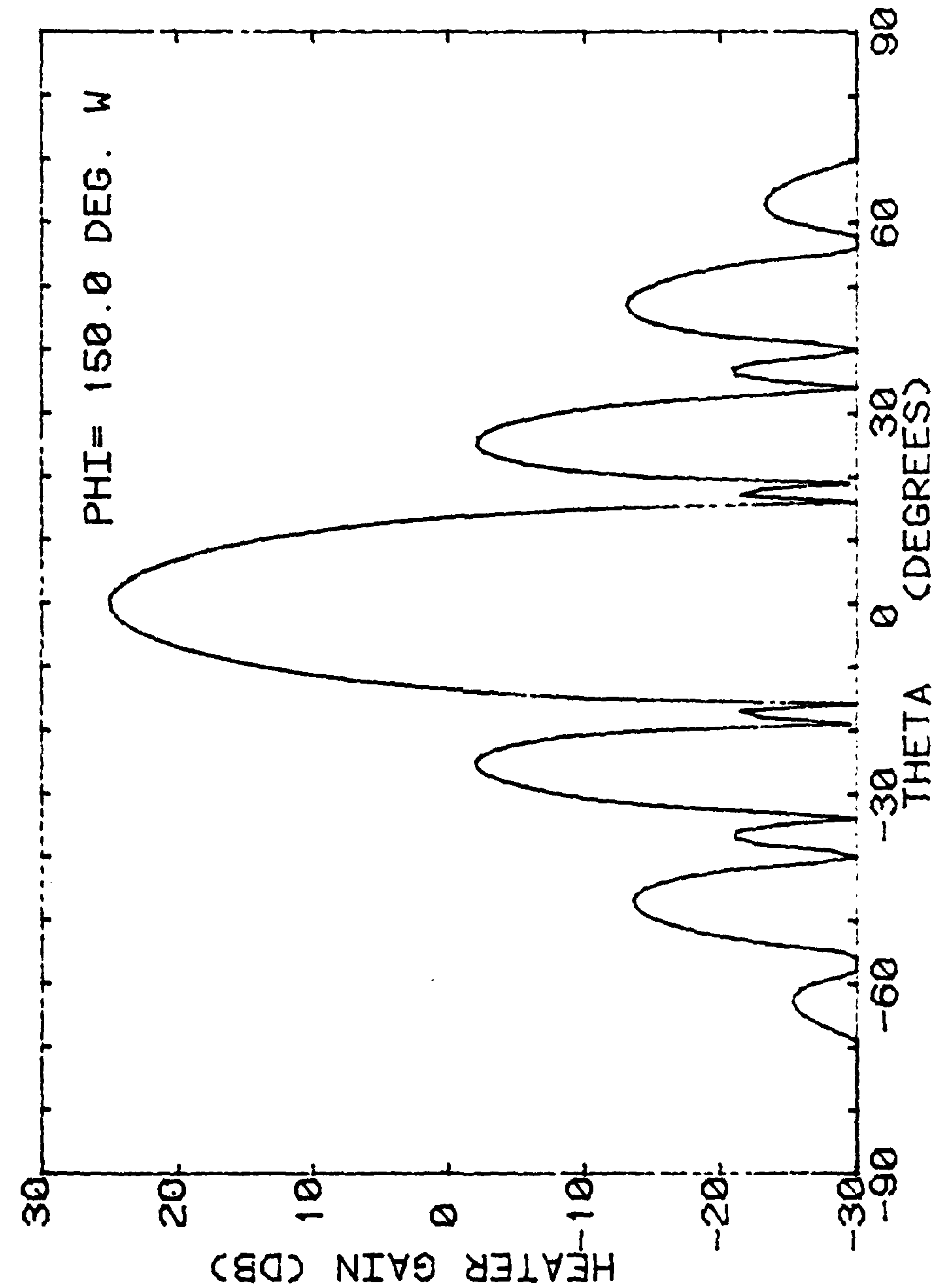
PHI= 150.0 DEG. W
HEATER GAIN (DB)
THETA (DEGREES)
30
20
10
0
-10
-20
-30
-90
-60
-30
0
30
60
90

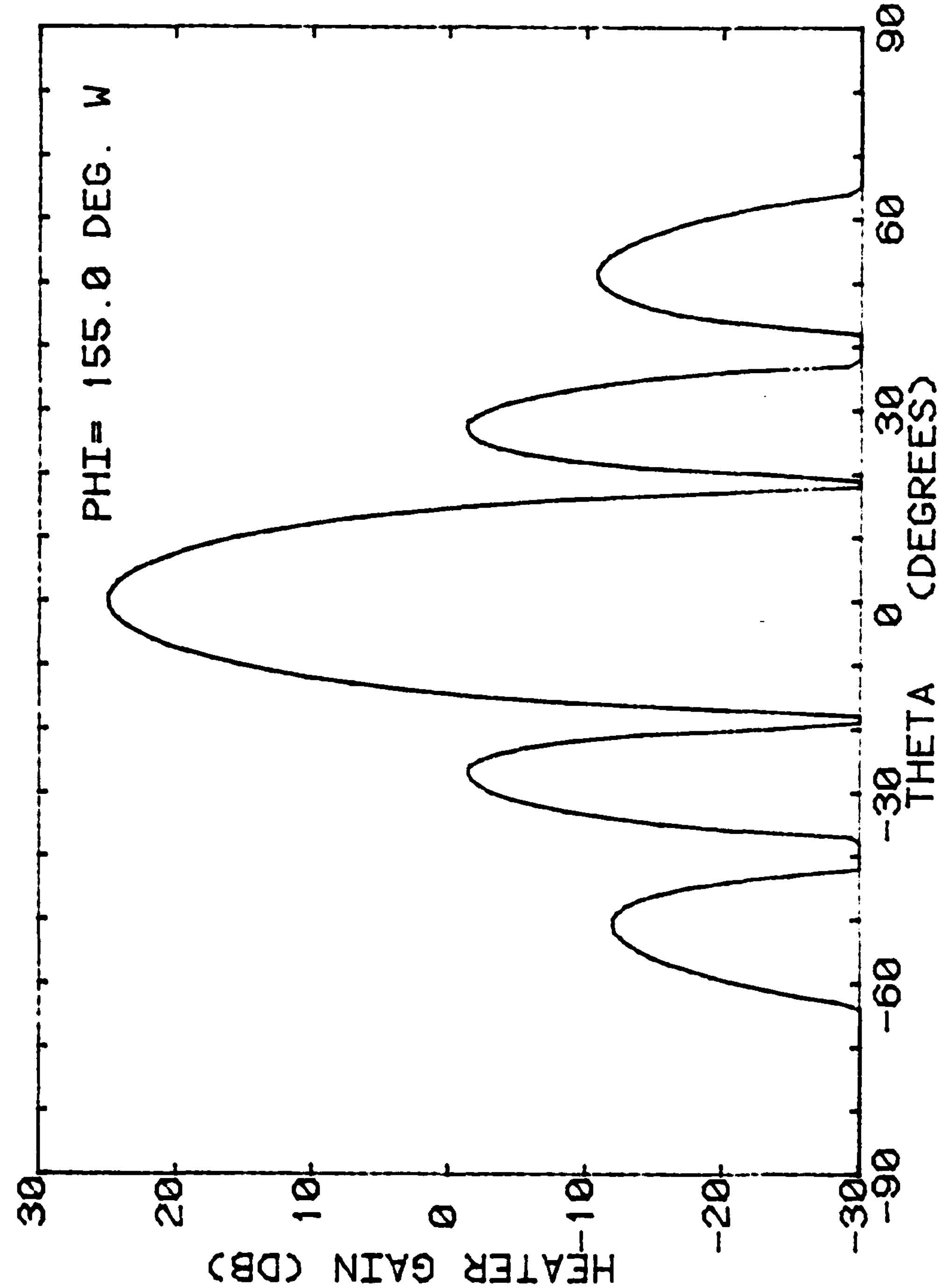
PHI= 155.0 DEG. W
HEATER GAIN (DB)
THETA (DEGREES)
30
20
10
0
-10
-20
-30
-90
-60
-30
0
30
60
90

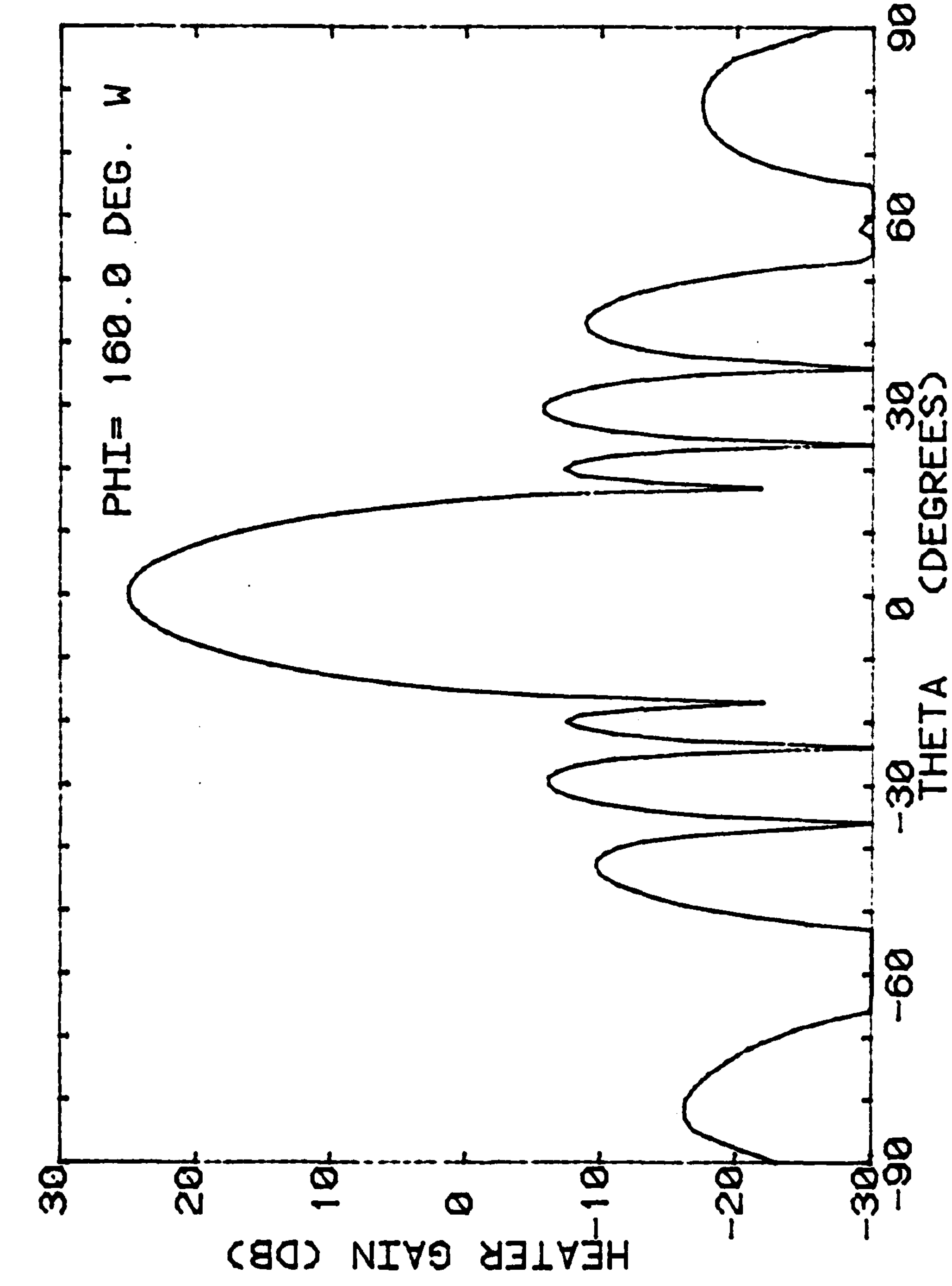
PHI= 160.0 DEG. W
HEATER GAIN (DB)
30
20
10
0
-10
-20
-30
-90
-60
-30
0
30
60
90
THETA (DEGREES)

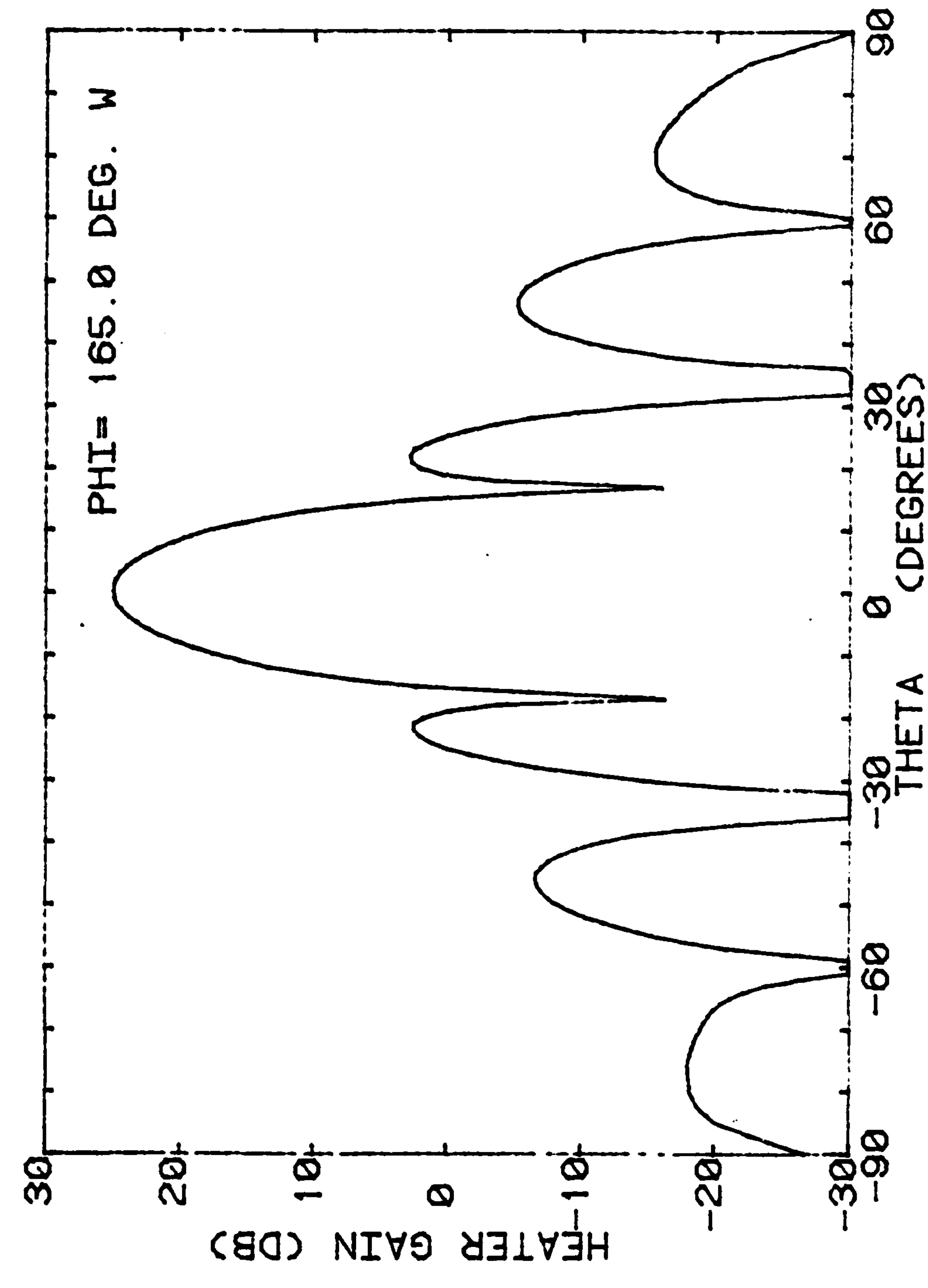
PHI= 165.0 DEG. W
HEATER GAIN (DB)
30
20
10
0
-10
-20
-30
-90
-60
-30
0
30
60
90
THETA (DEGREES)

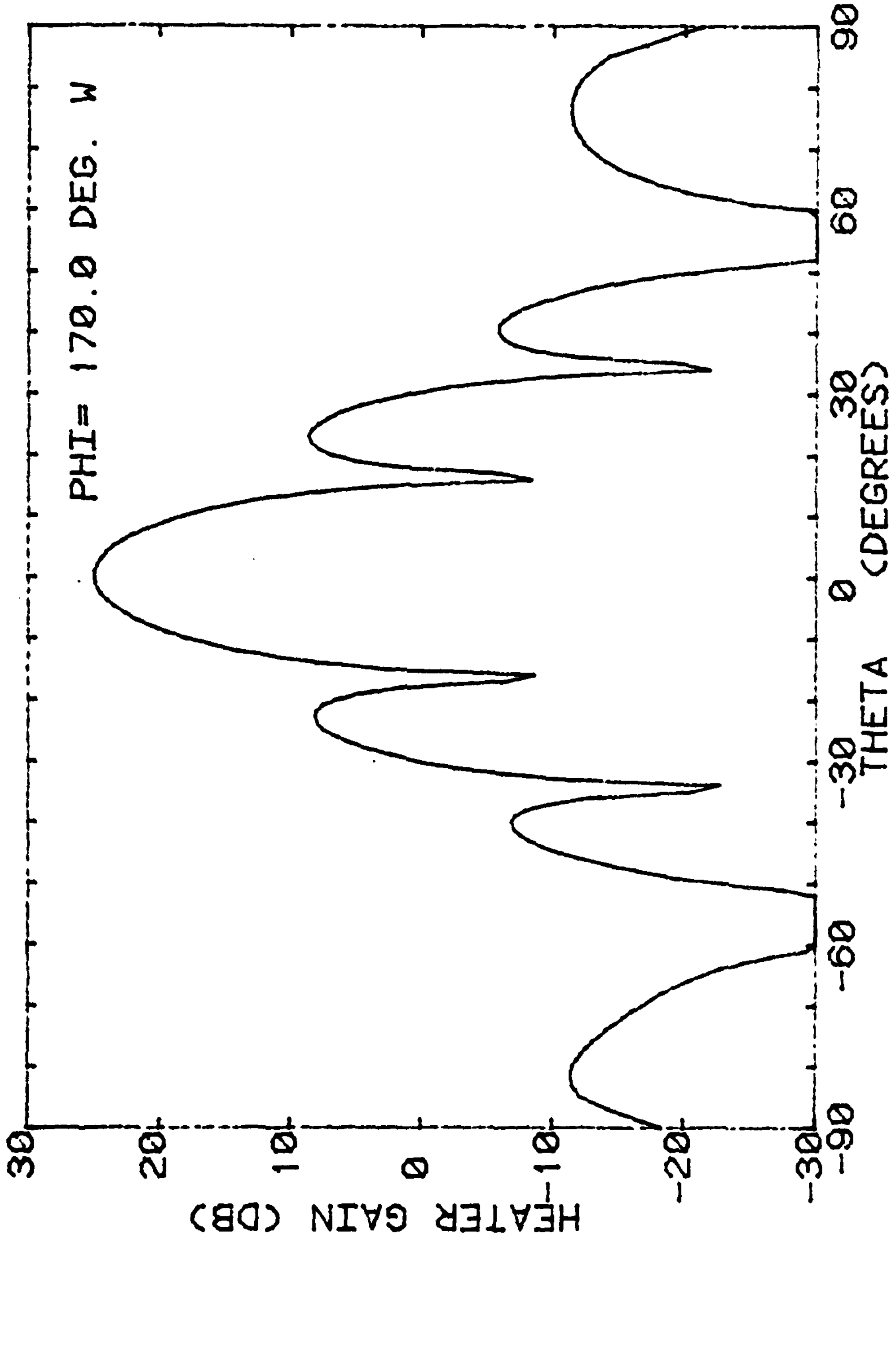
PHI= 170.0 DEG. W
HEATER GAIN (DB)
30
20
10
0
-10
-20
-30
-90
-60
-30
0
30
60
90
THETA (DEGREES)

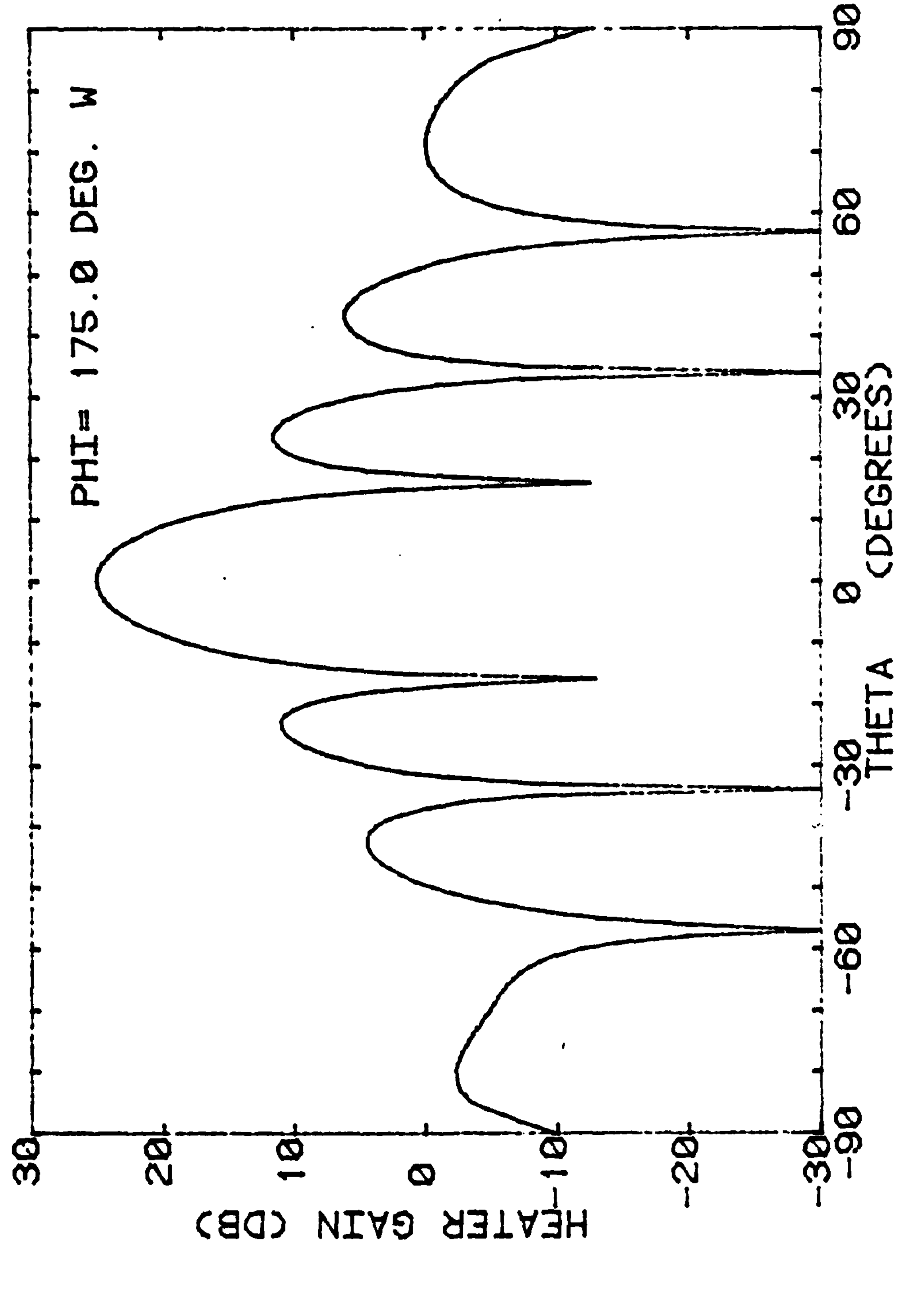
PHI= 175.0 DEG. W
HEATER GAIN (DB)
30
20
10
0
-10
-20
-30
-90
-60
-30
0
30
60
90
THETA (DEGREES)

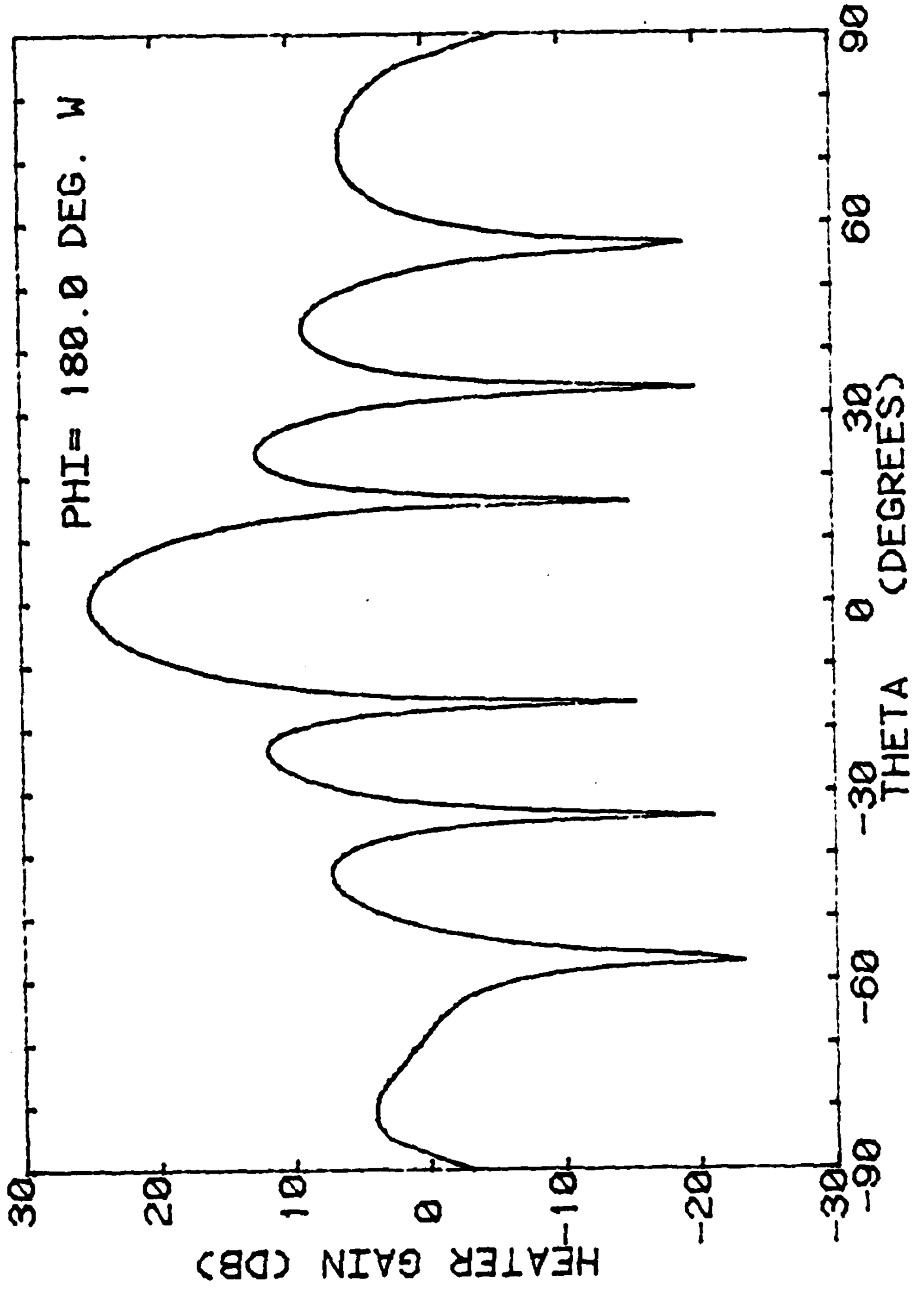
PHI= 180.0 DEG. W
HEATER GAIN (DB)
30
20
10
0
-10
-20
-30
-90
-60
-30
0
30
60
90
THETA (DEGREES)

Figure 1-11 Directive gain pattern for Arecibo Observatory HF heating array. Frequency = 5.1 MHz.

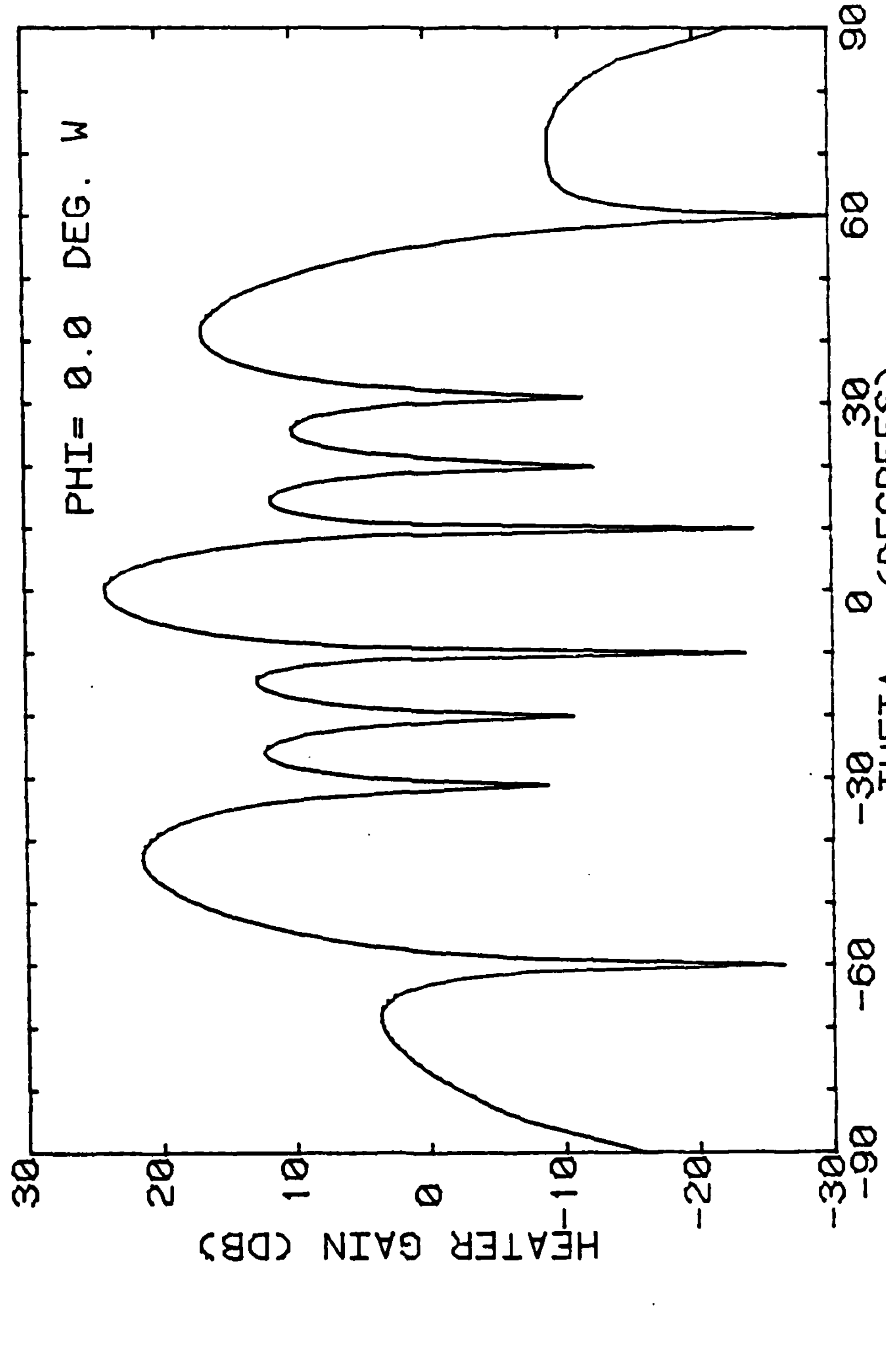
PHI= 0.0 DEG. W
HEATER GAIN (DB)
30
20
10
0
-10
-20
-30
-90
-60
-30
0
30
60
90
THETA (DEGREES)

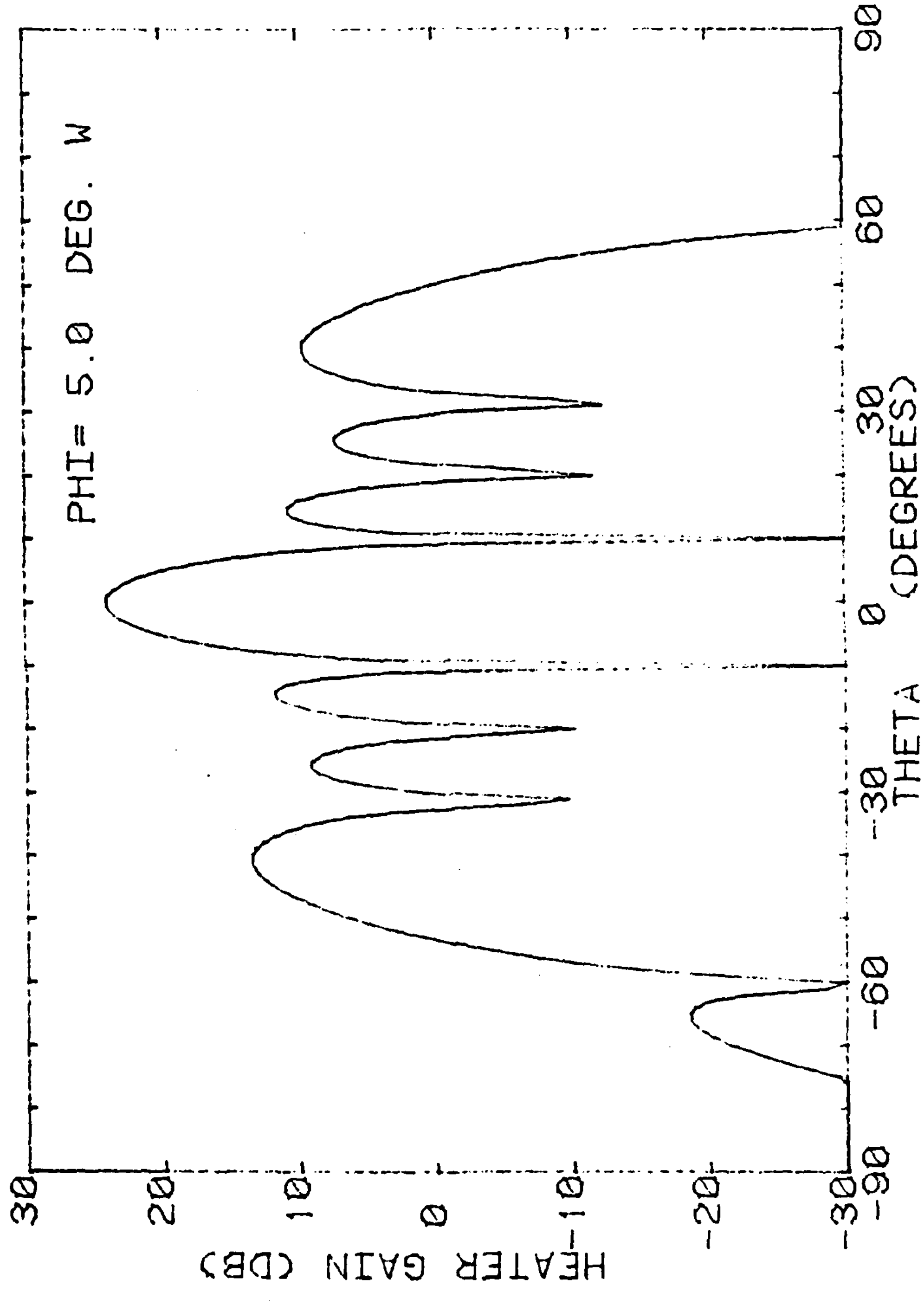
PHI= 5.0 DEG. W
HEATER GAIN (DB)
30
20
10
0
-10
-20
-30
-90
-60
-30
0
30
60
90
THETA (DEGREES)

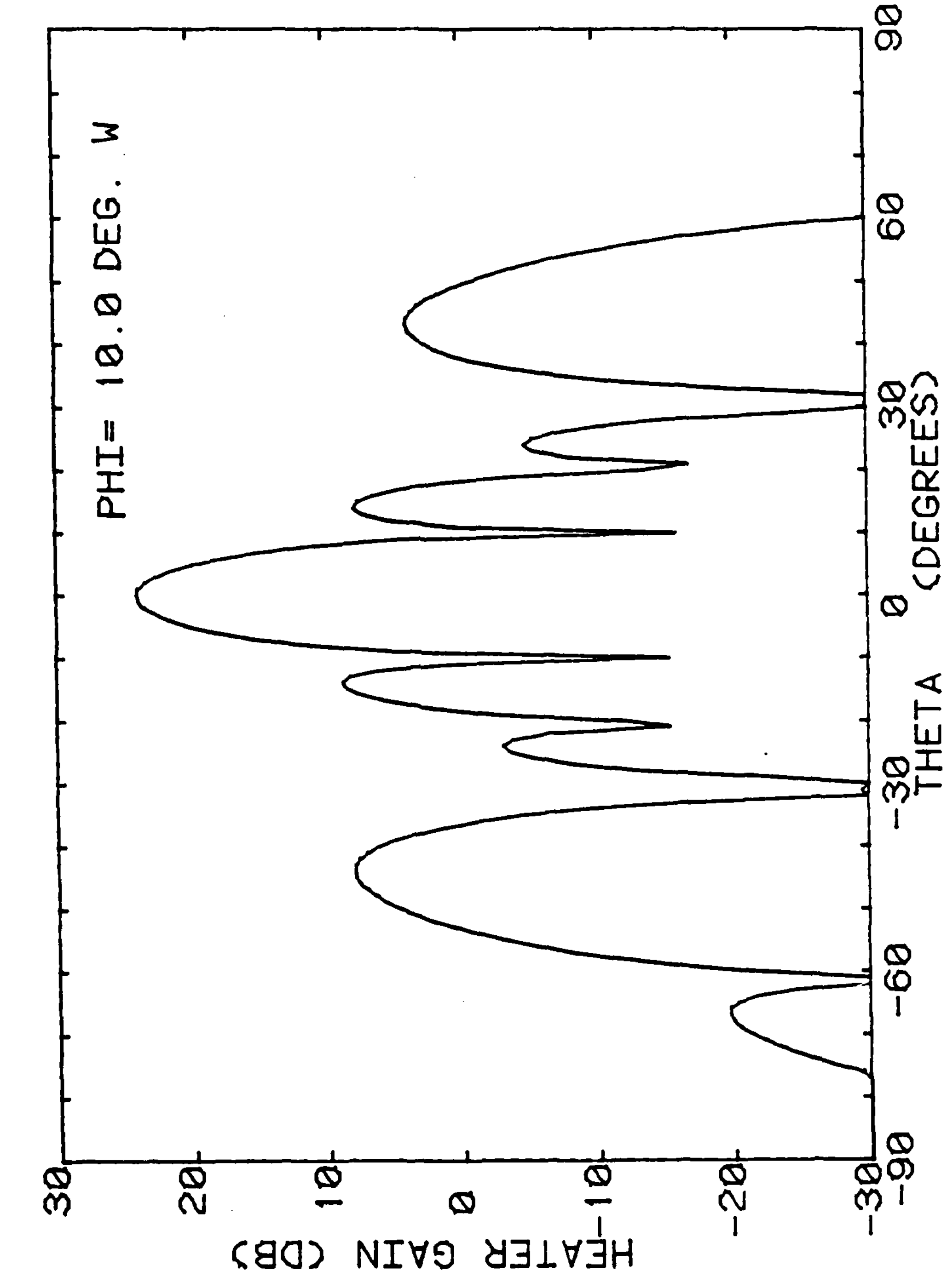
PHI= 10.0 DEG. W
HEATER GAIN (DB)
30
20
10
0
-10
-20
-30
-90
-60
-30
0
30
60
90
THETA (DEGREES)

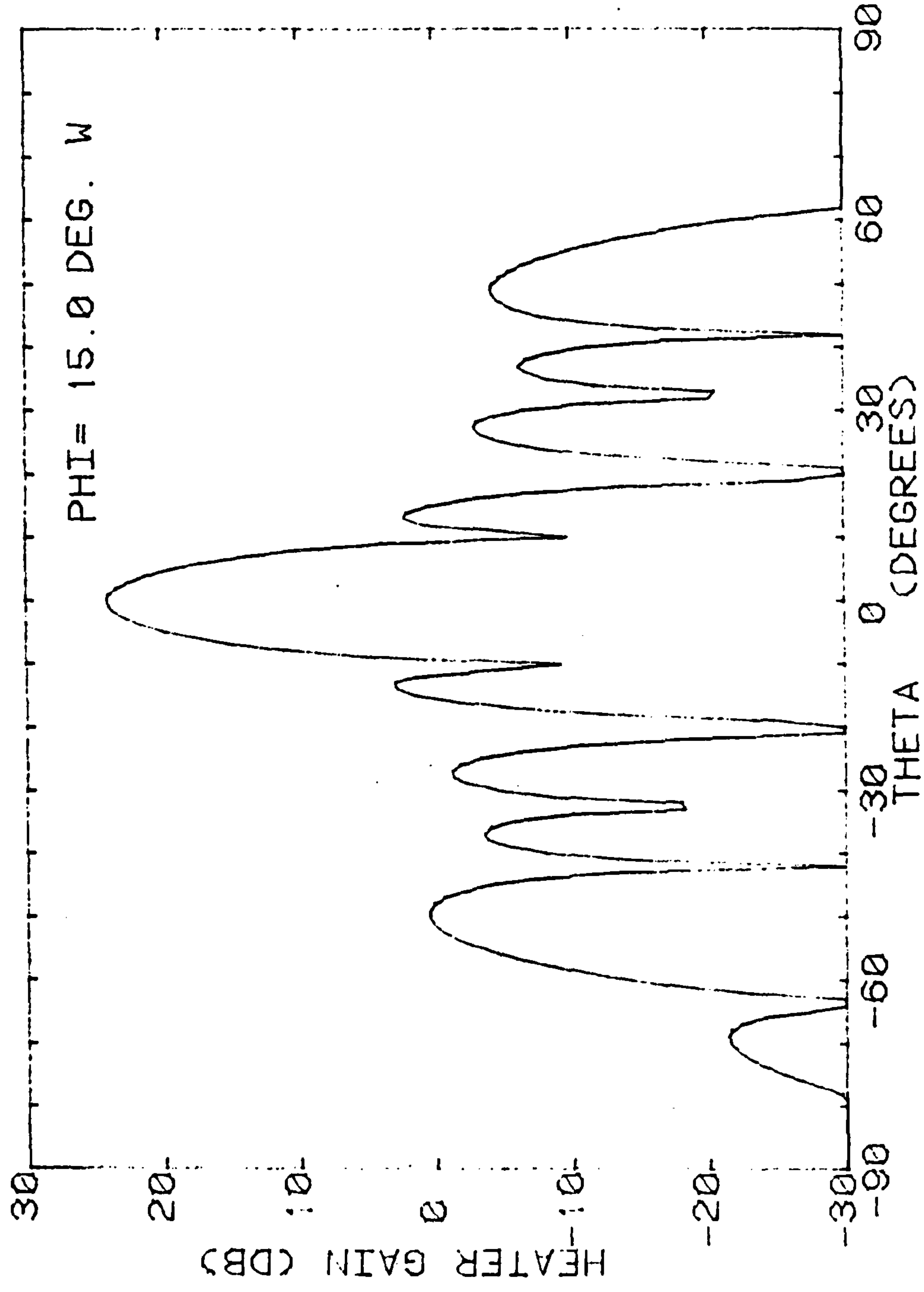
PHI= 15.0 DEG. W
HEATER GAIN (DB)
30
20
10
0
-10
-20
-30
-90
-60
-30
0
30
60
90
THETA (DEGREES)

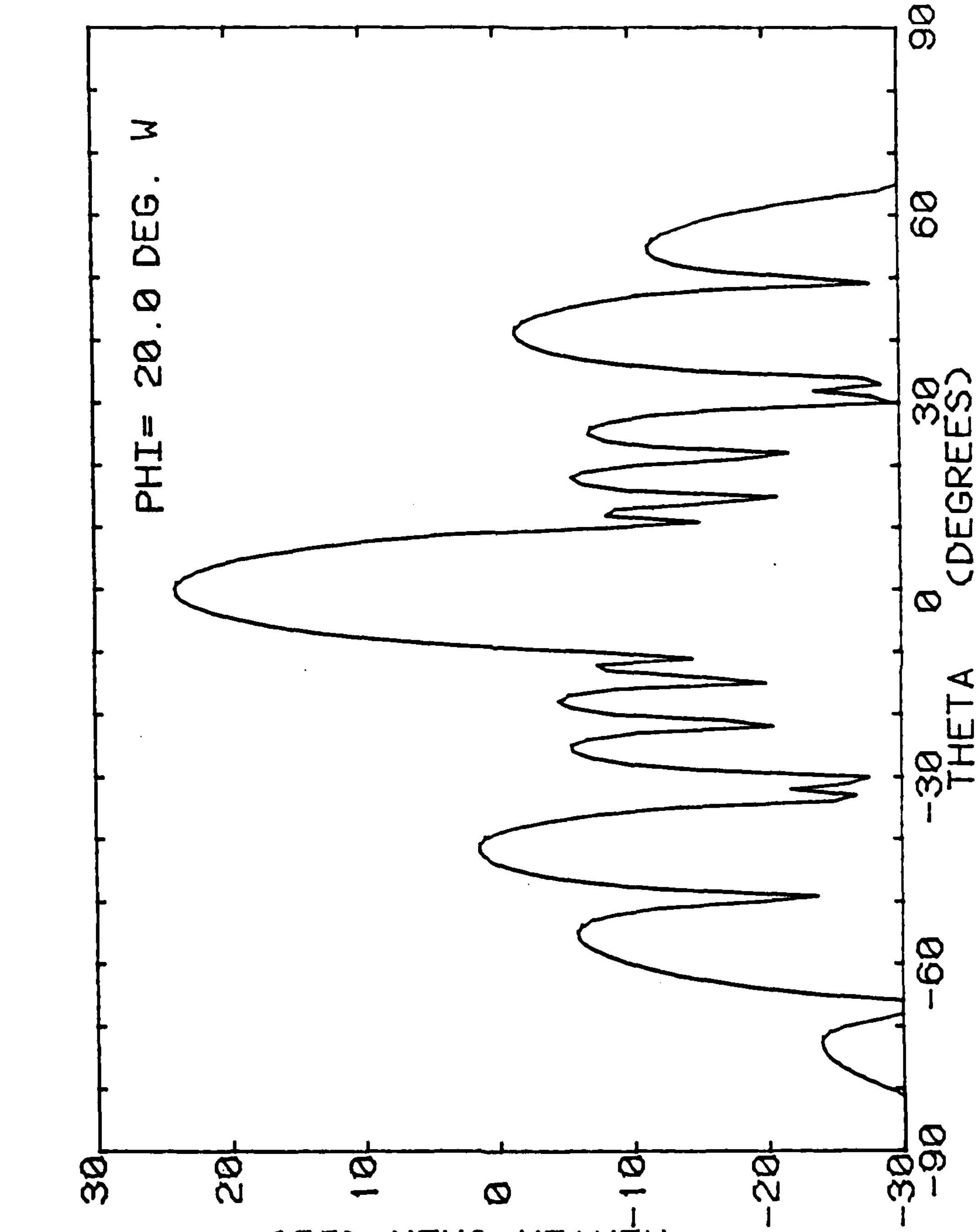
PHI= 20.0 DEG. W
HEATER GAIN (DB)
THETA (DEGREES)
30
20
10
0
-10
-20
-30
-90
-60
-30
0
30
60
90

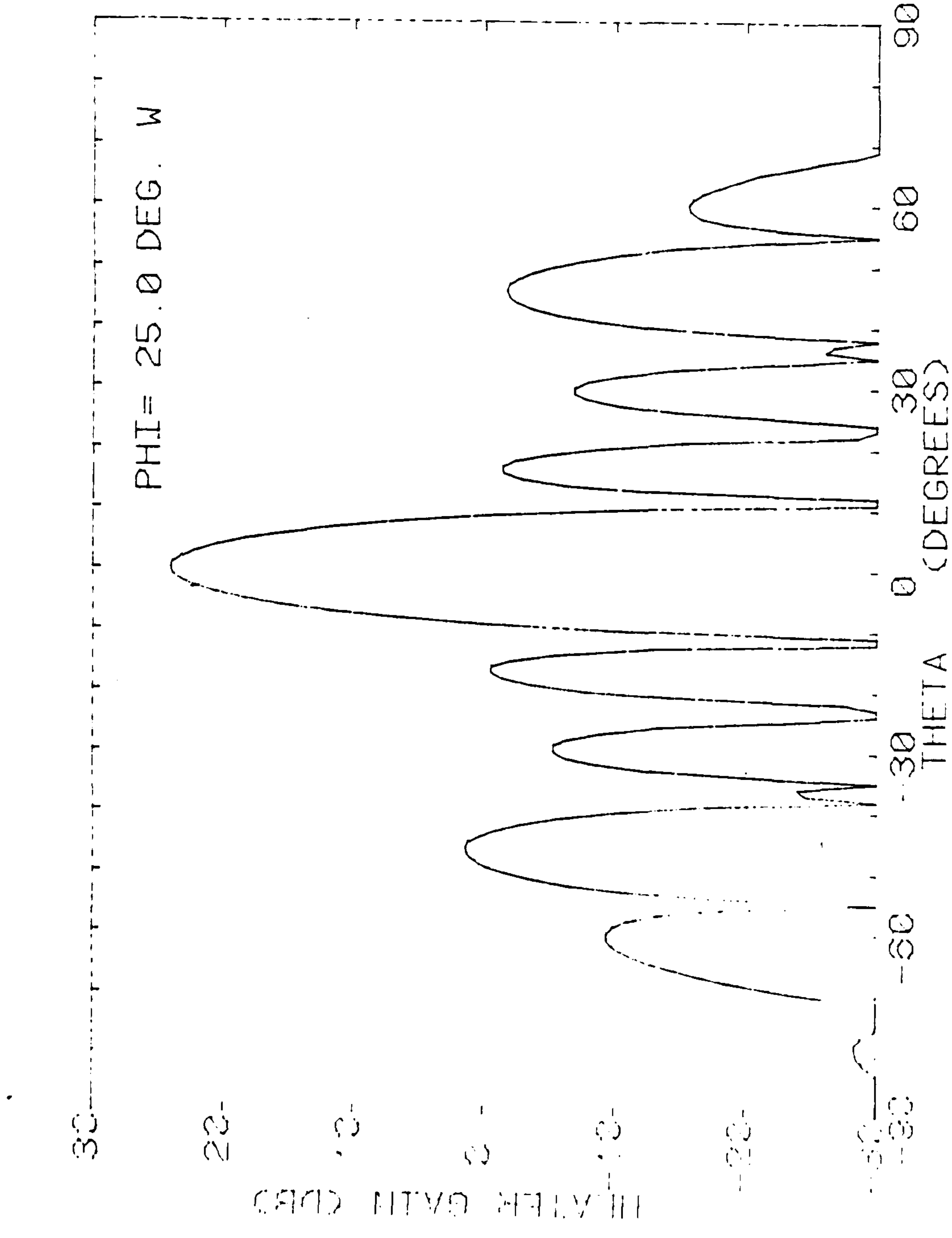
PHI= 25.0 DEG. W
THETA (DEGREES)
-90
-60
-30
0
30
60
90
30
20

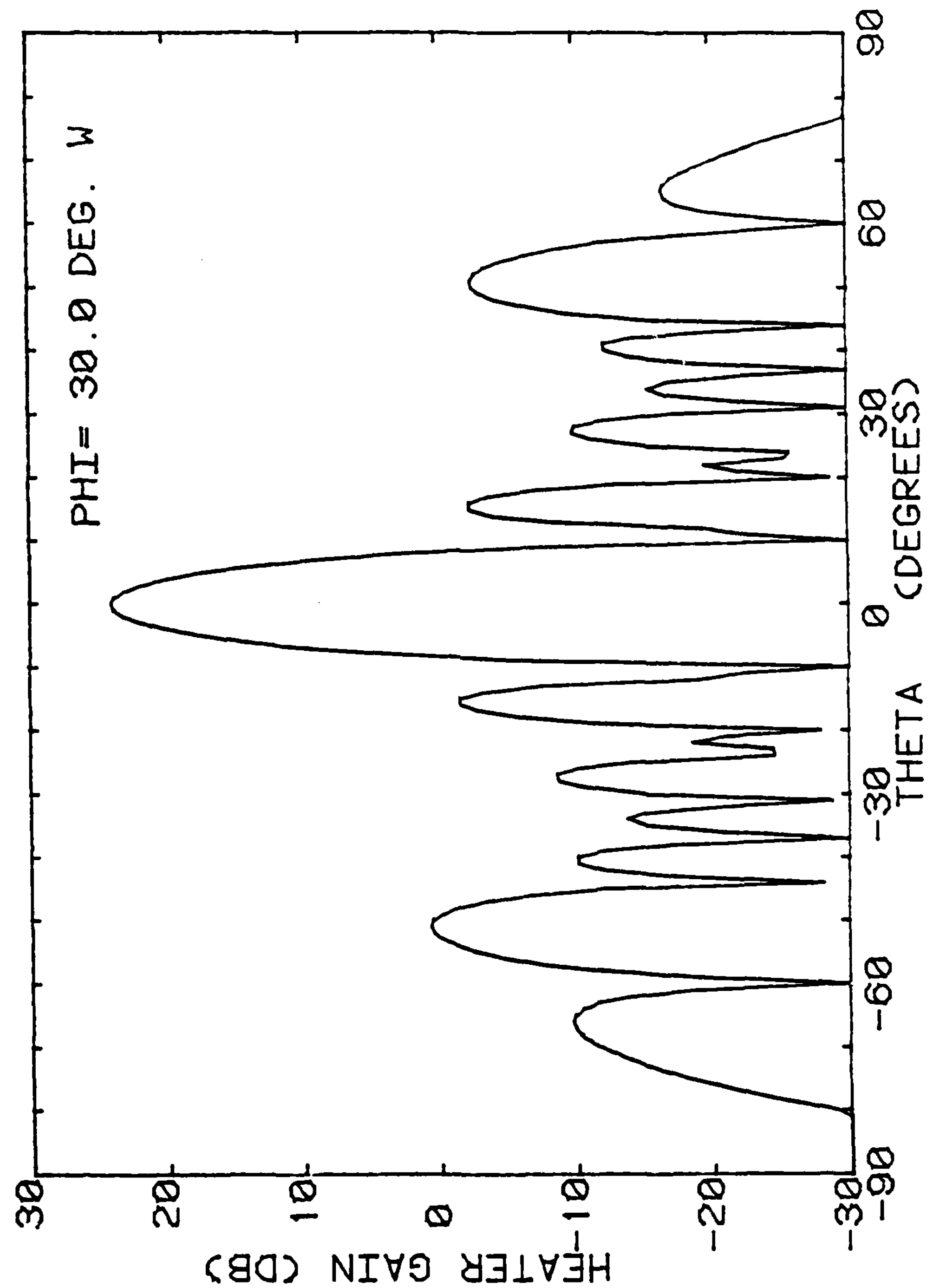
PHI= 30.0 DEG. W
HEATER GAIN (DB)
30
20
10
0
-10
-20
-30
THETA (DEGREES)
-90
-60
-30
0
30
60
90

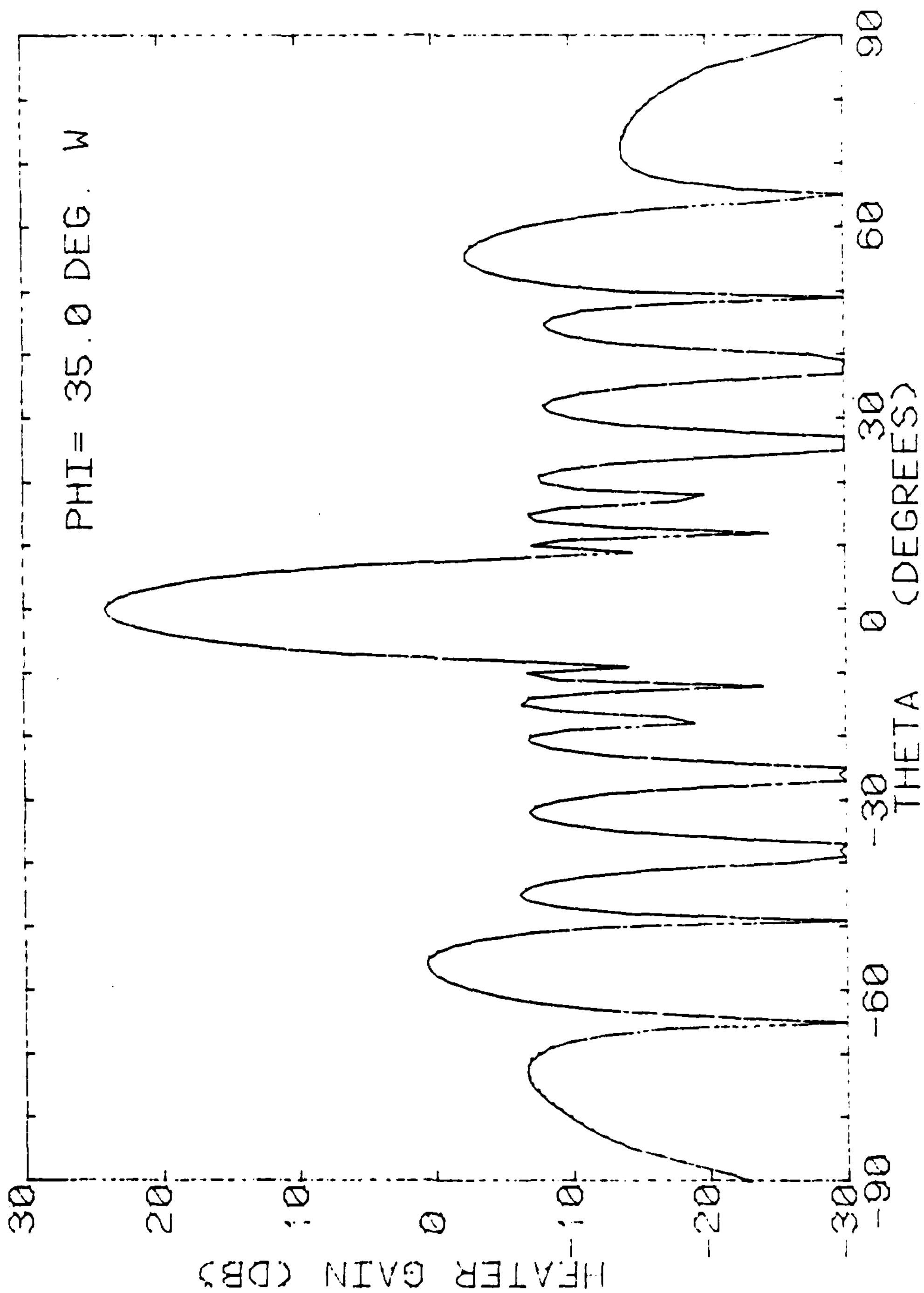
PHI= 35.0 DEG. W
30
20
10
0
-10
-20
-30
HEATER GAIN (DB)
-90
-60
-30
0
30
60
90
THETA (DEGREES)

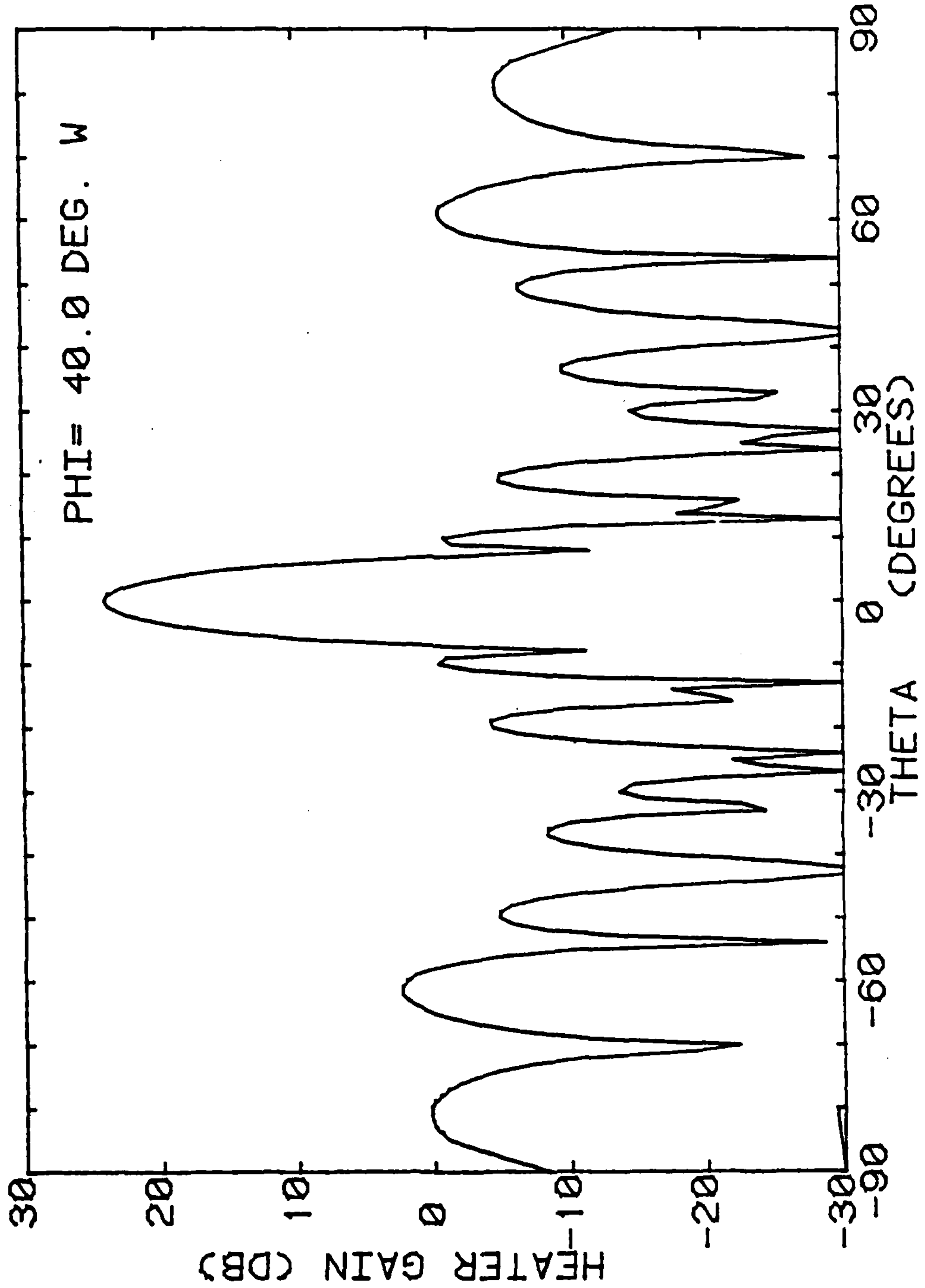
PHI= 40.0 DEG. W
HEATER GAIN (DB)
30
20
10
0
-10
-20
-30
-90
-60
-30
0
30
60
90
THETA (DEGREES)

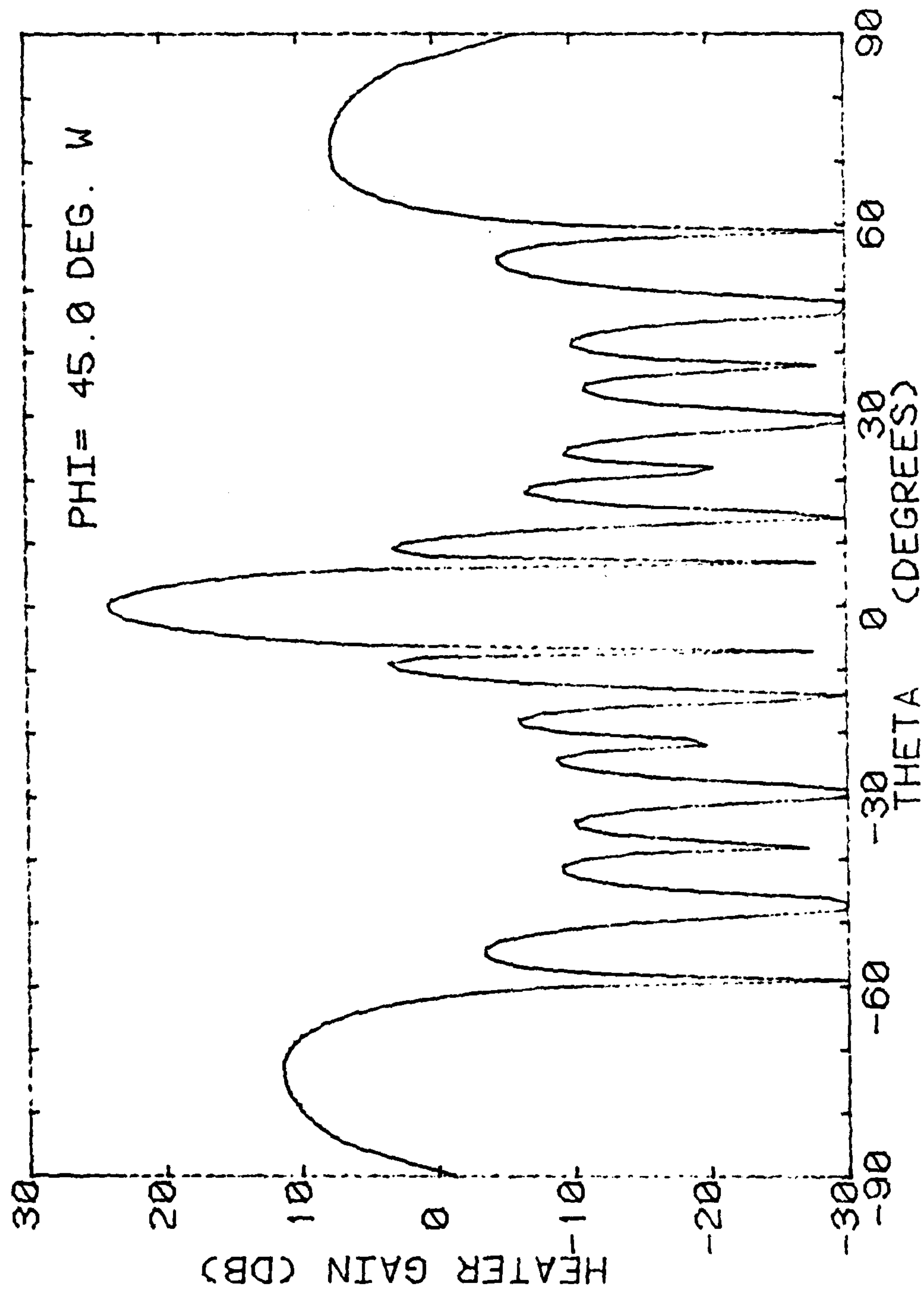
PHI= 45.0 DEG. W
HEATER GAIN (DB)
30
20
10
0
-10
-20
-30
-90
-60
-30
0
30
60
90
THETA (DEGREES)

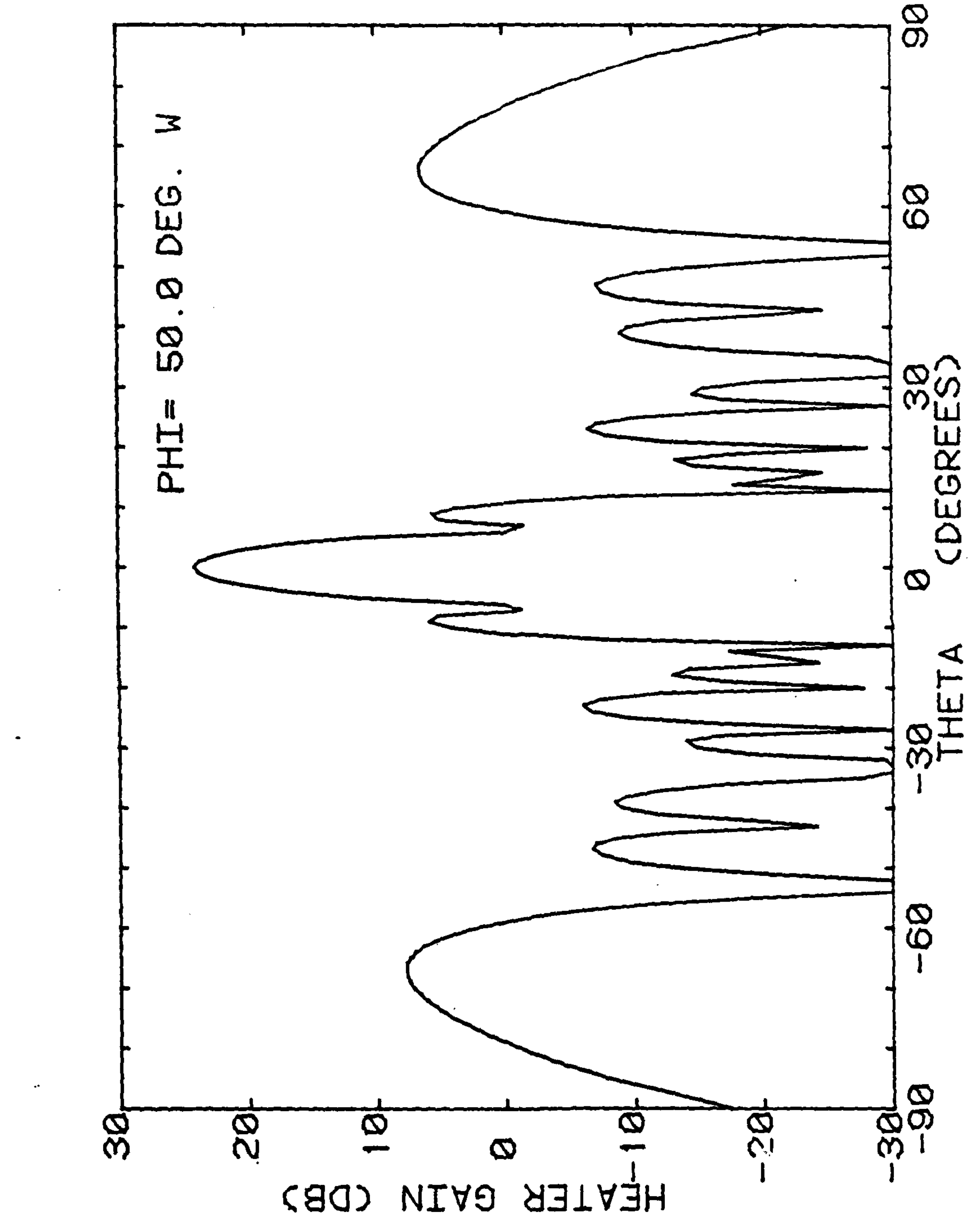
PHI= 50.0 DEG. W
HEATER GAIN (DB)
THETA (DEGREES)
30
20
10
0
-10
-20
-30
-90
-60
-30
0
30
60
90

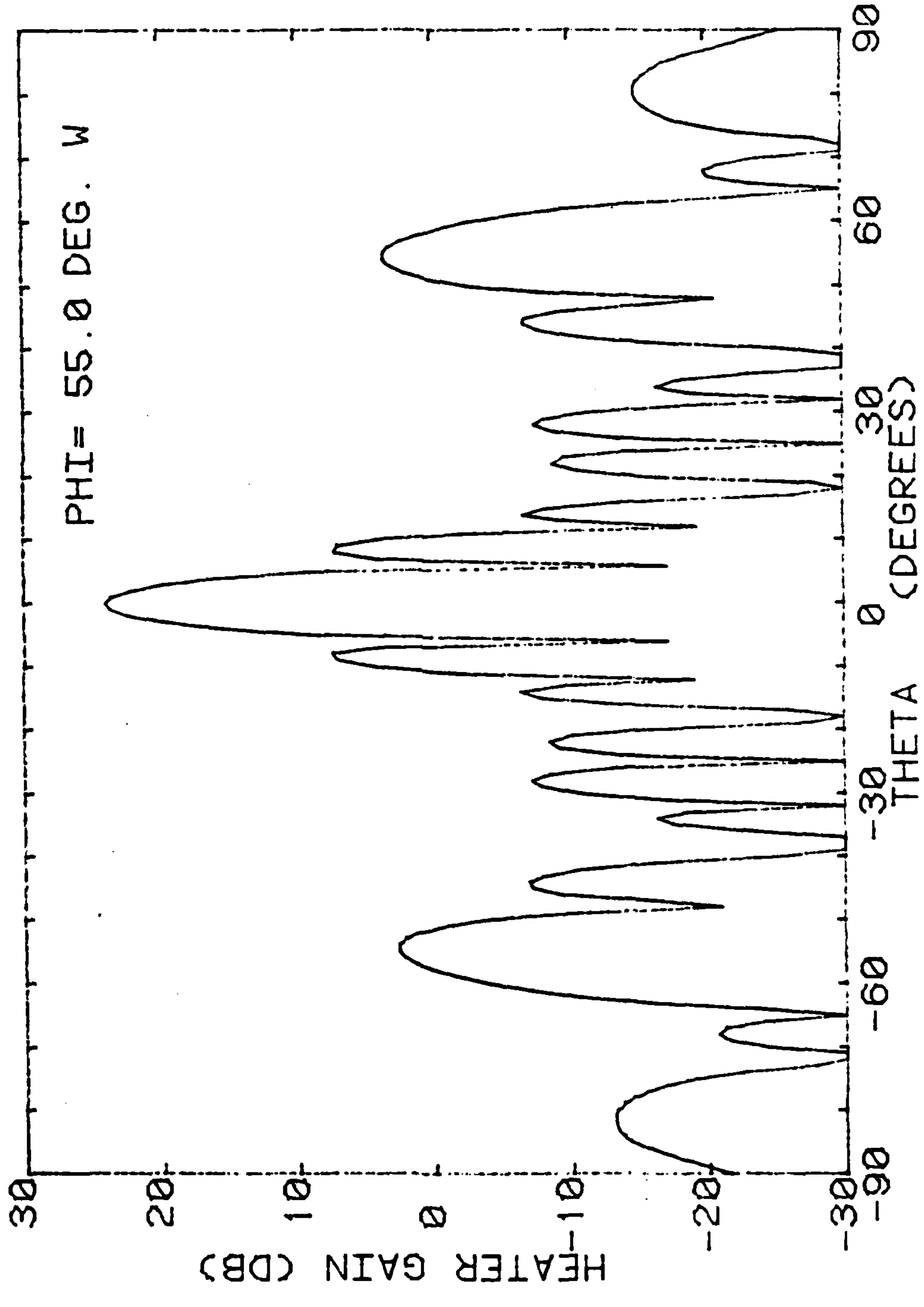

PHI= 55.0 DEG. W
HEATER GAIN (DB)
THETA (DEGREES)
30
20
10
0
-10
-20
-30
-90
-60
-30
0
30
60
90

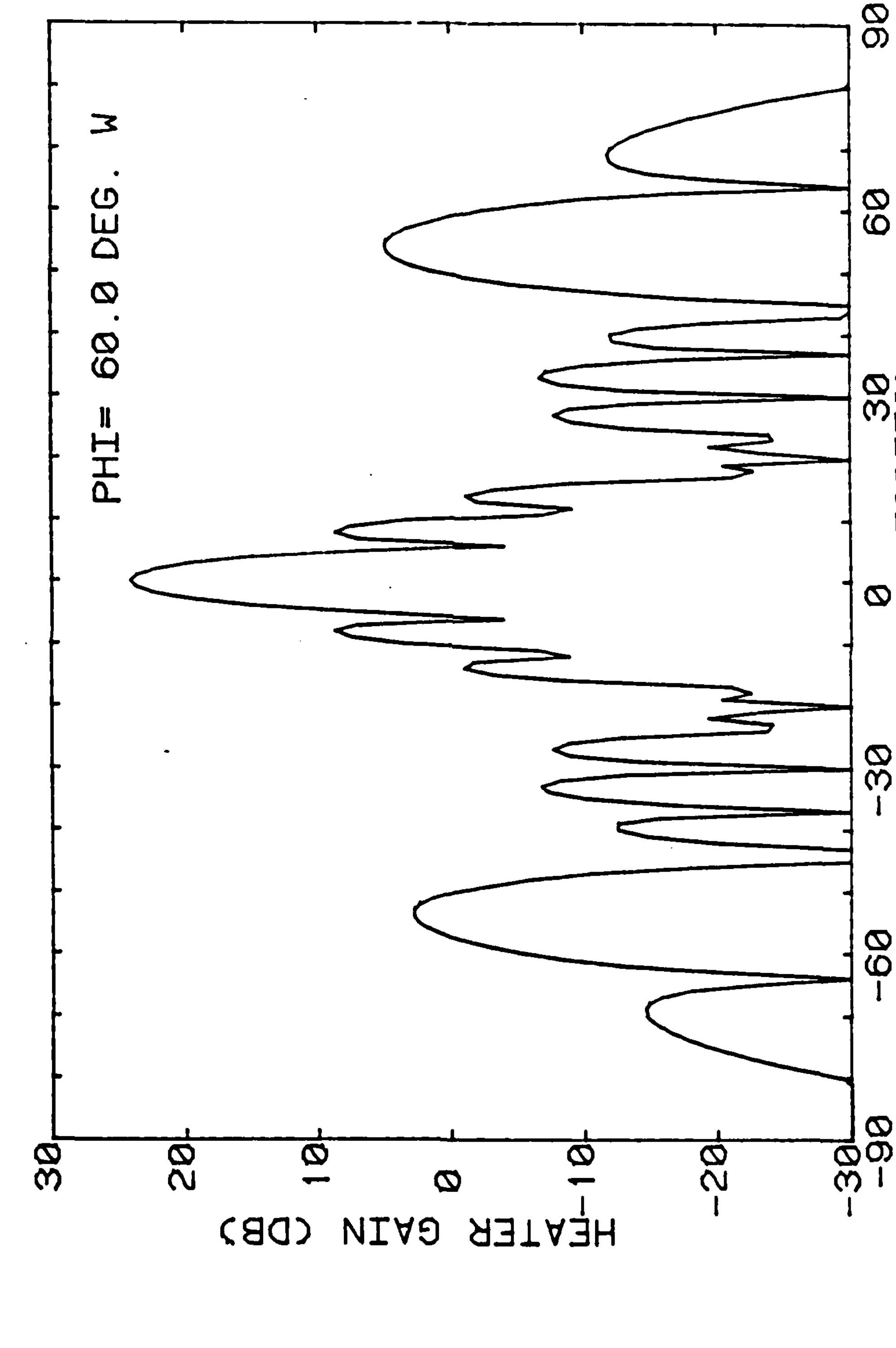
PHI= 60.0 DEG. W
HEATER GAIN (DB)
30
20
10
0
-10
-20
-30
-90
-60
-30
0
30
60
90
THETA (DEGREES)

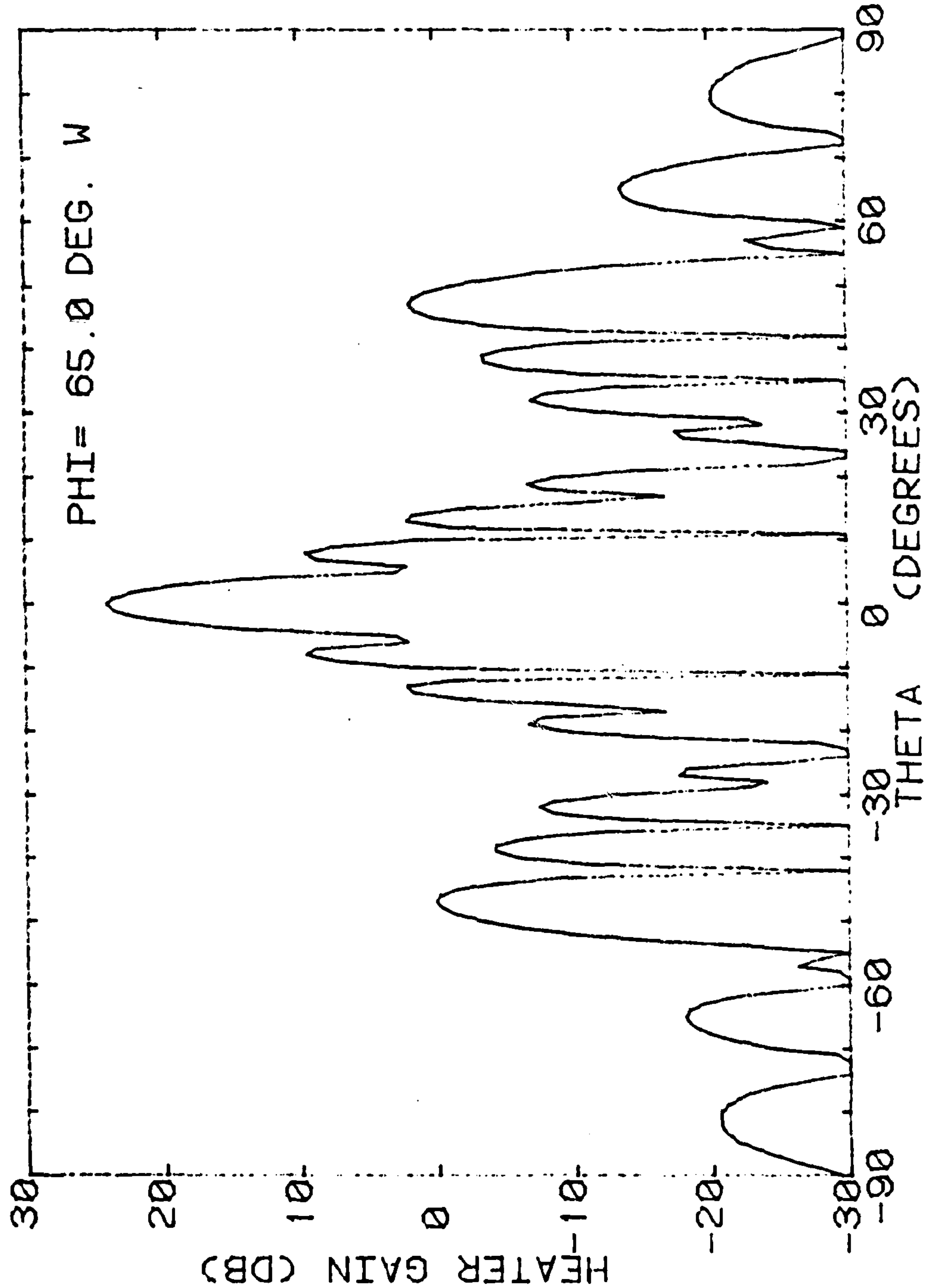
PHI= 65.0 DEG. W
HEATER GAIN (DB)
30
20
10
0
-10
-20
-30
-90
-60
-30
0
30
60
90
THETA (DEGREES)

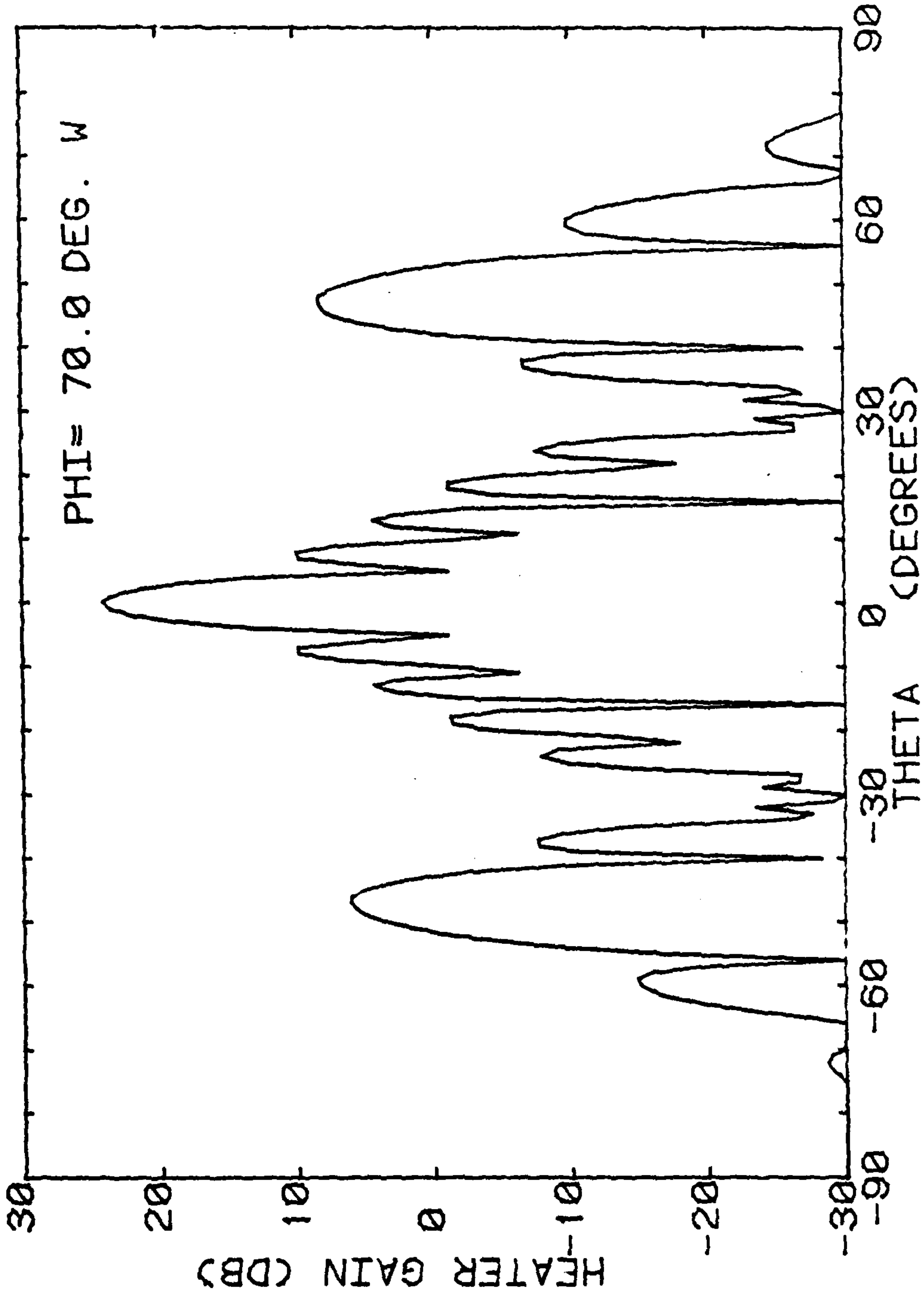
PHI= 70.0 DEG. W
HEATER GAIN (DB)
30
20
10
0
-10
-20
-30
-90
-60
-30
0
30
60
90
THETA (DEGREES)

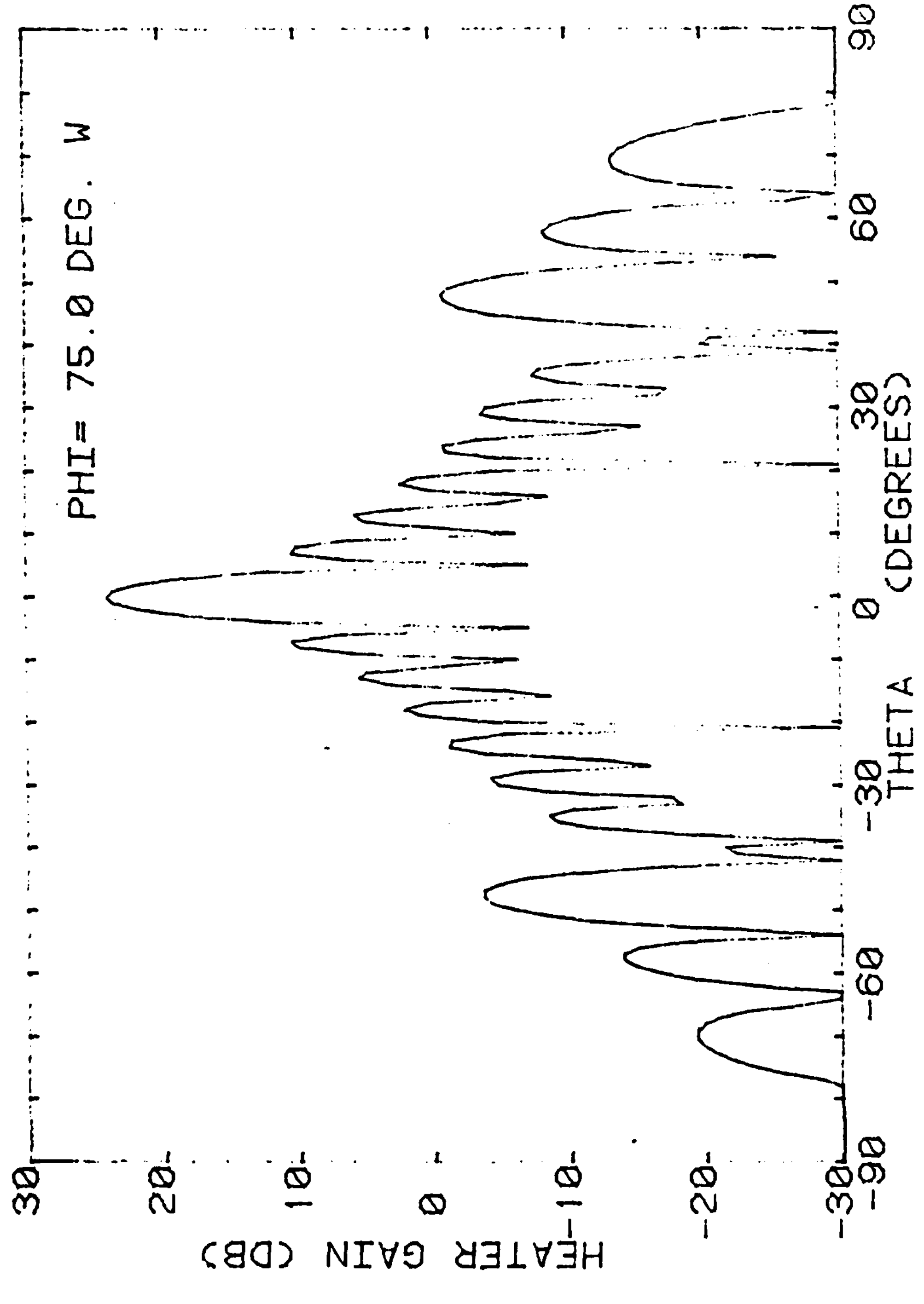
PHI= 75.0 DEG. W
HEATER GAIN (DB)
30
20
10
0
-10
-20
-30
-90
-60
-30
0
30
60
90
THETA (DEGREES)

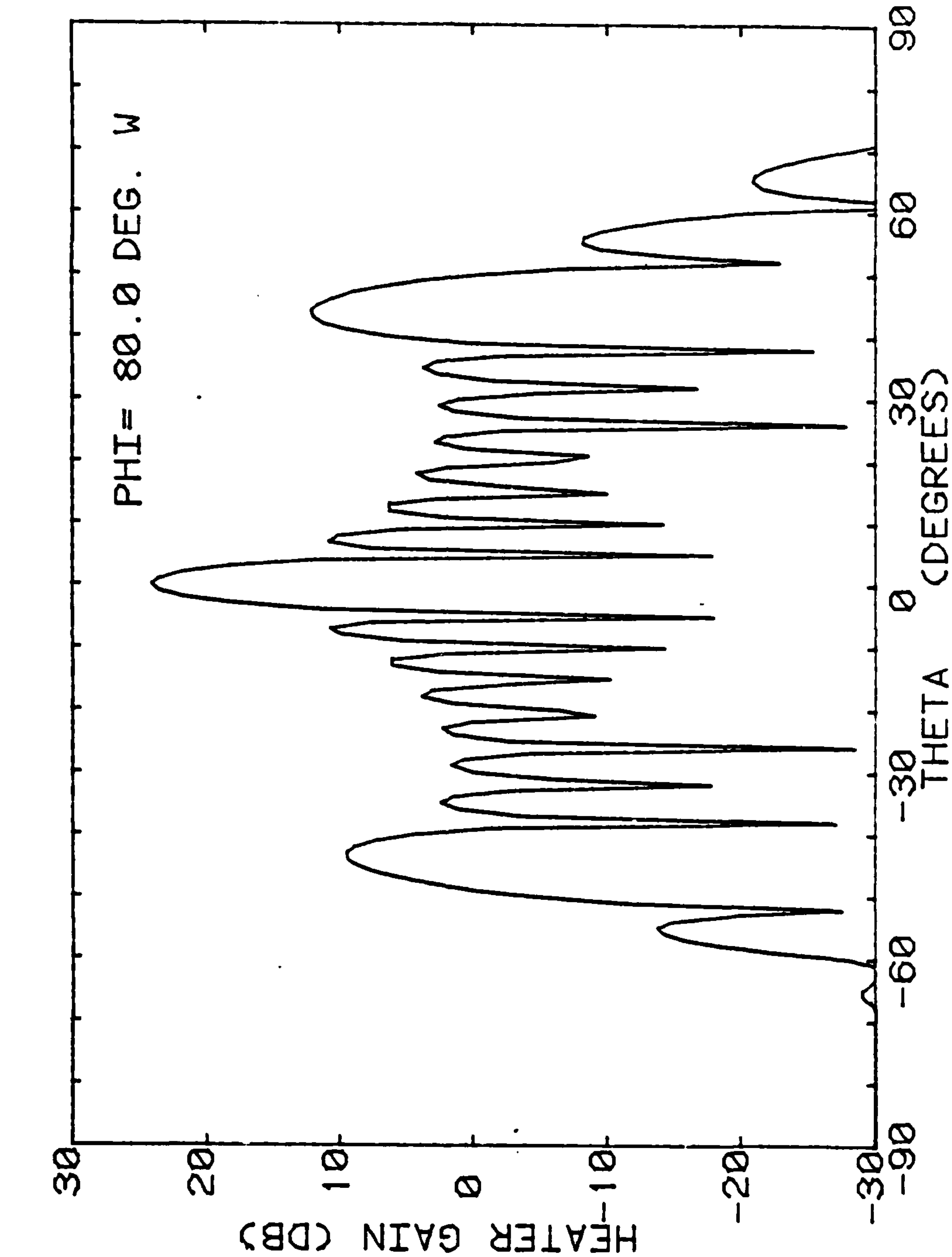
PHI= 80.0 DEG. W
HEATER GAIN (DB)
THETA (DEGREES)
30
20
10
0
-10
-20
-30
-90
-60
-30
0
30
60
90

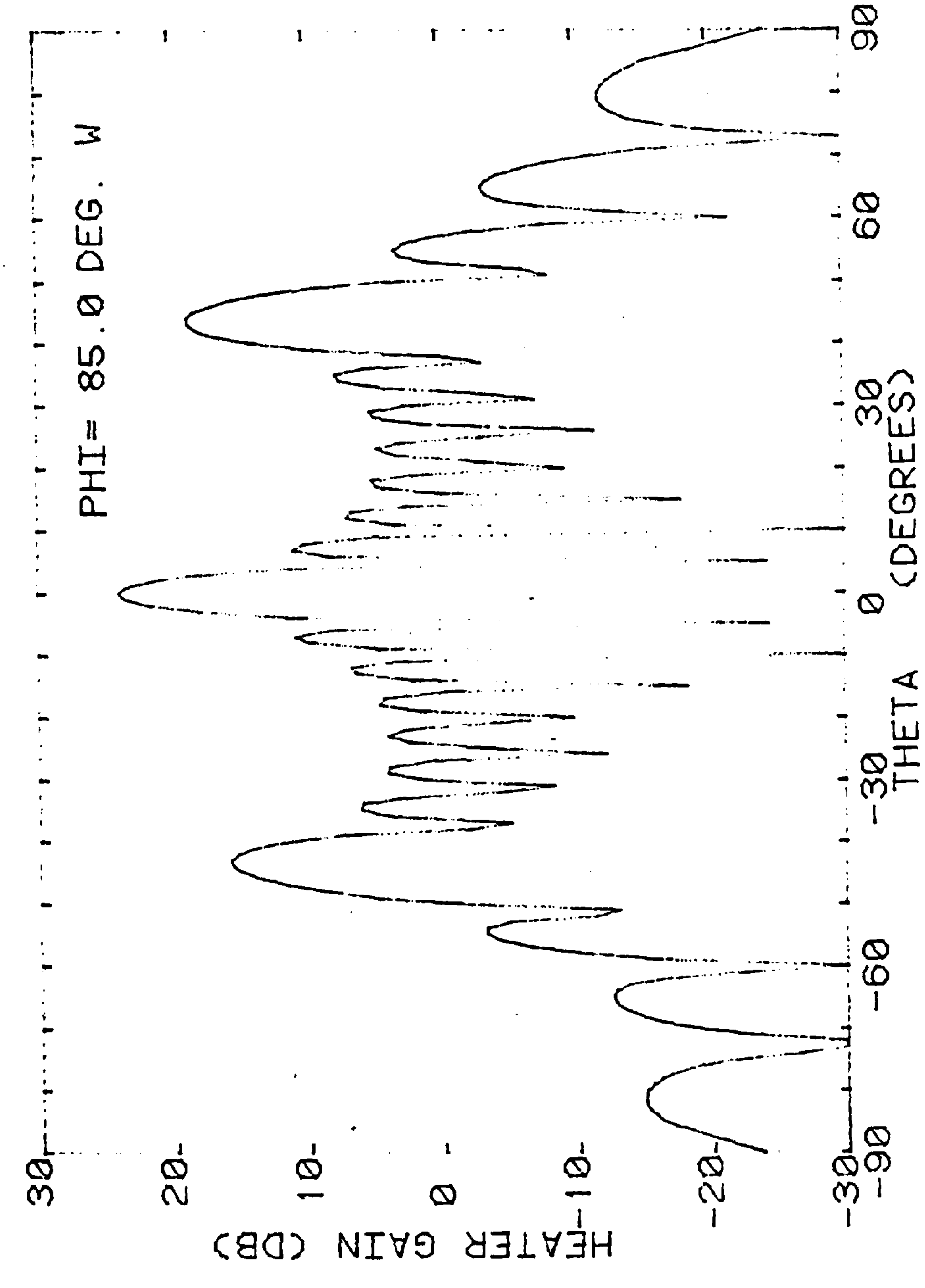
PHI= 85.0 DEG. W
HEATER GAIN (DB)
30
20
10
0
-10
-20
-30
-90
-60
-30
0
30
60
90
THETA (DEGREES)

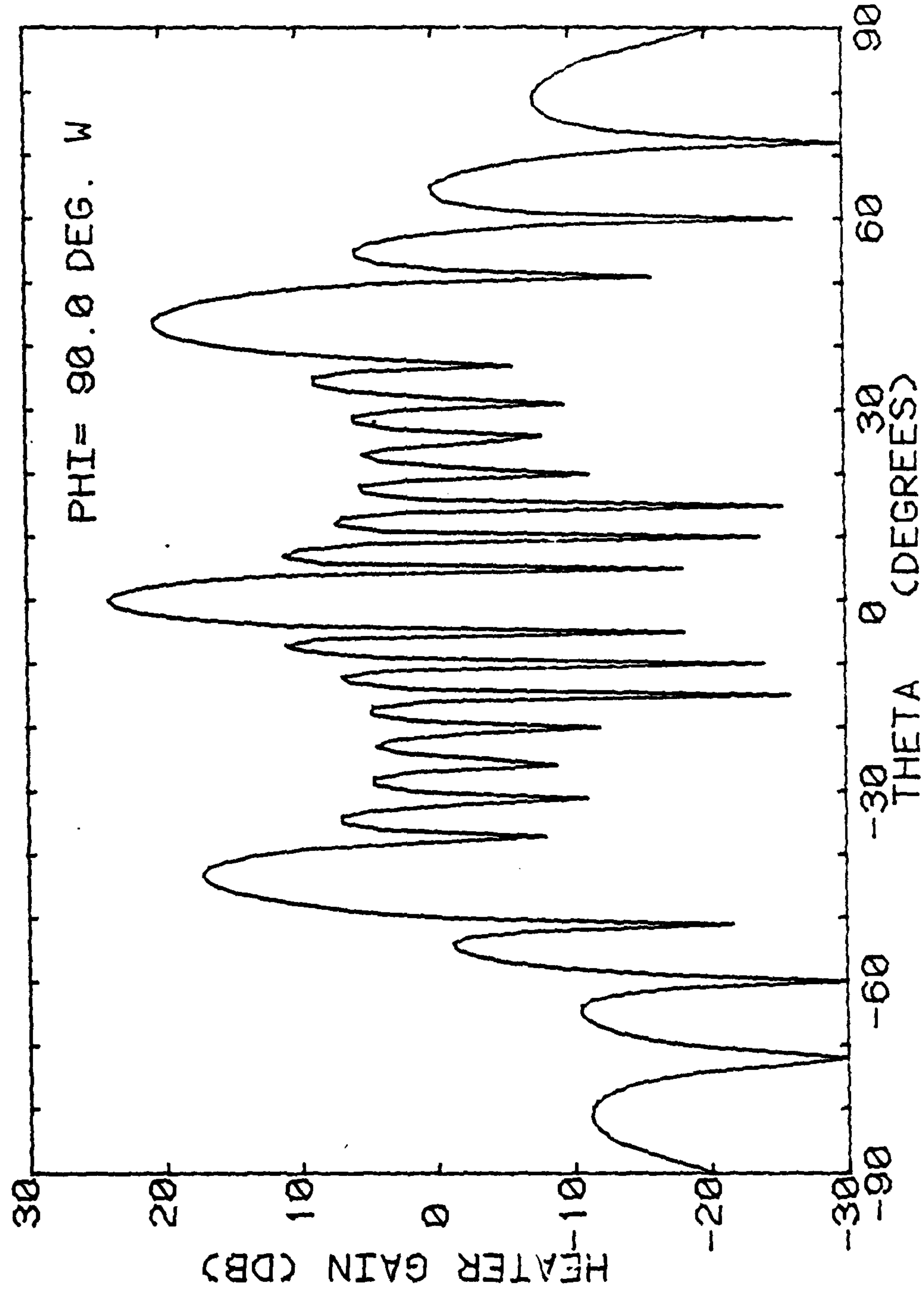
PHI= 90.0 DEG. W
HEATER GAIN (DB)
THETA (DEGREES)
30
20
10
0
-10
-20
-30
-90
-60
-30
0
30
60
90

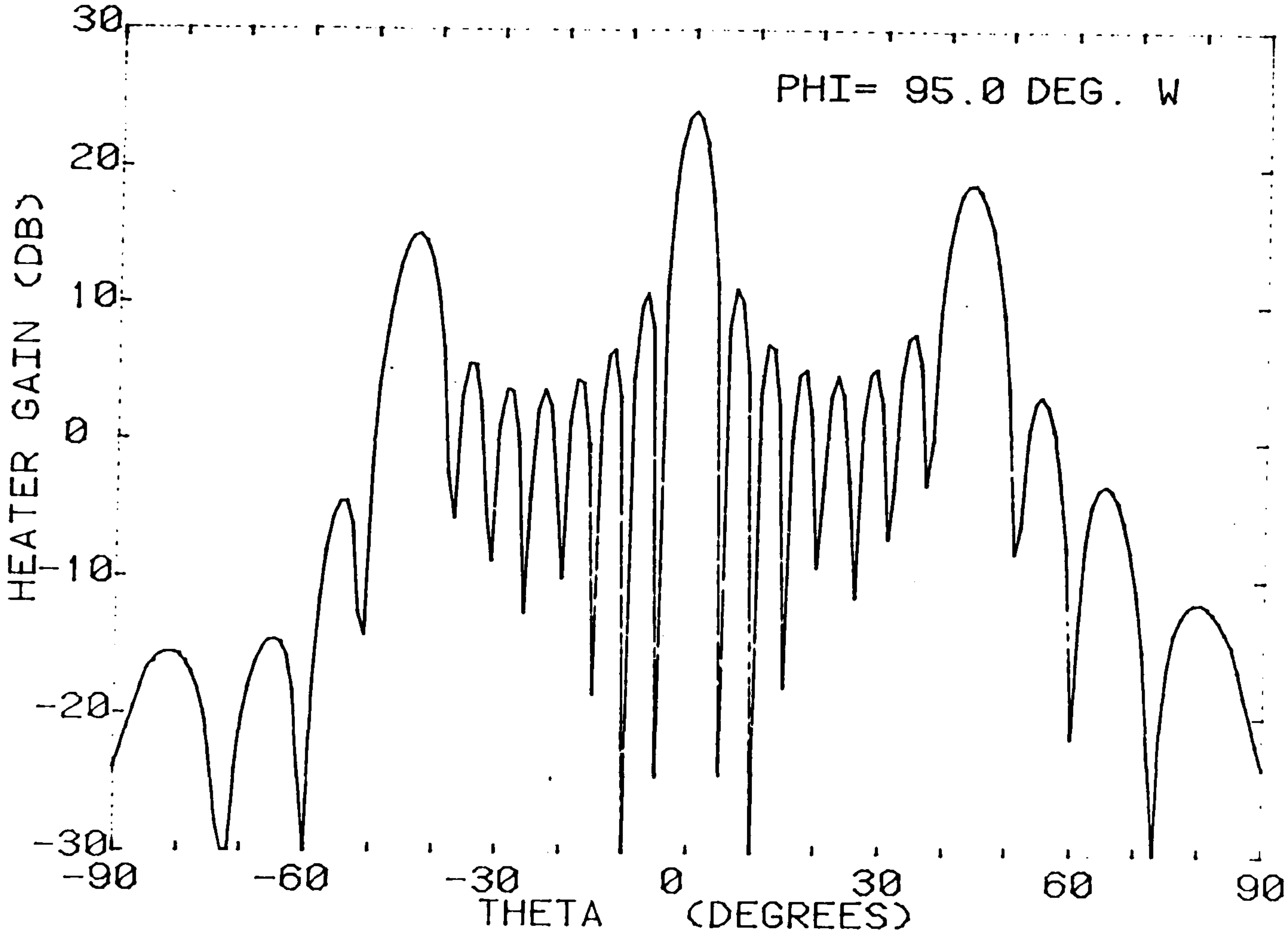
PHI= 95.0 DEG. W
HEATER GAIN (DB)
30
20
10
0
-10
-20
-30
-90
-60
-30
0
30
60
90
THETA (DEGREES)

AD-A126 809 EFFECT OF HF HEATING ARRAY DIRECTIVITY PATTERN ON THE FREQUENCY RESPONSE O..(U) PENNSYLVANIA STATE UNIV UNIVERSITY PARK IONOSPHERE RESEARCH L.. 2/3

UNCLASSIFIED K J CARROLL ET AL. JAN 83 PSU-IRL-SCI-475 F/G 20/14 NL

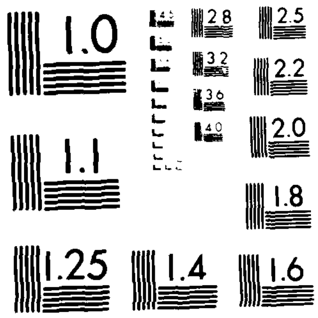

MICROCOPY RESOLUTION TEST CHART
NATIONAL BUREAU OF STANDARDS-1963-A

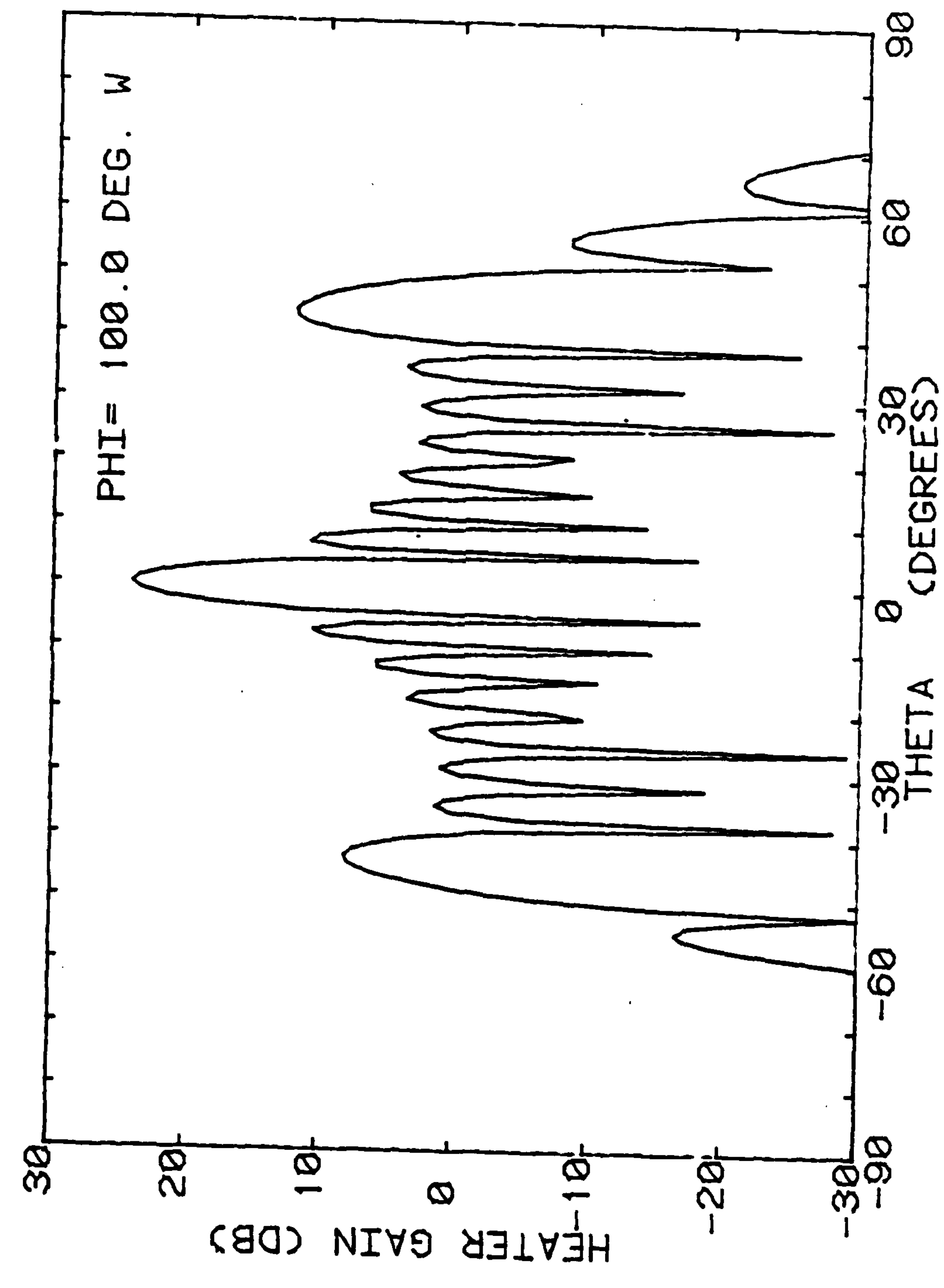
PHI= 100.0 DEG. W
HEATER GAIN (DB)
30
20
10
0
-10
-20
-30
-90
-60
-30
0
30
60
90
THETA (DEGREES)

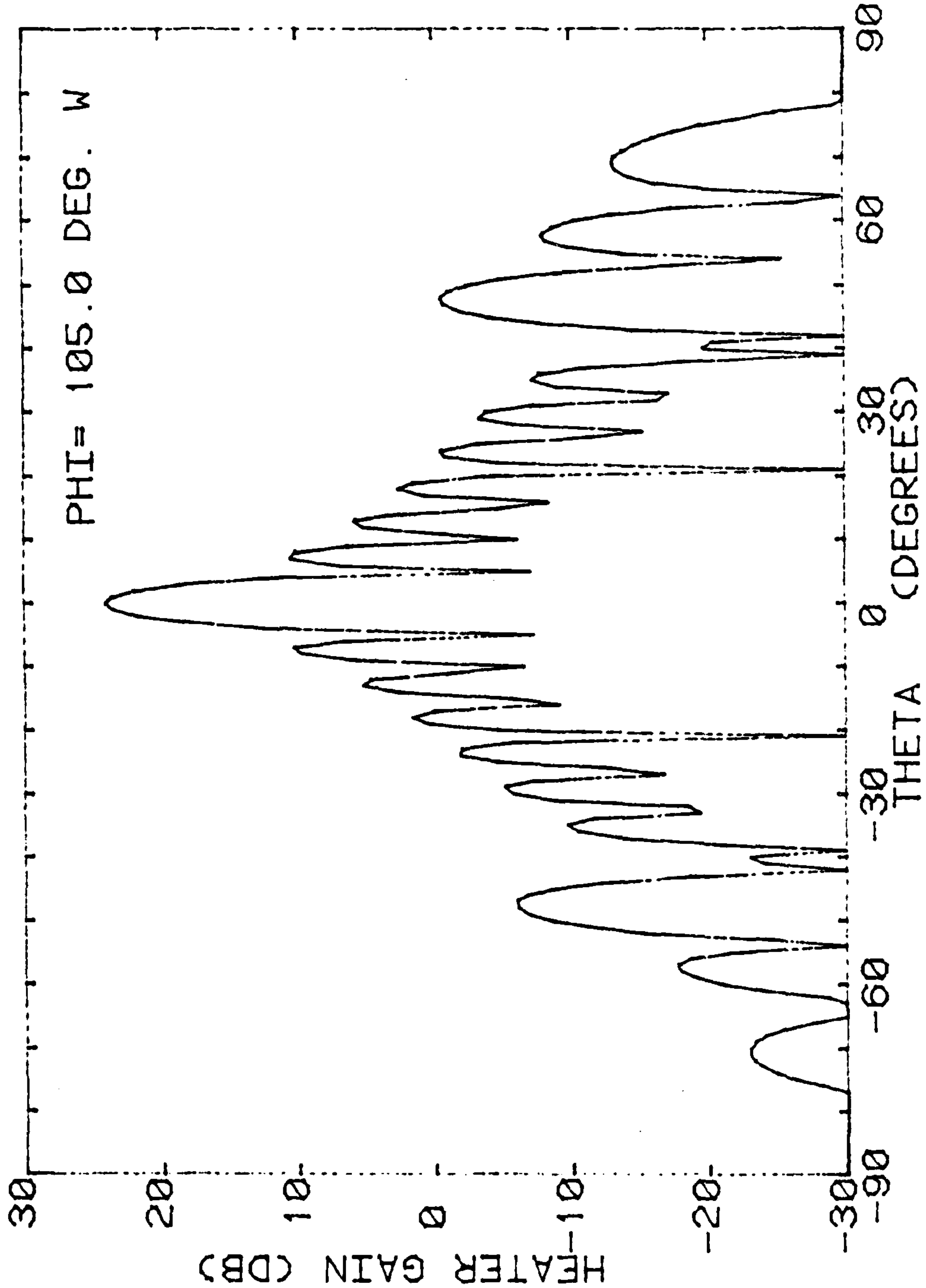
PHI= 105.0 DEG. W
THETA (DEGREES)
HEATER GAIN (DB)
-90 -60 -30 0 30 60 90
30 20 10 0 -10 -20 -30

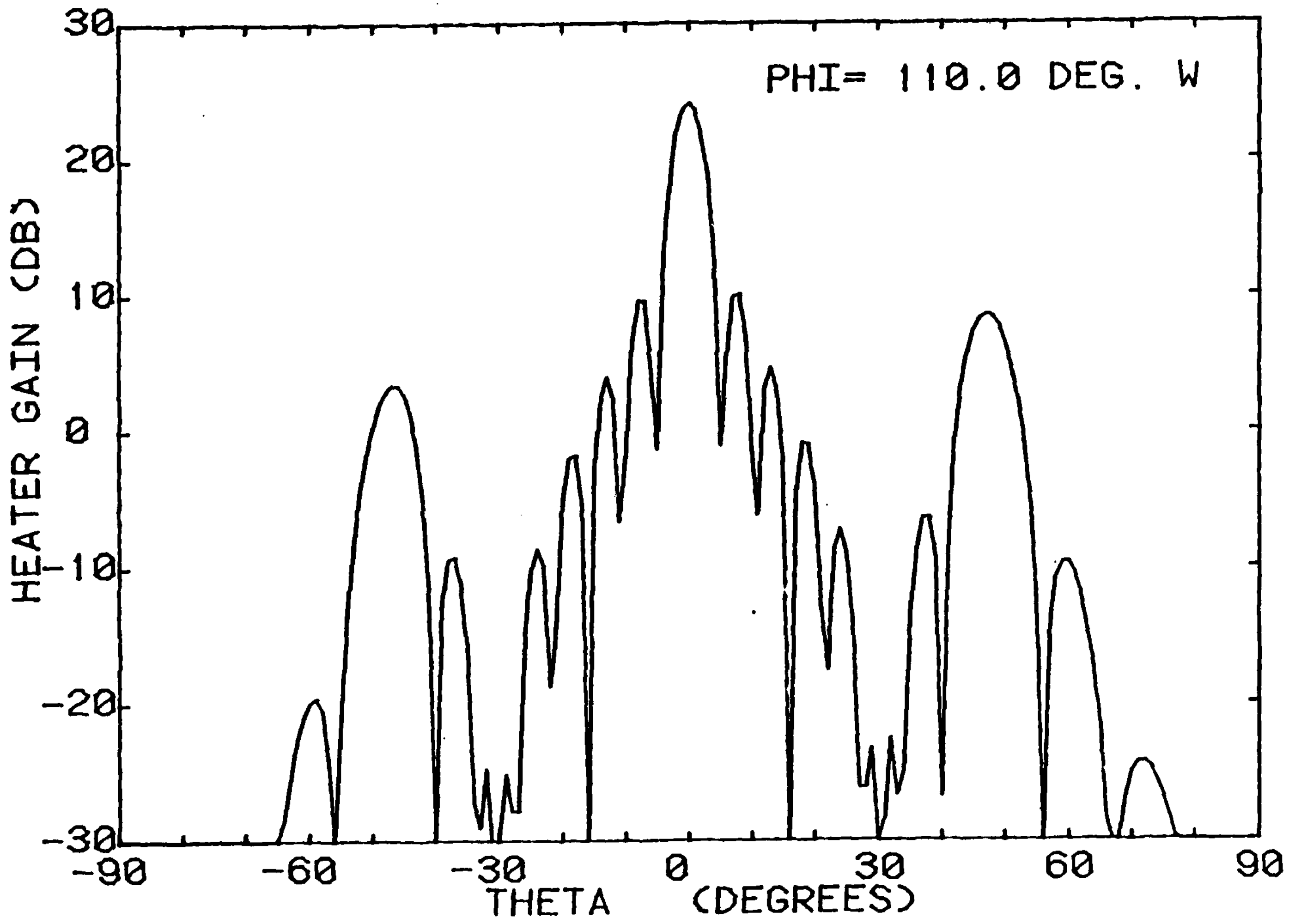
PHI= 110.0 DEG. W
HEATER GAIN (DB)
30
20
10
0
-10
-20
-30
-90
-60
-30
0
30
60
90
THETA (DEGREES)

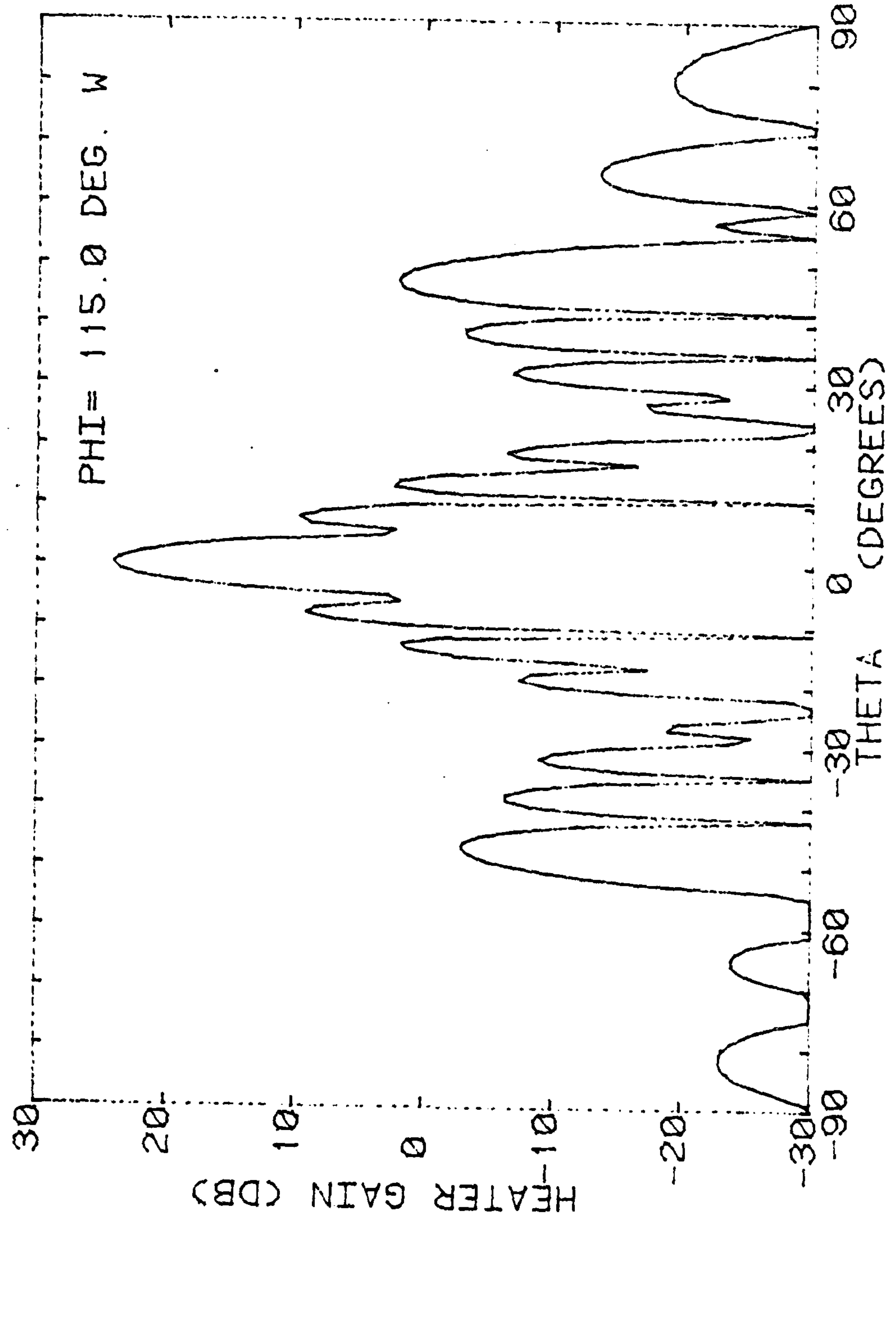
PHI= 115.0 DEG. W
HEATER GAIN (DB)
THETA (DEGREES)
30
20
10
0
-10
-20
-30
-90
-60
-30
0
30
60
90

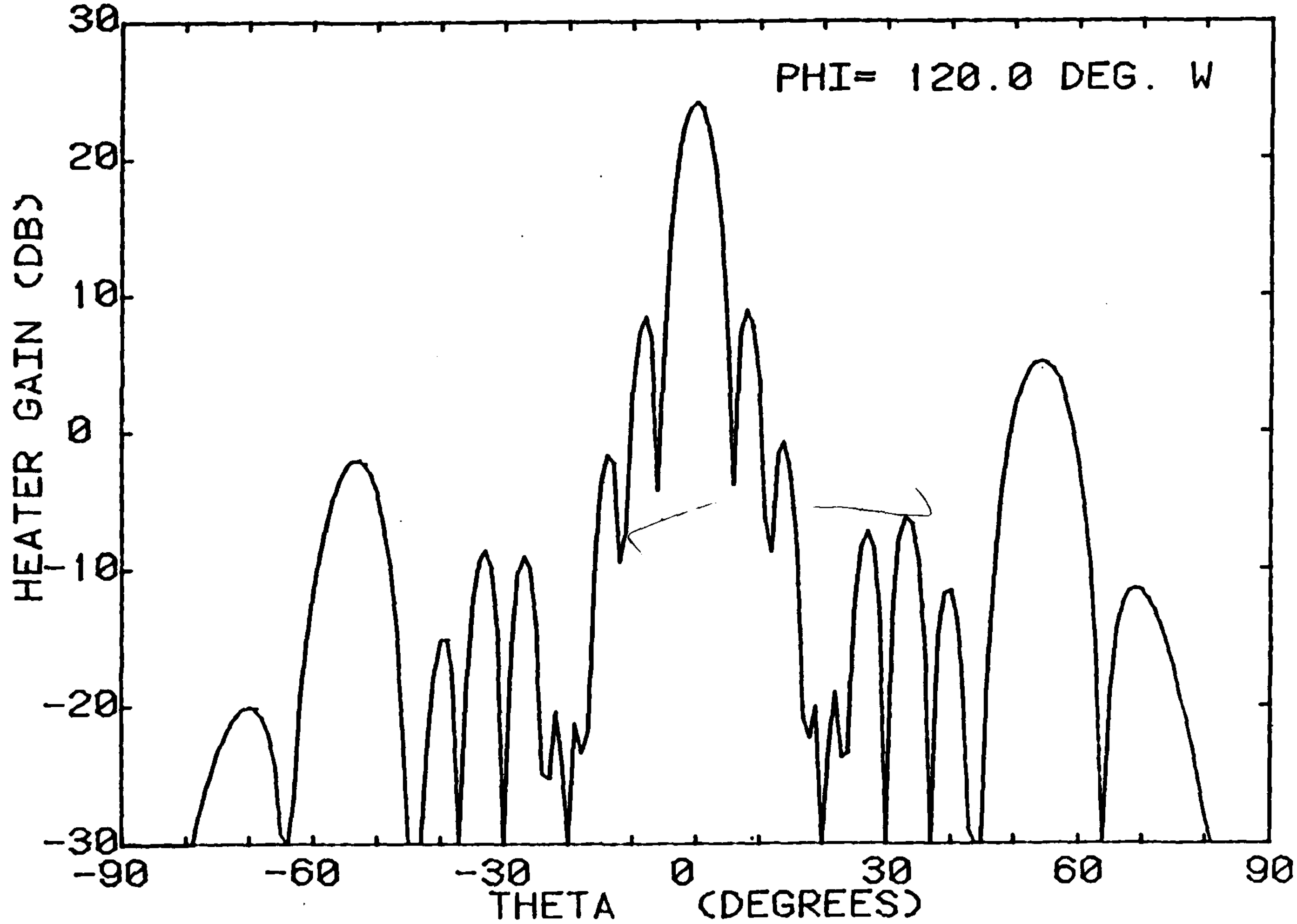
PHI= 120.0 DEG. W
HEATER GAIN (DB)
30
20
10
0
-10
-20
-30
-90
-60
-30
0
30
60
90
THETA (DEGREES)

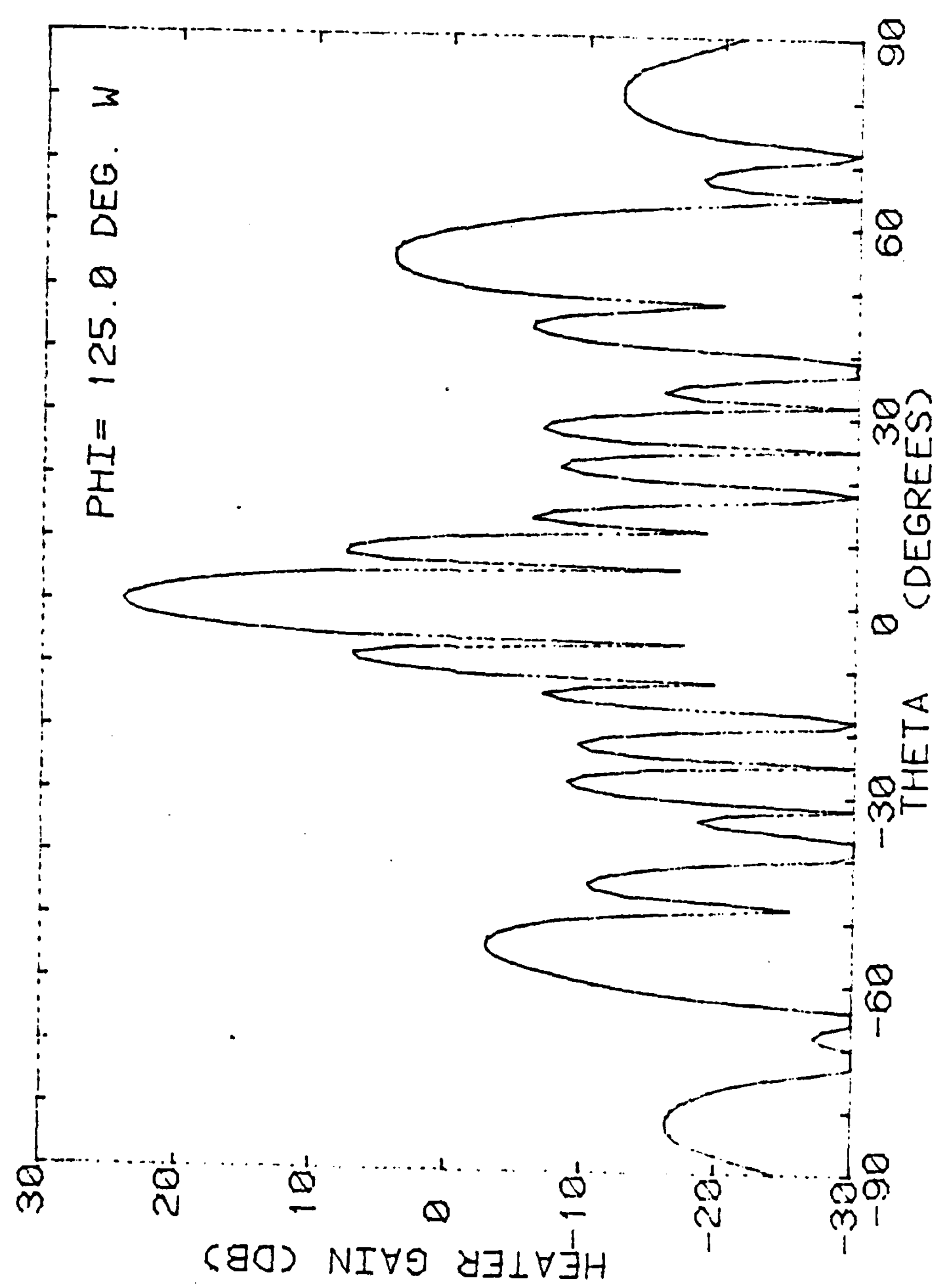
PHI= 125.0 DEG. W
HEATER GAIN (DB)
30
20
10
0
-10
-20
-30
THETA (DEGREES)
-90
-60
-30
0
30
60
90

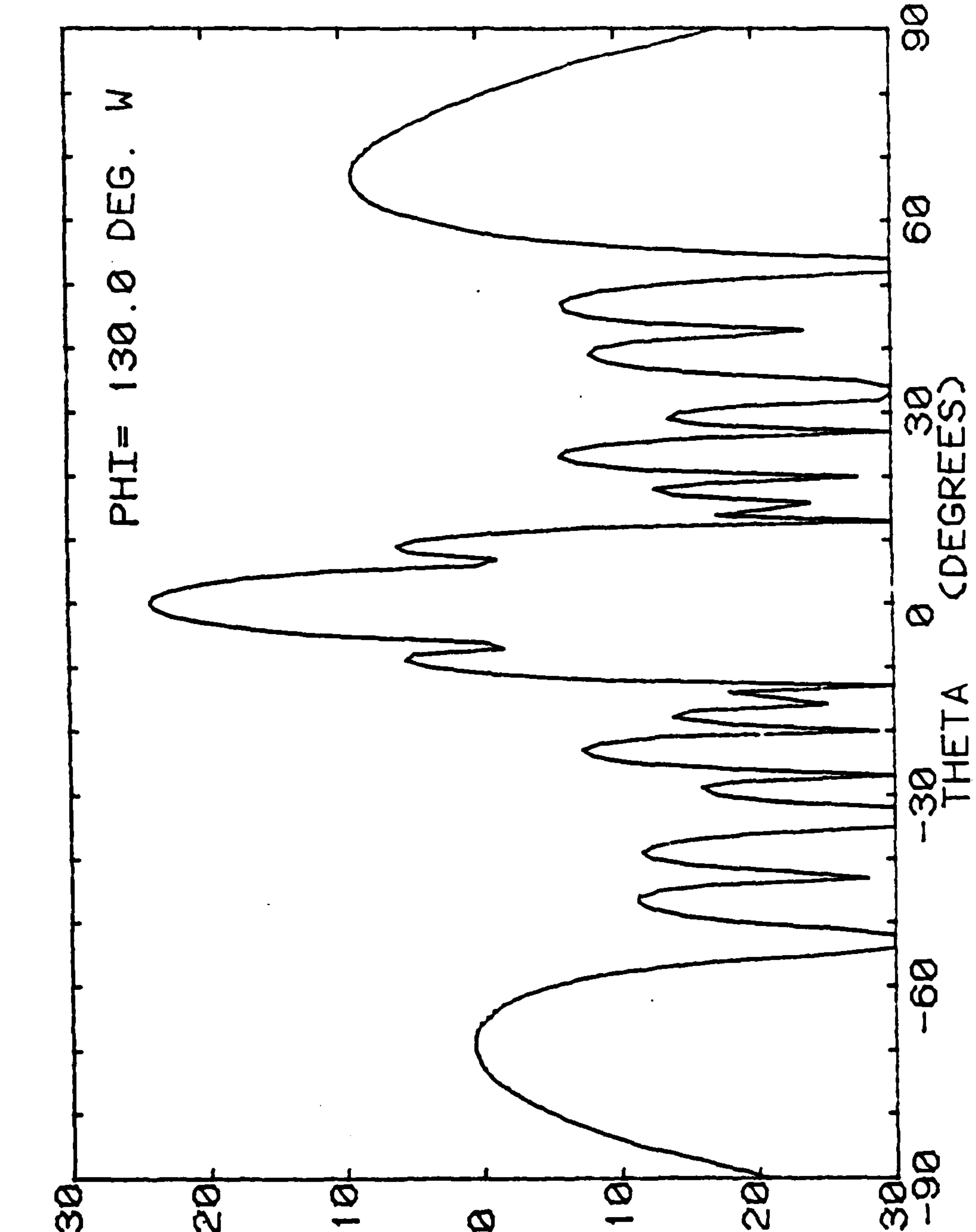
PHI= 130.0 DEG. W
HEATER GAIN (DB)
THETA (DEGREES)
30
20
10
0
-10
-20
-30
-90
-60
-30
0
30
60
90

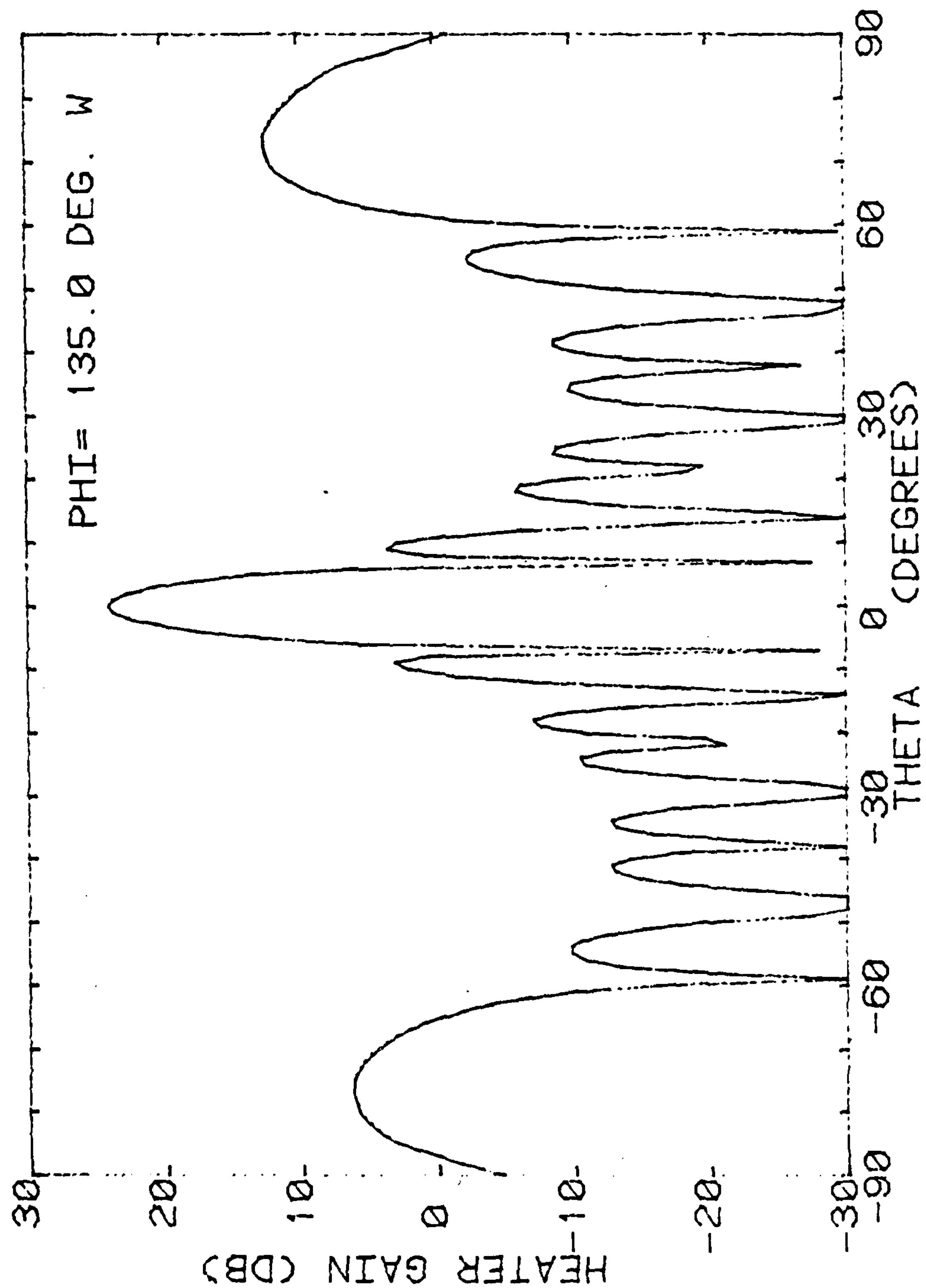
PHI= 135.0 DEG. W
HEATER GAIN (DB)
30
20
10
0
-10
-20
-30
THETA (DEGREES)
-90
-60
-30
0
30
60
90

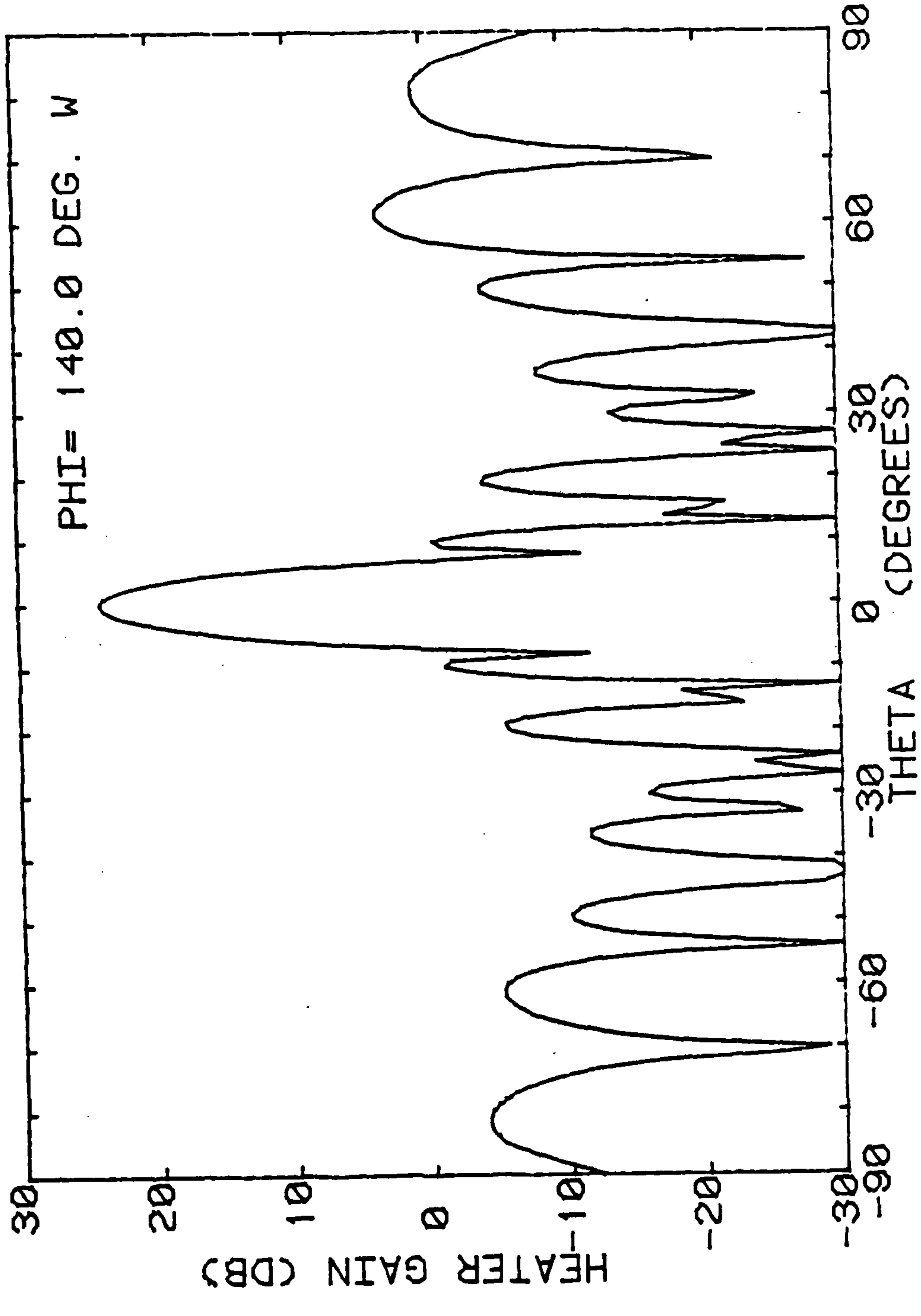
PHI= 140.0 DEG. W
HEATER GAIN (DB)
30
20
10
0
-10
-20
-30
-90
-60
-30
0
30
60
90
THETA
(DEGREES)

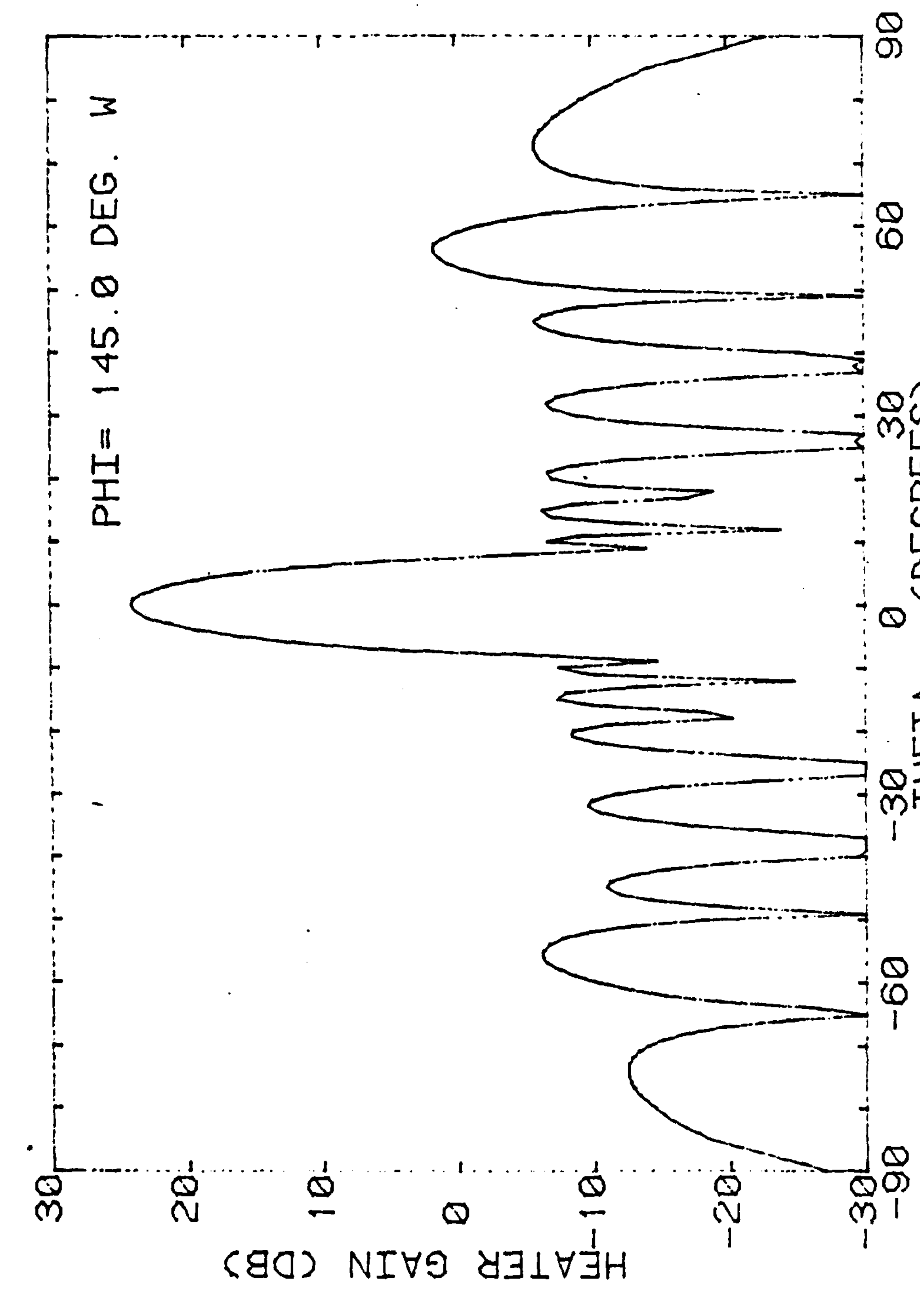
PHI= 145.0 DEG. W
HEATER GAIN (DB)
30
20
10
0
-10
-20
-30
-90
-60
-30
0
30
60
90
THETA (DEGREES)

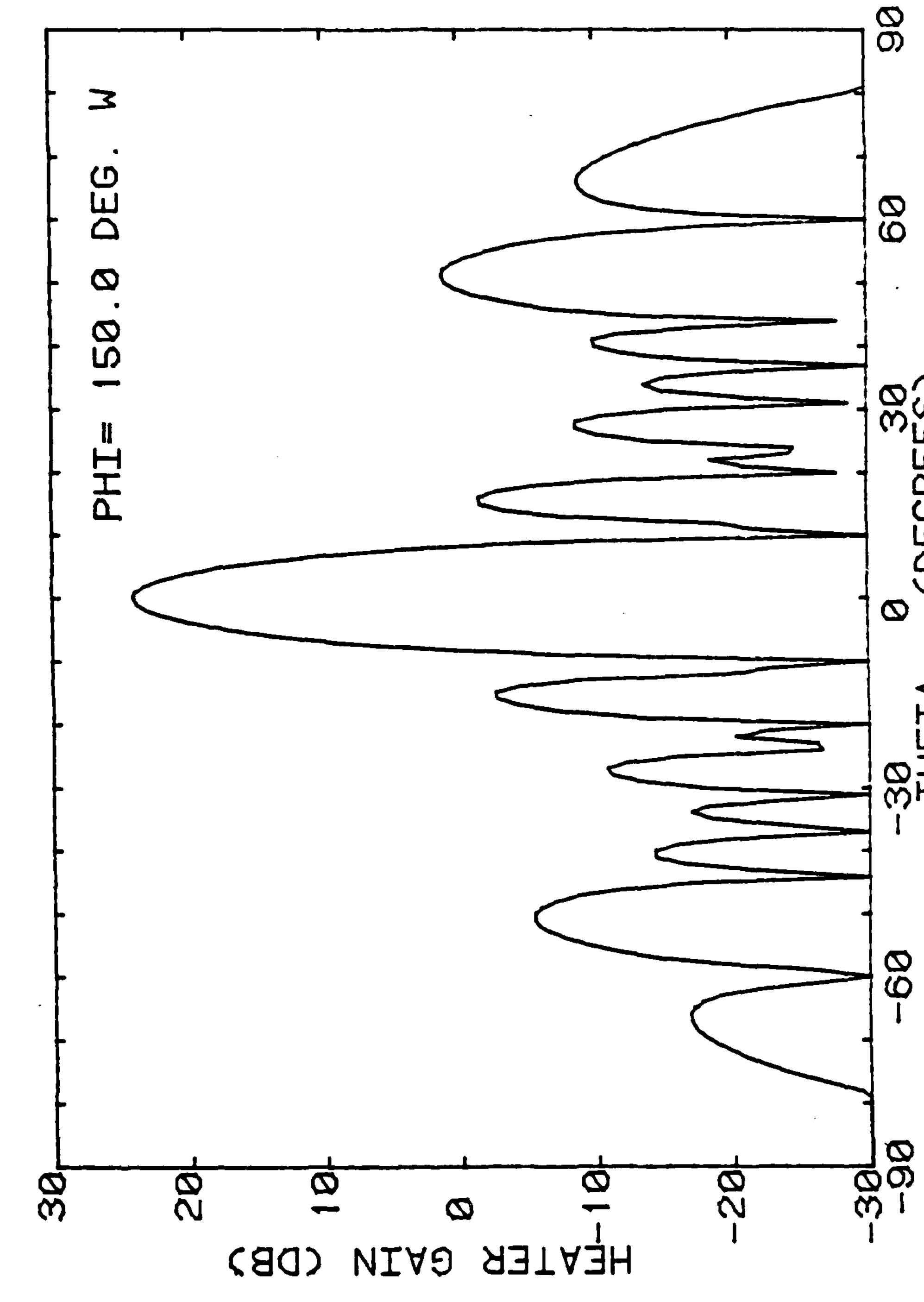
PHI= 150.0 DEG. W
HEATER GAIN (DB)
THETA (DEGREES)
30
20
10
0
-10
-20
-30
-90
-60
-30
0
30
60
90

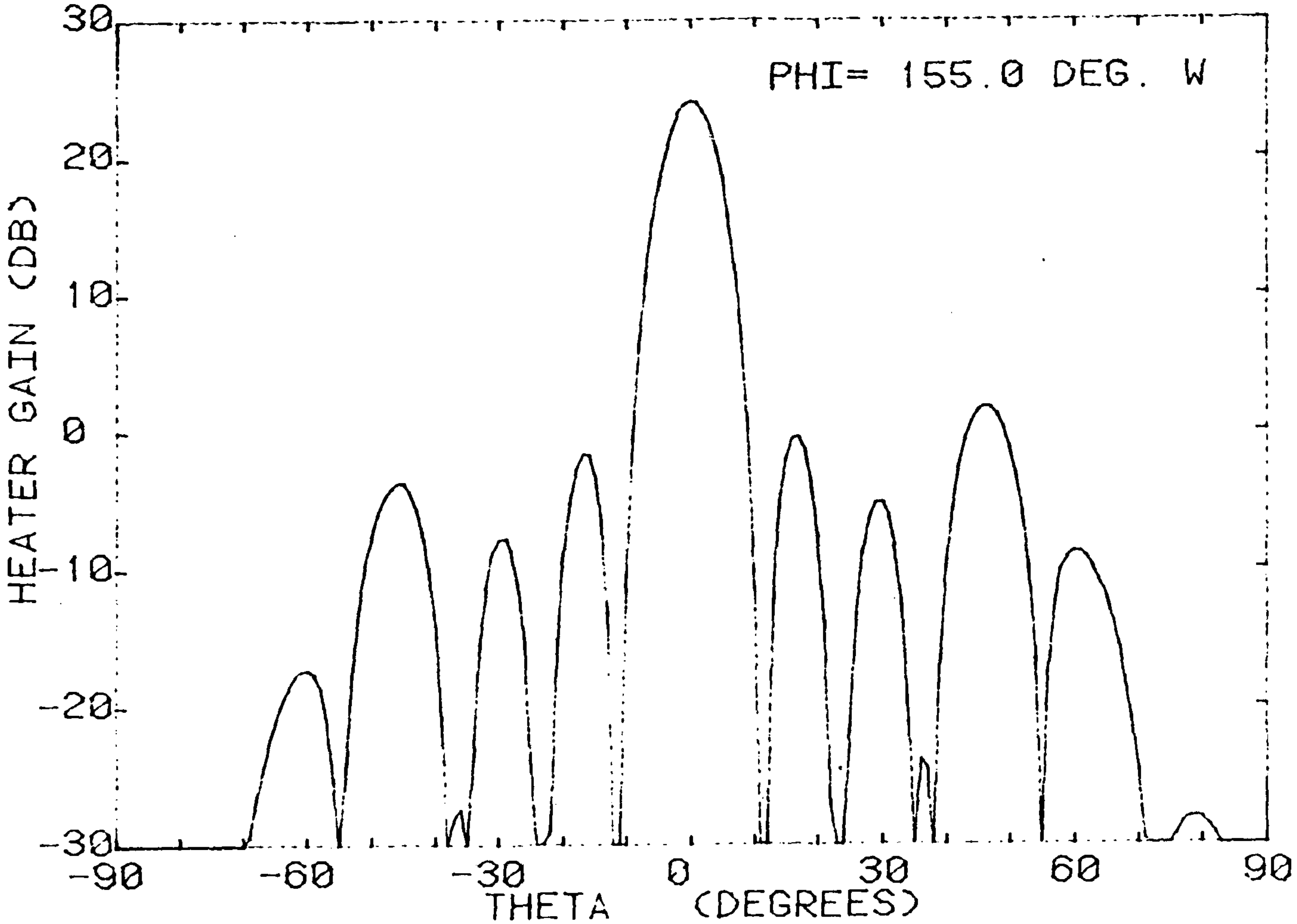
PHI= 155.0 DEG. W
HEATER GAIN (DB)
30
20
10
0
-10
-20
-30
-90
-60
-30
0
30
60
90
THETA (DEGREES)

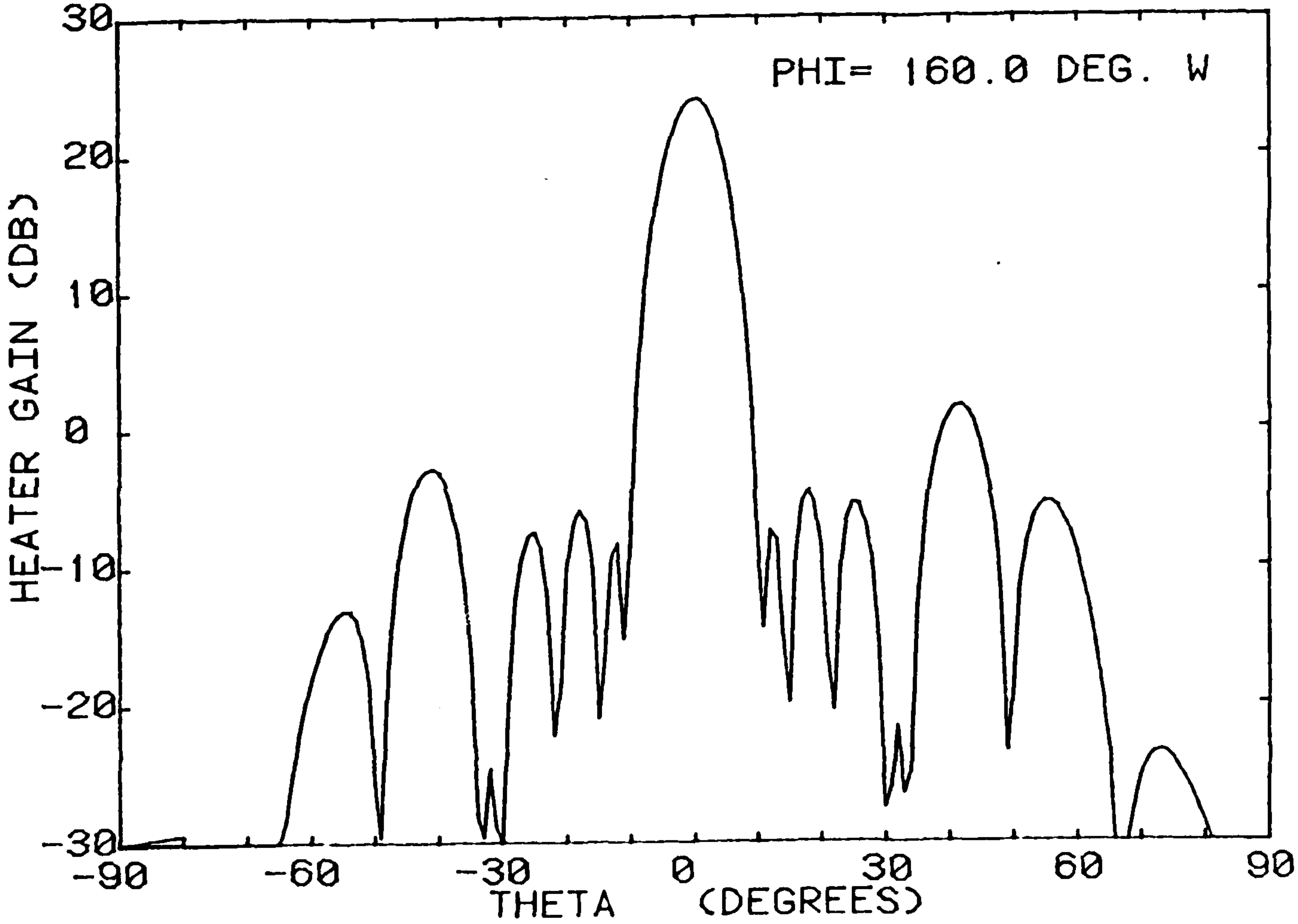

PHI= 160.0 DEG. W
HEATER GAIN (DB)
30
20
10
0
-10
-20
-30
-90
-60
-30
0
30
60
90
THETA (DEGREES)

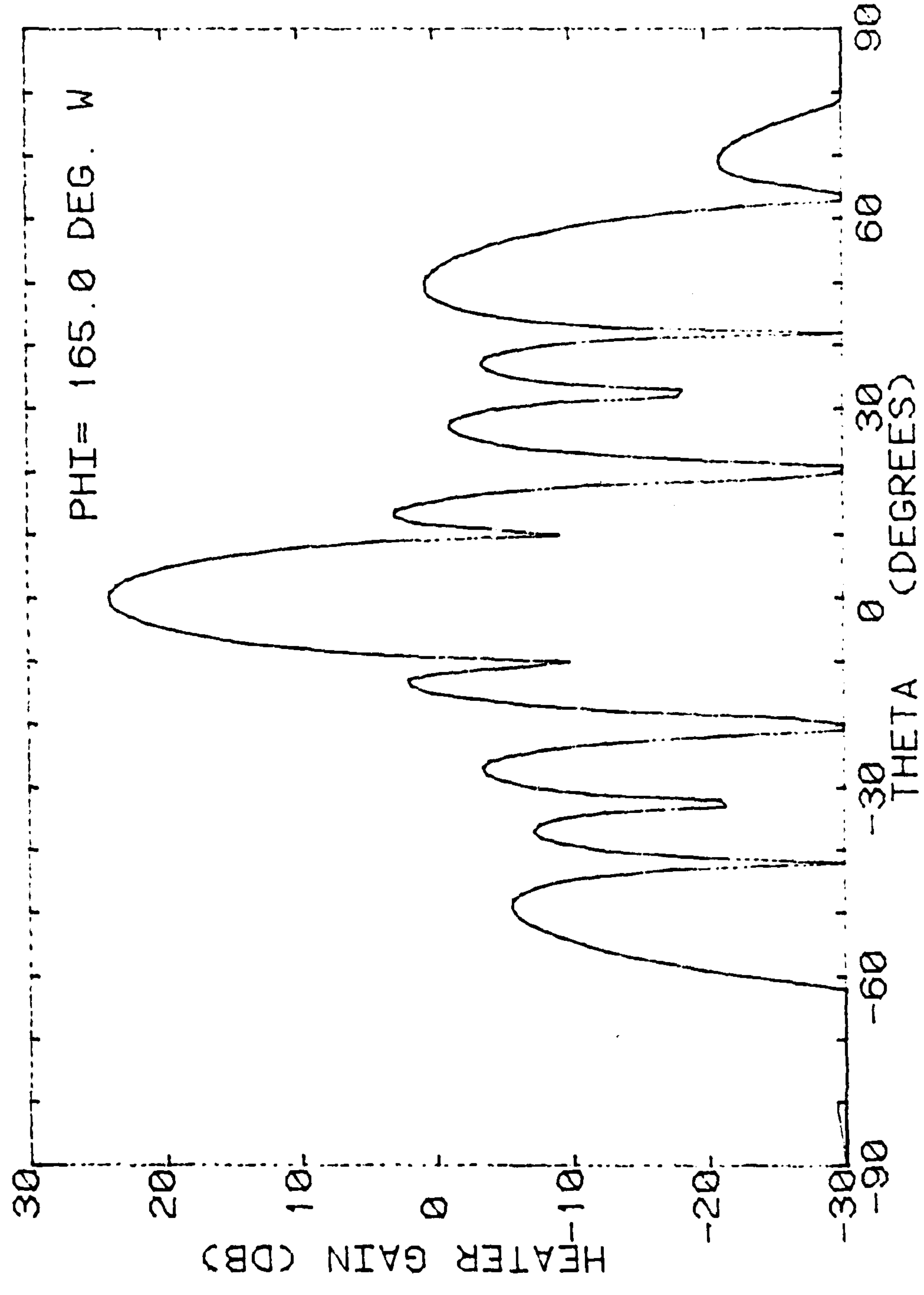
PHI= 165.0 DEG. W
HEATER GAIN (DB)
THETA (DEGREES)
30
20
10
0
-10
-20
-30
-90
-60
-30
0
30
60
90

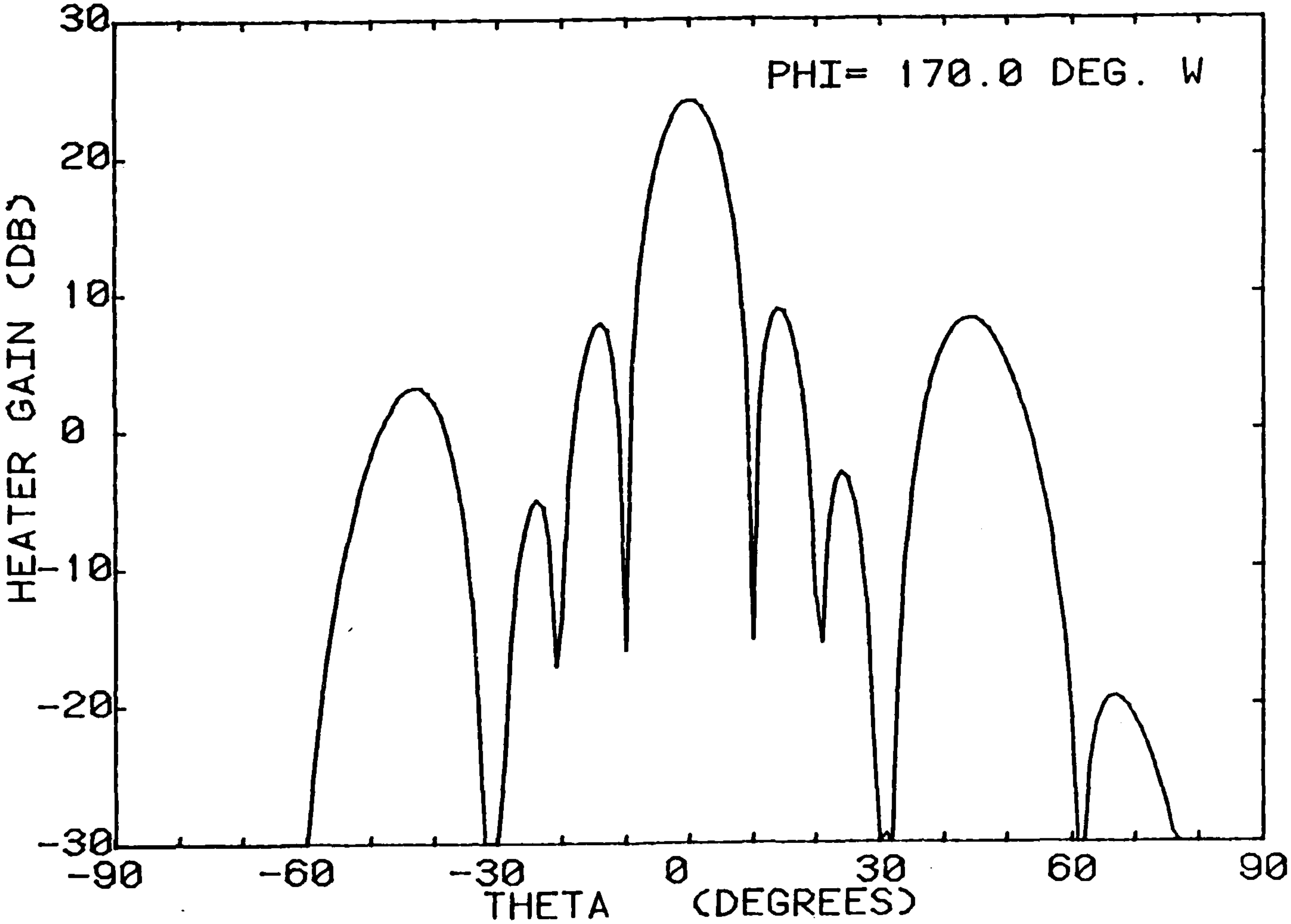
PHI= 170.0 DEG. W
HEATER GAIN (DB)
30
20
10
0
-10
-20
-30
-90
-60
-30
0
30
60
90
THETA (DEGREES)

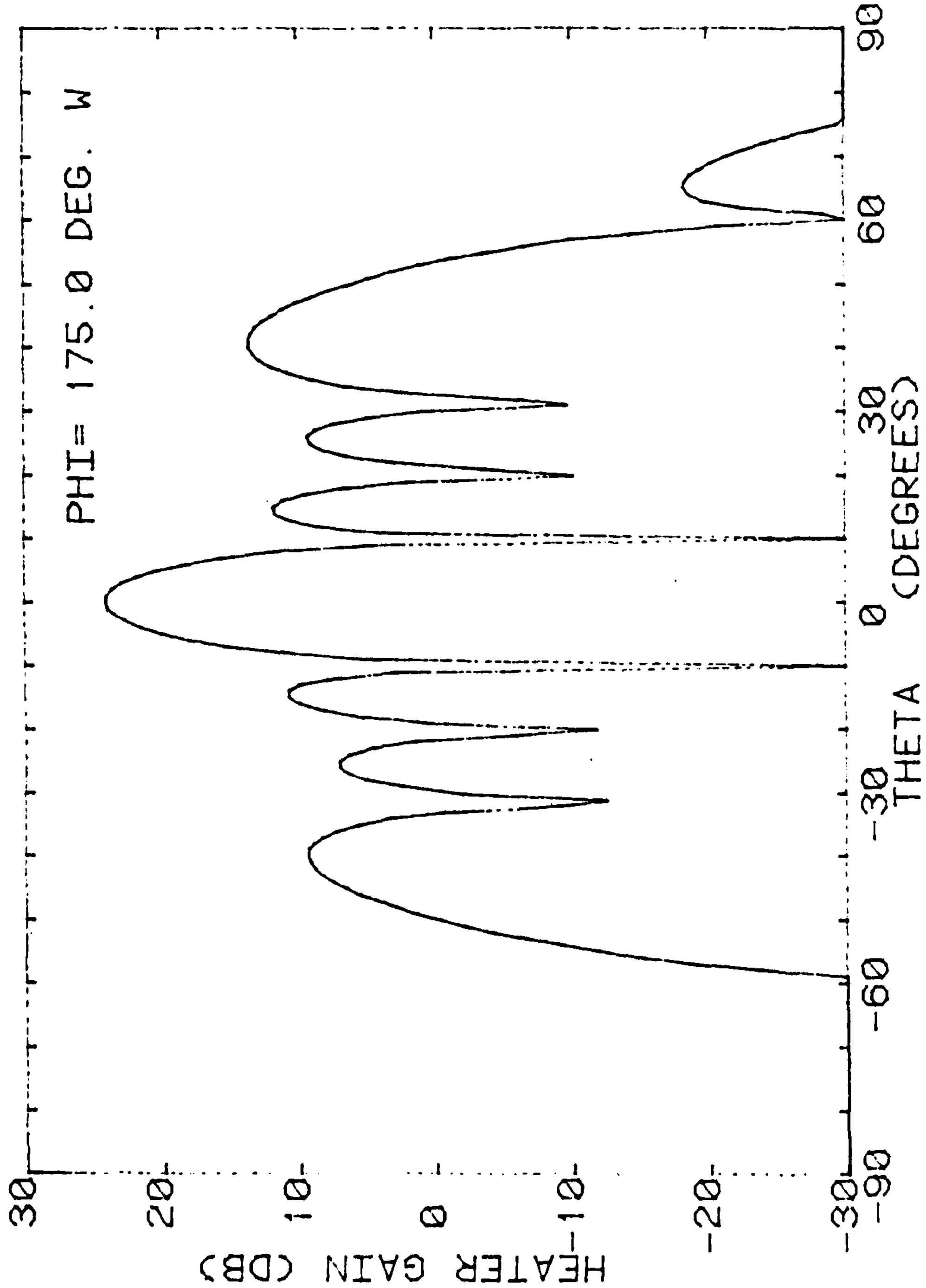
PHI= 175.0 DEG. W
HEATER GAIN (DB)
30
20
10
0
-10
-20
-30
-90
-60
-30
0
30
60
90
THETA (DEGREES)

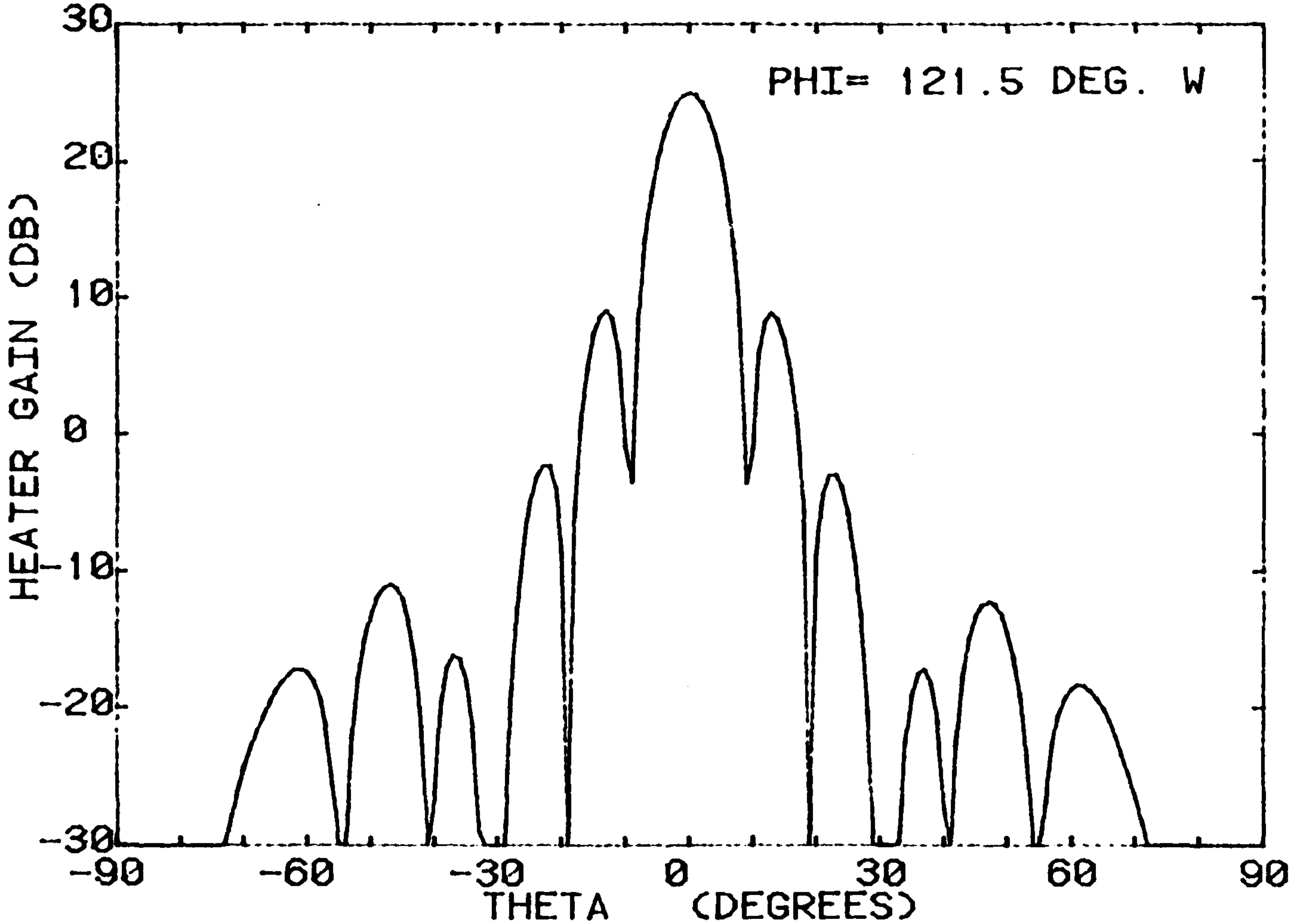

Figure 1-12.a Directive gain pattern in direction of Los Canos (3.17 Mhz)

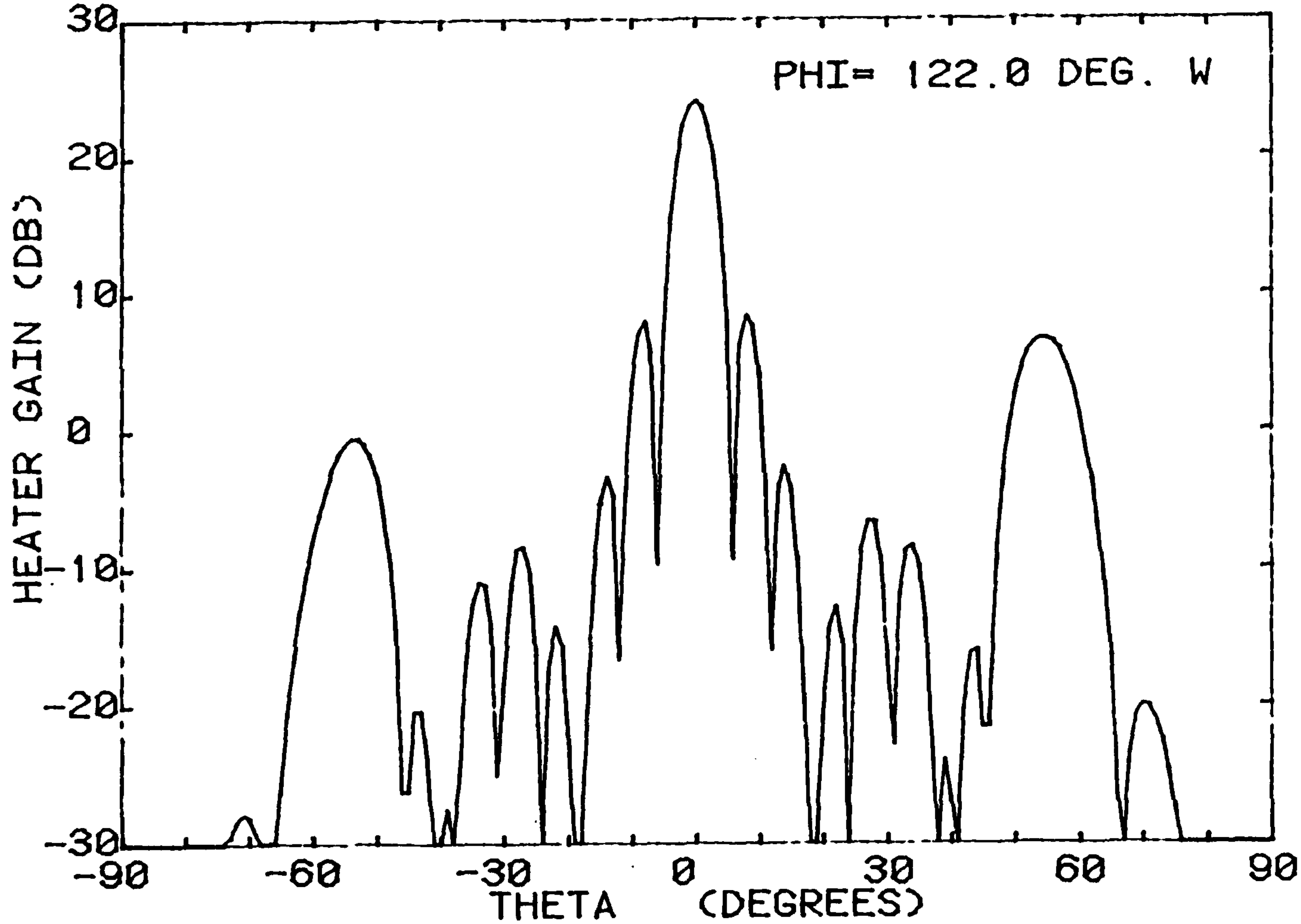

Figure 1-12.b Directive gain pattern in direction of Los Canos (5.1MHz)

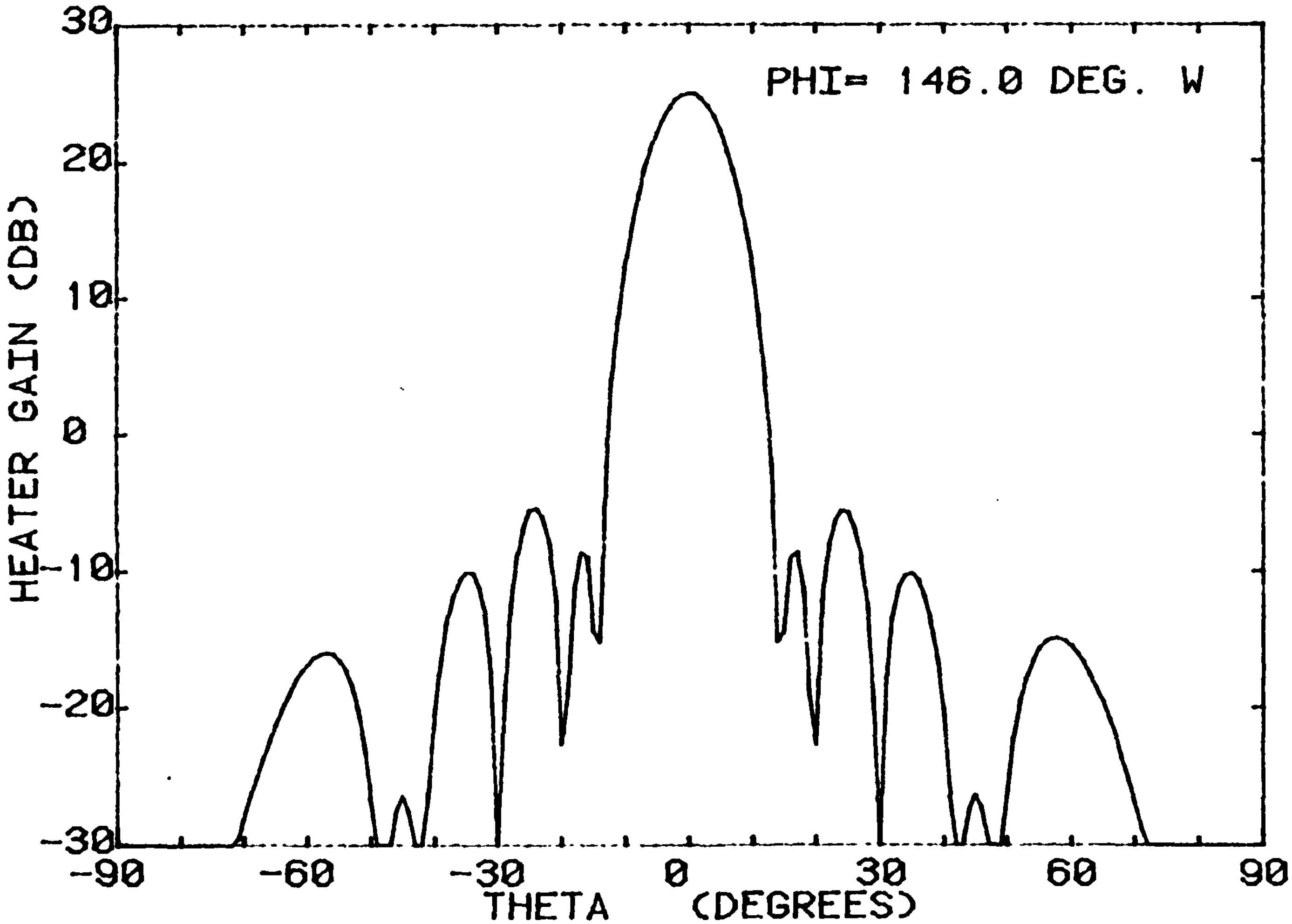

Figure 1-13.a Directive gain pattern in direction of Arecibo Observatory (3.17 Mhz)

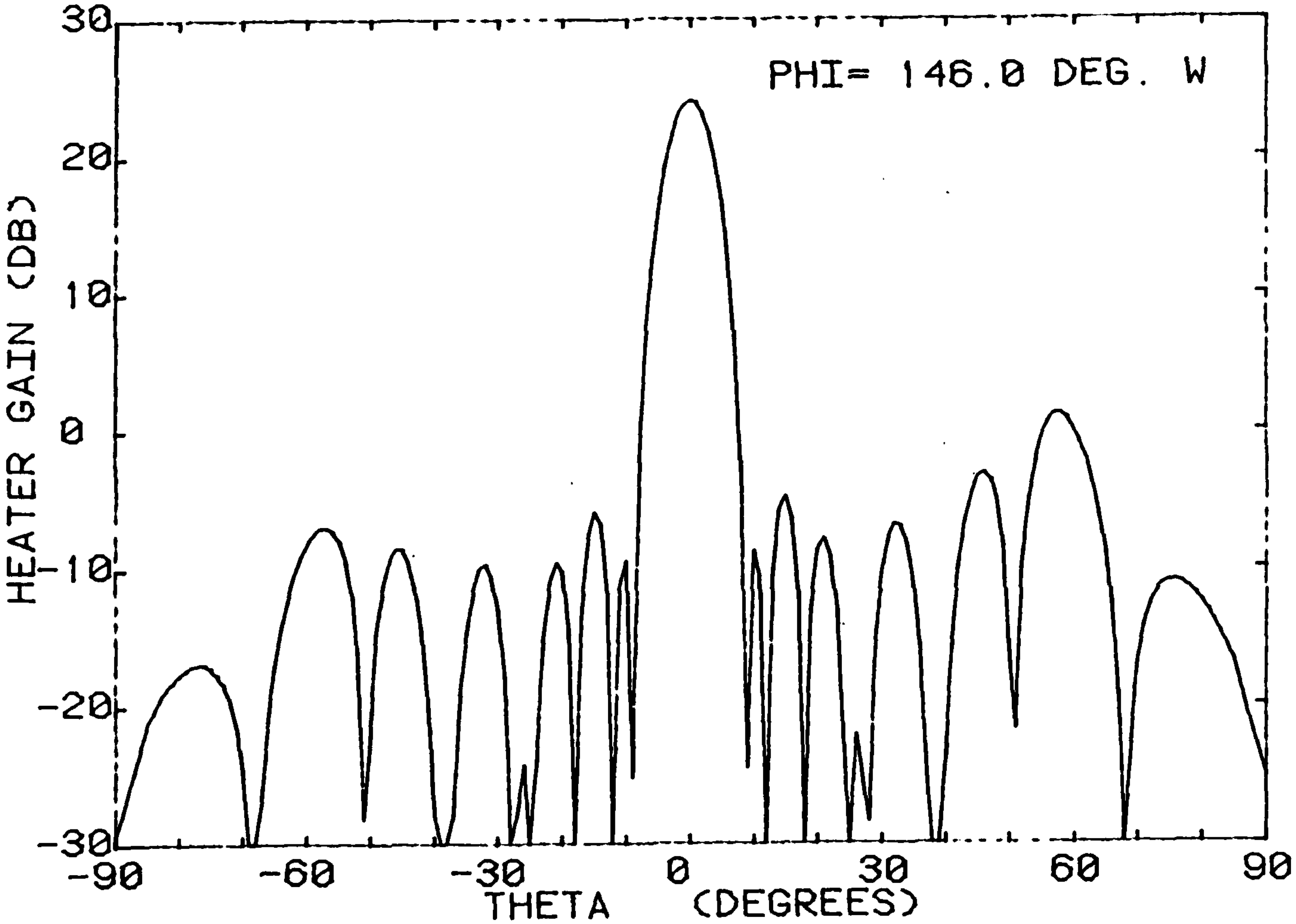

Figure 1-13.b Directive gain pattern in direction of Arecibo Observatory (5.1 MHz)

Grating lobes (lobes which have the same intensity as the main beam[2]) in the antenna factor will occur when both the numerator and denominator of both terms of equation (1-15) are zero. This will occur when equation (1-20) is satisfied.

$$\begin{aligned} \beta(d/2)\sin\Theta\sin\phi &= 0 \text{ or } \pi \\ \beta(d/2)\sin\Theta\cos\phi &= 0 \text{ or } \pi \end{aligned} \qquad (1\text{-}20)$$

For the A.O. array $\beta d/2$ is equal to 2.82 and 4.54 for 3.17 and 5.1 MHz respectively. Since $\sin\Theta\sin\phi$ and $\sin\Theta\cos\phi$ are never larger than 1, the 3.17 MHz pattern does not and should not have grating lobes. However, grating lobes will be present in the 5.1 MHz pattern because 4.54 is larger than π.

These grating lobes will occur for the angles given in table II. As can be seen in the plots of figure (1-11) major lobes do occur at these angles. They are attenuated when they are multiplied by the elemental pattern during the calculations of the total array pattern.

Θ(deg)	ϕ(deg)
43.8	0
43.8	90
43.8	180
43.8	270
78.1	45
78.1	135
78.1	225
78.1	315

Table II. Location of Grating Lobes in 5.1 MHz pattern

ELF/VLF ARRAY MODEL

Having established a directive gain pattern, it remains to relate the pattern to the heating of the ionosphere. Richardson[8] has shown that the largest change in conductivity caused by the heating occurs

at approximately a 70 km altitude. As a zero order approximation, the heating pattern can be projected on a plane located at a 70 km altitude. The location and relative intensity of the major heated regions can be found. By placing elementary dipoles with the same relative amplitude of current at the respective heated regions, a field intensity at a receiving site on the ground can be calculated.

A correction factor is needed to project the pattern onto a 70 km altitude plane. The pattern shows the relative distribution of the power on a sphercial surface of radius "R." Since the distance to a plane increases when "theta" is greater than zero, the power density on the plane will decrease from that indicated by the pattern. The power is being spread over a larger spherical surface as "R" is increased. The projection of the pattern on a plane surface requires multiplying the pattern by an attenuation factor of $\cos^2\theta$. This attenuation is plotted as a function of "theta" in figure (1-14).

Programs 6 and 7 in Appendix I were used to compute a pattern on a square section of a plane (122 km north and south by 122 km east and west of the main beam) at a 70 km altitude. The data were then plotted using Statistical Analysis System (SAS).[9,10] Figures (1-15) and (1-16) show the relative power density on a 70 km altitude plane for 3.17 MHz and 5.1 MHz respectively. Only levels above that of an isotropic radiator (0 db) were plotted.

The 122 km dimension of the plotted data corresponds to an angle of "theta" equal to 60.2 degrees. The major lobes created by the antenna factor grating lobes at 78.1 degrees are not seen in figure (1-16). These lobes are for the most part attenuated to the zero reference level by the long propagation path. Table III gives the

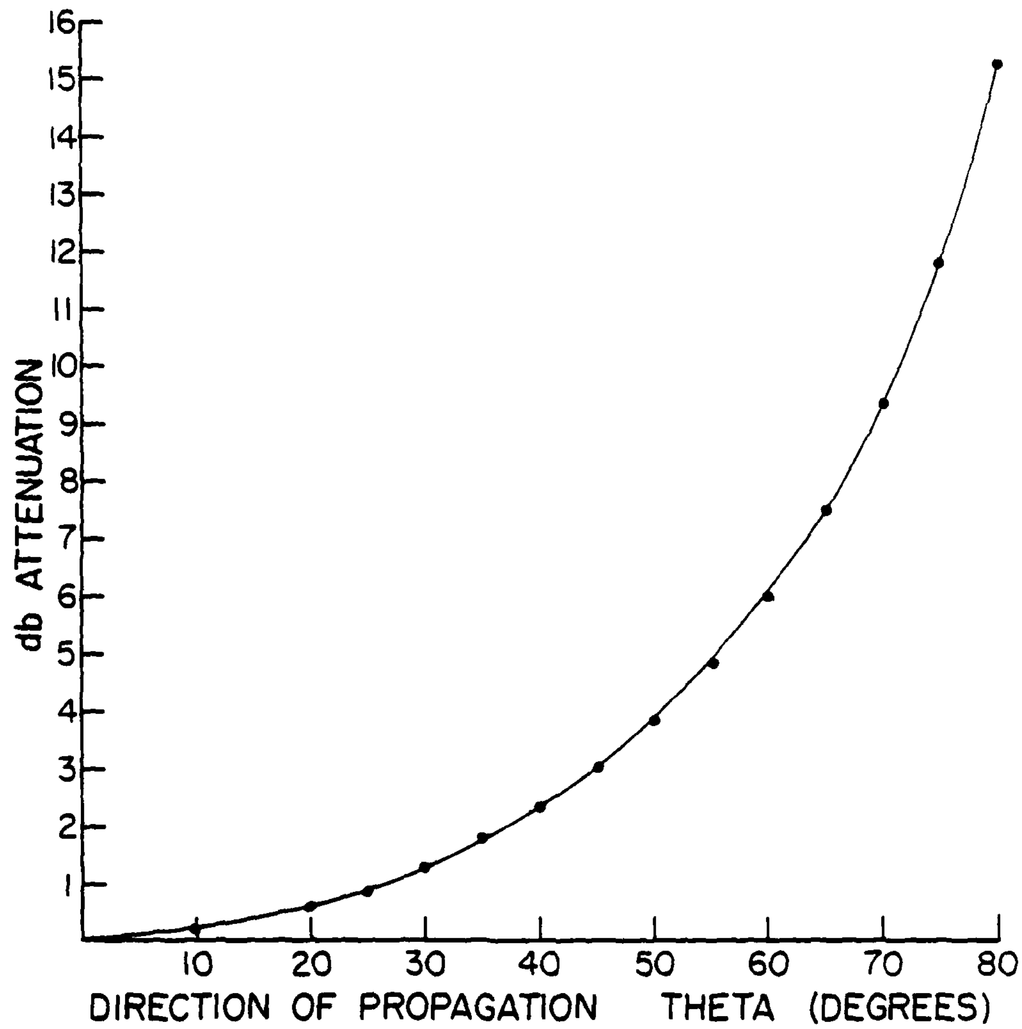

Figure 1-14 Propagation loss due to power spreading

RELATIVE POWER AT 70 KM

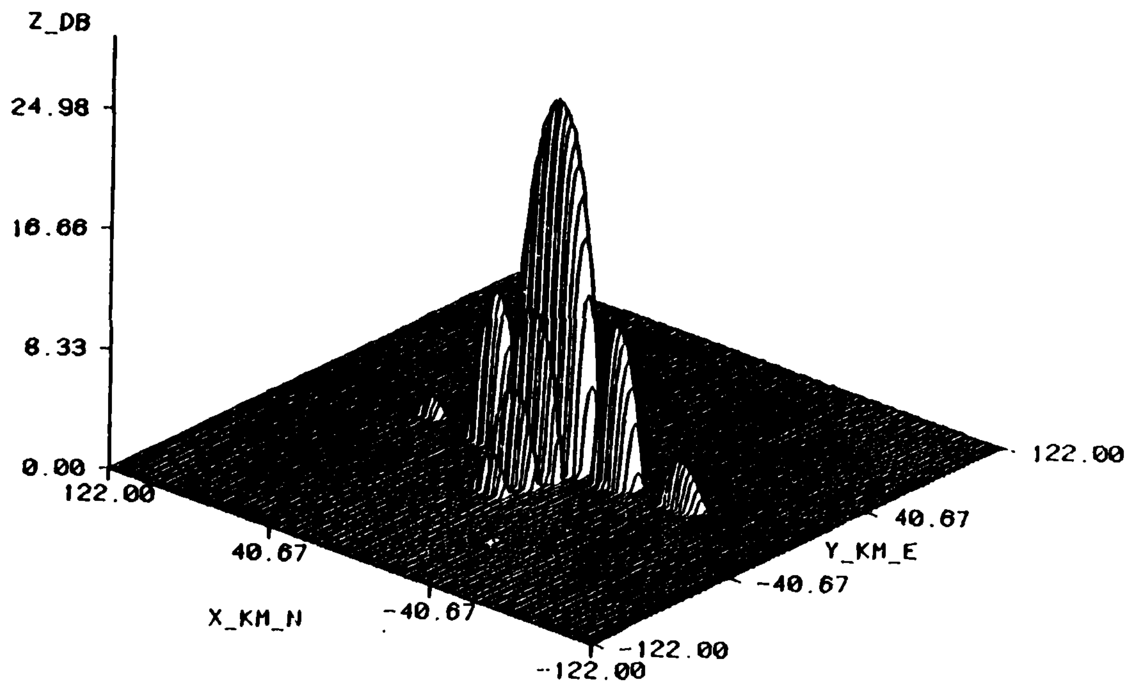

Figure 1-15 Relative HF power above isotropic on a 70 km altitude plane (3.17 MHz)

RELATIVE POWER AT 70 KM

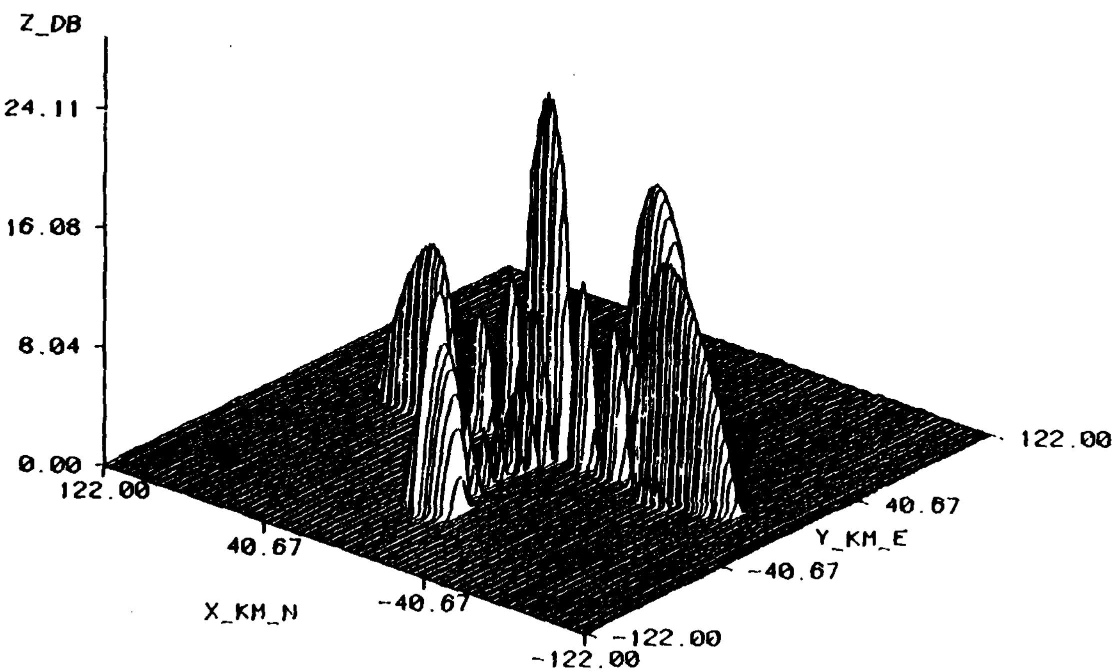

Figure 1-16 Relative HF power above isotropic on a 70 km altitude plane (5.1 MHz)

(deg)	(deg)	Directive Gain (db)	Path Attenuation (db)	Relative Power Density at 70 km altitude (db)	Location Center x (km)	Location Center y (km)
77	45	6.251	-12.96	-6.71	214.4	214.4
71	135	7.568	- 9.75	-2.18	143.8	143.8
72	225	12.486	-10.20	2.29	152.3	152.3
73	315	11.399	-10.68	.72	161.9	161.9

Table III. Grating lobes location and power density on 70 km altitude plane.

location and relative power density of these lobes on the 70 km altitude plane.

Data on the lobes shown in figures (1-15) and (1-16) are given in tables IV and V. The current was assumed to be proportional to the square root of the power density. To find the average current per unit length for each lobe, the current was integrated over the area of the plane disturbed by the lobe and divided by the length of the region. The current distribution on the plane was approximated using a pyramid with a quadrilateral as a base. The length and width of the heated region are the diagonals of the quadrilateral base; the peak current is the altitude. The volume of the pyramid is equal to one third of the area of the base times the altitude.[10] The area of the quadrilateral base is one half of the product of the diagonals times the sine of the angle between the diagonals.[11] So the formula for calculating the average current per unit length becomes equation (1-21).

$$I_{av} = (1/3)[(1/2)a \cdot b \sin 90](I_p/a) = (1/6)\, bI_p \qquad (1\text{-}21)$$

a = length (diagonal)
b = width (diagonal)
I_p = peak current (altitude)

In this zero order approximation each of the lobes is represented as an elementary current element source. The source has a current equal to the average current calculated in equation (1-21), a length equal to the length of the lobe, and is located at the x,y coordinates of the peak power density for the lobe on the 70 km altitude plane. The location, length, and average current are summarized in tables IV and V.

Location x(km)	y(km)	P_d Relative Power Density (db)	a Length (km)	b Width (km)	I_p Peak Current ($10^{p_d/20}$)	I_{av} Average Current ($1/6\ a \cdot b \cdot I_p$)a
-63	0	3.022	24	12	1.416	2.832
-30	0	10.87	22	18	3.495	7.485
0	0	24.983	40	20	17.748	59.16
30	0	10.215	22	16	3.242	8.645
62	0	1.295	15	7	1.161	1.355
0	-38	1.624	19	7	1.207	1.408
0	-25	5.875	26	9	1.967	2.951
0	-14	11.239	32	9	3.647	5.471
0	14	11.239	32	9	3.647	5.471
0	25	5.875	26	9	1.967	2.951
0	38	1.624	16	7	1.206	1.407

Table IV. Lobe Statistics for Frequency = 3.17 MHz

Location x(km)	y(km)	P_d Relative Power Density (db)	a Length (km)	b Width (km)	I_p Peak Current $(10^{P_d/20})$	I_{av} Average Current $(1/6\ a \cdot b \cdot I_p)/a$
-60.5	0	15.519	54	14	5.970	13.93
-34.0	0	10.141	14	14	3.214	7.499
-18.0	0	12.205	12	10	4.076	6.793
0	0	24.113	24	12	16.056	32.113
18.0	0	11.134	12	10	3.603	6.006
33.0	0	8.306	14	10	2.530	4.217
59.0	0	11.279	43	14	3.664	8.549
0	-65	14.301	26	28	5.189	24.213
0	-48	5.331	15	8	1.847	2.463
0	-38	3.715	12	6	1.534	1.534
0	-30	3.586	12	5	1.511	1.259
0	-22	4.825	14	5	1.743	1.452
0	-15	6.969	16	5	2.231	1.859
0	-9	11.079	20	6	3.581	3.581
0	9	11.079	20	6	3.581	3.581
0	15	6.969	17	5	2.231	1.859
0	22	4.825	15	5	1.743	1.452
0	30	3.586	14	5	1.511	1.259
0	38	3.715	14	6	1.534	1.534
0	48	5.331	18	8	1.847	2.463
0	65	14.301	28	28	5.189	24.213

Table V. Lobe Statistics for Frequency = 5.1 MHz.

The magnetic field due to a current element is given in equation[5] (1-22). The source is located at the origin and along the Z' axis. H_ϕ' is the magnetic field intensity in the source coordinate system X',Y',Z'. Since H_ϕ' is a vector and there are a number of sources at different locations whose fields need to be superimposed at the observation point, it would be beneficial to translate the fields to the observation frame of reference, X,Y,Z.

$$H_\phi' = [(Idl)/4\pi r']\sin\Theta' e^{-j\beta r'}[j\beta + (1/r')] \qquad (1\text{-}22)$$

The source and observation coordinate systems are shown in figure (1-17). The source is located at point O(XO,YO,ZO) and along the Z'-axis, which is parallel to the X-axis in the observation point coordinate system. The Y- and Y'-axis are also parallel and the X'-axis is in the negative z direction. From the geometry of the figure the relationships given in equation (1-23) can be found. In addition, using the transformation from spherical coordinates to Cartesian coordiantes, equation[12] (1-24), the expression for the magnetic field, equation (1-22), can be transformed to the observation point coordinates.

$$\begin{aligned} X' &= XP-XO \\ Y' &= YP-YO \\ Z' &= ZP-ZO \\ r' &= (XP-XO)^2+(YP-YO)^2+(ZP-ZO)^2)^{1/2} \end{aligned} \qquad (1\text{-}23)$$

$$\sin\Theta' = \frac{[(ZP-ZO))^2+(YP-YO)^2]^{1/2}}{r'}$$

$$\begin{aligned} H_y &= H_y' = H_\phi'(x')/\sqrt{x'^2+y'^2} \\ -H_z &= H_x' = -H_\phi'(y')/\sqrt{y'^2+x'^2} \\ H_x &= H_z' = 0 \end{aligned} \qquad (1\text{-}24)$$

The phase term $e^{-j\beta r'}$ is important when performing the superposition of the fields from all of the sources at the observation

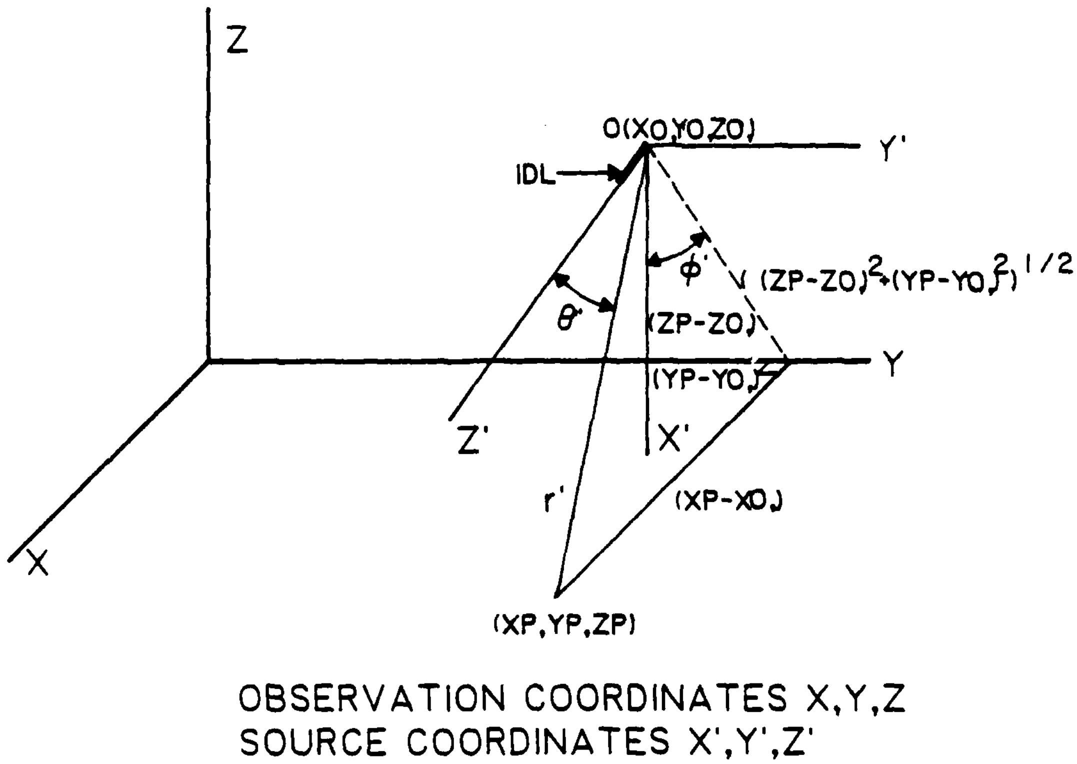

Figure 1-17 Relative orientation of observation and source coordinates

point. Small differences in the value of r' can be magnified by causing a significant change in the term's value. Thus it would affect the summation of the real and imaginary parts of all the sources.

An additional term must be added to $\beta r'$ to maintain the proper relationship between the sources. This is because the HF heating pulse must travel different path lengths to the source region. The difference in path lengths causes a time delay between the sources, equation (1-25). This delay can be expressed in terms of an additonal path length ΔR, equation (1-26). This allows the phase term, $e^{-j\beta r'}$, in equation (1-22) to be expressed as $e^{-j\beta(r'+\Delta R)}$. By combining the phase delay, equations (1-23) and (1-24) into equation (1-22), an expression for the magnetic field intensity at the point of observation and in terms of the observation point coordinate system can be found, equation (1-27).

$$\text{Time delay} = \frac{(ZO^2+YO^2+XO^2)^{1/2}-70}{C} \qquad (1\text{-}25)$$

$$\begin{aligned}\text{Phase delay} = \frac{(ZO^2+YO^2+XO^2)^{1/2}-70}{C} &= (2\pi/\lambda)[(ZO^2+YO^2+XO^2)^{1/2}-70] \\ &= \beta\Delta R \qquad (1\text{-}26)\end{aligned}$$

$$\begin{aligned}\overline{H} = {} & \frac{Idl[(ZP-ZO)^2+(YP-YO^2)^{1/2}}{4\pi[(XP-XO)^2+(YP-YO)^2+(ZP-ZO^2)]^{1/2}}\, e^{-j\beta[(XP-XO)^2+(YP-YO)^2 + (ZP-ZO)^2)^{1/2} + (ZP^2+YO^2+XO^2)^{1/2}-70]} \left[\frac{(XP-XO)}{((XP-XO)^2+(YP-YO)^2)^{1/2}}\,\hat{a}_y + {}\right. \\ & \left.\frac{(YP-YO)}{((XP-XO)^2+(YP-YO)^2)^{1/2}}\,\hat{a}_z\right] X \left[j\beta + \frac{1}{[(XP-XO)^2+(YP-YO)^2+(ZP-ZO)^2)]^{1/2}}\right]\end{aligned}$$

$$(1\text{-}27)$$

Programs 8 and 9 Appendix I were written to calculate the strength of the magnetic field at an observation point due to the two source patterns of figures (1-15) and (1-16). For each of the two cases a current element was placed at the location of the lobes, and a total magnetic field was calculated at an observation point corresponding to Los Canos. The calculations were carried out for the frequencies listed in table VI. These frequencies correspond to the frequencies used during the ELF/VLF experiments conducted in Puerto Rico. Figure (1-18) shows the result of the calculation. It is a plot of relative magnetic field strength as a function of frequency.

Frequency (kHz)	Frequency (kHz)
.479386	2.5
1.0	2.793296
1.25	3.144654
1.506024	3.448276
2.0	4.0
2.293578	4.464286
	5.0

Table VI. Experimental Frequencies

In order to determine the effect of the lobes on the value of the magnetic field at the observation point, a calculation was done with only the main lobe acting as the source. The plot of the relative field strength as a function of frequency is given in figure (1-19). A comparison of figures (1-18) and (1-19) shows that the lobes have a significant effect on determining the frequency response of the ELF/VLF radiating source. The location of the relative maximums and minimums in both 5.1 MHz and 3.17 MHz generated ELF/VLF response have shifted in frequency. A significant reduction in the field strength occurs between 2.5 to 4.5 kHz for the 5.1 MHz generated Y component.

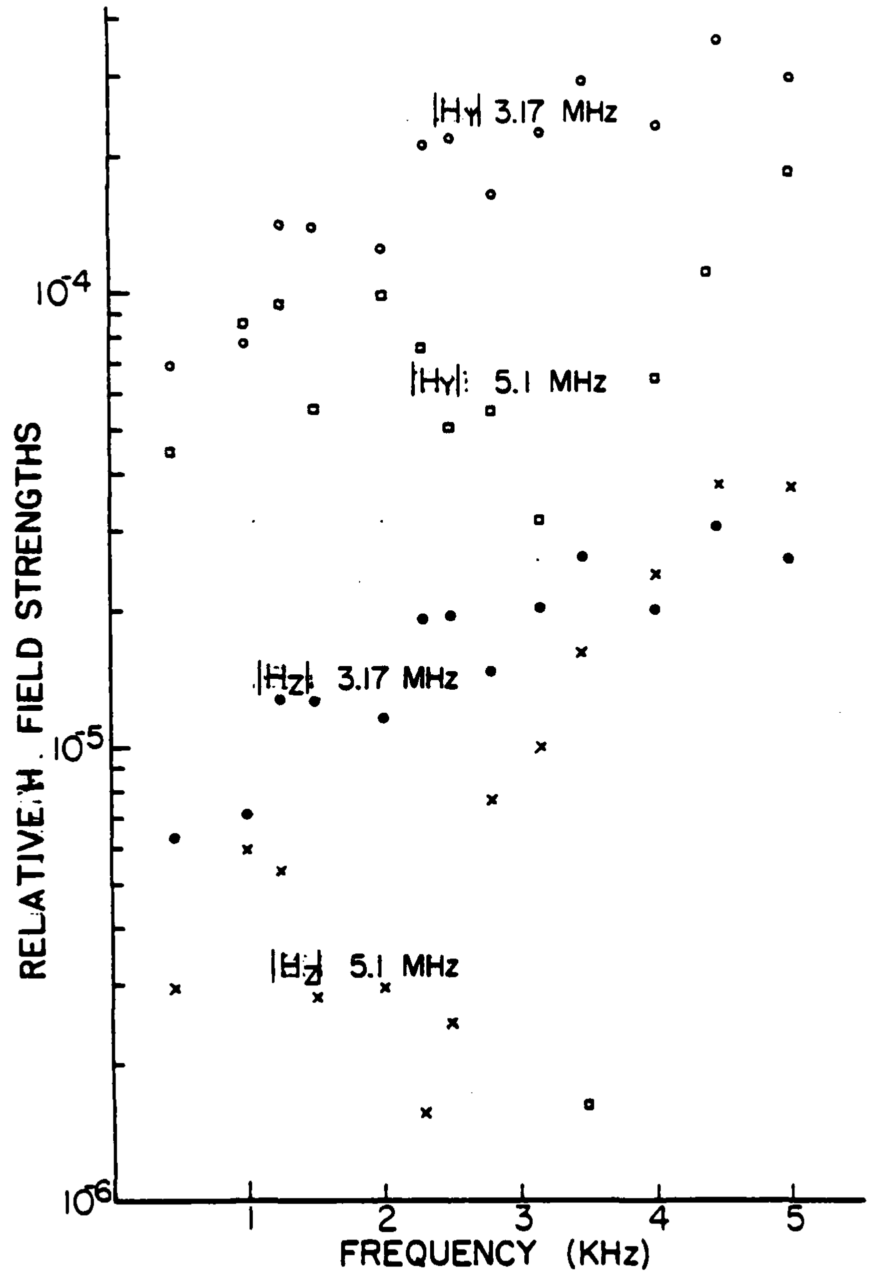

Figure 1-18 Current element array VLF/ELF response

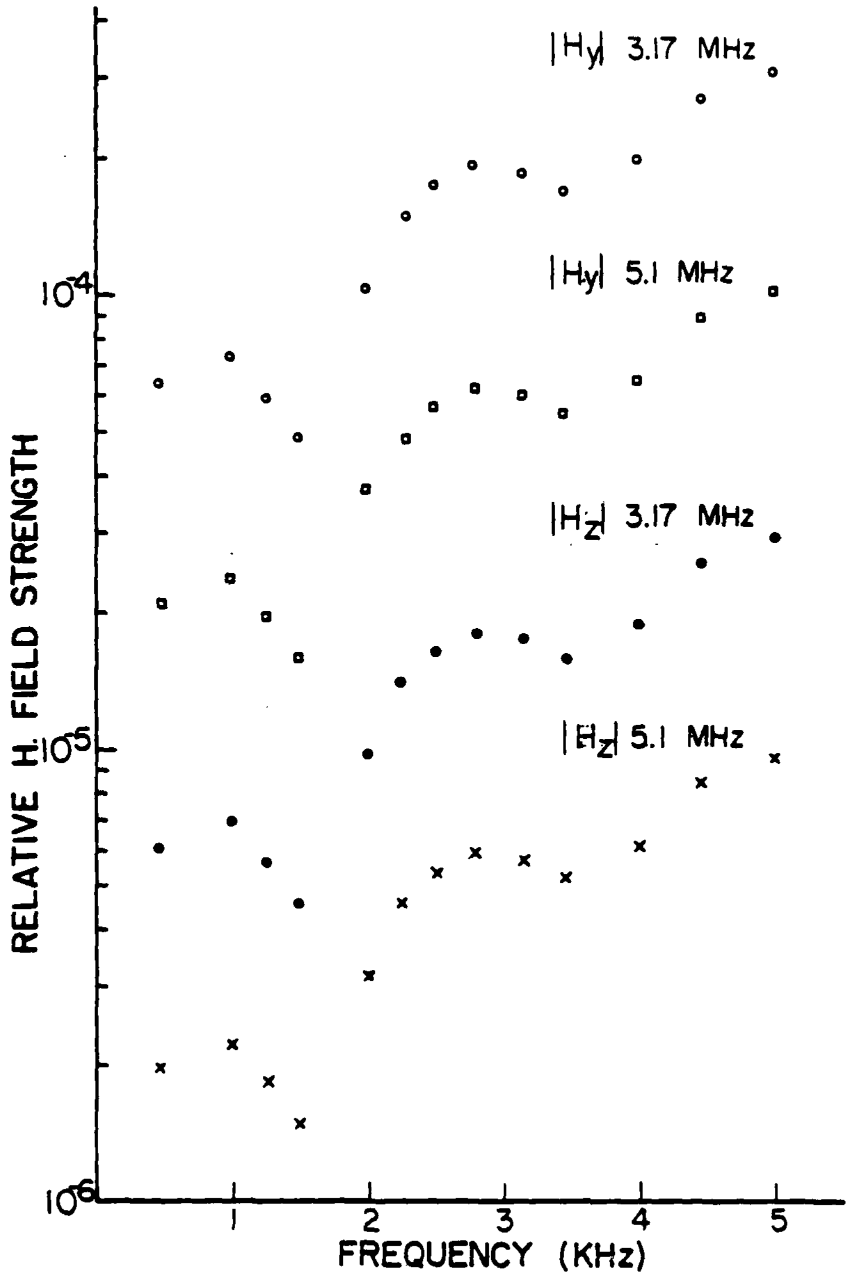

Figure 1-19 Main beam current element VLF/ELF response

In addition to computing the relative field strengths for the test frequencies, a calculation was made in 100 Hz frequency steps from from 500 Hz to 5 kHz. The result is plotted in figure (1-20). As can readily be seen from the figure, two deep minimums occur for the 5.1 MHz generated ELF/VLF. One occurs between 600 Hz and 700 Hz, and the other occurs between 3400 Hz and 3600 Hz. The 3.17 MHz generated ELF/VLF has only one deep minimum, which is located between 700 Hz and 900 Hz.

A calculation was made for an alternate receiving site. This site is located at Salinas, Puerto Rico, 17.98° N and 66.30° W geographic latitude and longitude respectively. The frequency response results for the two HF heating patterns are shown in figure (1-21). Comparison of figures (1-20) and (1-21) shows the changes in the response due to the different propagation paths. The first striking difference is the disappearance of the null in between 3 and 4 KHz in the 5.1 MHz pattern generated VLF. Second, the relative maximums and minimums for the Salinas location have been shifted to a lower frequency. In general, the relative field strengths are lower for the Salinas site due to the increase in propagation distance.

CONCLUSION

This completes the description of the zero order approximation. In summary, a pattern for the Arecibo Observatory has been calculated using the technique of pattern multiplication and AMP. The calculated pattern for the "PHI" equal "0" plane compares with the experimentally measured pattern. The pattern shows that there is enough power in the side lobes and grating lobes to cause significant heating at a 70 km

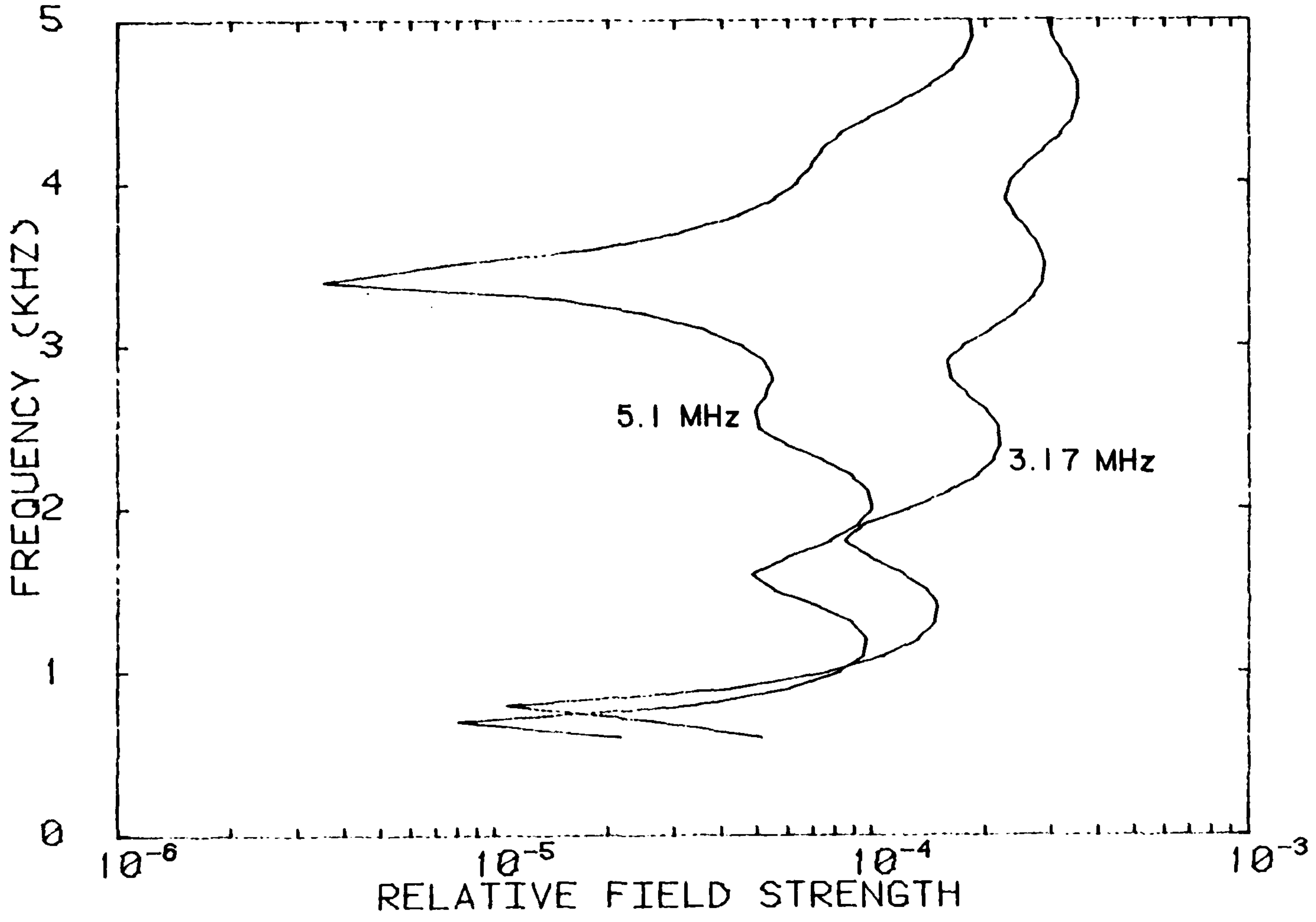

Figure 1-20 Current element array VLF/ELF response. Y component of magnetic field

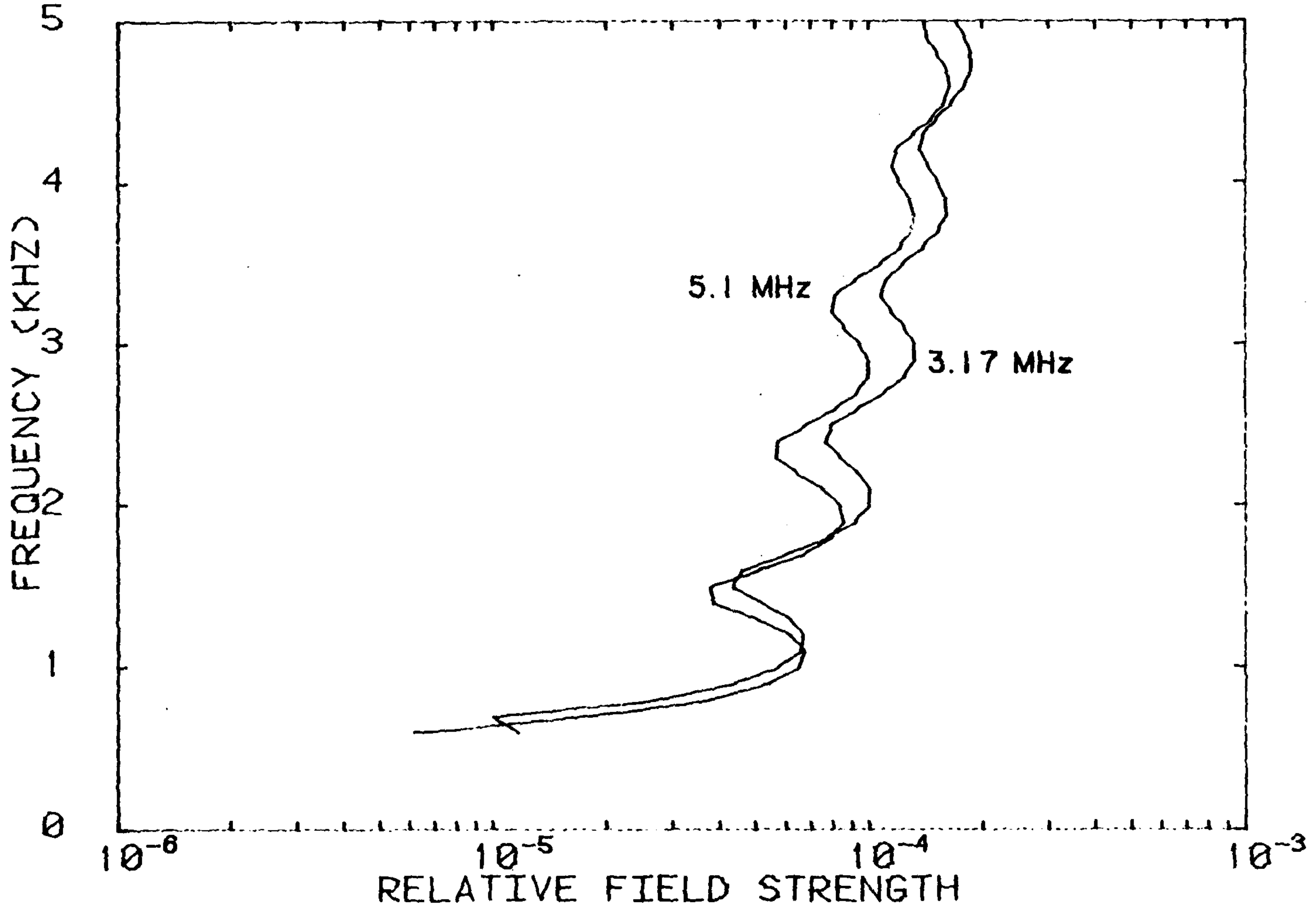

Figure 1-21 Current element array VLF/ELF response at Salinas. Y component of magnetic field

altitude. Using the HF antenna pattern, a zero order approximation of the model for the ELF/VLF radiating system was determined. The frequency responses of the ELF/VLF radiation system for observation points corresponding to Los Canos and Salinas were calculated. The calculations determined that the regions heated by the side lobes and grating lobes have a significant effect on the strength of the received signal.

REFERENCES

1. Antenna Modeling Program, Engineering Manual, MBA Associates, Bollinger Canyon Road, San Ramon, Calif., MB-R-74162, 1974.

2. Stutzman, W. L., Thiele, G. A., Antenna Theory and Design, John Wiley and Sons, New York, N.Y., 1981.

3. Mittra, R., Computer Techniques for Electromagnetics, Pergamon Press, New York, NY, 1982.

4. Trask, C., A high gain vertical beam antenna array using orthogonal non-planar log-periodic structures in a backfire configuration, M.S. Thesis, The Pennsylvania State University, 1979.

5. Jordan, E. C., Balmain, K. G., Electromagnetic Waves and Radiating Systems, Prentice-Hall, Inc., Englewood Cliffs, New Jersey, 1968.

6. Leithold, L., The Calculus with Analytic Geometry, Harper and Row, Publishers, New York, NY, 1968.

7. Preliminary Comparison of Theoretical and Observed Antenna Patterns for the Arecibo HF Heating Facility, Rice University, Houston, Texas, Feb. 18, 1982.

8. Richardson, C. G., An Analysis of the Ionospheric Antenna at VLF and ELF, M.S. Thesis, The Pennsylvania State University, 1982.

9. Helwig, J. T., SAS Introductory Guide, SAS Institute Inc., Cary, North Carolina, 1978.

10. SAS/GRAPH User's Guide, SAS Institute, Cary, North Carolina, 1978.

11. Selby, S. M. Girling, B., Standard Mathematical Tables, 14th edition, The Chemical Rubber Co., Cleveland, Ohio, 1965.

12. Hayt, Jr., W. H., Engineering Electromagnetics, 2nd edition, McGraw-Hill Book Company, 1967.

13. Robinson, R. W., Chebyshev's Polynomials, Thesis, The Pennsylvania State University, King of Prussia Graduate Center, March 1974.

Appendix I

Computer Programs

Program I

AMP data file

```
CM        THE DECK MUST BEGIN WITH CM,CE CARDS
CM   HEATER ARRAY ELEMENT AT ARECIBO P.R.    FREQ=3.170 MHZ.
CE    EE 438 FALL TERM 1981
GW001   5     0.000     0.000     0.000     0.000     5.763    0.000    0.0020
GW002   4     0.000     5.763     0.000    -4.175     5.763    0.000    0.0020
GW003   1     0.000     5.763     0.000     0.000     6.776    0.000    0.0020
GW004   4     0.000     6.776     0.000     4.745     6.776    0.000    0.0020
GW005   1     0.000     6.776     0.000     0.000     7.700    0.000    0.0020
GW006   4     0.000     7.700     0.000    -5.392     7.700    0.000    0.0020
GW007   1     0.000     7.700     0.000     0.000     8.750    0.000    0.0020
GW008   5     0.000     8.750     0.000     6.127     8.750    0.000    0.0020
GW009   1     0.000     8.750     0.000     0.000     9.944    0.000    0.0020
GW010   5     0.000     9.944     0.000    -6.963     9.944    0.000    0.0020
GW011   1     0.000     9.944     0.000     0.000    11.299    0.000    0.0020
GW012   5     0.000    11.299     0.000     7.912    11.299    0.000    0.0020
GW013   1     0.000    11.299     0.000     0.000    12.840    0.000    0.0020
GW014   5     0.000    12.840     0.000    -8.991    12.840    0.000    0.0020
GW015   1     0.000    12.840     0.000     0.000    14.591    0.000    0.0020
GW016   5     0.000    14.591     0.000    10.217    14.591    0.000    0.0020
GW017   1     0.000    14.591     0.000     0.000    16.581    0.000    0.0020
GW018   5     0.000    16.581     0.000   -11.610    16.581    0.000    0.0020
GW019   1     0.000    16.581     0.000     0.000    18.842    0.000    0.0020
GW020   5     0.000    18.842     0.000    13.193    18.842    0.000    0.0020
GW021   1     0.000    18.842     0.000     0.000    21.412    0.000    0.0020
GW022   6     0.000    21.412     0.000   -14.992    21.412    0.000    0.0020
GW023   1     0.000    21.412     0.000     0.000    24.331    0.000    0.0020
GW024   7     0.000    24.331     0.000    17.037    24.331    0.000    0.0020
GW025   2     0.000    24.331     0.000     0.000    27.649    0.000    0.0020
GW026   8     0.000    27.649     0.000   -19.360    27.649    0.000    0.0020
GW027   2     0.000    27.649     0.000     0.000    31.420    0.000    0.0020
GW028   9     0.000    31.420     0.000    22.000    31.420    0.000    0.0020
GW029   2     0.000    31.420     0.000     0.000    35.704    0.000    0.0020
GW030  10     0.000    35.704     0.000   -25.000    35.704    0.000    0.0020
GM000   0    45.000     0.000     0.000     0.000     0.000    0.000
GM030   1    90.000     0.000     0.000     0.000     0.000    0.000
GW061   5     0.000     0.000     0.000     5.775     0.000    0.000    0.0020
GW062   4     5.775     0.000     0.000     5.775    -4.344    0.000    0.0020
GW063   1     5.775     0.000     0.000     6.563     0.000    0.000    0.0020
GW064   4     6.563     0.000     0.000     6.563     4.546    0.000    0.0020
GW065   1     6.563     0.000     0.000     7.458     0.000    0.000    0.0020
GW066   4     7.458     0.000     0.000     7.458    -5.222    0.000    0.0020
GW067   1     7.458     0.000     0.000     8.475     0.000    0.000    0.0020
GW068   5     8.475     0.000     0.000     8.475     5.934    0.000    0.0020
GW069   1     8.475     0.000     0.000     9.631     0.000    0.000    0.0020
GW070   5     9.631     0.000     0.000     9.631    -6.7[illegible]    0.000    0.0020
GW071   1     9.631     0.000     0.000    10.944     0.000    0.000    0.0020
GW072   5    10.944     0.000     0.000    10.944    -7.663    0.000    0.0020
GW073   1    10.944     0.000     0.000    12.436     0.000    0.000    0.0020
GW074   5    12.436     0.000     0.000    12.436    -8.708    0.000    0.0020
GW075   1    12/436     0.000     0.000    14.132     0.000    0.000    0.0020
GW076   5    14.132     0.000     0.000    14.132     9.396    0.000    0.0020
GW077   1    14.132     0.000     0.000    16.059     0.000    0.000    0.0020
GW078   5    16.059     0.000     0.000    16.059   -11.245    0.000    0.0020
GW079   1    16.059     0.000     0.000    18.249     0.000    0.000    0.0020
GW080   5    18.249     0.000     0.000    18.249    12.778    0.000    0.0020
GW081   1    18.249     0.000     0.000    20.739     0.000    0.000    0.0020
GW082   6    20.739     0.000     0.000    20.739   -14.520    0.000    0.0020
GW083   1    20.739     0.000     0.000    23.566     0.000    0.000    0.0020
GW084   7    23.566     0.000     0.000    23.566    16.501    0.000    0.0020
GW085   2    23.566     0.000     0.000    26.779     0.000    0.000    0.0020
GW086   8    26.779     0.000     0.000    26.779   -18.751    0.000    0.0020
GW087   2    26.779     0.000     0.000    30.432     0.000    0.000    0.0020
GW088   9    30.432     0.000     0.000    30.432    21.308    0.000    0.0020
GW089   2    30.432     0.000     0.000    34.581     0.000    0.000    0.0020
GW090  10    34.581     0.000     0.000    34.581   -24.214    0.000    0.0020
GM000   0     0.000   -45.000     0.000     0.000     0.000    0.000      61.0
GM030   1     0.000   -90.000     0.000     0.000     0.000    0.000      61.0
GE001
GN000   0                20.0       .03
FR000   1               3.170     0.000
EX000 001   001    00   1.000     0.000
EX000 031   001    00   1.000     0.000
EX000 051   001    00   1.000     0.000
EX000 091   001    00   1.000     0.000
RP000  45    72  1000     0.0       0.0       2.5       5.0    7.5E 04
EN000
```

Program II

Total Array Pattern Simpson Integration, 3.17 MHz

```
// EXEC FWCG
//SYSIN DD *
      DIMENSION A(145)
      AX=0.
      BX=1.570797
      AY=0.
      BY=6.283185
C     NHT MUST BE EVEN AND GREATER THAN 4. NHT+1 IS # OF THETA ANGLES.
      NHT=90
C     NHP MUST BE EVEN AND GREATER THAN 4. NHP+1 IS # OF PHI ANGLES
      NHP=144
      TOT=0.
      HT=(BX-AX)/NHT
      HP=(BY-AY)/NHP
      X=AX
      Y=AY
      DO 300 J=1,145
      A(J)=0.
300   CONTINUE
C     NI=# OF ANGLES THETA-4. (FIRST AND LAST TWO OF SERIES PLUS SECOND IN LOOP
      NI=NHT-3
C     NJ=# OF ANGLES PHI AT WHICH INTEGRALS IN THETA ARE EVALUATED.
      NJ=NHP+1
      DO 200 J=1,NJ
      C1=FLOAT(J)
      A(J)=A(J)+PWR(X,Y)
      DO 100 I=1,NI,2
      C=FLOAT(I)
      X=AX+C*HT
      A(J)=A(J)+4.*PWR(X,Y)
      X=AX+(C+1.)*HT
      A(J)=A(J)+2.*PWR(X,Y)
100   CONTINUE
      X=AX+(NHT-1)*HT
      A(J)=A(J)+4.*PWR(X,Y)
      X=AX+NHT*HT
      A(J)=A(J)+PWR(X,Y)
      X=AX
      Y=AY+C1*HP
200   CONTINUE
      TOT=TOT+A(1)
      NP=NHP-2
      DO 400 J=2,NP,2
      TOT=TOT+4.*A(J)
      TOT=TOT+2.*A(J+1)
400   CONTINUE
      TOT=TOT+4.*A(NHP)
      TOT=TOT+A(NJ)
      ANS=TOT*HT*HP/9.
      WRITE(6,600) ANS,(A(I),I=1,145)
600   FORMAT(' THE TOTAL INTEGRAL IS =',1PE15.7,15(/' ',10(1PE10.3,2X)))
      STOP
      END
      FUNCTION PWR(X,Y)
      REAL*4 PWR,X,Y,PI
      PI=3.14159300
      X1=X
      THETA=(X/PI)*180.
      PHI=(Y/PI)*180.
      PWR=AF(THETA,PHI)*FF(THETA,PHI)*SIN(X1)
```

```
C     WRITE(6,100) PWR
C 100  FORMAT(' ','PWR=',1PE10.3)
      RETURN
      END
      FUNCTION AF(THETA,PHI)
      THETAR=(THETA/180.)*3.14159
      PHIR=(PHI/180.)*3.14159
      BETA=2.822564
      BETA4=4.*BETA
      BETA8=8.*BETA
      STHETA=SIN(THETAR)
      SPHI=SIN(PHIR)
      CPHI=COS(PHIR)
C     AFT=(SIN(BETA4*STHETA*SPHI)/SIN(BETA*STHETA*SPHI))*(SIN(BETA8*STHE
C    1TA*CPHI)/SIN(BETA*STHETA*CPHI))
      IF( ABS(THETA-0.) .LE. .2 .OR. ABS(THETA-180.) .LE. .2 .OR. ABS(PH
     1I-0.) .LE. .2 .OR. ABS(PHI-180.) .LE. .2) GO TO 100
      GO TO 200
 100  AFT1=4.
      GO TO 300
 200  AFT1=ABS(SIN(BETA4*STHETA*SPHI)/SIN(BETA*STHETA*SPHI))
 300  IF(ABS(THETA-0.) .LE. .2 .OR. ABS(THETA-180.) .LE. .2 .OR. ABS(PHI
     1-90.) .LE. .2 .OR. ABS(PHI-270.) .LE. .2) GO TO 400
      GO TO 500
 400  AFT2=8.
      GO TO 600
 500  AFT2=ABS(SIN(BETA8*STHETA*CPHI)/SIN(BETA*STHETA*CPHI))
 600  CONTINUE
C     600   DBAFT1=20.*.434294*ALOG(AFT1)
C     DBAFT2=20.*.434294*ALOG(AFT2)
C     WRITE(6,700) THETA,PHI,DBAFT1,DBAFT2
C  700   FORMAT(' ','THETA=',F6.2,'DEG    PHI=',F6.2,'DEG    4 ELEMENT=',F7.
C    12,' DB    8 ELEMENT=',F7.2,' DB')
C     AFT=ABS(AFT)
C     IF (ABS(AFT) .LT. 1.E-10) GO TO 10
C     AF=20.*.434294*ALOG(AFT)
C     AF=DBAFT1+DBAFT2
      AF=AFT1*AFT2
      AF=AF*AF
C     WRITE(6,800) AF,THETA,PHI
C 800   FORMAT(' AF=',1PE10.3,'   THETA=',1PE10.3,'   PHI=',1PE10.3)
      RETURN
C 10  - AF=-99.
C     RETURN
      END
      FUNCTION ELF(THETA,PHI)
      DIMENSION FF(7,37),APHI(8),ATHETA(37),T1(7,34),T2(7,3)
      DATA APHI/0.,90.,130.,180.,210.,270.,320.,360./,ATHETA/0.,2.5,5.,7
     1.5,10.,12.5,15.,17.5,20.,22.5,25.,27.5,30.,32.5,35.,37.5,40.,42.5,
     145.,47.5,50.,52.5,55.,57.5,60.,62.5,65.,67.5,70.,72.5,75.,77.5,80.,
     1,82.5,85.,87.5,90./
      DATA T1/7*3.5,3.52,3.45,3.43,3.44,3.46,3.51,3.53,3.51,3.37,3.35,3.
     135,3.38,3.5,3.55,3.47,3.26,3.26,[illegible]
     1,3.08,3.12,3.38,3.51,3.30,2.97,2.95,[illegible],3.20,3.65,3.16,2.75,
     12.76,2.67,2.71,3.15,3.36,2.99,2.51,2.56,2.61,2.46,2.98,3.25,[illegible]
     [illegible]
     [illegible]
     [illegible]
     [illegible]
     16,-1.68,-.61,-1.05,-1.77,-.11,[illegible]
```

```
     14.,54.,-1.63,-3.29,-1.67,-3.36,-3.69,-1.22,.09,-2.45,-4.22,-2.25,-6
     1.16,-6.42,-1.83,-.6,-3.12,-5.25000,-2.860,-5.03,-5.21,-2.69,-.92,-
     13.95,-6.48,-3.51,-5.95,-6.15,-3.10,-1.60,-6.0?,-7.61,-6.19,-7.91,-
     17.14,-3.91,-2.07,-5.73,-8.93,-6.90,-7.90,-8.17,-4.88,-2.71,-6.65,-
     110.33,-5.66,-8.92,-9.25,-5.49,-3.38,-7.57,-11.73,-6.4,-9.95,-10.36
     1,-6.34,-4.10,-8.45,-13.00,-7.19,-10.97,-11.48,-7.22,-4.86,-9.26,-1
     13.99,-8.00,-11.97,-12.61,-8.13,-5.66,-9.96,-14.54,-8.84,-12.95,-13
     1.72,-9.09,-6.52,-10.55,-14.76000,-9.70,-13.90,-14.81,-10.09,-7.44,
     1-11.05,-16.52,-10.59,-14.83,-15.85,-11.15,-8.43,-11.51,-14.33,-11.
     154,-15.77,-16.87,-12.28,-9.51,-12.03,-14.30,-12.60,-16.79,-17.91,-
     113.52,-10.73,-12.80,-14.64,-13.90,-18.01,-19.11,-14.99,-12.21/
      DATA T2/-14.19,-15.73,-15.77,-19.78,-20.84,-16.98,-14.26,-17.54,-1
     18.90,-19.51,-23.4,-24.41,-20.76,-18.15,-0.0,0.0,0.0,0.0,0.0,0.0,0.
     10/
      I1=1
      DO 300 I=1,34
      DO 400 J=1,7
      FF(J,I)=T1(J,I)
400   CONTINUE
300   CONTINUE
      DO 500 I=35,37
      DO 600 J=1,7
      IT=I-34
      FF(J,I)=T2(J,IT)
600   CONTINUE
500   CONTINUE
C     WRITE(6,2000) ((FF(I,J),I=1,7),J=1,37)
C 2000 FORMAT(' ',37(' ',7(F7.2,3X),/))
      J1=1
      DO 100 I=2,8
      I3=I
      IF(APHI(I) .GT. PHI) GO TO 1000
      I1=I1+1
100   CONTINUE
1000  DO 200 J=2,36
      J3=J
      IF(ATHETA(J) .GT. THETA) GO TO 1100
      J1=J1+1
200   CONTINUE
      J3=36
      J1=J3-1
1100  FRACT=(THETA-ATHETA(J1))/(ATHETA(J3)-ATHETA(J1))
      FRACP=(PHI-APHI(I1))/(APHI(I3)-APHI(I1))
      IF(I3 .EQ. 8) I3=1
      FF1=FRACP*(FF(I3,J1)-FF(I1,J1))+FF(I1,J1)
      FF2=FRACP*(FF(I3,J3)-FF(I1,J3))+FF(I1,J3)
      ELF=FRACT*(FF2-FF1)+FF1
      ELFE=ELF/10.
      ELF=10.**ELFE
C     WRITE(6,700) ELF,ATHETA(J3),ATHETA(J1),APHI(I3),APHI(I1)
C  700   FORMAT(' ','ELEMENTAL FACTOR=',F6.2,' DB',4(3X,F6.2))
      RETURN
      END
//DATA.INPUT DD *
```

Program III

Total Array Pattern Simpson Integration, 5.1 MHz

```
// EXEC FWCG
/*JP SERVICE=DEFER
//SYSIN DD *                                                        00000100
      DIMENSION A(145)
      AX=0.
      BX=1.570297
      AY=0.
      BY=6.283185
C     NHT MUST BE EVEN AND GREATER THAN 4. NHT+1 IS # OF THETA ANGLES.
      NHT=90
C     NHP MUST BE EVEN AND GREATER THAN 4. NHP+1 IS # OF PHI ANGLES
      NHP=144
      TOT=0.
      HT=(BX-AX)/NHT
      HP=(BY-AY)/NHP
      X=AX
      Y=AY
      DO 300 J=1,145
      A(J)=0.
300   CONTINUE
C     NI=#.OF ANGLES THETA-4. (FIRST AND LAST TWO OF SERIES PLUS SECOND IN LOOP
      NI=NHT-3
C     NJ=# OF ANGLES PHI AT WHICH INTEGRALS IN THETA ARE EVALUATED.
      NJ=NHP+1
      DO 200 J=1,NJ
      C1=FLOAT(J)
      A(J)=A(J)+PWR(X,Y)
      DO 100 I=1,NI,2
      C=FLOAT(I)
      X=AX+C*HT
      A(J)=A(J)+4.*PWR(X,Y)
      X=AX+(C+1.)*HT
      A(J)=A(J)+2.*PWR(X,Y)
100   CONTINUE
      X=AX+(NHT-1)*HT
      A(J)=A(J)+4.*PWR(X,Y)
      X=AX+NHT*HT
      A(J)=A(J)+PWR(X,Y)
      X=AX
      Y=AY+C1*HP
200   CONTINUE
      TOT=TOT+A(1)
      NP=NHP-2
      DO 400 J=2,NP,2
      TOT=TOT+4.*A(J)
      TOT=TOT+2.*A(J+1)
400   CONTINUE
      TOT=TOT+4.*A(NHP)
      TOT=TOT+A(NJ)
      ANS=TOT*HT*HP/9.
      WRITE(6,600) ANS,(A(I),I=1,145)
600   FORMAT(' THE TOTAL INTEGRAL IS =',1PE15.7,15(/' ',10(1PE10.3,2X)))
      STOP
      END
      FUNCTION PWR(X,Y)
      REAL*4 PWR,X,Y,PI
      PI=3.1415930 00
      XI=X
      TH=(A-(Z/PI))*100.
      PHI=(Y/PI)*100.
```

```
      PWR=AF(THETA,PHI)*ELE(THETA,PHI)*SIN(X))
C     WRITE(6,100) PWR
C 100    FORMAT(' ','PWR=',1PE10.3)
      RETURN
      END
      FUNCTION AF(THETA,PHI)
      THETAR=(THETA/180.)*3.14159
      PHIR=(PHI/180.)*3.14159
C     BETA=2*PI*(F/C)*B5/2.    B5=DISTANCE BETWEEN RADIATORS.
      BETA=4.539601
      BETA4=4.*BETA
      BETA8=8.*BETA
      STHETA=SIN(THETAR)
      SPHI=SIN(PHIR)
      CPHI=COS(PHIR)
C     AFT=(SIN(BETA4*STHETA*SPHI)/SIN(BETA*STHETA*SPHI))*(SIN(BETA8*STHE
C    1TA*CPHI)/SIN(BETA*STHETA*CPHI))
      IF( ABS(THETA-0.) .LE. .2 .OR. ABS(THETA-180.) .LE. .2 .OR. ABS(PH
     1I-0.) .LE. .2 .OR. ABS(PHI-180.) .LE. .2) GO TO 100
      GO TO 200
 100  AFT1=4.
      GO TO 300
 200  AFT1=ABS(SIN(BETA4*STHETA*SPHI)/SIN(BETA*STHETA*SPHI))
 300  IF(ABS(THETA-0.) .LE. .2 .OR. ABS(THETA-180.) .LE. .2 .OR. ABS(PHI
     1-90.) .LE. .2 .OR. ABS(PHI-270.) .LE. .2) GO TO 400
      GO TO 500
 400  AFT2=8.
      GO TO 600
 500  AFT2=ABS(SIN(BETA8*STHETA*CPHI)/SIN(BETA*STHETA*CPHI))
C     USE .434294 TO CONVERT NATURAL LOG TO BASE 10
 600  CONTINUE
C 600    DBAFT1=20.*.434294*ALOG(AFT1)
C     DBAFT2=20.*.434294*ALOG(AFT2)
C     WRITE(6,700) THETA,PHI,DBAFT1,DBAFT2
C 700    FORMAT(' ','THETA=',F6.2,'DEG   PHI=',F6.2,'DEG   4 ELEMENT=',F7.
C    12,' DB    8 ELEMENT=',F7.2,' DB')
C     AFT=ABS(AFT)
C     IF (ABS(AFT) .LT. 1.E-10) GO TO 10
C     AF=20.*.434294*ALOG(AFT)
C     AF=DBAFT1+DBAFT2
      AF=AFT1*AFT2
      AF=AF*AF
      RETURN
C 10     AF=-99.
C     RETURN
      END
      FUNCTION ELE(THETA,PHI)
      DIMENSION EE(9,37),APHI(10),ATHETA(37),E1(7,33),E2(7,4),E3(2,37)
      DATA APHI/10.,60.,70.,110.,150.,180.,[illegible]/,ATHETA/0
     1.,2.5,5.,7.5,10.,12.5,15.,17.5,20.,22.5,25.,27.5,30.,32.5,35.,37.5
     1,40.,42.5,45.,47.5,50.,52.5,55.,57.5,60.,62.5,65.,67.5,70.,72.5,75
     1.,77.5,80.,82.5,85.,87.5,90./
      DATA E1/[illegible]
     1[illegible]
     1[illegible]
     1[illegible]
     1[illegible]
     1[illegible]
     1[illegible]
     1[illegible]
```

```
     1.3,1.36,2.,-2.37,-3.03,-2.55,-1.56,0.93,0.93,1.62,-3.34,-3.95,-3.4
     16,-2.33,.55,.46,1.21,-4.42,-4.93,-4.47,-3.18,0.15,-.04,.77,-5.64,-
     15.97,-5.59,-4.13,-.27,-.57,.29,-7.0,-7.06,-6.42,-5.17,-.70,-1.1400
     1,-.22,-8.53,-8.19,-8.19,-6.34,-1.14,-1.73,-.76,-10.22,-9.40,-9.700
     1,-7.63,-1.59,-2.35,-1.34,-12.05,-10.36,-11.34,-9.07,-2.06,-2.29,-1
     1.94,-13.90,-11.3,-13.10,-10.68,-2.56,-3.65,-2.57,-15.46,-12.08,-14
     1.8700,-12.47,-3.1,-4.34,-3.22,-16.27,-12.65,-16.48,-14.40,-3.68,-5
     1.04,-3.89,-16.19,-13.05,-17.62,-16.39,-4.42,-5.76,-4.59,-15.54,-13
     1.32,-18.11,-18.16,-5.04,-6.5,-5.32,-14.78,-13.54,-18.06,-19.32,-5.
     1860000,-7.26,-6.09,-14.15,-13.79,-17.8,-19.66,-6.81,-8.07,-6.91,-1
     13.78,-16.15,-17.61,-19.5,-7.93,-8.94,-7.81,-13.76,-14.71,-17.7,-19
     1.330,-9.30,-9.95,-8.87/
      DATA T2/-14.23,-15.65,-18.25,-19.58,-11.05,-11.22,-10.21,-15.57,-1
     17.35,-19.69,-20.72,-13.52,-13.13,-12.22,-19.12,-21.19,-23.37,-24.1
     17,-18.01,-17.03,-16.23,7*0.0/
      DATA T3/3.83,3.83,3.80,3.85,3.75,3.84,3.68,3.82,3.58,3.76,3.47,3.6
     18,3.32000,3.57,3.16,3.44,2.97,3.27,2.76,3.07,2.52,2.83,2.25,2.5600
     1,1.96,2.24,1.64,1.89,1.29,1.49,.92,1.05,0.52,0.56,.10,.03,-.36,-.5
     15,-.84,-1.18,-1.35,-1.85,-1.89,-2.56,-2.45,-3.30,-3.05,-4.06,-3.68
     1,-4.84,-4.36,-5.61,-5.08,-6.37,-5.85,-7.09,-6.70,-7.76,-7.64,-8.40
     1,-8.69,-9.01,-9.89,-9.66,-11.33,-10.43,-13.13,-11.49,-15.66,-13.24
     1,-20.2200,-17.07,0.,0./
      I1=1
      IF( PHI .LT. 10.) PHI=PHI+360.
      DO 300 I=1,33
      DO 400 J=1,4
      EF(J,I)=T1(J,I)
400   CONTINUE
      EF(5,I)=T3(1,I)
      DO 450 J=5,7
      EF(J+1,I)=T1(J,I)
450   CONTINUE
      EF(9,I)=T3(2,I)
300   CONTINUE
      DO 500 I=34,37
      DO 600 J=1,4
      IT=I-33
      EF(J,I)=T2(J,IT)
600   CONTINUE
      EF(5,I)=T3(1,I)
      DO 650 J=5,7
      EF(J+1,I)=T2(J,IT)
650   CONTINUE
      EF(9,I)=T3(2,I)
500   CONTINUE
C     WRITE(6,2000) ((EF(I,J),I=1,9),J=1,37)
C   2000  FORMAT(' ',37(' ',9(F7.2,4X),/))
      J1=1
      DO 100 I=2,10
      I3=I
      IF(APHI(I) .GT. PHI) GO TO 1000
      I1=I1+1
100   CONTINUE
1000  DO 200 J=2,36
      J3=J
      IF(ATHETA(J) .GT. THETA) GO TO 1100
      J1=J1+1
200   CONTINUE
      J3=36
      J1=J3-1
```

```
1100  FRACT=(THETA-ATHETA(J1))/(ATHETA(J3)-ATHETA(J1))
      IF (I1 .EQ. I3) WRITE(6,800) PHI
      FRACP=(PHI-APHI(I1))/(APHI(I3)-APHI(I1))
      IF(I3 .EQ. 10) I3=1
      FF1=FRACP*(FF(I3,J1)-FF(I1,J1))+FF(I1,J1)
      FF2=FRACP*(FF(I3,J3)-FF(I1,J3))+FF(I1,J3)
      ELF=FRACT*(FF2-FF1)+FF1
      ELFE=ELF/10.
      ELF=10.**ELFE
C     WRITE(6,700) ELF,ATHETA(J3),ATHETA(J1),APHI(I3),APHI(I1)
C   700   FORMAT(' ','ELEMENTAL FACTOR=',F6.2,' DB',4(3X,F6.2))
800   FORMAT(' ',F10.3,'  PHI NOT IN RANGE 10 DEG TO 370 DEG')
      RETURN
      END
//DATA.INPUT DD *
```

Program IV

Directive Gain Pattern Calculation and Plotting, 3.17MHz

```
//SCR EXEC PGM=IEFBR14
//SCR DD DISP=(OLD,DELETE),VOL=REF=VOL001,
// DSN=MEN.U84490.KJC.PLOT.OUTPUT
// EXEC FXCG
/*JP SERVICE=DEFER
/*JP FULLSKIPS
//SYSIN DD *
      COMMON /BLOCK1/XVAL(181),YVAL(181),IYBCD(4),IXBCD(8)
C     4 CHARACTERS PER INTEGER IN INTEGER ARRAYS. SEE BLOCK DATA SUBPROG
      DIMENSION ATHA(91),ADB(91),CHECK(5),CHEKP(5)
      CHECK(1)=0.
      CHECK(2)=32.5
      CHECK(3)=55.
      CHECK(4)=87.5
      CHECK(5)=90.
      CHEKP(1)=90.
      CHEKP(2)=270.
      CHEKP(3)=90.
      CHEKP(4)=130.
      CHEKP(5)=250.
      DO 400 J=11,19
      JINC=1
      DO 1003 I=1,181
      XVAL(I)=0.
1003  YVAL(I)=0.
      J1=J-1
      PHI=FLOAT(J1)*5.0+90.
C     PHI=CHEKP(J)
      PHIL=PHI-90.
      DO 500 I=1,91
      ATHA(I)=0.
      ADB(I)=0.
 500  CONTINUE
      DO 2000 J2=1,2
      THETA=0.
      DO 100 I=1,91
C     THETA=CHECK(I)
C     FIND TOTAL FIELD. 8.62 IS FACTOR TO NORMALIZE TO GAIN OVER ISOTROPIC
      DB=AF(THETA,PHI)+ELE(THETA,PHI)-8.62
      ATHA(I)=THETA
      ADB(I)=DB
      THETA=THETA+1.
 100  CONTINUE
      WRITE(6,200) (ATHA(I),PHI,ADB(I),I=1,91)
 200  FORMAT(' ',5(F6.2,1X,F6.2,1X,F8.3,2X))
      WRITE(6,300)
 300  FORMAT(' ')
      JP=91
      NEND=NUI+1
      DO 1001 I=1,91
      XVAL(JP)=ATHA(I)*JINC
      YVAL(JP)=ADB(I)
      JP=JP+JINC
1001  CONTINUE
      IF(JINC .EQ. 1) JINC=-1
      PHI=PHI+180
      IF(PHI .GT. 360.) PHI=PHI-360.
2000  CONTINUE
      WRITE(6,1006)(XVAL(I),YVAL(I),I=1,181)
1006  FORMAT(' ',5(F[illegible]),/' ')) [illegible]
```

```
      IF(J .GT. 11) CALL NXTPLT(18,6,-90.,90.,-30.,30.,181)
      IF(J .GT. 11) GO TO 2100
      CALL ANTPLT(18,6,-90.,90.,-30.,30.,181)
2100  Y=4.58
      X=4.00
      CALL LETTER(X,Y,.15,'PHI= ',0,0,5)
      CALL NUMBER(X,Y,.15,PHI,0,0,1)
      X=X+.95
      Y=4.58
      CALL LETTER(X,Y,.15,'DEG. W',0,0,6)
      CALL NEWPEN(3)
400   CONTINUE
      CALL FINISH
1002  CONTINUE
      STOP
      END
      FUNCTION AF(THETA,PHI)
      THETAR=(THETA/180.)*3.14159
      PHIR=(PHI/180.)*3.14159
      BETA=2.822564
      BETA4=4.*BETA
      BETA8=8.*BETA
      STHETA=SIN(THETAR)
      SPHI=SIN(PHIR)
      CPHI=COS(PHIR)
C     AFT=(SIN(BETA4*STHETA*SPHI)/SIN(BETA*STHETA*SPHI))*(SIN(BETA8*STHE
C    1TA*CPHI)/SIN(BETA*STHETA*CPHI))
      IF( ABS(THETA-0.) .LE. .2 .OR. ABS(THETA-180.) .LE. .2 .OR. ABS(PH
     1I-0.) .LE. .2 .OR. ABS(PHI-180.) .LE. .2) GO TO 100
      GO TO 200
100   AFT1=4.
      GO TO 300
200   AFT1=ABS(SIN(BETA4*STHETA*SPHI)/SIN(BETA*STHETA*SPHI))
300   IF(ABS(THETA-0.) .LE. .2 .OR. ABS(THETA-180.) .LE. .2 .OR. ABS(PHI
     1-90.) .LE. .2 .OR. ABS(PHI-270.) .LE. .2) GO TO 400
      GO TO 500
400   AFT2=8.
      GO TO 600
500   AFT2=ABS(SIN(BETA8*STHETA*CPHI)/SIN(BETA*STHETA*CPHI))
600   DBAFT1=20.*.434294*ALOG(AFT1)
      DBAFT2=20.*.434294*ALOG(AFT2)
C     WRITE(6,700) THETA,PHI,AFT1,AFT2
700   FORMAT(' ','THETA=',F6.2,'DEG     PHI=',F6.2,'DEG    4 ELEMENT=',F7.
     12,'      8 ELEMENT=',F7.2,'    ')
C     AFT=ABS(AFT)
C     IF (ABS(AFT) .LT. 1.E-10) GO TO 10
C     AF=20.*.434294*ALOG(AFT)
      AF=DBAFT1+DBAFT2
      RETURN
C  10     AF=-99.
C     RETURN
      END
      FUNCTION ELE(THETA,PHI)
      DIMENSION [illegible](7,37),APHI(8),ATHETA(37),T1(7,36),T2(7,3)
      DATA APHI/0.,90.,130.,180.,210.,270.,320.,360./,ATHETA/0.,2.5,5.,7
     1.5,10.,12.5,15.,17.5,20.,[illegible],27.5,30.,[illegible],37.5,40.,[illegible]
     165.,47.5,50.,52.5,55.,57.5,60.,62.5,65.,67.5,70.,72.5,75.,77.5,80.
     1,82.5,85.,87.5,90./
      DATA T1/[illegible]
     1[illegible]
```

```
     1,3.08,3.12,3.38,3.51,3.30,2.96,2.95,2.89,2.93,3.28,3.45,3.16,2.75,
     12.76,2.67,2.71,3.15,3.36,2.99,2.51,2.56,2.41,2.44,2.98,3.25,2.79,2
     1,23,2.32,2.11,2.13,2.78,3.12,2.54,1.92,2.06,1.77,1.78,2.55,2.95,2.
     176,1.56,1.77,1.39,1.38,2.28,2.76,1.94,1.15,1.45,.97,.94,1.98,2.53,
     11.57,.70,1.10,.5,.46,1.64,2.28,1.16,.19,.72,-.01,-.08,1.26,2.,.71,
     1-.37,.31,-.58,-.66,.84,1.68,.20,-.99,-.14,-1.19,-1.29,.39,1.33,-.3
     16,-1.68,-.61,-1.85,-1.97,-.11,.95,-.97,-2.45,-1.12,-2.57,-2.70,-.6
     14,.54,-1.63,-3.29,-1.67,-3.34,-3.49,-1.22,.09,-2.35,-4.22,-2.25,-4
     1.16,-4.32,-1.83,-.4,-3.12,-5.25000,-2.860,-5.03,-5.21,-2.49,-.92,-
     13.95,-6.38,-3.51,-5.95,-6.15,-3.18,-1.48,-4.82,-7.81,-4.19,-6.91,-
     17.14,-3.91,-2.07,-5.73,-8.93,-4.90,-7.90,-8.17,-4.68,-2.71,-6.65,-
     110.33,-5.64,-8.92,-9.25,-5.49,-3.38,-7.57,-11.73,-6.4,-9.95,-10.36
     1,-6.34,-4.10,-8.45,-13.00,-7.19,-10.97,-11.48,-7.22,-4.86,-9.26,-1
     13.99,-8.00,-11.97,-12.61,-8.13,-5.66,-9.96,-14.54,-8.84,-12.95,-13
     1.72,-9.09,-6.52,-10.55,-14.66000,-9.70,-1 .90,-14.81,-10.09,-7.44,
     1-11.05,-14.52,-10.59,-14.83,-15.85,-11.15,-8.43,-11.51,-14.33,-11.
     154,-15.77,-16.87,-12.28,-9.51,-12.03,-14.30,-12.60,-16.79,-17.91,-
     113.52,-10.73,-12.80,-14.64,-13.90,-18.01,-19.11,-14.99,-12.21/
      DATA T2/-14.19,-15.73,-15.77,-19.78,-20.84,-16.98,-14.26,-17.54,-1
     18.90,-19.51,-23.4,-24.41,-20.76,-18.15,-0.0,0.0,0.0,0.0,0.0,0.0,0.
     10/
      I1=1
      DO 300 I=1,34
      DO 400 J=1,7
      EF(J,I)=T1(J,I)
400   CONTINUE
300   CONTINUE
      DO 500 I=35,37
      DO 600 J=1,7
      IT=I-34
      EF(J,I)=T2(J,IT)
600   CONTINUE
500   CONTINUE
C     WRITE(6,2000) ((EF(I,J),I=1,7),J=1,37)
C  2000  FORMAT(' ',37(' ',7(F7.2,3X),/))
      J1=1
      DO 100 I=2,8
      I3=I
      IF(APHI(I) .GE. PHI) GO TO 1000
      I1=I1+1
100   CONTINUE
1000  DO 200 J=2,36
      J3=J
      IF(ATHETA(J) .GT. THETA) GO TO 1100
      J1=J1+1
200   CONTINUE
C   SET J3 FOR LINEAR EXTRAPOLATION OUT TO 90 DEGREES.
      J3=36
      J1=J3-1
1100  FRACT=(THETA-ATHETA(J1))/(ATHETA(J3)-ATHETA(J1))
      FRACP=(PHI-APHI(I1))/(APHI(I3)-APHI(I1))
      IF(I3 .EQ. 8) I3=1
      EF1=FRACP*(EF(I3,J1)-EF(I1,J1))+EF(I1,J1)
      EF2=FRACP*(EF(I3,J3)-EF(I1,J3))+EF(I1,J3)
      ELF=FRACT*(EF2-EF1)+EF1
C     WRITE(6,700) ELF,ATHETA(J3),ATHETA(J1),APHI(I3),APHI(I1)
700   FORMAT(' ','ELEMENTAL FACTOR=',F6.2,' DB',4(X,F6.2))
      RETURN
      END
      SUBROUTINE ANTPLT(NUM,NUMD,XMIN,XMAX,YMIN,YMAX,[illegible])
```

```
      COMMON /BLOCK1/XVAL(181),YVAL(181),IYHCD(4),IXHCD(8)
      DIMENSION XVVV(36),YVVV(36)
      INTEGER*4 YSCALE,XSCALE
C     NUM=# OF DIVISIONS ON X AXIS
C     NUMD = # OF DIVISIONS ON Y AXIS
C     XMIN = VALUE OF X AT ORIGIN
C     XMAX = VALUE OF X AT END OF AXIS
C     YMIN = VALUE OF Y AT ORIGIN
C     YMAX = VALUE OF Y AT TOP OF Y AXIS
C     NPNTS = # OF POINTS TO BE PLOTED. MUST BE LESS THAN 81
      CALL PLTTYP(4662,6,37)
      CALL START
      CALL PLOT(0.0,0.0,3)
      CALL PLOT(0.0,1.0,2)
      CALL PLOT(0.0,7.0,3)
      CALL PLOT(0.0,8.0,2)
      CALL PLOT(11.0,0.0,3)
      CALL PLOT(10.0,0.0,2)
      CALL PLOT(1.0,0.0,3)
      CALL PLOT(0.0,0.0,2)
      CALL NEWPEN(1)
C     DEFINE NEW ORIGIN FOR PLOT AXIS
      CALL PLOT(2.22,1.88,-3)
      CALL FACTOR(1.0)
C     DRAW AXIS
      ENTRY NXTPLT(NUM,NUMD,XMIN,XMAX,YMIN,YMAX,NPNTS)
      CALL RECT(0.0,0.0,7.0,5.0)
C     DRAW TIC MARKS ON AXIS. CSIZE=DIVISION SIZE IN INCHES X AXIS.
C     DSIZE=DIVISION SIZE IN INCHES Y AXIS
      CSIZE=7.0/FLOAT(NUM)
      DSIZE=5.0/FLOAT(NUMD)
      X1=0.0
      Y1=0.0
      Y2=Y1+.05
      X2=X1+.05
      DO 400 K=1,2
      DO 200 J=1,NUM
      XBASE=FLOAT(NUM-J)*CSIZE
      X=XBASE
      CALL PLOT(X,Y1,3)
      CALL PLOT(X,Y2,2)
  200 CONTINUE
      CALL PLOT(X1,Y1,3)
      CALL PLOT(X2,Y1,2)
      DO 300 J=1,NUMD
      YBASE=FLOAT(NUMD-J)*DSIZE
      CALL PLOT(X1,YBASE,3)
      CALL PLOT(X2,YBASE,2)
  300 CONTINUE
      X1=7.0
      Y1=5.0
      X2=X1-.05
      Y2=Y1-.05
  400 CONTINUE
C     PUT SCALE ON Y AXIS
C     UNITS = UNITS PER DIV ON Y AXIS
      UNITS=((YMAX-YMIN)/FLOAT(NUMD))
      YSCALE=AINT(ABS(YMIN)+.5 )
      IF(YMIN .LT. 0) YSCALE=YSCALE+(0.1)
      LL2=NUMD+1
```

```
      DO 900 I=1,II2
      ULOC=DSIZE*(I-1)-.04
      X=-.46
      IF(YSCALE .GE. 0) X=-.307
      CALL INUMBR(X,ULOC,.15,YSCALE,0,0)
      YSCALE=YSCALE+AINT(UNITS+.5 )
900   CONTINUE
      XT=-.5
      YT=1.5
      CALL LETTER(XT,YT,.15,IYHCD,90,0,16)
C PUT SCALES ON X AXIS
C    UNITX    UNITS PER DIV ON X AXIS
      UNITX=((XMAX-XMIN)/FLOAT(NUM))
      XSCALE=AINT(ABS(XMIN)+.5 )
      IF(XMIN .LT. 0) XSCALE=XSCALE*(0-1)
C    LABEL X AXIS SCALES
750   IT1=NUM+1
      DO 700 I=1,IT1,3
      ULOC=CSIZE*(I-1)-.125
      IF( XSCALE .LT. 0 ) ULOC=ULOC-.15
      CALL INUMBR(ULOC,-.24,.15,XSCALE,0,0)
      XSCALE=XSCALE+AINT(UNITX+.5 )*3
700   CONTINUE
      XT=1.0
      YT=-.44
      CALL LETTER(XT,YT,.15,IXHCD,0,0,32)
C     UNITS = UNITS PER DIV ON Y AXIS
C    PLOT DATA
      ENTRY PLINE(NPNTS)
      DO 600 I=1,NPNTS
      IF(XVAL(I) .LT. XMIN) XVAL(I)=XMIN
      IF(XVAL(I) .GT. XMAX) XVAL(I)=XMAX
      IF(YVAL(I) .LT. YMIN) YVAL(I)=YMIN
      IF(YVAL(I) .GT. YMAX) YVAL(I)=YMAX
600   CONTINUE
C     WRITE(6,1001)(XVAL(I),YVAL(I),I=1,181)
1001  FORMAT(' ',23(8(F7.2,',',F7.2),/' '))
      X=(XVAL(1)-XMIN)/(UNITX/CSIZE)
      Y=(YVAL(1)-YMIN)/(UNITS/DSIZE)
      CALL PLOT(X,Y,3)
C    NPNTS = # OF POINTS TO BE PLOTED
      DO 500 I=2,NPNTS
      X=(XVAL(I)-XMIN)/(UNITX/CSIZE)
      Y=(YVAL(I)-YMIN)/(UNITS/DSIZE)
      CALL PLOT(X,Y,2)
500.  CONTINUE
C    PLOT RICE PAPER DATA
C     DATA XVVV/-68.9,-52.8,-56.2,-42.3,-40.2,-38.0,-34.0,-28.6,-25.8,-2
C    10.,-16.2,-15.3,-13.8,-10.3,-6.8,-4.16,5.20,0.,6.8,9.8,11.3,14.3,15
C    1.8,17.7,20.,23.6,25.8,28.6,31.4,34.,36.1,38.0,40.5,42.3,49.4,53.4/
C     DATA YVVV/7.11,-3.39,-23.89,15.61,15.61,11.61,-1.39,-1.89,2.11000,
C    1-29.39,-15.69,-7.89,-8.79,-20.89,0.11,19.51,23.11,24.11,8.11,-7.39
C    1,-3.89,7.11,6.61,4.61,-12.89,2.31,4.61,-.89,-17.89,-1.39,7.11,13.1
C    11,13.61,14.11,11.61,1.61/
C     DO 1002 I=1,36
C     X=(XVVV(I)-XMIN)/(UNITX/CSIZE)
C     Y=(YVVV(I)-YMIN)/(UNITS/DSIZE)
C     CALL SYMBOL(X,Y,.05,4,0.0,-1)
C   1002 CONTINUE
C     WRITE(6,1001)(XVVV(I),YVVV(I),I=1,36 )
```

```
      RETURN
      END
      BLOCK DATA
      COMMON /BLOCK1/XVAL(181),YVAL(181),IYBCD(4),IXBCD(8)
      DATA IYBCD/'HEAT','FR G','AIN ','(DB)'/
      DATA IXBCD/'    ','    ','THET','A   ','(DEG','REES',')   ','    '
     1/
      END
//DATA.FT37F001 DD VOL=REF=MFN.UB4490.KJC.LIB,DISP=(NEW,KEEP),
// DSN=MFN.UB4490.KJC.PLOT.OUTPUT,SPACE=(CYL,(1,1),RLSE),
// DCB=(RECFM=FB,LRECL=80,BLKSIZE=3120)
//DATA.INPUT DD *
```

Program V

Directive Gain Pattern Calculation and Plotting, 5.1 MHz

```
//SCR EXEC PGM=IEFBR14
//SCR DD DISP=(OLD,DELETE),VOL=REF=VOL001,
// DSN=MEN,UB6490,KJC,PLOT,OUTPUT
// EXEC FXCG
/*JP SERVICE=DEFER
/*JP FULLSKIPS
//SYSIN DD *
      COMMON /BLOCK1/XVAL(181),YVAL(181),IYBCD(4),IXBCD(8)
C     4 CHARACTERS PER INTEGER IN INTEGER ARRAYS. SEE BLOCK DATA SUBPROG
      DIMENSION ATHA(91),ADB(91),CHECK(5),CHEKP(5)
      CHECK(1)=0.
      CHECK(2)=32.5
      CHECK(3)=55.
      CHECK(4)=87.5
      CHECK(5)=90.
      CHEKP(1)=90.
      CHEKP(2)=270.
      CHEKP(3)=90.
      CHEKP(4)=130.
      CHEKP(5)=250.
      DO 400 J=1,5
      JINC=1
      DO 1003 I=1,181
      XVAL(I)=0.
 1003 YVAL(I)=0.
      J1=J-1
      PHI=FLOAT(J1)*10.+90.
C     PHI=CHEKP(J)
      PHIL=PHI-90.
      DO 500 I=1,91
      ATHA(I)=0.
      ADB(I)=0.
  500 CONTINUE
      DO 2000 J2=1,2
      THETA=0.
      DO 100 I=1,91
C     THETA=CHECK(I)
C   FIND TOTAL FIELD. 9.82 IS FACTOR TO NORMALIZE TO GAIN OVER ISOTROPIC
     , DB=AF(THETA,PHI)+ELE(THETA,PHI)-9.82
      ATHA(I)=THETA
      ADB(I)=DB
      THETA=THETA+1.
  100 CONTINUE
      WRITE(6,200) (ATHA(I),PHI,ADB(I),I=1,91)
  200 FORMAT(' ',5(F6.2,1X,F6.2,1X,F8.3,2X))
      WRITE(6,300)
  300 FORMAT(' ')
      JP=91
      NEND=NHT+1
      DO 1001 I=1,91
      XVAL(JP)=ATHA(I)*JINC
      YVAL(JP)=ADB(I)
      JP=JP+JINC
 1001 CONTINUE
      IF(JINC .EQ. 1) JINC=-1
      PHI=PHI+180
      IF(PHI .GT. 360.) PHI=PHI-360.
 2000 CONTINUE
      WRITE(6,1006)(XVAL(I),YVAL(I),I=1,181)
 1006 FORMAT(' ',23(8(F7.2,',',F7.2),/' '))
```

```
      IF(J .GT. 1) CALL NXTPLT(18.6,-90.,90.,-30.,30.,181)
      IF(J .GT. 1) GO TO 2100
      CALL ANTPLT(18.6,-90.,90.,-30.,30.,181)
 2100 Y=4.58
      X=4.00
      CALL LETTER(X,Y,.15,'PHI= ',0.0,5)
      CALL NUMBER(X,Y,.15,PHIL,0.0,1)
      X=X+.75
      Y=4.58
      CALL LETTER(X,Y,.15,'DEG. W',0.0,6)
      CALL NEWPEN(3)
  400 CONTINUE
      CALL FINISH
 1002 CONTINUE
      STOP
      END
      FUNCTION AF(THETA,PHI)
      THETAR=(THETA/180.)*3.14159
      PHIR=(PHI/180.)*3.14159
C    BETA=2*PI*(F/C)*85/2.    85=DISTANCE BETWEEN RADIATORS.
      BETA=4.539601
      BETA4=4.*BETA
      BETA8=8.*BETA
      STHETA=SIN(THETAR)
      SPHI=SIN(PHIR)
      CPHI=COS(PHIR)
C     AFT=(SIN(BETA4*STHETA*SPHI)/SIN(BETA*STHETA*SPHI))*(SIN(BETA8*STHE
C    1TA*CPHI)/SIN(BETA*STHETA*CPHI))
      IF( ABS(THETA-0.) .LE. .2 .OR. ABS(THETA-180.) .LE. .2 .OR. ABS(PH
     1I-0.) .LE. .2 .OR. ABS(PHI-180.) .LE. .2) GO TO 100
      GO TO 200
  100 AFT1=4.
      GO TO 300
  200 AFT1=ABS(SIN(BETA4*STHETA*SPHI)/SIN(BETA*STHETA*SPHI))
  300 IF(ABS(THETA-0.) .LE. .2 .OR. ABS(THETA-180.) .LE. .2 .OR. ABS(PHI
     1-90.) .LE. .2 .OR. ABS(PHI-270.) .LE. .2) GO TO 400
      GO TO 500
  400 AFT2=8.
      GO TO 600
  500 AFT2=ABS(SIN(BETA8*STHETA*CPHI)/SIN(BETA*STHETA*CPHI))
C    USE .434294 TO CONVERT NATURAL LOG TO BASE 10
  600 DBAFT1=20.*.434294*ALOG(AFT1)
      DBAFT2=20.*.434294*ALOG(AFT2)
C     WRITE(6,700) THETA,PHI,DBAFT1,DBAFT2
C 700   FORMAT(' ','THETA=',F6.2,'DEG    PHI=',F6.2,'DEG    4 ELEMENT=',F7.
C    12,' DB    8 ELEMENT=',F7.2,' DB')
C     AFT=ABS(AFT)
C     IF (ABS(AFT) .LT. 1.E-10) GO TO 10
C     AF=20.*.434294*ALOG(AFT)
      AF=DBAFT1+DBAFT2
      RETURN
C  10 .  AF=-99.
C     RETURN
      END
      FUNCTION ELF(THETA,PHI)
      DIMENSION EE(9,37),APHI(10),ATHETA(37),I1(7,33),I2(7,6),I3(2,37)
      DATA APHI/10.,60.,90.,110.,150.,180.,215.,270.,320.,370./,ATHETA/0
     1.,2.5,5.,7.5,10.,12.5,15.,17.5,20.,22.5,25.,27.5,30.,32.5,35.,37.5
     1,40.,42.5,45.,47.5,50.,52.5,55.,57.5,60.,62.5,65.,67.5,70.,72.5,75
     1.,77.5,80.,82.5,85.,87.5,90./
```

```
      DATA T1/7*3.83,3.76,3.72,3.73,3.74,3.85,3.89,3.90,3.67,3.58,3.6,3.
     164,3.84,3.92,3.95,3.54,3.40,3.44,3.50,3.81,3.92,3.97000,3.38,3.19,
     13.24,3.34,3.74,3.88,3.97,3.19,2.94,3.02,3.15,3.66,3.82,3.93,2.96,2
     1.65,2.7600,2.93,3.54,3.72,3.88,2.68,2.32,2.46,2.68,3.40,3.6,3.79,2
     1.36,1.94,2.12,2.39,3.23,3.44,3.68,1.99,1.52,1.74,2.07,3.03,3.24,3.
     1530,1.57,1.05,1.31,1.70,2.81,3.01,3.36,1.09,.52,.82,1.29,2.56,2.75
     1,3.15,.55,-.06,.28,.83,2.28,2.46,2.91,-.06,-.71,-.32,.33,1.98,2.13
     1,2.64,-.74,-1.41,-.99,-.24,1.65,1.76,2.34,-1.51,-2.19,-1.73,-.87,1
     1.3,1.36,2.,-2.37,-3.03,-2.55,-1.56,0.93,0.93,1.62,-3.34,-3.95,-3.4
     16,-2.33,.55,.46,1.21,-4.42,-4.93,-4.47,-3.18,0.15,-.04,.77,-5.64,-
     15.97,-5.59,-4.13,-.27,-.57,.29,-7.0,-7.06,-6.82,-5.17,-.70,-1.1400
     1,-.22,-8.53,-8.19,-8.19,-6.34,-1.14,-1.73,-.76,-10.22,-9.30,-9.700
     1,-7.63,-1.59,-2.35,-1.34,-12.05,-10.36,-11.34,-9.07,-2.06,-2.29,-1
     1.94,-13.90,-11.3,-13.10,-10.68,-2.56,-3.65,-2.57,-15.46,-12.08,-14
     1.8700,-12.47,-3.1,-4.34,-3.22,-16.27,-12.65,-16.48,-14.40,-3.68,-5
     1.04,-3.89,-16.19,-13.05,-17.62,-16.39,-4.32,-5.76,-4.59,-15.54,-13
     1.32,-18.11,-18.16,-5.04,-6.5,-5.32,-14.78,-13.54,-18.06,-19.32,-5.
     1860000,-7.26,-6.09,-14.15,-13.79,-17.8,-19.66,-6.81,-8.07,-6.91,-1
     13.78,-14.15,-17.61,-19.5,-7.93,-8.94,-7.81,-13.76,-14.71,-17.7,-19
     1.330,-9.30,-9.95,-8.87/
      DATA T2/-14.23,-15.65,-18.25,-19.58,-11.05,-11.22,-10.21,-15.57,-1
     17.35,-19.69,-20.72,-13.52,-13.13,-12.22,-19.12,-21.19,-23.37,-24.1
     17,-18.01,-17.03,-16.23,7*0.0/
      DATA T3/3.83,3.83,3.80,3.85,3.75,3.84,3.68,3.82,3.58,3.76,3.47,3.6
     18,3.32000,3.57,3.16,3.44,2.97,3.27,2.76,3.07,2.52,2.83,2.25,2.5600
     1,1.96,2.24,1.64,1.89,1.29,1.49,.92,1.05,0.52,0.56,.10,.03,-.36,-.5
     15,-.84,-1.18,-1.35,-1.85,-1.89,-2.56,-2.45,-3.30,-3.05,-4.06,-3.68
     1,-4.84,-4.36,-5.61,-5.08,-6.37,-5.85,-7.09,-6.70,-7.76,-7.64,-8.40
     1,-8.69,-9.01,-9.89,-9.66,-11.33,-10.43,-13.13,-11.49,-15.66,-13.74
     1,-20.2200,-17.07,0.,0./
      I1=1
      IF( PHI .LT. 10.) PHI=PHI+360.
      DO 300 I=1,33
      DO 400 J=1,4
      EF(J,I)=T1(J,I)
400   CONTINUE
      EF(5,I)=T3(1,I)
      DO 450 J=5,7
      EF(J+1,I)=T1(J,I)
450   CONTINUE
      EF(9,I)=T3(2,I)
300   CONTINUE
      DO 500 I=34,37
      DO 600 J=1,4
      IT=I-33
      EF(J,I)=T2(J,IT)
600   CONTINUE
      EF(5,I)=T3(1,I)
      DO 650 J=5,7
      EF(J+1,I)=T2(J,IT)
650   CONTINUE
      EF(9,I)=T3(2,I)
500   CONTINUE
C     WRITE(6,2000) ((EF(I,J),I=1,9),J=1,37)
C  2000  FORMAT(' ',37(' ',9(F7.2,3X),/))
      J1=1
      DO 100 I=2,10
      I4=I
      IF(APHI(I) .GT. PHI) GO TO 1000
      I1=I1+1
```

```
 100   CONTINUE
1000   DO 200 J=2,36
       J3=J
       IF(ATHETA(J) .GT. THETA) GO TO 1100
       J1=J1+1
 200   CONTINUE
       J3=36
       J1=J3-1
1100   FRACT=(THETA-ATHETA(J1))/(ATHETA(J3)-ATHETA(J1))
       IF (I1 .EQ. I3) WRITE(6,800) PHI
       FRACP=(PHI-APHI(I1))/(APHI(I3)-APHI(I1))
       IF(I3 .EQ. 10) I3=1
       EF1=FRACP*(FF(I3,J1)-FF(I1,J1))+FF(I1,J1)
       EF2=FRACP*(FF(I3,J3)-FF(I1,J3))+FF(I1,J3)
       ELF=FRACT*(EF2-EF1)+EF1
C      WRITE(6,700) ELF,ATHETA(J3),ATHETA(J1),APHI(I3),APHI(I1)
C   700    FORMAT(' ','ELEMENTAL FACTOR=',F6.2,' DB',4(3X,F6.2))
 800   FORMAT(' ',F10.3,'  PHI NOT IN RANGE 10 DEG TO 370 DEG')
       RETURN
       END
       SUBROUTINE ANTPLT(NUM,NUMD,XMIN,XMAX,YMIN,YMAX,NPNTS)
       COMMON /BLOCK1/XVAL(181),YVAL(181), /HCD(4),IXHCD(8)
       DIMENSION XVVV(36),YVVV(36)
       INTEGER*4 YSCALE,XSCALE
C     NUM=# OF DIVISIONS ON X AXIS
C     NUMD = # OF DIVISIONS ON Y AXIS
C     XMIN = VALUE OF X AT ORIGIN
C    XMAX = VALUE OF X AT END OF AXIS
C     YMIN = VALUE OF Y AT ORIGIN
C     YMAX = VALUE OF Y AT TOP OF Y AXIS
C     NPNTS = # OF POINTS TO BE PLOTED. MUST BE LESS THAN 81
       CALL PLTTYP(4662,6,37)
       CALL START
       CALL PLOT(0.0,0.0,3)
       CALL PLOT(0.0,1.0,2)
       CALL PLOT(0.0,7.0,3)
       CALL PLOT(0.0,8.0,2)
       CALL PLOT(11.0,0.0,3)
       CALL PLOT(10.0,0.0,2)
       CALL PLOT(1.0,0.0,3)
       CALL PLOT(0.0,0.0,2)
       CALL NEWPEN(1)
C     DEFINE NEW ORIGIN FOR PLOT AXIS
       CALL PLOT(2.22,1.88,-3)
       CALL FACTOR(1.0)
C     DRAW AXIS
       ENTRY NXTPLT(NUM,NUMD,XMIN,XMAX,YMIN,YMAX,NPNTS)
       CALL RECT(0.0,0.0,7.0,5.0)
C     DRAW TIC MARKS ON AXIS. CSIZE=DIVISION SIZE IN INCHES X AXIS.
C     DSIZE=DIVISION SIZE IN INCHES Y AXIS
       CSIZE=7.0/FLOAT(NUM)
       DSIZE=5.0/FLOAT(NUMD)
       X1=0.0
       Y1=0.0
       Y2=Y1+.05
       X2=X1+.05
       DO 400 K=1,2
       DO 200 J=1,NUM
       XHASH=FLOAT(NUM-1)*CSIZE
       X=XHASH
```

```
      CALL PLOT(X,Y1,3)
      CALL PLOT(X,Y2,2)
 200  CONTINUE
      CALL PLOT(X1,Y1,3)
      CALL PLOT(X2,Y1,2)
      DO 300 J=1,NUMD
      YBASE=FLOAT(NUMD-J)*DSIZE
      CALL PLOT(X1,YBASE,3)
      CALL PLOT(X2,YBASE,2)
 300  CONTINUE
      X1=7.0
      Y1=5.0
      X2=X1-.05
      Y2=Y1-.05
 400  CONTINUE
C   PUT SCALE ON Y AXIS
C     UNITS = UNITS PER DIV ON Y AXIS
      UNITS=((YMAX-YMIN)/FLOAT(NUMD))
      YSCALE=AINT(ABS(YMIN)+.5 )
      IF(YMIN .LT. 0) YSCALE=YSCALE*(0-1)
      IT2=NUMD+1
      DO 900 I=1,IT2
      ULOC=DSIZE*(I-1)-.04
      X=-.46
      IF(YSCALE .GE. 0) X=-.307
      CALL INUMBR(X,ULOC,.15,YSCALE,0,0)
      YSCALE=YSCALE+AINT(UNITS+.5 )
 900  CONTINUE
      XT=-.5
      YT=1.5
      CALL LETTER(XT,YT,.15,IYBCD,90,0,16)
C PUT SCALES ON X AXIS
C   PUT SCALES ON X AXIS
C   UNITX = UNITS PER DIV ON X AXIS
      UNITX=((XMAX-XMIN)/FLOAT(NUM))
      XSCALE=AINT(ABS(XMIN)+.5 )
      IF(XMIN .LT. 0) XSCALE=XSCALE*(0-1)
C   LABEL X AXIS SCALES
 750  IT1=NUM+1
      DO 700 I=1,IT1,3
      ULOC=CSIZE*(I-1)-.125
      IF( XSCALE .LT. 0 ) ULOC=ULOC-.15
      CALL INUMBR(ULOC,-.24,.15,XSCALE,0,0)
      XSCALE=XSCALE+AINT(UNITX+.5 )*3
 700  CONTINUE
      XT=1.0
      YT=-.44
      CALL LETTER(XT,YT,.15,IXBCD,0,0,32)
C     UNITS = UNITS PER DIV ON Y AXIS
C   PLOT DATA
      ENTRY PLINE(NPNTS)
      DO 600 I=1,NPNTS
      IF(XVAL(I) .LT. XMIN) XVAL(I)=XMIN
      IF(XVAL(I) .GT. XMAX) XVAL(I)=XMAX
      IF(YVAL(I) .LT. YMIN) YVAL(I)=YMIN
      IF(YVAL(I) .GT. YMAX) YVAL(I)=YMAX
 600  CONTINUE
      WRITE(6,1001)(XVAL(I),YVAL(I),I=1,100)
 1001 FORMAT( [illegible] )
      X=(XVAL(I)-XMIN)/(UNITX/CSIZE)
```

```
      Y=(YVAL(1)-YMIN)/(UNITS/DSIZE)
      CALL PLOT(X,Y,3)
C     NPNTS = # OF POINTS TO BE PLOTED
      DO 500 I=2,NPNTS
      X=(XVAL(I)-XMIN)/(UNITX/CSIZE)
      Y=(YVAL(I)-YMIN)/(UNITS/DSIZE)
      CALL PLOT(X,Y,2)
500   CONTINUE
C    PLOT RICE PAPER DATA
C     DATA XVVV/-48.9,-52.8,-56.2,-42.3,-40.2,-38.0,-34.0,-28.6,-25.8,-2
C    10.,-16.2,-15.3,-13.8,-10.3,-6.8,-4.16,5.20.0,.6.8,9.8,11.3,14.3,15
C    1.8,17.7,20.,23.6,25.8,28.6,31.4,34.,36.1,38.0,40.5,42.3,49.4,53.4/
C     DATA YVVV/7.11,-3.39,-23.89,15.61,15.61,11.61,-1.39,-1.89,2.11000,
C    1-29.39,-15.69,-7.89,-8.79,-29.89,0.11,19.51,23.11,24.11,8.11,-7.39
C    1,-3.89,7.11,6.61,4.61,-12.89,2.31,4.61,-.89,-17.89,-1.39,7.11,13.1
C    11,13.61,14.11,11.61,1.61/
C     DO 1002 I=1,36
C     X=(XVVV(I)-XMIN)/(UNITX/CSIZE)
C     Y=(YVVV(I)-YMIN)/(UNITS/DSIZE)
C     CALL SYMBOL(X,Y,.05,4,0.0,-1)
C    1002 CONTINUE
C     WRITE(6,1001)(XVVV(I),YVVV(I),I=1,36 )
      RETURN
      END
      BLOCK DATA
      COMMON /BLOCK1/XVAL(181),YVAL(181),IYBCD(4),IXBCD(8)
      DATA IYBCD/'HEAT','FR G','AIN ','(DH)'/
      DATA IXBCD/'    ','    ','(HEI','A   ','(DEG','REES',')   ','    '
     1/
      END
//DATA.FT37F001 DD VOL=REF=MEN.U84490.KJC.LIB,DISP=(NEW,KEEP),
// DSN=MEN.U84490.KJC.PLOT.OUTPUT,SPACE=(CYL,(1,1),RLSE),
// DCB=(RECFM=FB,LRECL=80,BLKSIZE=3120)
//DATA.INPUT DD *
```

Program VI

*Program to compute relative HF power above isotropic on a 70km altitude plane. Frenquency=3.17 MHz

*note: Function subprograms AF (Theta, Phi) and ELF (Theta, Phi) are not shown. They are the same as in program IV.

```
DATE ... 3.17                                                                                    09/04/82      PAGE   1
                                                                                                           1     1     1
           1         2         3         4         5         6         7         8         9         0     1     2
  1234567890123456789012345678901234567890123456789012345678901234567890123456789012345678901234567890123456789012345678901234567890

      //M 2XXXXX JOB
      //SCR EXEC PGM=IEFBR14
      //SCR DD DISP=(OLD,DELETE),VOL=REF=VOL031,
      // DSN=MEN.UP4490.KJC.PLCT.OUTPUT
      // EXEC FVG
      /*JP SERVICE=DEF62
      /*JP FULLSKIPS
      //SYSIN DD *
            DO 400 J=1,245,2
            J1=J-123
            Y=FLOAT(J1)
            DO 100 I=1,245,2
            I1=I-123
            X=FLOAT(I1)
            XY=SQRT(X*X+Y*Y)
            THETA=ATAN(XY/70.)*180./3.14159
            IF( ABS(X) .LT. .1) PHI=90.
            IF ( ABS(X) .GT. .1) PHI=ATAN(Y/X)*180./3.14159
            IF( X .LT. -.1) PHI=PHI+180.
            IF( PHI .LT. 0.) PHI=PHI+360.
            PHI=PHI+90.
            IF( PHI .GT. 360) PHI=PHI-360.
            THETAR=(THETA/180.)*3.14159
            DPPDP=20.*ALOG(COS(THETAR))
      C    FIND TOTAL FIELD. 8.62 IS FACTOR TO NORMALIZE TO GAIN OVER ISOTROPIC
            DP=AF(THETA,PHI)+ELF(THETA,PHI)+PPDP-8.62
            Z=DP
            IF( DP .LT. 0.) Z=0.
            THETA=THETA+1.
            WRITE(27,200) X,Y,Z
      100   CONTINUE
      200   FORMAT(' ',F9.3,2X,F9.3,2X,F9.3)
      400   CONTINUE
      1002  CONTINUE
            STOP
            END
      //DATA.FT27F001 DD VOL=REF=MEN.U8449C.KJC.LIB,DISP=(NEW,KEEP),
      // DSN=MEN.UP4490.KJC.PLCT.OUTPUT,SPACE=(CYL,(1,1),RLSE),
      // DCB=(RECFM=FB,LRECL=80,BLKSIZE=3120)
      //DATA.INPUT DD *
```

Program VII

*Program to compute relative HF power above isotropic on a 70km altitude plane. Frequency=5.1MHz.

*note: Function subprograms AF (Theta,Phi) and ELF (Theta, Phi) are not shown. They are the same as those in program V.

```
DATA, F..5.1.5. .                                                                                      09/04/82      PAGE   1

                 1         2         3         4         5         6         7         8         9         1         1         1
                                                                                                          0         1         2
        1234567890123456789012345678901234567890123456789012345678901234567890123456789012345678901234567890123456789012345678901234567890

        //ME2XXXXX JOB
        //SCR EXEC PGM=IEFBR14
        //SCR  DD DISP=(OLD,DELETE),VOL=REF=VEL001,
        // DSN=MEN.UR4490.KJC.PLOT.OUTPUT
        // EXEC FORT
        /*JP SERVICE=DEFER
        /*JP FULLSKIPS
        //SYSIN DD *
              DO 400 J=1,245,2
              J1=J-123
              Y=FLOAT(J1)
              DO 100 I=1,245,2
              I1=I-123
              X=FLOAT(I1)
              XY=SQRT(X*X+Y*Y)
              THETA=ATAN(XY/70.)*180./3.14159
              IF( ABS(X) .LT. .1) PHI=90.
              IF( ABS(X) .GT. .1) PHI=ATAN(Y/X)*180./3.14159
              IF(X .LT. -.1) PHI=PHI+180.
              IF( PHI .LT. 0.) PHI=PHI+360.
              PHI=PHI+90.
              IF (PHI .GT. 360.) PHI=PHI-360.
              THTAR=(THETA/180.)*3.14159
              RPROP=20.*ALOG(COS(TETAR))
        C     THETA=CHECK(I)
        C   FIND TOTAL FIELD. 9.82 IS FACTOR TO NORMALIZE TO GAIN OVER ISOTROPIC
              DB=AF(THETA,PHI)+ELF(THETA,PHI)+RPROP-9.82
              Z=DB
              IF( DB .LT. 0.) Z=0.
              WRITE(37,200) X,Y,Z
        100   CONTINUE
        200   FORMAT(' ',F9.3,2X,F9.3,2X,F9.3)
        400   CONTINUE
              STOP
              END
        //DATA.FT37F001 DD VOL=REF=MEN.UR4490.KJC.LIB,DISP=(NEW,KEEP),
        // DSN=MEN.UR4490.KJC.PLOT.OUTPUT,SPACE=(CYL,(1,1),RLSE),
        // DCB=(RECFM=FB,LRECL=80,BLKSIZE=3120)
        //DATA.INPUT DD *
```

Program VIII

Program to compute relative magnetic field strength at observation point for ionospheric ELF/VLF current element array. 3.17 HF pattern.

```
[illegible]                                   TOP V01-VC1001                         09/04/82    PAGE  1
         1         2         3         4         5         6         7         8         9         0         1         2
1234567890123456789012345678901234567890123456789012345678901234567890123456789012345678901234567890123456789012345678901234567890

//*XXXXXXX JOB
//SCR EXEC PGM=IEFBR14
//SCR DD DISP=(OLD,DELETE),VOL=SER=VC1001,
// DSN=[illegible].F0C.PICT.OUTPUT
// EXEC FWCG
/*JE SERVICE=[illegible]
/*IE [illegible]
//SYSIN DD *
      DIMENSION XO(15),YO(15),ZO(15),DLO(15),AZE(15),AZI(15),AYE(15),AYI
     1(15),FREC(15)
      REAL*4 IO(15)/2.332,7.465,59.9,8.645,1.355,1.408,2.951,5.471,5.47
     11,2.951,1.407,4*0./
      DATA XO/-63.,-31.,0.,30.,62.,10*0./,YO/5*0.,-38.,-25.,-14.,14.,25.
     1,38.,4*0./,ZO/15*70./
      DATA DLO/24.,22.,40.,22.,15.,10.,26.,32.,32.,26.,16.,4*0./
      DATA FREC/1.,1.25,1.50E024,2.,2.293578,2.5,2.793296,3.149654,3.448
     1276,4.,4.464286,5.,.956016,.479386,.0/
      DATA XP,YP,ZP/-4.02,-6.57,0./
      NFREQ=14
      DO 1001 I=1,NFREQ
      FREQ(I)=FREQ(I)*1000.
 1001 CONTINUE
      DO 3000 K=1,NFREQ
      NPTS=11
      DO 1000 J=1,NPTS
      XO(J)=XO(J)*1000.
      YO(J)=YO(J)*1000.
      ZO(J)=ZO(J)*1000.
      DLO(J)=DLO(J)*1000.
 1000 CONTINUE
      XP=XP*1000.
      YP=YP*1000.
      ZP=ZP*1000.
      PI=3.141596
      I=1
      BETA=2.*PI*FREQ(K)/(3.E 08)
      DO 1100 I=1,NPTS
      RO=SQRT(XO(I)*XO(I)+YO(I)*YO(I)+ZO(I)*ZO(I))
      DELAY=RO-ZO.
      RDIST=SQRT((XO(I)-XP)*(XO(I)-XP)+(YO(I)-YP)*(YO(I)-YP)+(ZO(I)-ZP)*
     1(ZO(I)-ZP))
      BTARP=BETA*(RDIST+DELAY)
      CBETA=COS(BTARP)
      SBETA=SIN(BTARP)
      RXYP=SQRT(XO(I)*XO(I)+(XO(I)-XP)*(YO(I)-YP))
      STHP=RXYP/RDIST
      SPHIP=(YP-YO(I))/RXYP
      CPHIP=XO(I)/RXYP
      FACT=(IO(I)*DLO(I)*STHP)/(4.*PI*RDIST)
      EPHI=FACT*(CBETA/RDIST+BETA*SBETA)
      EPHII=FACT*(SBETA/RDIST-BETA*CBETA)
      AZE(I)=SPHIP*EPHIE
      AZI(I)=SPHIP*EPHII
      AYE(I)=CPHIP*EPHIE
      AYI(I)=CPHIP*EPHII
```

```
                                                                                                    1         1         1
         1         2         3         4         5         6         7         8         9         0         1         2
123456789012345678901234567890123456789012345678901234567890123456789012345678901234567890123456789012345678901234567890

      1100  CONTINUE
            AYPT=0.
            AYIT=0.
            AZRT=0.
            AZIT=0.
            DO 400 I=1,NPTS
            AZRT=AZRT+AZR(I)
            AZIT=AZIT+AZI(I)
            AYRT=AYRT+AYR(I)
            AYIT=AYIT+AYI(I)
       400  CONTINUE
            AZM=SQRT(AZRT*AZRT+AZIT*AZIT)
            AYM=SQRT(AYRT*AYRT+AYIT*AYIT)
            DO 1300 I=1,NPTS
            ZO(I)=ZO(I)/1000.
            YO(I)=YO(I)/1000.
            XO(I)=XO(I)/1000.
            ELO(I)=ELO(I)/1000.
      1300  CONTINUE
            XR=XR/1000.
            YR=YR/1000.
            ZR=ZR/1000.
            FREC(K)=FREC(K)/1000.
            WRITE(6,500) FREQ(K),ZO(K),XR,YR,ZR
       500  FORMAT(' ','FREQUENCY=',F12.7,'  SOURCE ALTITUDE= ',F5.1,' KM RCVR
           1 SITE AT (',F5.2,' KM,',F5.2,' KM,',F5.2,' KM)')
            WRITE(6,550)
       550  FORMAT(' ')
            WRITE(6,600)
       600  FORMAT(' SOURCE LOCATION    STRENGTH  LENGTH  Z-REAL      Z-IMAG
           1   Y-REAL       Y-IMAG      Z-MAG       Y-MAG')
            DO 2000 I=1,NPTS
            YM=SQRT(AYR(I)*AYR(I)+AYI(I)*AYI(I))
            ZM=SQRT(AZR(I)*AZR(I)+AZI(I)*AZI(I))
            WRITE(6,650) XO(I),YO(I),IO(I),ELO(I),AZR(I),AZI(I),AYR(I),AYI(I),
           1ZM,YM
      2000  CONTINUE
       650  FORMAT(' ',4X,'(',F5.1,',',F5.1,')',2X,F7.3,2X,F6.1,2X,1PE10.3,1X,
           11PE10.3,1X,1PE10.3,1X,1PE10.3,1X,1PE10.3,1X,1PE10.3)
            WRITE(6,550)
            WRITE(6,700) AZRT,AZIT,AYRT,AYIT,AZM,AYM
       700  FORMAT(' ','AZRT=',E10.3,' AZIT=',E10.3,' AYRT=',E10.3,' AYIT=',E1
           10.3,' AZM= ',E10.3,' AYM= ',E10.3)
            WRITE(6,550)
            WRITE(6,550)
      1000  CONTINUE
            STOP
            END
//FT15F001 DD VOL=SER=MFR,UE4990,KJC,III,DISP=(NEW,KEEP),
// DSN=MEN,UE4990,KJC,PLOT,OUTPUT,SPACE=(CYL,(1,1),RLSE),
// DCB=(RECFM=FB,LRECL=80,BLKSIZE=3120)
//DATA.INPUT DD *
```

Program IX

Program to compute relative magnetic field strength of an observation point for an ionspheric ELF/VLF current element array. 5.1 MHz HF pattern.

```
DSN=...PN.H.SP ... .LIPT.,PILEY,E,A,2          ......           FOR VOL=VCI001                09/04/82   PAGE  1
                                                                                                      1      1    1
            1         2         3         4         5         6         7         8         9         0      1    2
   1234567890123456789012345678901234567890123456789012345678901234567890123456789012345678901234567890123456789012345678901234567890
//*NEBRITT) JOI
/SEP EXEC PGM=IPTIFIN
/SCR ...  =(OLD,DELETE),VOL=SER=VCI001,
// DSN=EN.34449).JC.FICT.COUTPUT
// EXEC FORT
/*JE SERVICE=EFFSP
.*JE ENTISTIES
//SYSIN DD *
      DIMENSION X0(21),Y0(21),Z0(21),DLO(21),AZF(21),AZI(21),AYP(21),AYI
     1(21),FREQ(15)
      DATA  10(21)/11.93,7.499,6.793,32.113,6.996,4.217,8.549,24.213,2.
     1463,1.534,1.259,1.452,1.459,1.561,3.581,1.959,1.452,1.259,1.534,2.
     1463,24.213/
      DATA X0/-60.5,-39.,-18.,0.,18.,33.,59.,1440./,Y0/7*0.,-65.,-48.,-3
     15.,-11.,-22.,-15.,-9.,9.,15.,22.,30.,39.,48.,65./,Z0/21*70./
      DATA DLO/59.,14.,12.,24.,12.,14.,43.,26.,15.,12.,12.,15.,16.,20.,2
     17.,17.,15.,14.,14.,16.,28./
      DATA FREQ/1.,1.25,1.506020,2.,2.293578,2.5,2.793296,3.144654,3.448
     1276,4.,4.464286,5.,.956016,.479346,.0/
      DATA XP,YP,ZP/-4.02,-6.57,0./
      NFREQ=14
      DO 1001 I=1,NFREQ
      FREQ(I)=FREQ(I)*1000.
 1001 CONTINUE
      DO 1002 K=1,NFREQ
      NPTS=21
      DO 1002 J=1,NPTS
      X0(J)=X0(J)*1000.
      Y0(J)=Y0(J)*1000.
      Z0(J)=Z0(J)*1000.
      DLO(J)=DLO(J)*1000.
 1002 CONTINUE
      XP=XP*1000.
      YP=YP*1000.
      ZP=ZP*1000.
      PI=3.141596
      I=1
      BETA=2.*PI*FREQ(K)/(3.E 09)
      DO 1100 I=1,NPTS
      R0=SQRT(X0(I)*X0(I)+Y0(I)*Y0(I)+Z0(I)*Z0(I))
      DELAY=R0-70.
      RPRIM=SQRT((X0(I)-XP)*(X0(I)-XP)+(Y0(I)-YP)*(Y0(I)-YP)+(Z0(I)-ZP)*
     1(Z0(I)-ZP))
      DTASP=BETA*(RPRIM+DELAY)
      CDTASP=COS(DTASP)
      SDTASP=SIN(DTASP)
      EXYP=SQRT(Z0(I)*Z0(I)+(Y0(I)-YP)*(Y0(I)-YP))
      STETF=EXYP/RPRIM
      CPHIP=(YP-Y0(I))/EXYP
      SPHIP=Z0(I)/EXYP
      FACT=(I0(I)*DLO(I)*STETF)/(4.*PI*RPRIM)
      RPHID=FACT*(CPHIP/RPRIM+BETA*SDTASP)
      HPHII=FACT*(SPHIP/RPRIM+BETA*CDTASP)
      AZF(I)=SPHIP*HPHIE
      AZI(I)=SPHIP*HPHII
```

```
DCP MFN,H84490,KJC,PLIOT,PRIC,APPEX,5.1.2          FOR V.I VCI221
                                                                        09/04/82    PAGE  2
          1         2         3         4         5         6         7         8         9         1         1         1
                                                                                                    0         1         2
 123456789012345678901234567890123456789012345678901234567890123456789012345678901234567890123456789012345678901234567890
             AYF(I)=CPRIP*RPHIP
             AYI(I)=CPRIP*RPHII
      1100   CONTINUE
             AYFT=0.
             AYIT=0.
             AZIT=0.
             AZIT=0.
             DO 400 I=1,NPTS
             AZFT=AZFT+AZF(I)
             AZIT=AZIT+AZI(I)
             AYFT=AYFT+AYF(I)
             AYIT=AYIT+AYI(I)
       400   CONTINUE
             AZM=SQRT(AZFT*AZFT+AZIT*AZIT)
             AYM=SQRT(AYFT*AYFT+AYIT*AYIT)
             DO 1300 I=1,NPTS
             Z0(I)=Z0(I)/1000.
             Y0(I)=Y0(I)/1000.
             X0(I)=X0(I)/1000.
             DL0(I)=DIC(I)/1000.
      1300   CONTINUE
             XP=XP/1000.
             YP=YP/1000.
             ZP=ZP/1000.
             FREQ(K)=FREQ(K)/1000.
             WRITE(6,500) FREQ(K),Z0(K),XP,YP,ZP
       500   FORMAT(' ','FREQUENCY=',F12.7,'  SOURCE ALTITUDE= ',F5.1,' KM RCVR
            1 SITE AT (',F5.2,' KM,',F5.2,' KM,',F5.2,' KM)')
             WRITE(6,550)
       550   FORMAT(' ')
             WRITE(6,600)
       600   FORMAT(' SOURCE LOCATION     STRENGTH  LENGTH  Z-REAL      Z-IMAG
            1    Y-REAL       Y-IMAG        Z-MAG         Y-MAG')
             DO 2000 I=1,NPTS
             YM=SQRT(AYF(I)*AYF(I)+AYI(I)*AYI(I))
             ZM=SQRT(AZF(I)*AZF(I)+AZI(I)*AZI(I))
             WRITE(6,650) X0(I),Y0(I),Z0(I),DL0(I),AZF(I),AZI(I),AYF(I),AYI(I),
            1ZM,YM
      2000   CONTINUE
       650   FORMAT(' ',4X,'(',F5.1,',',F5.1,')',2X,F7.3,1X,F6.1,2X,1PE10.3,1X,
            11PE10.3,1X,1PE10.3,1X,1PE10.3,1X,1PE10.3,1X,1PE10.3)
             WRITE(6,550)
             WRITE(6,700) AZFT,AZIT,AYFT,AYIT,AZM,AYM
       700   FORMAT(' ','AZFT=',F10.3,' AZIT=',F10.3,' AYFT=',F10.3,' AYIT=',F1
            10.3,' AZM= ',F10.3,' AYM= ',F10.3)
             WRITE(6,550)
             WRITE(6,550)
      3000   CONTINUE
             STOP
             END
 //DATA.FT17F001 DD VOL=REF=YFN.H84490.KJC.LIB,DISP=(NEW,KEEP),
 // DSN=YFN.H84490.KJC.PLOT,CUTPUT,SPACE=(CYL,(1,1),RLSE),
 // DCB=(RECFM=FB,LRECL=80,BLKSIZE=3120)
 //DATA.INPUT DD *
```

APPENDIX II

USE OF CHEBYSHEV'S POLYNOMIALS TO SIMPLIFY ANTENNA FACTORS

The Chebyshev's polynomials are the solution to the Chebyshev differential equation (A-1). The solution has the form of equation (A-2)

$$(1 - x^2)\frac{d^2y}{dx^2} - x\frac{dy}{dx} + n^2y = 0 \qquad \text{(A-1)}$$

With a recursive formula given in equation (A-3)[13]

$$T_m(x) = \cos\,(m \cos^{-1}x) \qquad m \geq 0,\ |x| \leq 1 \qquad \text{(A-2)}$$

$$T_{m+1}(x) = 2x\ T_m(x) - T_{m-1}(x) \qquad \text{(A-3)}$$

Equation (A-4) and (A-5) follow from substitution of 0 and 1 for m in (A-2)

$$T_0 = 1 \qquad \text{(A-4)}$$
$$T_1 = x \qquad \text{(A-5)}$$

By using the recursion relationship (A-3), the following polynomials are obtained:

$$T_2(x) = 2x^2 - 1$$
$$T_3(x) = 4x^3 - 3x$$
$$T_4(x) = 8x^4 - 8x^2 + 1$$
$$T_5(x) = 16x^5 - 20x^3 + 5x$$
$$T_6(x) = 32x^6 - 48x^4 + 18x^2 - 1$$
$$T_7(x) = 64x^7 - 112x^5 + 56x^3 - 7x$$
$$T_8(x) = 128x^8 - 256x^6 + 160x^4 - 32x^2 + 1$$

Let "w" equal "$\cos^{-1}x$" then "x" is equal to "cos w."

Substitution for "x" in equation (A-2) gives (A-6).

$$T_m(\cos w) = \cos\,(m\ w) \qquad \text{(A-6)}$$

By using equation (A-6) with the polynomials, trigonometric identities can be found for expressing "cos (m w)" or "sin (m w)" in terms of "sin w" and "cos w." For example, using "$T_2(x)$" and letting "x" equal "cos w", equation (A-7) is obtained.

$$T_2(\cos w) = \cos (2w) = 2 (\cos^2 w) - 1 \tag{A-7}$$

Expressions for sin(m w) can be obtained by taking the derivative of the "cos (m w)" identity. Equation (A-8) was obtained by taking the derivative of (A-7).

$$\sin (2w) = 2 (\cos w) \sin w \tag{A-8}$$

To obtain the antenna factors in the form of equation (1-13) and (1-14), equation (1-7) must be expanded. Equation (A-9) is the expansion for the 8-element case. Let $w = \beta (d/2) \sin\theta$.

$$AF = \sum_{m=1,3,5...}^{8-1} \cos (m \beta d/2 \sin \theta) = \cos(w) + \cos (3w) + \cos (5w) + \cos (7w) \tag{A-9}$$

Use the Chebyshev's polynomials to find trigonometric identities to reduce (A-9) into an equation in terms of powers of cos w. These identities are given in equation (A-10).

$$\begin{aligned} T_1 &= \cos w = \cos w \\ T_3 &= \cos 3w = 4\cos^3 w - 3 \cos w \\ T_5 &= \cos 5w = 16\cos^5 w - 20\cos^3 w + 5\cos w \\ T_7 &= \cos 7w = 64\cos^7 w - 112\cos^5 w + 56\cos^3 w - 7\cos w \end{aligned} \tag{A-10}$$

Substituting (A-10) into (A-9), the expression for the antenna factor becomes (A-11).

$$AF = 64\cos^7 w - 96\cos^5 w + 40\cos^3 w - 4\cos w \tag{A-11}$$

An identity for "cos(8w)" can be found from polynomial "T_8." By taking the derivative of "cos (8w)", an identity for "sin (8w)" can be found, (A-12).

$$\sin 8w = 1024 \cos^7 w \sin w - 1536 \cos^5 w \sin w + 640 \cos^3 w \sin w - 64 \cos w \sin w = 16 \sin w (64\cos^7 w - 96 \cos^5 w + 40 \cos^3 w - 4\cos w) \tag{A-12}$$

Equation (A-12) can be rearranged into (A-13).

$$\frac{1}{16}\frac{\sin 8w}{\sin w} = 64 \cos^7 w - 96 \cos^5 w + 40 \cos^3 w - 4 \cos w \tag{A-13}$$

Equation (A-14) can be obtained by subtituting equation (A-13) into (A-11).

$$AF = \frac{1}{16}\frac{\sin 8w}{\sin w} \tag{A-14}$$

This is identical with equation (1-14) for the 8-element array antenna factor with the exception of the 1/16 constant in (A-14). The constant can be neglected at this point, due to the fact that when the directive gain is calculated, the AF will be normalized.

A similiar calculation can be performed to obtain the 4-element array factor, (1-13).

APPENDIX III

REVISED ARECIBO HF ANTENNA ARRAY GEOMETRY

After completion of the work described in the main body of this report, a preliminary copy was reviewed by the Arecibo Observatory. At this time the Arecibo Observatory made available additional information about the HF array. The following differences were reported between the model used in the main text and the actual A.O. array:

1. The τ for the antenna is .774.
2. The pyramid structure is elevated five feet above ground.
3. The feed point of each face is capacitively loaded.

This appendix presents the information provided by the A.O. and discusses its possible effects on the work presented in the main body of this report.

The τ of the NPLA is .774. It is obtained by taking the ratio of the lengths of two consecutive elements of a face on the same side of the feed line. Table III-1 provides a list of the element lengths and the length of the feed line to that element. The even numbered elements represent the dimensions for the scaled faces of the pyramid structure.

Figure (III-1) provides a view of the structure at the vertex of the pyramid. It was concluded from this figure that height of the vertex of the pyramid was 1.524 m (60 inches).

Element Number	Element Length (m)	Feed Line Length (m)
1	25.000	35.704
2	23.454	33.49
3	22.001	31.42
4	20.638	29.47
5	19.361	27.65
6	18.163	25.94
7	17.035	24.33
8	15.984	22.82
9	14.993	21.41
10	14.064	20.01
11	13.195	18.84
12	12.378	17.68
13	11.610	16.58
14	10.891	15.55
15	10.217	14.59
16	9.586	13.69
17	8.992	12.84
18	8.434	12.05
19	7.913	11.30
20	7.422	10.60
21	6.902	9.94
22	6.532	9.33
23	6.126	8.75
24	5.749	8.21
25	5.392	7.70
26	5.060	7.22
27	4.746	6.78
28	4.450	6.36
29	4.176	5.96
30	3.917	5.59

Table III-1. NPLA Element and Feed Line Lengths Provided by A.O. Even element numbers are for the scaled faces. $\tau = .774$.

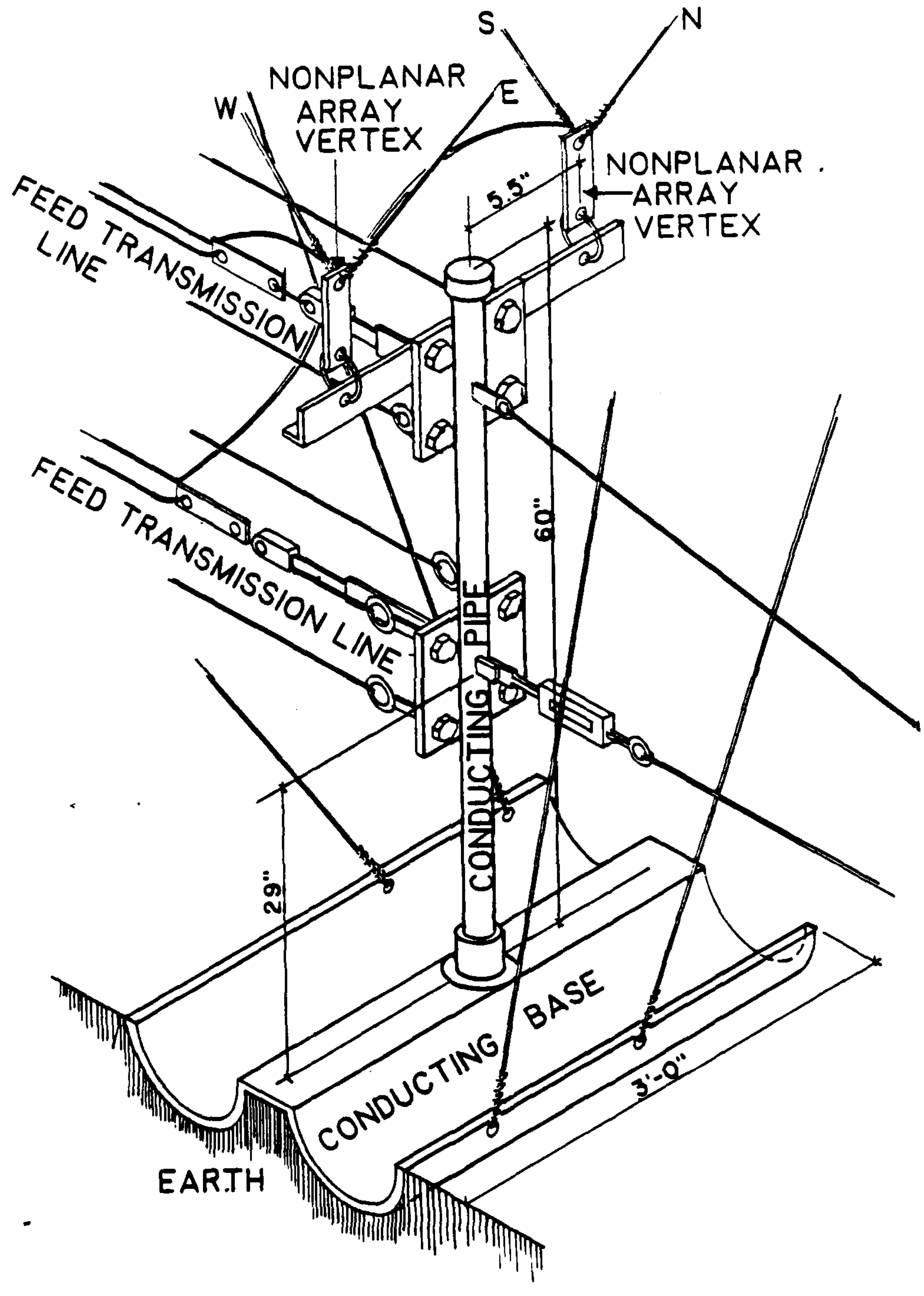

Figure III-1 Vertex of pyramid for Arecibo Observatory HF non-planar log-periodic array

Figure (III-2) shows a sketch of a feed point of one of the faces of the pyramid. The wires detailed by "A" are in addition to previously used geometry. All of the conducting elements of the antenna consist of three #12 twisted steel wires with 10% aluminum coating.

The additional information on the array elements was combined into a new geometry description for AMP. Discrepancies exist within the new information provided. Figure (III-1) depicts the height of the vertex at five feet, while figure (III-2) shows a six-foot height. Table III-1 and figure (III-2) give different distances between the feed point and the bottom element. It is unclear whether figure (III-2) represents a scaled face or unscaled face of the pyramid and whether the dimensions of the additional wires are also scaled between the two sets of faces. For the new geometry description to be used with AMP the following geometry was decided upon:

1. The height of the vertex is 1.524 m.
2. The lengths of all the feed lines to the elements are all taken from table III-1 (including the length to the bottom element).
3. Figure (III-2) was taken to be an unscaled face of a pyramid. The 144" dimension was taken to be correct and the other dimensions were adjusted to correspond to table III-1.
4. All wires and dimensions from the unscaled face were scaled by the fourth root of τ (τ = .774) for the scaled face. This includes the additional wires shown in figure (III-2).

The final AMP geometry deck incorporating these changes is given in figure (III-3). The computer results of the power gain

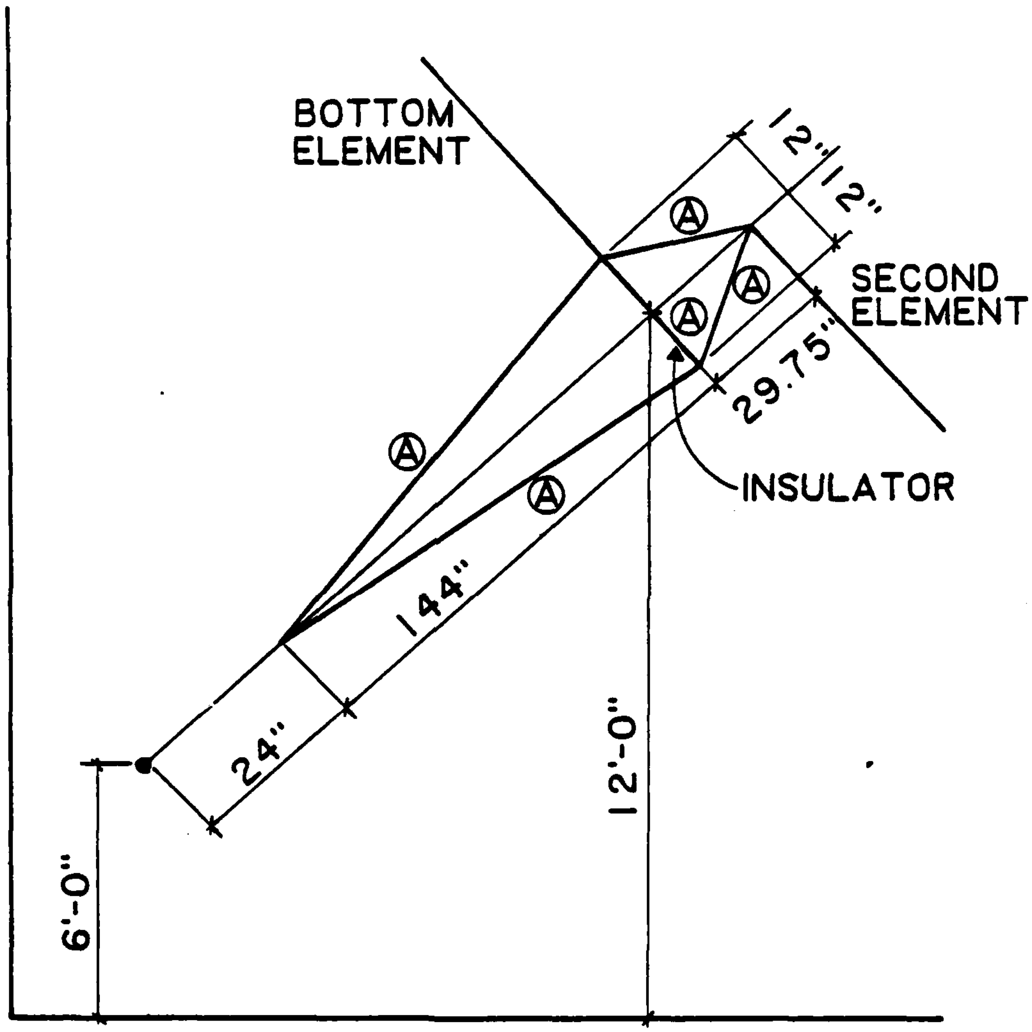

Figure III-2 Capacitvely loaded feed region for one face of pyramid element in Arecibo Observatory HF heating non-planar log-periodic array

1.	//DATA.INPUT DD *								
2.	CM	THE DECK MUST BEGIN WITH CM,CE CARDS							
3.	CM	HEATER ARRAY ELEMENT AT ARECIBO P.R. FREQ=3.170 MHZ.							
3.5	CM	MODIFIED GEOMETRY TAU=.774 ELEMENT ELEVATION 60 INCHES							
4.	CE	EE 438 FALL TERM 1981							
5.	GW001	2	0.000	0.000	0.000	0.000	2.305	0.000	0.0020
6.	GW002	3	0.000	2.305	0.000	0.304	5.963	0.000	0.0020
7.	GW003	3	0.000	2.305	0.000	0.000	5.963	0.000	0.0020
8.	GW004	3	0.000	2.305	0.000	-0.304	5.963	0.000	0.0020
9.	GW005	1	0.000	5.963	0.000	-0.304	5.963	0.000	0.0020
10.	GW006	4	-0.304	5.963	0.000	-4.176	5.963	0.000	0.0020
11.	GW007	1	0.000	5.963	0.000	0.000	6.776	0.000	0.0020
12.	GW008	1	0.304	5.963	0.000	0.000	6.776	0.000	0.0020
13.	GW009	1	-0.304	5.963	0.000	0.000	6.776	0.000	0.0020
16.	GW010	4	0.000	6.776	0.000	4.746	6.776	0.000	0.0020
17.	GW011	1	0.000	6.776	0.000	0.000	7.700	0.000	0.0020
18.	GW012	4	0.000	7.700	0.000	-5.392	7.700	0.000	0.0020
19.	GW013	1	0.000	7.700	0.000	0.000	8.750	0.000	0.0020
20.	GW014	5	0.000	8.750	0.000	6.126	8.750	0.000	0.0020
21.	GW015	1	0.000	8.750	0.000	0.000	9.944	0.000	0.0020
22.	GW016	5	0.000	9.944	0.000	-6.962	9.944	0.000	0.0020
23.	GW017	1	0.000	9.944	0.000	0.000	11.299	0.000	0.0020
24.	GW018	5	0.000	11.299	0.000	7.913	11.299	0.000	0.0020
25.	GW019	1	0.000	11.299	0.000	0.000	12.840	0.000	0.0020
26.	GW020	5	0.000	12.840	0.000	-8.992	12.840	0.000	0.0020
27.	GW021	1	0.000	12.840	0.000	0.000	14.591	0.000	0.0020
28.	GW022	5	0.000	14.591	0.000	10.217	14.591	0.000	0.0020
29.	GW023	1	0.000	14.591	0.000	0.000	16.581	0.000	0.0020
30.	GW024	5	0.000	16.581	0.000	-11.610	16.581	0.000	0.0020
31.	GW025	1	0.000	16.581	0.000	0.000	18.842	0.000	0.0020
32.	GW026	5	0.000	18.842	0.000	13.195	18.842	0.000	0.0020
33.	GW027	1	0.000	18.842	0.000	0.000	21.412	0.000	0.0020
34.	GW028	6	0.000	21.412	0.000	-14.993	21.412	0.000	0.0020
35.	GW029	1	0.000	21.412	0.000	0.000	24.331	0.000	0.0020
36.	GW030	7	0.000	24.331	0.000	17.035	24.331	0.000	0.0020
37.	GW031	2	0.000	24.331	0.000	0.000	27.649	0.000	0.0020
38.	GW032	8	0.000	27.649	0.000	-19.361	27.649	0.000	0.0020
39.	GW033	2	0.000	27.649	0.000	0.000	31.420	0.000	0.0020
40.	GW034	9	0.000	31.420	0.000	22.001	31.420	0.000	0.0020
41.	GW035	2	0.000	31.420	0.000	0.000	35.704	0.000	0.0020
42.	GW036	10	0.000	35.704	0.000	-25.000	35.704	0.000	0.0020
43.	GM000	0	45.000	0.000	0.000	0.000	0.000	0.000	
44.	GM036	1	90.000	0.000	0.000	0.000	0.000	0.000	
45.	GW073	2	0.000	0.000	0.000	2.162	0.000	0.000	0.0020
45.02	GW074	3	2.162	0.000	0.000	5.594	0.000	0.000	0.0020
45.04	GW075	3	2.162	0.000	0.000	5.594	0.286	0.000	0.0020
45.06	GW076	3	2.162	0.000	0.000	5.594	-0.286	0.000	0.0020
45.08	GW077	1	5.594	0.000	0.000	5.594	-0.286	0.000	0.0020
45.1	GW078	4	5.594	-0.286	0.000	5.594	-3.917	0.000	0.0020
45.12	GW079	1	5.594	0.000	0.000	6.356	0.000	0.000	0.0020
45.14	GW080	1	5.[illegible]	-0.286	0.000	6.356	0.000	0.000	0.0020
45.16	GW081	1	5.594	0.286	0.000	6.356	0.000	0.000	0.0020
48.	GW082	4	6.356	0.000	0.000	6.356	4.450	0.000	0.0020
49.	GW083	1	6.356	0.000	0.000	7.223	0.000	0.000	0.0020
50.	GW084	4	7.223	0.000	0.000	7.223	-5.060	0.000	0.0020

Figure III-3 AMP geometry deck containing structure modifications: τ=.774, capacitively loaded feed, and elevation of 1.524 m

51.	GW085	1	7.223	0.000	0.000	8.209	0.000	0.000	0.0020
52.	GW086	5	8.208	0.000	0.000	8.209	5.749	0.000	0.0020
53.	GW087	1	8.208	0.000	0.000	9.329	0.000	0.000	0.0020
54.	GW088	5	9.328	0.000	0.000	9.328	-6.532	0.000	0.0020
55.	GW089	1	9.328	0.000	0.000	10.599	0.000	0.000	0.0020
56.	GW090	5	10.599	0.000	0.000	10.599	7.422	0.000	0.0020
57.	GW091	1	10.599	0.000	0.000	12.045	0.000	0.000	0.0020
58.	GW092	5	12.045	0.000	0.000	12.045	-8.434	0.000	0.0020
59.	GW093	1	12.045	0.000	0.000	13.688	0.000	0.000	0.0020
60.	GW094	5	13.688	0.000	0.000	13.688	9.596	0.000	0.0020
61.	GW095	1	13.688	0.000	0.000	15.554	0.000	0.000	0.0020
62.	GW096	5	15.554	0.000	0.000	15.554	-10.891	0.000	0.0020
63.	GW097	1	15.554	0.000	0.000	17.675	0.000	0.000	0.0020
64.	GW098	5	17.675	0.000	0.000	17.675	12.378	0.000	0.0020
65.	GW099	1	17.675	0.000	0.000	20.086	0.000	0.000	0.0020
66.	GW100	6	20.086	0.000	0.000	20.086	-14.064	0.000	0.0020
67.	GW101	1	20.086	0.000	0.000	22.825	0.000	0.000	0.0020
68.	GW102	7	22.825	0.000	0.000	22.825	15.994	0.000	0.0020
69.	GW103	2	22.825	0.000	0.000	25.937	0.000	0.000	0.0020
70.	GW104	8	25.937	0.000	0.000	25.937	-18.163	0.000	0.0020
71.	GW105	2	25.937	0.000	0.000	29.475	0.000	0.000	0.0020
72.	GW106	9	29.475	0.000	0.000	29.475	20.638	0.000	0.0020
73.	GW107	2	29.475	0.000	0.000	33.493	0.000	0.000	0.0020
74.	GW108	10	33.493	0.000	0.000	33.493	-23.454	0.000	0.0020
75.	GM000	0	0.000	-45.000	0.000	0.000	0.000	0.000	75.0
76.	GM036	1	0.000	-90.000	0.000	0.000	0.000	0.000	73.0
77.	GM000	0	0.000	0.000	0.000	0.000	0.000	1.524	
78.	GW145	2	0.000	0.000	0.000	0.000	0.000	1.524	0.0020
79.	GE001								
80.	GN000	0		20.0	.03				
81.	FR000	1		3.170	0.000				
82.	EX000	001	001 00	1.000	0.000				
83.	EX000	037	001 00	1.000	0.000				
84.	EX000	073	001 00	1.000	0.000				
85.	EX000	109	001 00	1.000	0.000				
86.	RP000	45	72 1000	0.0	0.0	2.5	5.0	7.5E 04	
87.	EN000								

Figure III-3 (con.) AMP geometry deck containing structure modifications: τ=.774, capacitively loaded feed, and elevation of 1.524 m

for the two cases of 3.17 MHz and 5.1 MHz are shown in figures (III-4) and (III-5). In these figures the "x" denotes the results of the new modified geometry given in this appendix, and the "•" denotes the results of the "old" geometry used in the main body of this report. Figure (III-4) shows the power gain as a function of "phi" for selected constant values of "theta." These are the same values of "theta" used in figure (1-6). Figure (III-5) is a plot of power gain as a function of "theta" for selected values of "phi." The selected values of "phi" are the same values of "phi" used in figure (1-7) plus additional values corresponding to the "x" and "y" axis (i.e., $\phi = 0°, 90°, 180°, 270°$).

Examination of figures (III-4) and (III-5) leads to the conclusion that the changes in geometries between the two cases result in only a small difference in power gain for small values of "theta" and large differences for large values of "theta."

It is necessary to determine what effect the new geometry will have on the results of the main body of this report. The elemental power gain for $\Theta < 50°$ is approximately equal for the two geometries. Since a large portion of the radiated power is contained in this region, it is expected that the directivity of the total array would remain approximately the same. The results shown in figures (1-10) and (1-11) should be approximately the same for $\Theta < 50°$ but significant differences could occur for $\Theta > 50°$.

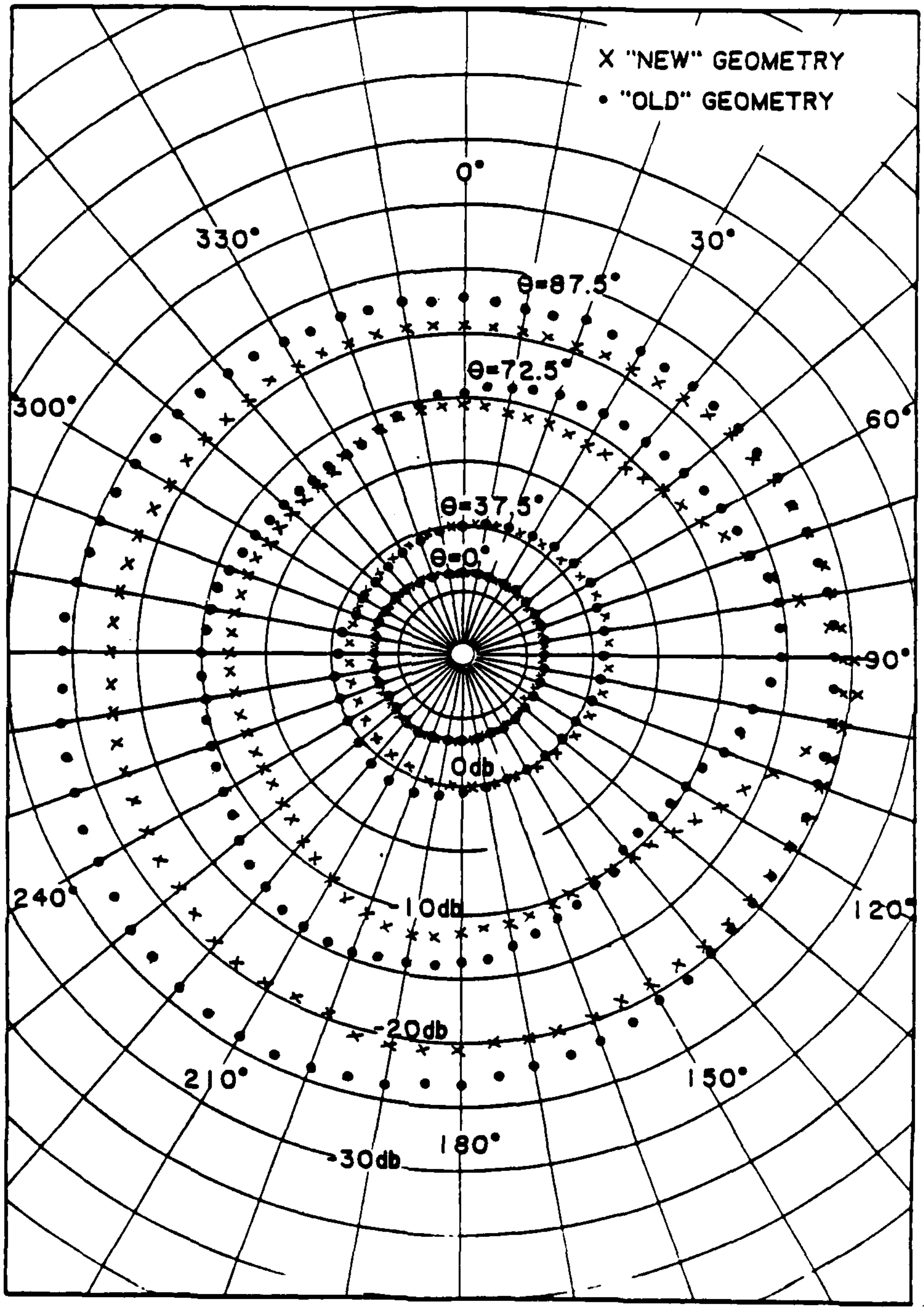

Figure III-4a Power gain vs. phi for constant theta. Comparison of "new" and "old" heating array element geometry. Frequency= 3.17 MHz

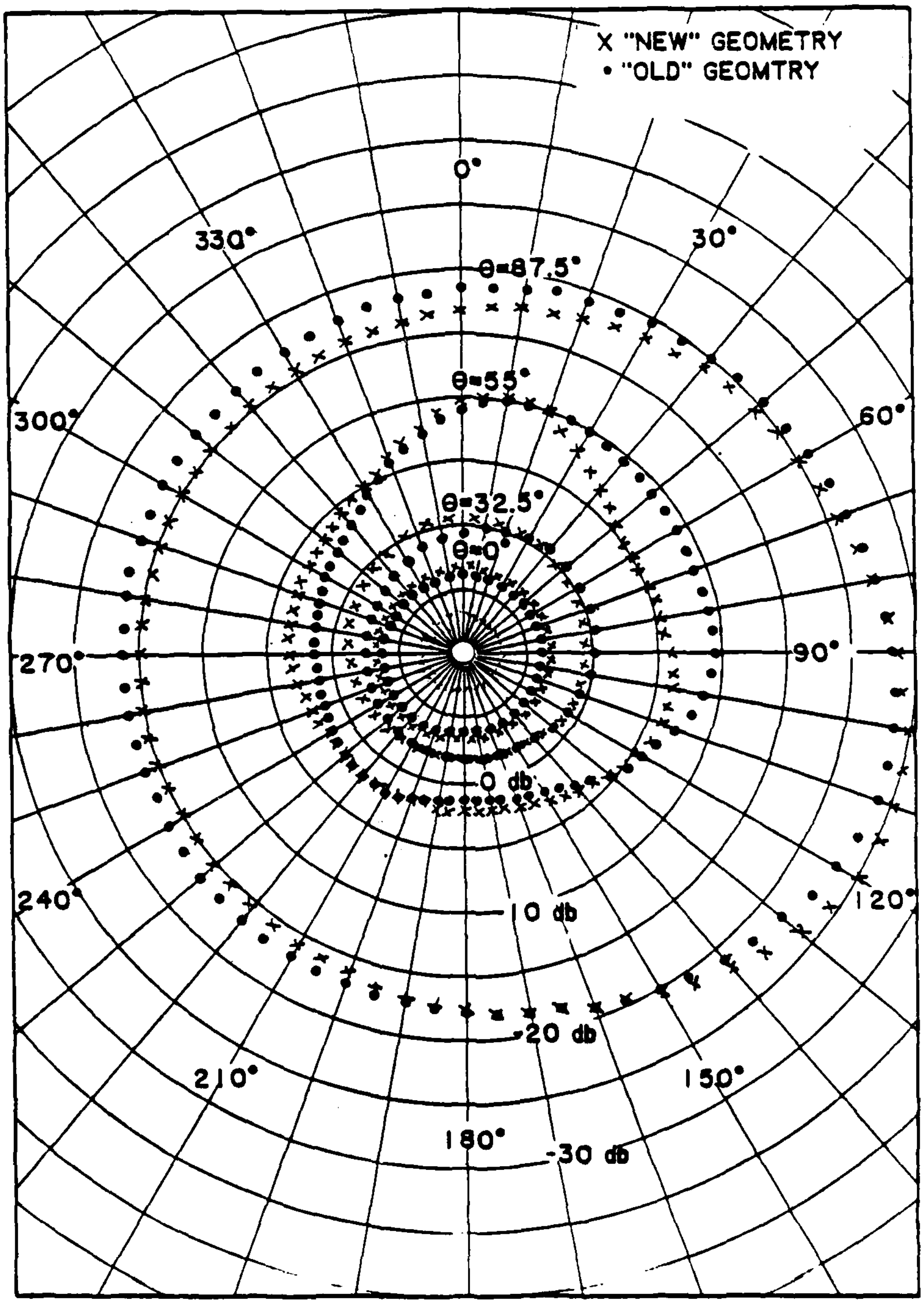

Figure III-4b Power gain vs. phi for constant theta. Comparison of "new" and "old" heating array element geometry. Frequency= 5.1 MHz

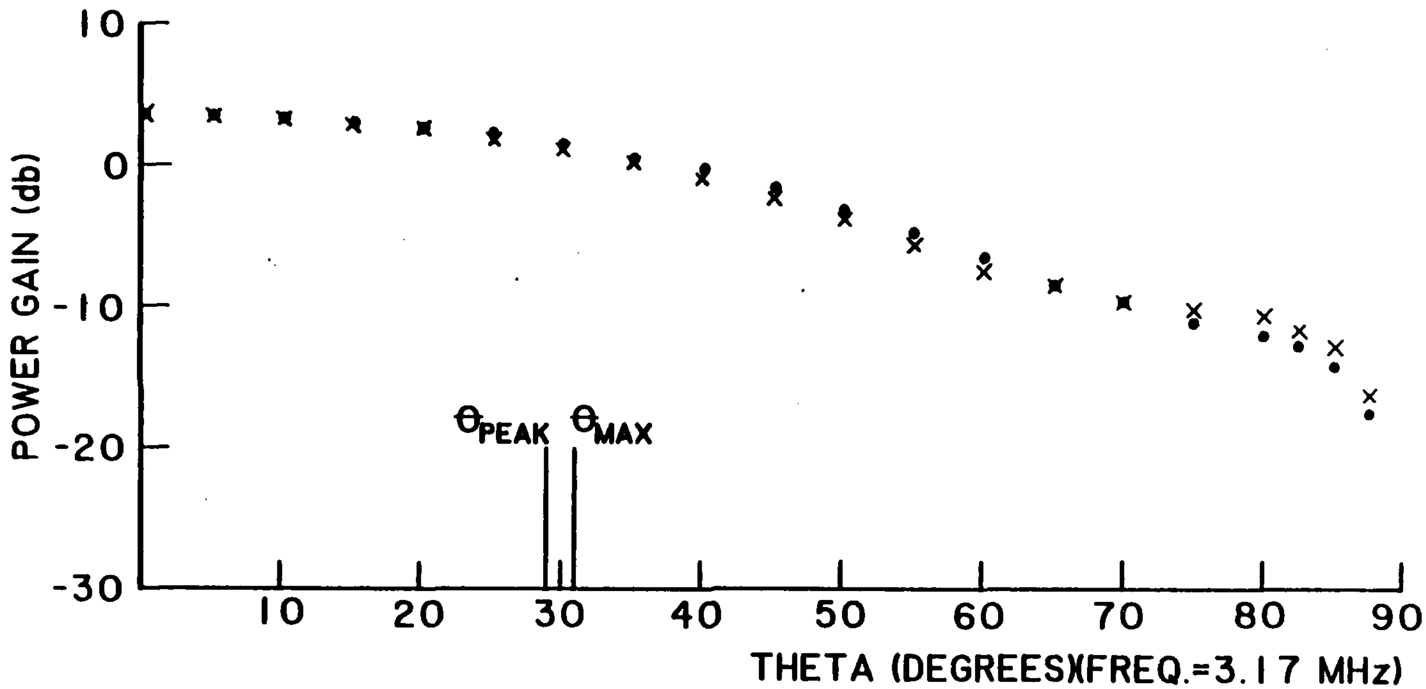

Figure III-5a.1 Power gain vs. 'theta' for constant 'phi'. Comparison of 'new' and 'old' heating array element geometry. Phi = 0^{o}
Frequency = 3.17 MHz

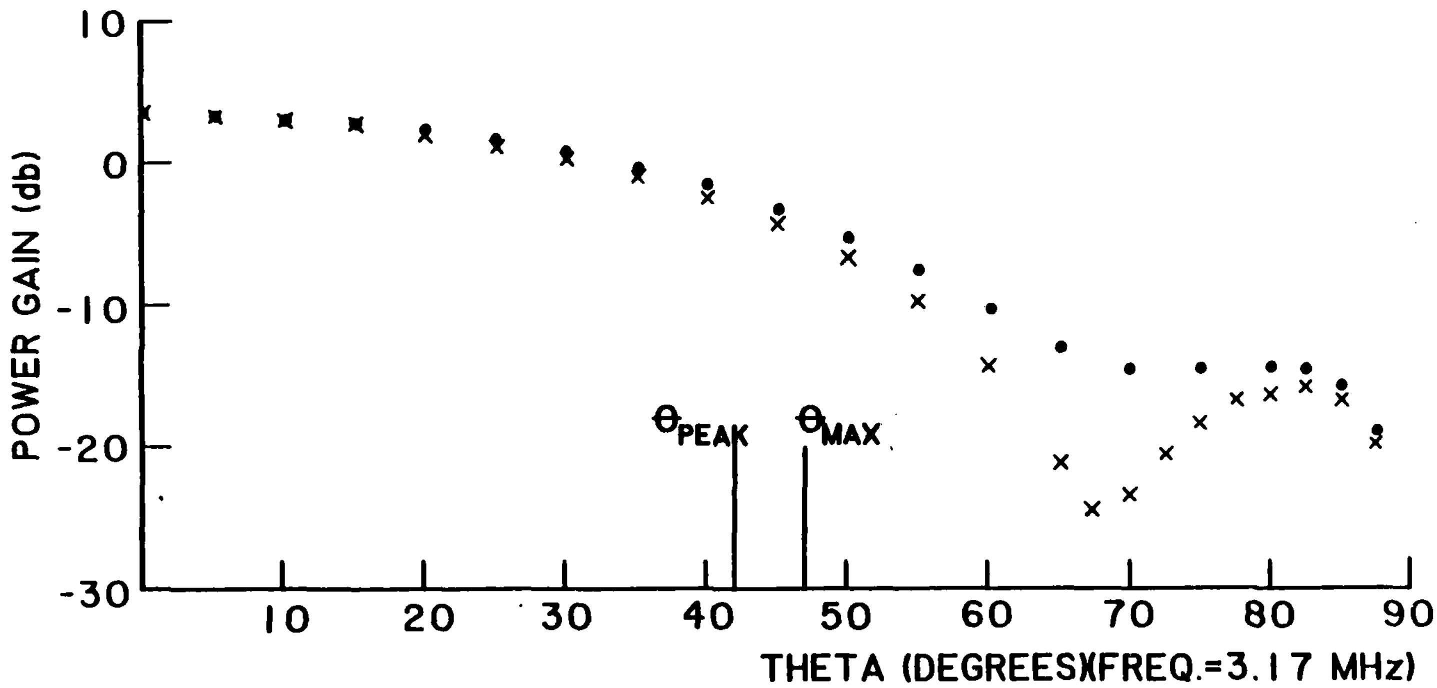

Figure III-5a.2 Power gain vs. 'theta' for constant 'phi'. Comparison of 'new' and 'old' heating array element geometry. Phi = 90° Frequency = 3.17 MHz

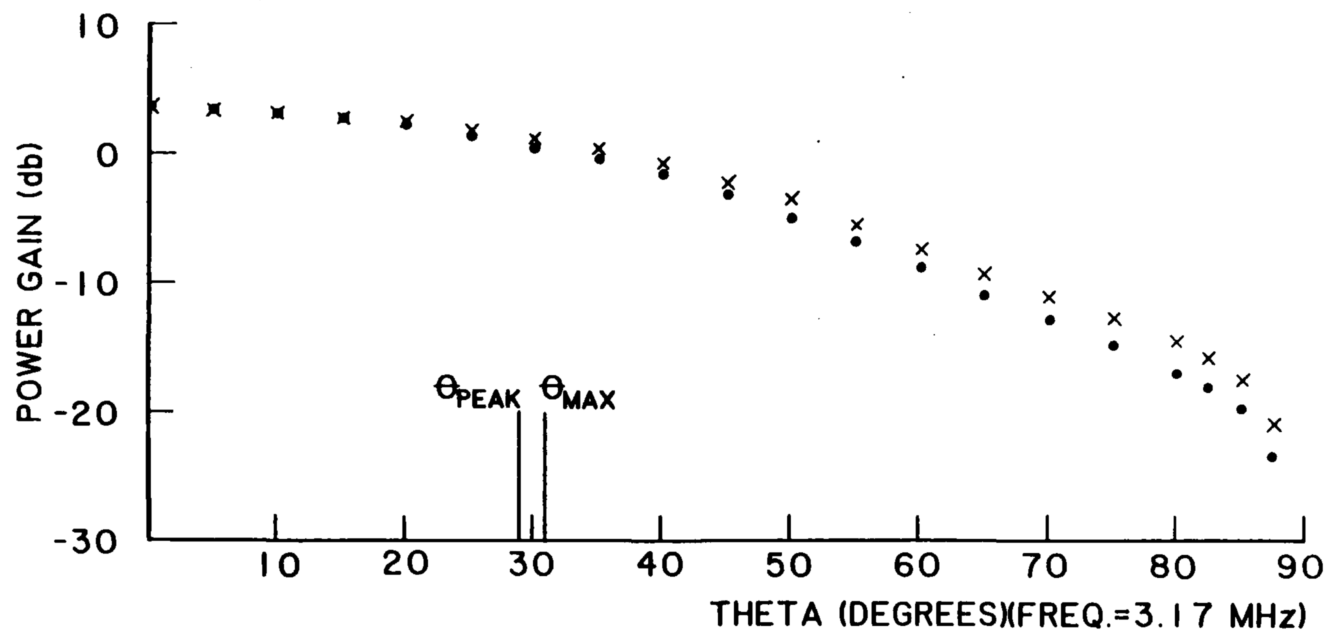

Figure III-5a.3 Power gain vs. 'theta' for constant 'phi'. Comparison of 'new' and 'old' heating array element geometry. Phi = 180°
Frequency = 3.17 MHz

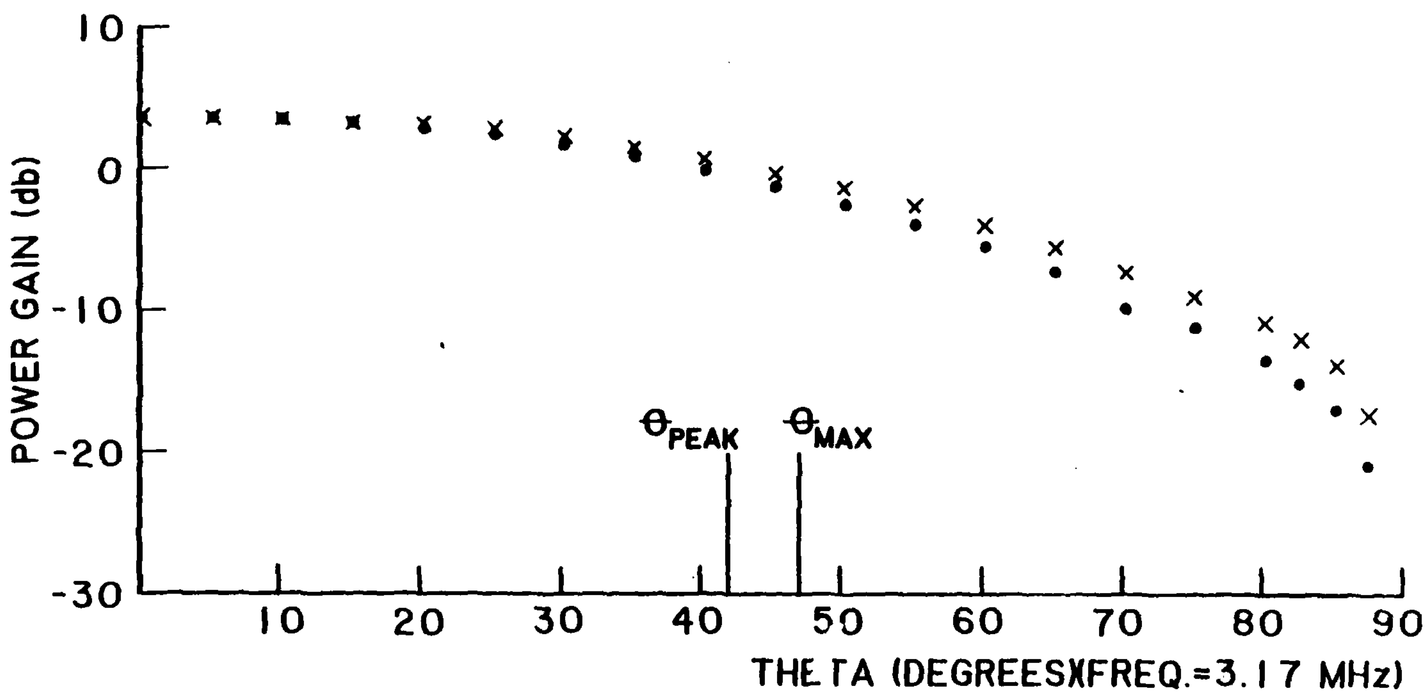

Figure III-5a.4 Power gain vs. 'theta' for constant 'phi'. Comparison of 'new' and 'old' heating array element geometry. Phi = 270° Frequency = 3.17 MHz

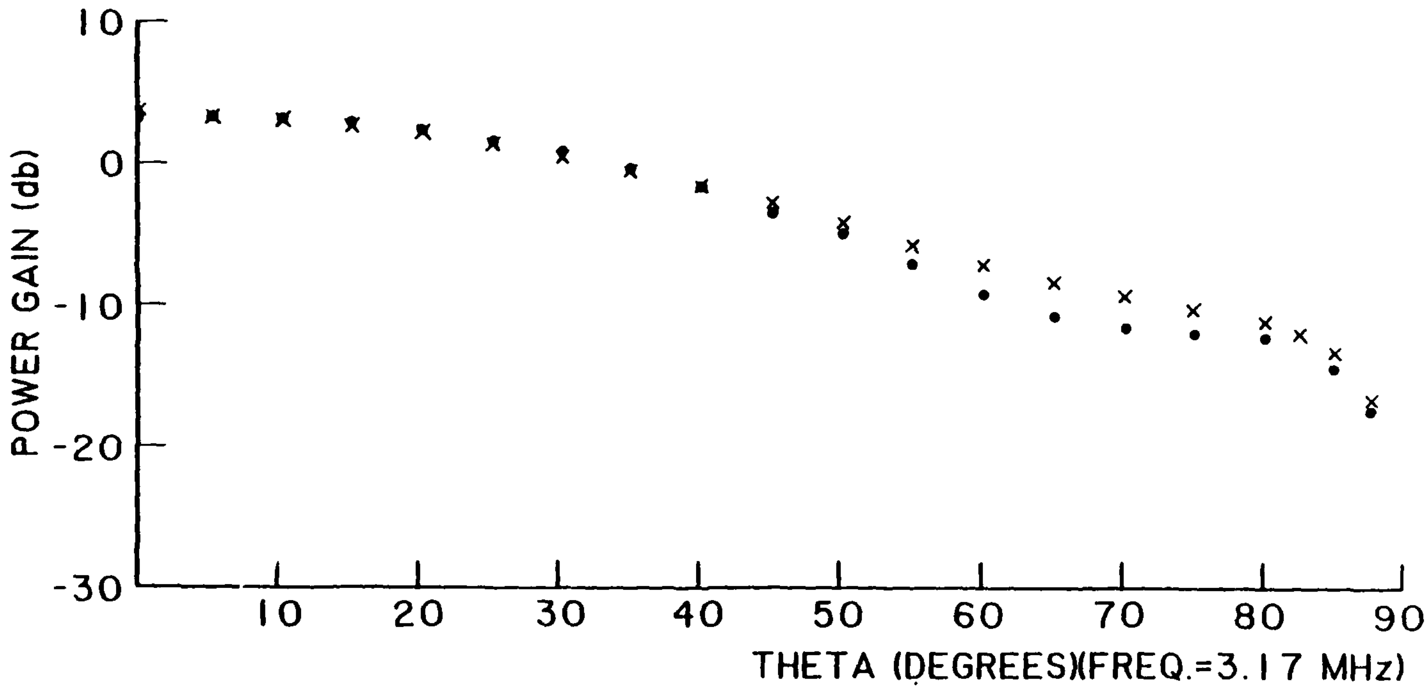

Figure III-5a.5 Power gain vs. 'theta' for constant 'phi'. Comparison of 'new' and 'old' heating array element geometry. Phi = 40° Frequency = 3.17 MHz

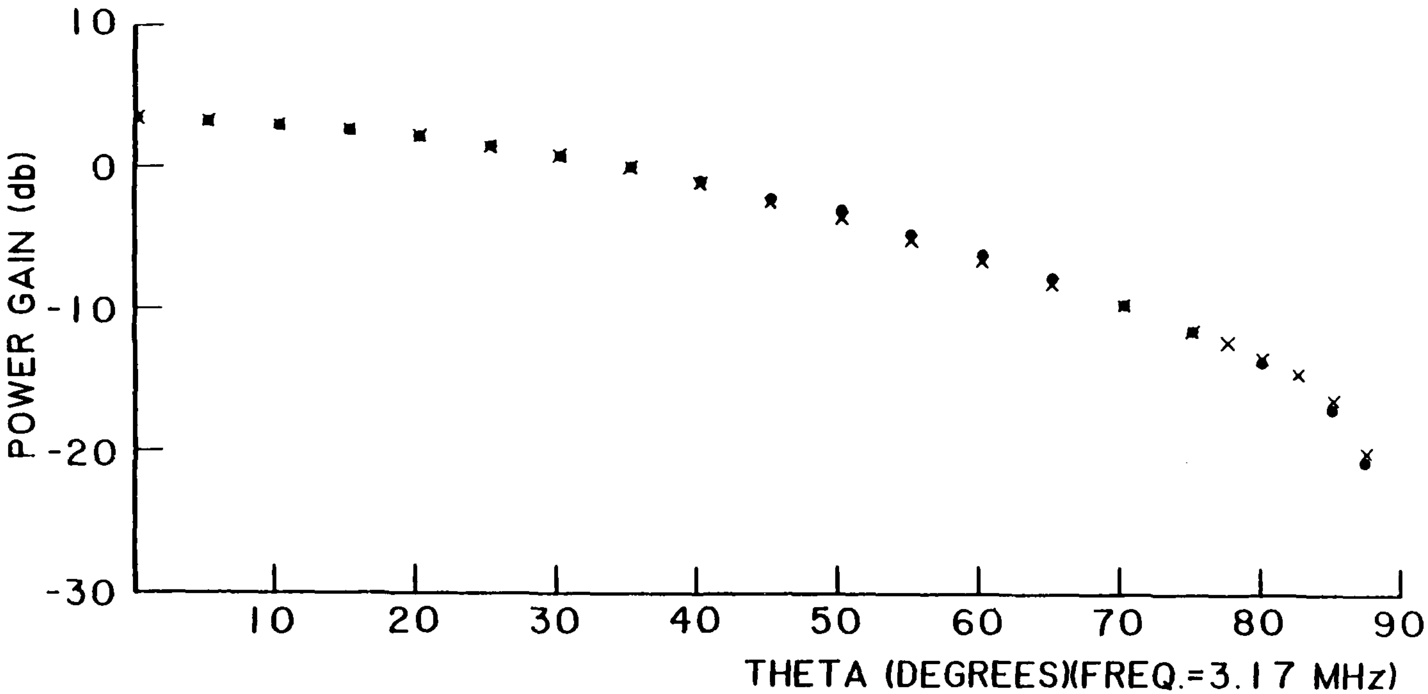

Figure III-5a.6 Power gain vs. 'theta' for constant 'phi'. Comparison of 'new' and 'old' heating array element geometry. Phi = 150° Frequency = 3.17 MHz

AD-A126 809 EFFECT OF HF HEATING ARRAY DIRECTIVITY PATTERN ON THE FREQUENCY RESPONSE O..(U) PENNSYLVANIA STATE UNIV UNIVERSITY PARK IONOSPHERE RESEARCH L.. 3/3

UNCLASSIFIED K J CARROLL ET AL. JAN 83 PSU-IRL-SCI-475 F/G 20/14 NL

END
DATE
FILMED
5-83
DTIC

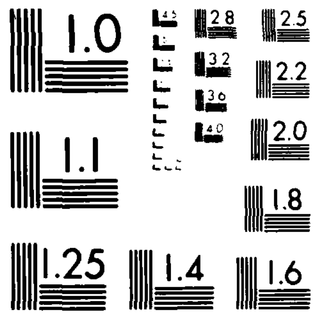

MICROCOPY RESOLUTION TEST CHART
NATIONAL BUREAU OF STANDARDS 1963-A

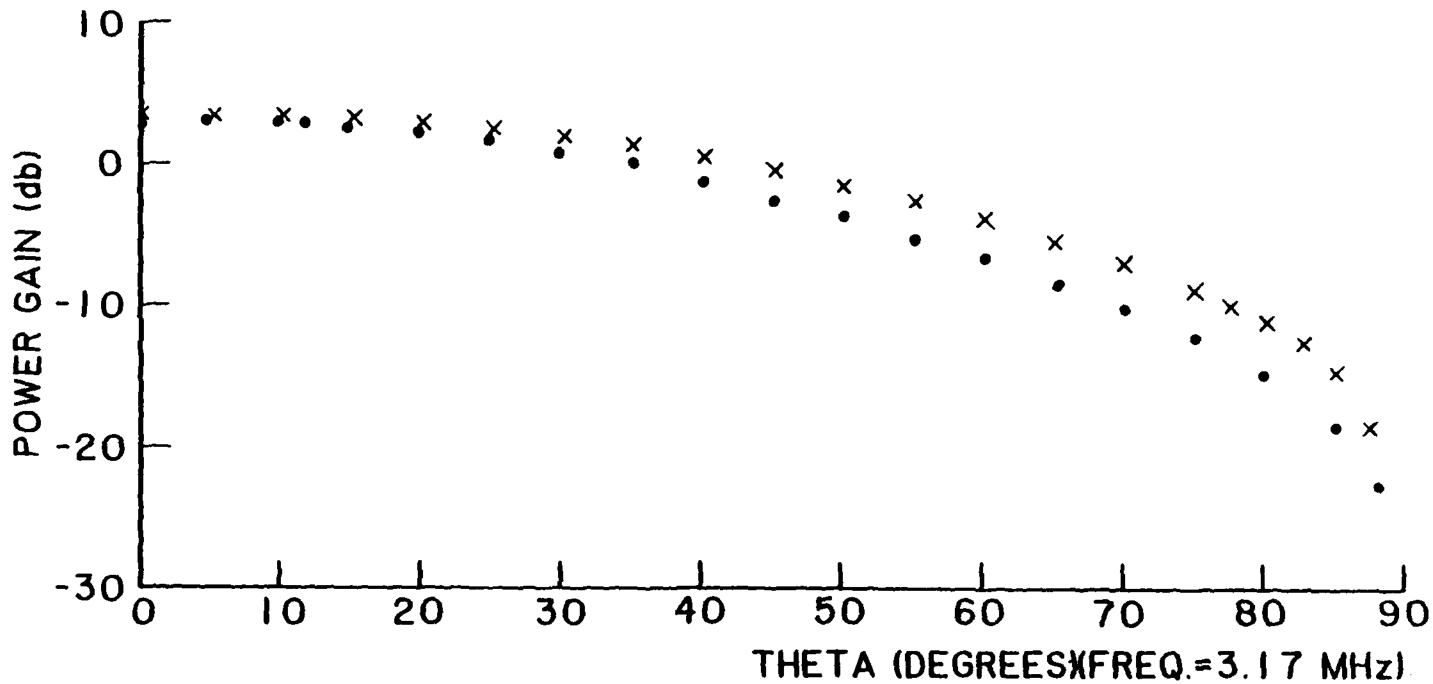

Figure III-5a.7 Power gain vs. 'theta' for constant 'phi'. Comparison of 'new' and 'old' heating array element geometry. Phi = 240° Frequency = 3.17 MHz

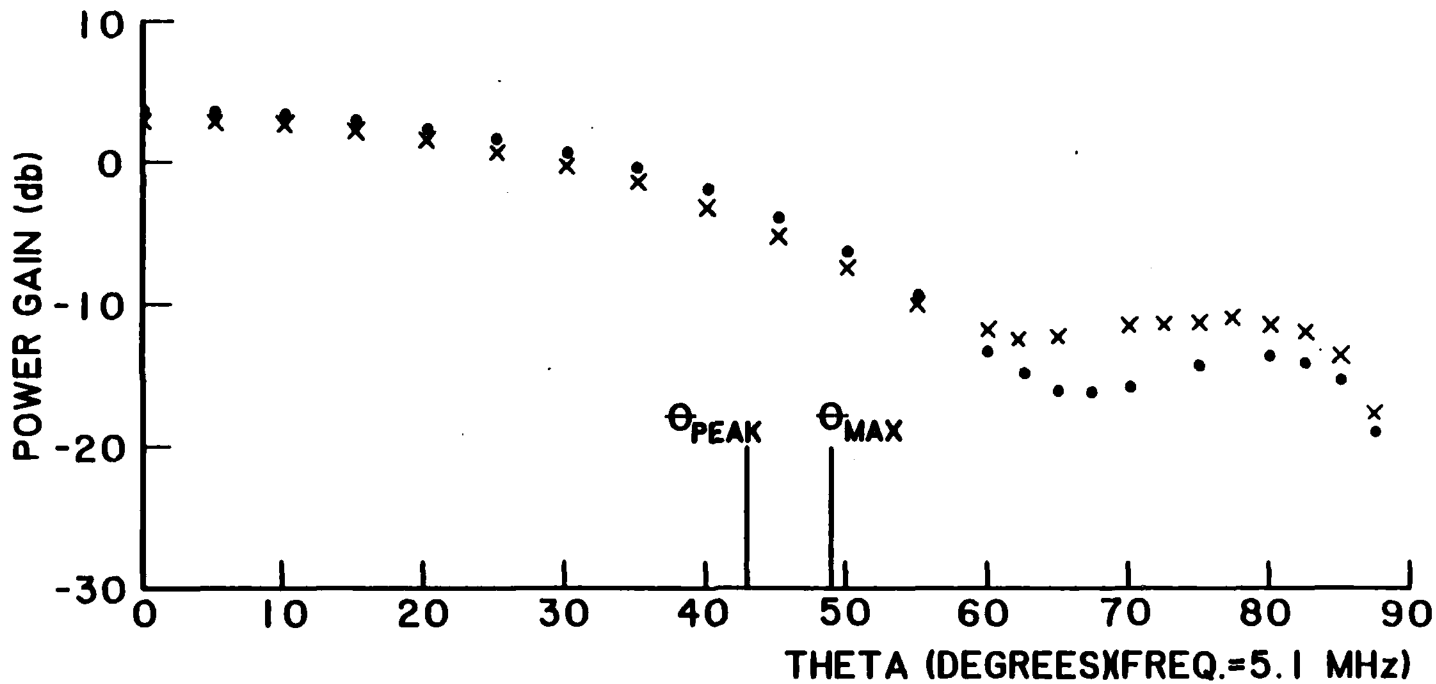

Figure III-5b.1 Power gain vs. 'theta' for constant 'phi'. Comparison of 'new' and 'old' heating array element geometry. Phi = 0 Frequency = 5.1 MHz

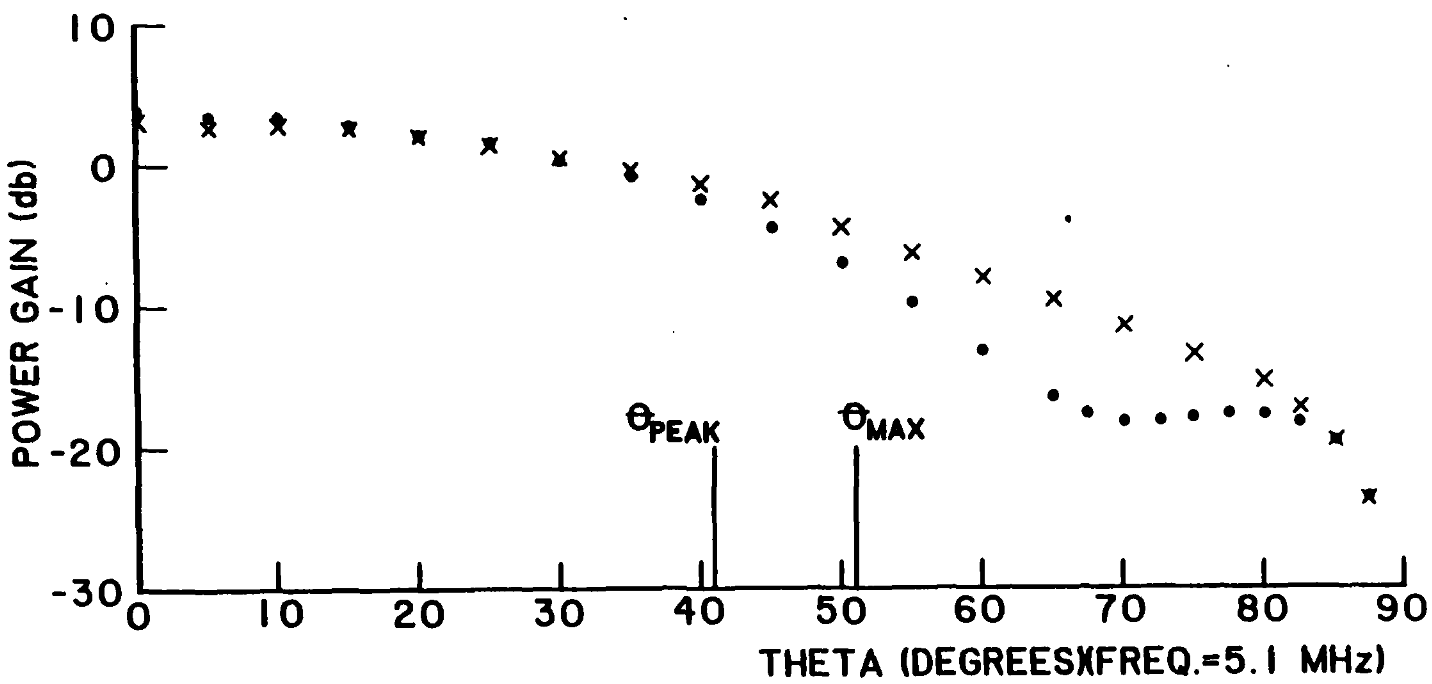

Figure III-5b.2 Power gain vs. 'theta' for constant 'phi'. Comparison of 'new' and 'old' heating array element geometry. Phi = 90^{o}
Frequency = 5.1 MHz

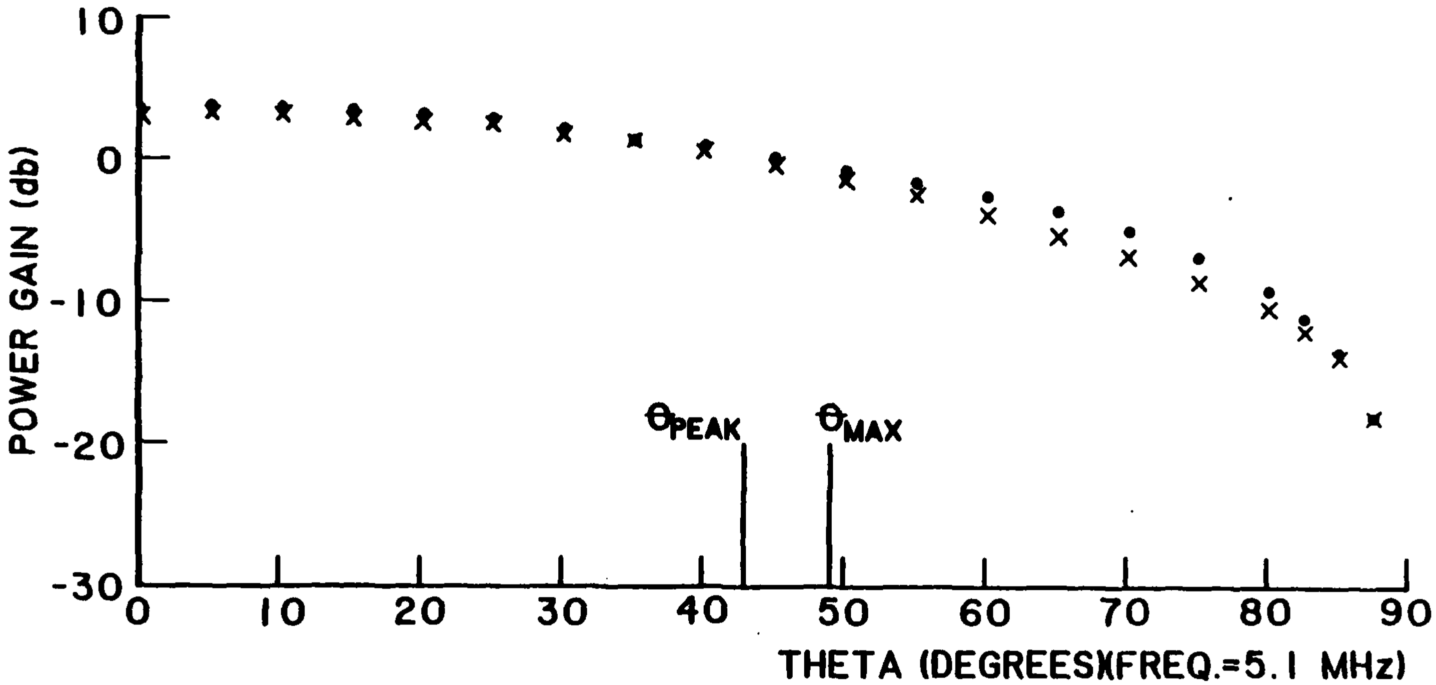

Figure III-5b.3 Power gain vs. 'theta' for constant 'phi'. Comparison of 'new' and 'old' heating array element geometry. Phi = 180° Frequency = 5.1 MHz

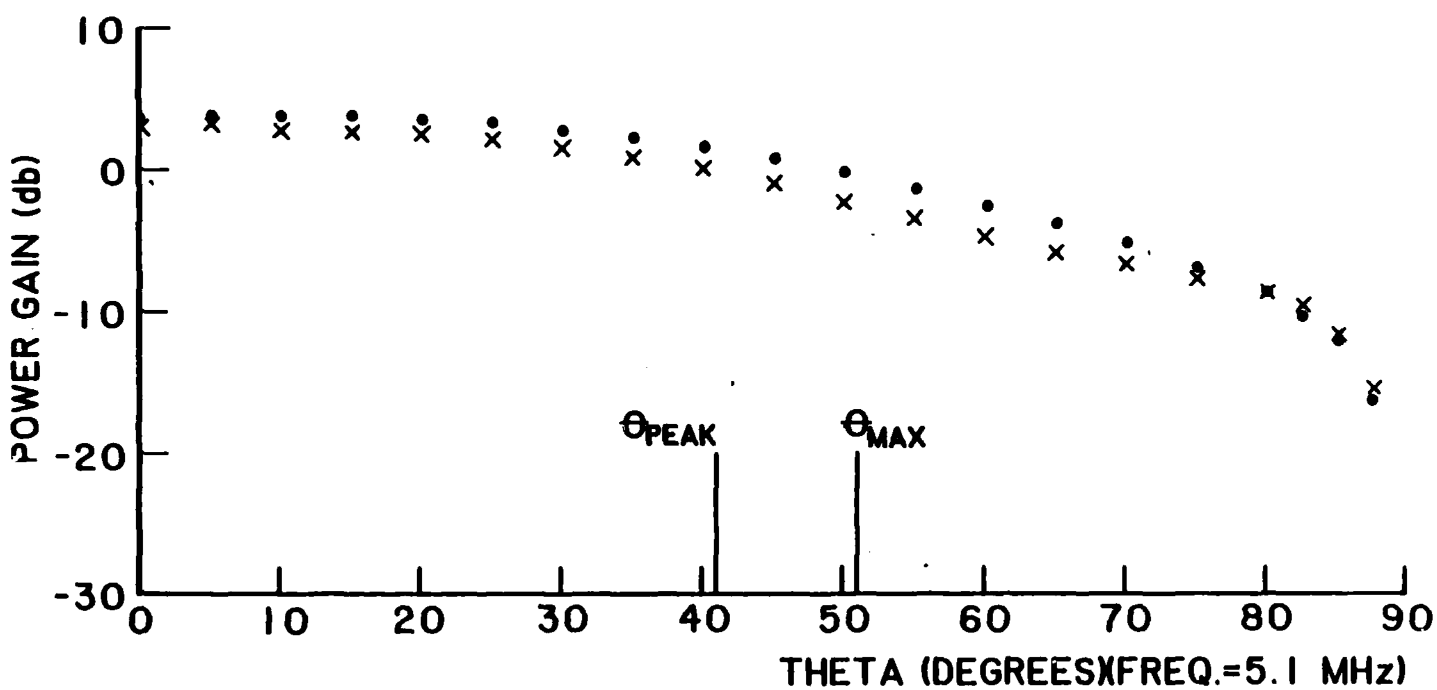

Figure III-5b.4 Power gain vs. *'theta' for constant 'phi'. Comparison of 'new'* and 'old' heating array element geometry. Phi = 270°
Frequency = 5.1 MHz

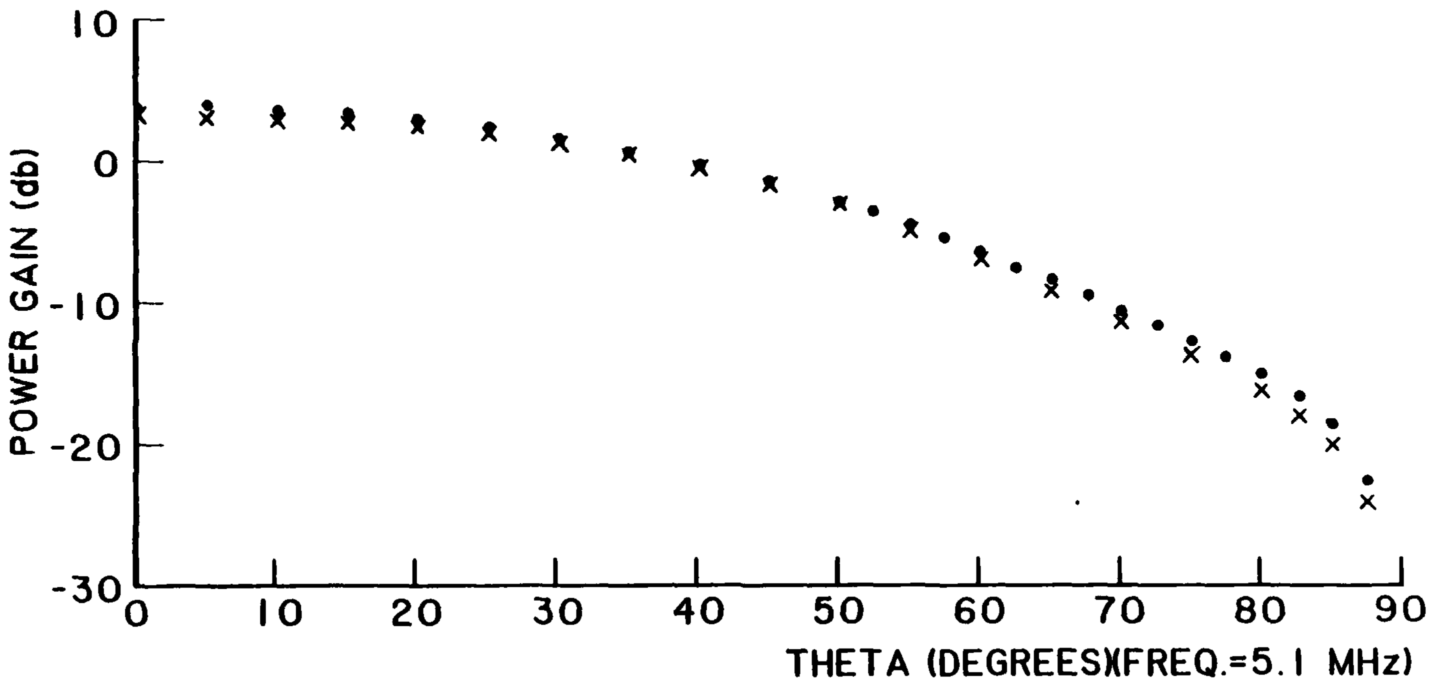

Figure III-5b.5 Power gain vs. 'theta' for constant 'phi'. Comparison of 'new' and 'old' heating array element geometry. Phi = 130°
Frequency = 5.1 MHz

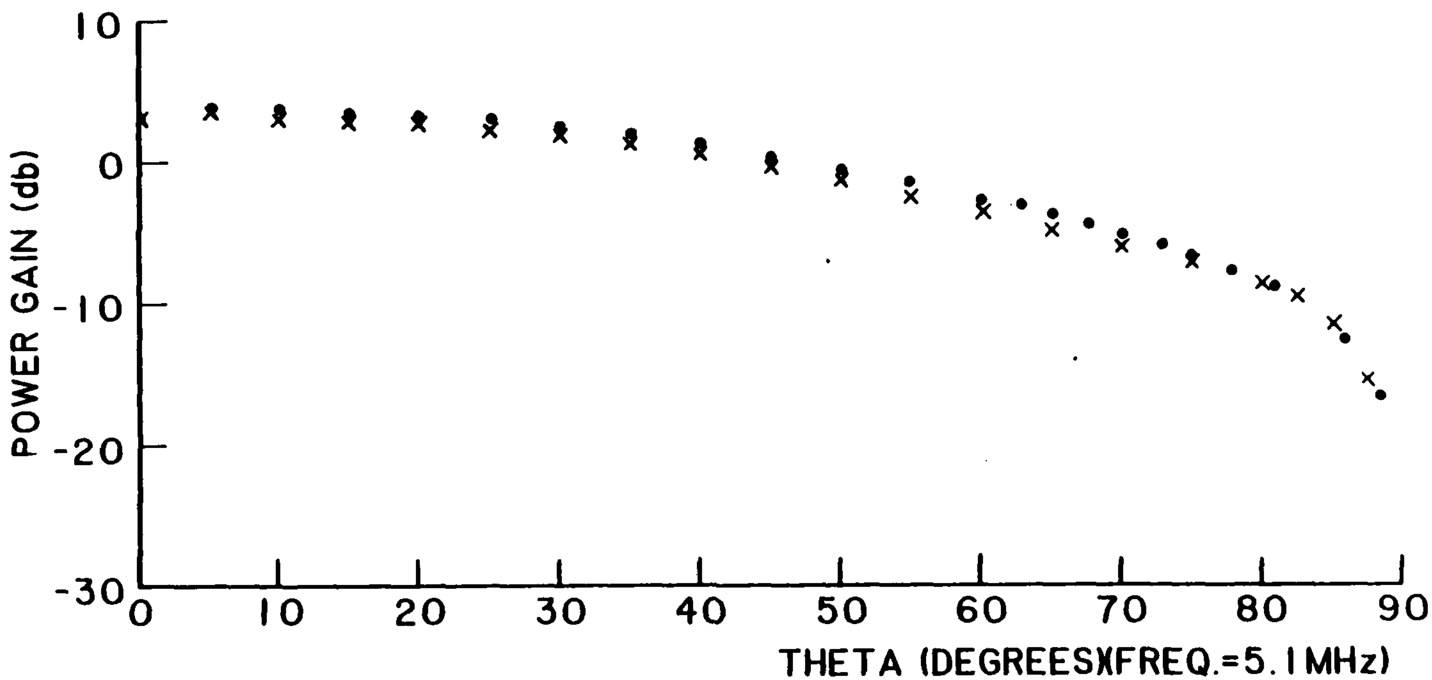

Figure III-5b.6 Power gain vs. 'theta' for constant 'phi'. Comparison of 'new' and 'old' heating array element geometry. Phi = 250^{o}
Frequency = 5.1 MHz

Of particular interest is the differences in directive gain along the "x" and "y" axis. The ELF/VLF source array orginates from the HF antenna response along these lines. Table III-2 shows the value of "theta" to the center and furthest edge of the ELF/VLF source region (shown in figures (1-15) and (1-16)) which is furthest from the origin.

Frequency	Source Location x	y	Length	Width	Center	Edge
3.17 MHz	63 km	0	24 km	-----	42°	47°
3.17 MHz	0	38 km	----	7 km	29°	31°
5.1 Mhz	60 km	0	54 km	---	41°	51°
5.1 MHz	0	65 km	---	28 km	43°	49°

Table III-2. Value for Θ to the Source Regions Furthest from Origin.

Since all the ELF/VLF sources are located in a region where "theta" is less than 50°, it is concluded that the new geometry will not significantly affect the zero approximation ELF/VLF array model. The plots of relative field intensity versus ELF/VLF frequency should remain essentially the same. The fundamental conclusion of the main body of the report that the ELF/VLF frequency response is affected by the geometry of the HF heating antenna pattern remains intact.

Distribution List for Pennsylvania State University
Contract No. N00014-81-K-0276
January 1983

Department of Defense

Director
Defense Advanced Research Projects Agency
1400 Wilson Boulevard
Arlington, VA 22209
1 cy ATTN: TIO
1 cy ATTN: STO
1 cy ATTN: NRMO

Director
Defense Communications Agency
8th Street and South Courhouse Road
Arlington, VA 22204
3 cys. ATTN: MEECN Office

Defense Documentation Center
Cameron Station
Alexandria, VA 22314
12 cys. ATTN: TC

Director
Defense Nuclear Agency
Washington, DC 20305
1 cy ATTN: STTL
1 cy ATTN: DDST
3 cys ATTN: RAAE
1 cy ATTN: RAEV

Joint Chiefs of Staff
Department of Defense
Washington, DC 20301
1 cy. ATTN: J-6

Director
National Security Agency
Fort George G. Meade, MD 20755
2 cys ATTN: Technical Library

Under Secretary of Defense (Research and Engineering)
Department of Defense
Washington, DC 20301
2 cys ATTN: DDS&SS

Assistant Deputy Under Secretary of Defense (C^3)
Department of Defense
Washington, DC 20301
2 cys ATTN: Dr. Quinn

Department of Commerce

U.S. Department of Commerce
Office of Telecommunications
Institute for Telecommunication Sciences
National Telecommunications and Information Administration
Boulder, Colorado 80303
2 cys ATTN: W.F. Utlaut

Department of the Army

Commander/Director
Atmospheric Sciences Laboratory
U.S. Army Electronics Command
White Sands Missile Range, NM 88002
1 cy ATTN: DRSEL-BL-SY-S
F.E. Niles

Director
U.S. Army Ballistic Research Laboratories
Aberdeen Proving Grounds, MD 21005
1 cy ATTN: George E. Keller

Commander
U.S. Army Foreign Sciences and Technology Center
220 7th Street, N.E.
Charlottesville, VA 22901
1 cy ATTN: Robert Jones

Department of the Navy

Office of Naval Research Detachment, Boston
495 Summer Street
Boston, MA 02210
2 cy

ONR Resident Representative
Carnegie-Mellon University
Room 407 Margaret Morrison Building
Pittsburgh, PA 15213
1 cy

Chief of Naval Operations
Department of the Navy
Washington, DC 20350
    1 cy ATTN: NOP 985
    1 cy ATTN: NOP 094H
    1 cy ATTN: NOP 943

Chief of Naval Research
Department of the Navy
800 North Quincy Street
Arlington, VA 22217
    1 cy ATTN: Code 414, R.G. Joiner
    1 cy ATTN: Code 210, Capt. Howard

Commander
Naval Electronic Systems Command
Department of the Navy
Washington, DC 20360
    1 cy ATTN: PME-110
    1 cy ATTN: PME-110T
    1 cy ATTN: PME 110-21
    1 cy ATTN: PME 110-112
    1 cy ATTN: PME 110-22

Director
Naval Ocean Systems Center
Electromagnetic Propagation Division
271 Catalina Boulevard
San Diego, CA 92152
    1 cy ATTN: Code 2200, J. Fergerson
    1 cy ATTN: Code 2200, J. Richter
    1 cy ATTN: Code 2200, John Bickel

Director
Naval Research Laboratory
4555 Overlook Avenue, S.W.
Washington, D.C. 20375
    1 cy ATTN: Code 1001, Timothy P. Coffey
    1 cy ATTN: Code 7709, Wahab Ali
    2 cys ATTN: Code 7750, John Davis
    1 cy ATTN: Code 2627
    1 cy ATTN: Code 4101, P. Mange

Commander
Naval Surface Weapons Center (White Oak)
Silver Spring, MD 20910
    1 cy ATTN: Technical Library

Director
Naval Underwater Systems Center
New London Lab
New London, CT 06320
2 cys ATTN: Peter Banister

Office of Naval Research Detachment, Pasadena
1030 East Green Street
Pasadena, CA 91106
2 cy ATTN: Dick Brandt

Department of the Air Force

Commander
Air Force Geophysical Laboratory,AFSC
L. G. Hanscom Air Force Base, MA 01731
1 cy ATTN: LKB, W. Swider
1 cy ATTN: LKB, K. Champion
1 cy ATTN: LKB, G. Sales

Director
Air Force Technical Applications Center
Patrick Air Force Base, FL 32920
1 cy ATTN: TD
1 cy ATTN: HQ 1035th TCHOG/TFS

National Aeronautics and Space Administration

Goddard Space Flight Center
Greenbelt, MD 20771
1 cy ATTN: Code 961 R. Goldberg

Department of Defense Contractors

General Electric Company
TEMPO - Center for Advanced Studies
816 State Street
Santa Barbara, CA 93102
1 cy ATTN: Warren S. Knapp
1 cy ATTN: DASIAC

Lockheed Missiles and Space Company
3251 Hanover Street
Palo Alto, CA 94304
1 cy ATTN: J. B. Reagan
1 cy ATTN: W. Imhof
1 cy ATTN: Martin Walt

Mission Research Corporation
735 State Street
Santa Barbara, CA 93101
1 cy ATTN: M. Scheibe
1 cy ATTN: D. Sowle

Pacific-Sierra Research Corporation
12340 Santa Monica Blvd.
Los Angeles, CA 90025
1 cy ATTN: E. C. Field

Pennsylvania State University
Ionospheric Research Laboratory
College of Engineering
318 Electrical Engineering - East Wing
University Park, Pennsylvania 16802
1 cy ATTN: J. Nisbet
1 cy ATTN: Les Hale
1 cy ATTN: A. J. Ferraro
1 cy ATTN: H. S. Lee
1 cy ATTN: J. Olivero
1 cy ATTN: L. Carpenter
1 cy ATTN: J. Brown
1 cy ATTN: W. Adams
1 cy ATTN: J. Mitchell

R & D Associates
4640 Admiralty Way
Marina Del Rey, CA 90291
1 cy ATTN: R. Lelevier
1 cy ATTN: F. Gilmore
1 cy ATTN: R. Turco

The Rand Corporation
1700 Main Street
Santa Monica, CA 90406
1 cy ATTN: Cullen Crain

Profesor Chalmers F. Sechrist
155 Electrical Engineering Building
University of Illinois
Urbana, IL 61801
1 cy ATTN: C. Sechrist

Stanford Research Institute
333 Ravenswood Avenue
Menlo Park, CA 94025
1 cy ATTN: Allen M. Peterson
1 cy ATTN: Ray L. Leadabrand

Stanford University
Radio Science Lab
Stanford, CA 94305
1 cy ATTN: A. C. Frazer-Smith
1 cy ATTN: R. Hellimell
1 cy ATTN: P. Banks

Dr. William Gordon
Rice University
Houston, Texas 77001
1 cy ATTN: W. Gordon

Dr. Peter Stubbe
Max-Planck-Institut fur Aeronomie
Postfach 20, D3411
Katlenburg-Lindau 3
West Germany
1 cy ATTN: P. Stubbe

S.A.I.
McLean, VA 22101
1 cy D. Papadopoulos

IIT Research Institute
5100 Forbes Boulevard
Lanham, MD 20706
1 cy ATTN: A. A. Tomko

Arecibo Observatory
Post Office Box 995
Arecibo, Puerto Rico 00612
1 cy ATTN: D. Campbell

University of Otago
Post Office Box 56
Dunedin, New Zealand
1 cy ATTN: R. L. Dowden

120 New Mark Esplanade
Rockville, MD 20850
1 cy ATTN: D. Newman

Global Analytics
10065 Old Grove Road
San Diego, CA 92131
1 cy ATTN: S. Weisbord

Carroll, Kenneth J., A. J. Ferraro, H. S. Lee, Roger Allshouse, Bruce Long and Ray J. Lunnen, Effect of HF Heating Array Directivity Pattern on the Frequency Response of Generated ELF/VLF, The Electrical Engineering Department, Ionosphere Research Laboratory, Electrical Engineering East, University Park, Pennsylvania, 16802

PSU-IRL-SCI-475

Classification Numbers

1.5.1 D-region
4.1.4 Numerical Techniques and Computations
3.2.1 Ground-Based Techniques and Measurements
3.1 Instrumentation and Facilities for Ionospheric Measurements

Directivity patterns at 3.17 MHz and 5.1 MHz are calculated for the HF antenna array at the high power HF heating facility at the Arecibo Observatory in Puerto Rico. The pattern was calculated using pattern multiplication and method of moment techniques. The calculated pattern is shown to be a good approximation to an experimentally measured pattern in one plane of the array. A simple model was used to approximate the effect of the pattern on the frequency response of ELF/VLF signals generated by the HF heating. The frequency response was determined at two ELF/VLF receiver sites. Results show that ELF/VLF generated by side lobes of the HF pattern have sufficient strength to create a ELF/VLF interference pattern at receiving locations.

Carroll, Kenneth J., A. J. Ferraro, H. S. Lee, Roger Allshouse, Bruce Long and Ray J. Lunnen, Effect of HF Heating Array Directivity Pattern on the Frequency Response of Generated ELF/VLF, The Electrical Engineering Department, Ionosphere Research Laboratory, Electrical Engineering East, University Park, Pennsylvania, 16802

PSU-IRL-SCI-475

Classification Numbers

1.5.1 D-region
4.1.4 Numerical Techniques and Computations
3.2.1 Ground-Based Techniques and Measurements
3.1 Instrumentation and Facilities for Ionospheric Measurements

Directivity patterns at 3.17 MHz and 5.1 MHz are calculated for the HF antenna array at the high power HF heating facility at the Arecibo Observatory in Puerto Rico. The pattern was calculated using pattern multiplication and method of moment techniques. The calculated pattern is shown to be a good approximation to an experimentally measured pattern in one plane of the array. A simple model was used to approximate the effect of the pattern on the frequency response of ELF/VLF signals generated by the HF heating. The frequency response was determined at two ELF/VLF receiver sites. Results show that ELF/VLF generated by side lobes of the HF pattern have sufficient strength to create a ELF/VLF interference pattern at receiving locations.

Carroll, Kenneth J., A. J. Ferraro, H. S. Lee, Roger Allshouse, Bruce Long and Ray J. Lunnen, Effect of HF Heating Array Directivity Pattern on the Frequency Response of Generated ELF/VLF, The Electrical Engineering Department, Ionosphere Research Laboratory, Electrical Engineering East, University Park, Pennsylvania, 16802

PSU-IRL-SCI-475

Classification Numbers

1.5.1 D-region
4.1.4 Numerical Techniques and Computations
3.2.1 Ground-Based Techniques and Measurements
3.1 Instrumentation and Facilities for Ionospheric Measurements

Directivity patterns at 3.17 MHz and 5.1 MHz are calculated for the HF antenna array at the high power HF heating facility at the Arecibo Observatory in Puerto Rico. The pattern was calculated using pattern multiplication and method of moment techniques. The calculated pattern is shown to be a good approximation to an experimentally measured pattern in one plane of the array. A simple model was used to approximate the effect of the pattern on the frequency response of ELF/VLF signals generated by the HF heating. The frequency response was determined at two ELF/VLF receiver sites. Results show that ELF/VLF generated by side lobes of the HF pattern have sufficient strength to create a ELF/VLF interference pattern at receiving locations.

Carroll, Kenneth J., A. J. Ferraro, H. S. Lee, Roger Allshouse, Bruce Long and Ray J. Lunnen, Effect of HF Heating Array Directivity Pattern on the Frequency Response of Generated ELF/VLF, The Electrical Engineering Department, Ionosphere Research Laboratory, Electrical Engineering East, University Park, Pennsylvania, 16802

PSU-IRL-SCI-475

Classification Numbers

1.5.1 D-region
4.1.4 Numerical Techniques and Computations
3.2.1 Ground-Based Techniques and Measurements
3.1 Instrumentation and Facilities for Ionospheric Measurements

Directivity patterns at 3.17 MHz and 5.1 MHz are calculated for the HF antenna array at the high power HF heating facility at the Arecibo Observatory in Puerto Rico. The pattern was calculated using pattern multiplication and method of moment techniques. The calculated pattern is shown to be a good approximation to an experimentally measured pattern in one plane of the array. A simple model was used to approximate the effect of the pattern on the frequency response of ELF/VLF signals generated by the HF heating. The frequency response was determined at two ELF/VLF receiver sites. Results show that ELF/VLF generated by side lobes of the HF pattern have sufficient strength to create a ELF/VLF interference pattern at receiving locations.